

The synthesis and evaluation of caffeine analogues as inhibitors of monoamine oxidase B and antagonists of the adenosine A_{2A} receptor

By

JUDEY PRETORIUS, B.Sc. HONS. M.Sc.

Thesis submitted for the degree Philosophiae Doctor in the School of
Pharmacy, Faculty of Health Sciences at the North-West University

Promotor: Dr. J.P. Petzer

Co-promotors: Prof. J.J Bergh
Prof. S.F. Malan

**2008
Potchefstroom**

This thesis is dedicated to God, Who has been gracious, loving, sovereign and in ultimate control throughout my whole life!

Abstract

The adenosine A_{2A} receptor has emerged as an attractive target for the treatment of Parkinson's disease (PD). Evidence suggests that antagonists of the A_{2A} receptor (A_{2A} antagonists) partially alleviate the symptoms of PD, prevent the development of motor complications and may also slow the underlying neurodegenerative process. It was recently reported that several members of the (*E*)-8-styrylcaffeine class of A_{2A} antagonists also are potent inhibitors of monoamine oxidase B (MAO-B). Since MAO-B inhibitors have also been employed as anti-parkinsonian agents, dual-target-directed drugs that block both MAO-B and A_{2A} receptors may have enhanced value in the management of PD. In an attempt to identify additional dual-acting compounds, we have, in the present study, synthesised 3 additional classes of C-8 substituted caffeine analogues. While 8-phenyl- and 8-benzylcaffeinines exhibited relatively weak MAO-B inhibition potencies, selected (*E,E*)-8-(4-phenylbutadien-1-yl)caffeine analogues and the expansion of the series with ethyl substitution at positions 1,3 and 7 of the caffeine ring were found to be exceptionally potent reversible inhibitors with enzyme-inhibitor dissociation constants (K_i values) ranging from 17–149 nM. Furthermore, these (*E,E*)-8-(4-phenylbutadien-1-yl)caffeinines also acted as potent A_{2A} antagonists with K_i values ranging from 59–153 nM. We conclude that (*E,E*)-8-(4-phenylbutadien-1-yl)caffeinines are a promising candidate class of dual-acting compounds. In this study we also compared experimentally obtained K_i values for reversible interaction with MAO-B with experimentally obtained IC_{50} values (concentration of inhibitor producing 50% inhibition) and test the validity of the Cheng–Prusoff equation which relates these two parameters. The results of this study showed that the Cheng–Prusoff equation may be used to interconvert IC_{50} and K_i values.

In conclusion, this study has identified (*E,E*)-8-(4-phenylbutadien-1-yl)caffeinines as a new class of adenosine A_{2A} antagonists. These compounds have potencies similar to that of (*E*)-8-(3-chlorostyryl)caffeine (CSC), an A_{2A} antagonist used as reference in pharmacological studies. The most potent A_{2A} antagonist of the series, (*E,E*)-1,3-diethyl-8-(4-phenylbutadien-1-yl)-7-methylxanthine, antagonized A_{2A} receptors with

a potency similar to that of (*E*)-1,2-diethyl-8-(3,4-dimethoxystyryl)-7-methylxanthine (KW-6002), an A_{2A} antagonist that is currently clinically evaluated as antiparkinsonian agent. Among the (*E,E*)-8-(4-phenylbutadien-1-yl)caffeines analogues, we have also identified congeners with potent MAO-B inhibition properties. These compounds were exceptionally potent reversible MAO-B inhibitors with K_i values in the low nanomolar range. We therefore conclude that (*E,E*)-8-(4-phenylbutadien-1-yl)caffeines are potent A_{2A} antagonists and MAO-B inhibitors. Since both these activities are relevant to PD, the compounds identified here may act as useful antiparkinsonian agents.

Uittreksel

Die adenosien A_{2A} -reseptor het na vore getree as 'n aantreklike teiken vir die behandeling van Parkinson se siekte (PS). Gegewens dui daarop dat antagonist van die A_{2A} -reseptor (A_{2A} -antagoniste), die simptome van PS gedeeltelik verlig, die ontwikkeling van motoriese komplikasies voorkom en ook die onderliggende neurodegeneratiewe prosesse mag vertraag.

Dit is onlangs gerapporteer dat verskeie lede van die (*E*)-8-stirielkafeïenklas A_{2A} -antagoniste, ook kragtige inhibeerders (of remmers) van monoamienoksidas B (MAO-B) is. Aangesien MAO-B-inhibeerders ook as teen-parkinsonistiese middels aangewend word, mag dubbelteikengerigte geneesmiddels, wat beide MAO-B- en A_{2A} -reseptore blokkeer, verhoogde waarde in die beheer van PS hê. In 'n poging om bykomende dubbelwerkende verbindings te identifiseer, het ons in die huidige studie, 3 bykomende klasse C-8-gesubstitueerde kafeïenanaloeë gesintetiseer. Terwyl 8-feniel- en 8-bensielkafeïene relatief swak MAO-B inhibisie- sterktes vertoon het, is bevind dat geselekteerde (*E,E*)-8-(4-fenielbutadien-1-iel)-kafeïen-analoë en die uitbreiding van die reeks met etielsubstitusie by posisies 1, 3 en 7 van die kafeïenring, besonder kragtige omkeerbare inhibeerders met ensiem-inhibeerderdissosiasiekonstantes (K_i -waardes), wat wissel van 17 – 49 nM, lewer. Boonop het hierdie (*E,E*)-8-(4-fenielbutadien-1-iel)kafeïene ook as kragtige A_{2A} -antagoniste opgetree, met K_i -waardes wat van 59 – 153 nM wissel. Ons kom tot die gevolgtrekking dat (*E,E*)-8-(4-fenielbutadien-1-iel)kafeïen 'n belowende kandidaatklas van dubbelwerkende verbindings is.

In hierdie studie het ons ook eksperimentverkreë K_i -waardes vir omkeerbare interaksie met MAO-B, met eksperimentverkreë IC_{50} -waardes (konsentrasie van die inhibeerder wat 50% inhibisie lewer) vergelyk en die geldigheid van die Cheng-Prusoff-vergelyking getoets wat met hierdie twee parameters verband hou. Die resultate van hierdie studie het getoon dat die Cheng-Prusoff-vergelyking interomskakeling van IC_{50} en K_i waardes moontlik maak.

In hierdie studie is bevind dat (*E,E*)-8-(4-fenielbutadieen-1-iel)kaffeïen-analoë ñ nuwe reeks adenosien A_{2A} antagonist is. Die vermoë waarmee die verbindings A_{2A} reseptore antagoneer, is ongeveer gelyk aan die van (*E*)-8-(3-chlorostiriel)kaffeïen (CSC) wat as verwysings A_{2A} antagonis dien vir farmakologiese studies. Die kragtigste A_{2A} antagonis in die reeks was (*E,E*)-1,3-dietiel-8-(4-fenielbutadieen-1-iel)-7-metielxantien wat ongeveer so potent was soos (*E*)-1,2-dietiel-8-(3,4-dimetoksiestiriel)-7-metielxantien (KW-6002). KW-6002 ondergaan tans kliniese proewe vir die behandeling van PS. Die studie het ook gevind dat sommige van die (*E,E*)-8-(4-fenielbutadieen-1-iel)kaffeïen-analoë as kragtige omkeerbare MAO-B-inhibeerders optree met K_i waardes in die lae nanomolaar konsentrasie gebied. Ons kom dus tot die gevolgtrekking dat (*E,E*)-8-(4-fenielbutadieen-1-iel)kaffeïen-analoë kragtige A_{2A} antagonist en MAO-B-inhibeerders is. Omdat beide A_{2A} antagonist en MAO-B-inhibeerders in PS aangewend kan word, kan die verbinding wat in die studie ondersoek is moontlik as nuwe geneesmiddels dien.

TABLE OF CONTENTS

	<i>Page</i>
LIST OF TABLES	i
LIST OF FIGURES	iii
LIST OF EQUATIONS	vi
LIST OF SYMBOLS AND ABBREVIATIONS	vii
ACKNOWLEDGEMENTS	xvi
CHAPTER ONE - INTRODUCTION	
1.1 Background	1
1.2 Problem statement.....	2
1.3 Objective.....	3
1.4 Concluding remarks.....	4
CHAPTER TWO - SYNTHESIS OF THE CAFFEINE ANALOGUES	
2.1 Introduction.....	6
2.2 Synthesis of (<i>E</i>)-8-styrylxanthinyl derivatives	7
2.3 Chemistry	7
2.4 Synthesis of test compounds.....	9
2.4.1 Chemicals and instrumentation.....	9
2.5 Preparation of synthetic targets.....	10
2.5.1 1,3-Dialkyl-5,6-aminouracil (5a, b).....	10
2.5.2 General procedure for the synthesis of (<i>E,E</i>)-5-phenyl-2,4-pentadienoic acids (10a-d).....	11
2.5.3 General procedure for the synthesis of caffeine analogues (1a-c, 2a-c and 3a-g).....	13
2.5.4 Characterisation.....	15
2.6 Concluding remarks.....	19

CHAPTER THREE - PARKINSON'S DISEASE AND MAO-B ENZYMOLOGY

3.1	Introduction	20
3.2	Clinical presentation and disease cause.....	21
3.3	Oxidative stress and modelling of PD in animals.....	22
	3.3.1 Oxidative stress.....	22
	3.3.2 Toxin-induced models of PD.....	24
3.4	Enzymology.....	25
	3.4.1 Monoamine oxidase-B (MAO-B).....	25
3.5	The role of MAO-B in Parkinson's disease.....	27
3.6	MMTP as a substrate.....	28
3.7	Experimental objectives and procedures.....	29
	3.7.1 Molecular Docking.....	29
	3.7.2 Enzyme kinetics: K_m determination.....	33
	3.7.3 K_i and IC_{50} determination.....	35
	3.7.4 MAO-B inhibition studies.....	36
3.8	Results and discussion.....	38
	3.8.1 8-Phenylcaffeine analogues.....	41
	3.8.2 8-Benzylcaffeine analogues.....	42
	3.8.3 (<i>E,E</i>)-8-(4-phenylbutadien-1-yl)caffeine analogues.....	43
3.9	Concluding remarks.....	46

CHAPTER FOUR - ADENOSINE A_{2A} RECEPTOR ANTAGONISM

4.1	Introduction.....	48
	4.1.1 Adenosine receptors.....	49
4.2	Adenosine A _{2A} receptor antagonists.....	51
	4.2.1 (<i>E</i>)-8-Styrylxanthinyl derivatives.....	52
	4.2.2 Non-xanthinyl heterocycles.....	54
4.3	Experimental design and procedures.....	55
	4.3.1 Tissue preparations.....	55
	4.3.2 Incubation conditions.....	55

Table of Contents

4.4	Results and Discussion.....	58
4.5	Concluding remarks.....	61

CHAPTER FIVE - CONCLUSION

5.1	Discussion	62
5.2	Concluding remarks	65

REFERENCES	66
-------------------------	-----------

APPENDIX A	81
-------------------------	-----------

LIST OF TABLES

CHAPTER ONE - INTRODUCTION

Table 1.1	Structures of the C-8 substituted caffeine analogues that were investigated for this study.....	4
-----------	---	---

CHAPTER TWO - SYNTHESIS OF THE CAFFEINE ANALOGUES

None

CHAPTER THREE - PARKINSON'S DISEASE AND MAO-B ENZYMOLOGY

Table 3.1	Clinical manifestations of Parkinson's disease.....	21
Table 3.2	Toxin based models.....	25
Table 3.3	The K_i values for the inhibition of MAO-B by 8-phenylcaffeine analogues (1a-c).....	42
Table 3.4	The K_i values for the inhibition of MAO-B by 8-benzylcaffeine analogues (2a-c).....	43
Table 3.5	The K_i and IC_{50} values for the inhibition of MAO-B by (<i>E,E</i>)-8-(4-phenylbutadien-1-yl)caffeine analogues (3a-g).....	45
Table 3.6	The K_i and IC_{50} values for the inhibition of MAO-B by (<i>E</i>)-8-styrylcaffeine analogues (4a-d).....	46

CHAPTER FOUR - ADENOSINE A_{2A} RECEPTOR ANTAGONISM

Table 4.1	Description of materials and suppliers of reagents and materials utilised for the A _{2A} assay.....	58
Table 4.2	The K_i values for the competitive inhibition of [³ H]NECA binding to rat striatal adenosine A _{2A} receptors by selected caffeine analogues.....	60

CHAPTER FIVE - CONCLUSION

Table 5.1	Structures of the C-8 substituted caffeine analogues that were investigated for this study.....	64
------------------	--	-----------

APPENDIX A

Table A.1	A summary of the ¹H-NMR.....	82
------------------	--	-----------

LIST OF FIGURES

CHAPTER ONE - INTRODUCTION

None

CHAPTER TWO - SYNTHESIS OF THE CAFFEINE ANALOGUES

Figure 2.1	(<i>E</i>)-8-(3-Chlorostyryl)caffeine (CSC).....	6
Figure 2.2	The structures of the C-8 substituted caffeine analogues that were investigated in the present study.....	9
Figure 2.3	Synthetic pathway to substituted 5,6-diaminouracil derivatives (5a, b).....	11
Figure 2.4	Synthetic pathway to the (<i>E,E</i>)-5-phenyl-2,4-pentadienoic acids (6a-e).....	12
Figure 2.5	Synthetic pathway to the C-8 substituted caffeine analogues 1a-c, 2a-c and 3a-g.....	14

CHAPTER THREE - PARKINSON'S DISEASE AND MAO-B ENZYMOLOGY

Figure 3.1	Representation of the production of ROS from molecular oxygen.....	24
Figure 3.2	Structures of MAO-B inhibitors, (<i>R</i>)-deprenyl, rasagiline, lazabemide and safinamide.....	27
Figure 3.3	The oxidation of MPTP by MAO-B.....	28
Figure 3.4	The MAO catalysed oxidation of MMTP.....	29
Figure 3.5	Docking orientations of selected caffeine analogues in the active site of MAO-B.....	
	a 8-(3-Trifluoromethylbenzyl)caffeine.....	31
	b 8-(3-Chlorophenyl)caffeine.....	31
	c (<i>E,E</i>)-8-[(4-(3-Bromophenylbutadien-1-yl))caffeine.....	32
	d (<i>E,E</i>)-8-(4-Phenylbutadien-1-yl)caffeine.....	32
Figure 3.6	Graphical representation of the Michaelis-Menten equation (V_i versus $[S]$).....	34
Figure 3.7	An example of the Lineweaver-Burke plot ($1/V_i$ versus $1/[S]$).....	35

Figure 3.8	Linearity in the oxidation of MMTP by baboon liver MAO-B.....	39
Figure 3.9	Lineweaver–Burke plots of the oxidation of MMTP by baboon liver MAO-B.....	40
Figure 3.10	The sigmoidal dose-response curve of the initial rates of oxidation of MMTP versus the logarithm of concentration of inhibitor.....	41
CHAPTER FOUR - ADENOSINE A_{2A} RECEPTOR ANTAGONISM		
Figure 4.1	Structures of adenosine and caffeine.....	52
Figure 4.2	Xanthinyl type adenosine receptor antagonists.....	53
Figure 4.3	Non-xanthinyl heterocyclic adenosine receptor antagonists.....	54
Figure 4.4	Competition study between [3f] and the radio labelled ligand.....	60
CHAPTER FIVE - CONCLUSION		
None		
APPENDIX A –		
None		

LIST OF EQUATIONS

CHAPTER THREE - PARKINSON'S DISEASE AND MAO-B ENZYMOLOGY

Equation 3.1	Michaelis-Menten.....	33
Equation 3.2	Lineweaver-Burke.....	34
Equation 3.3	K_i determination.....	35

CHAPTER FOUR - ADENOSINE A_{2A} RECEPTOR ANTAGONISM

Equation 4.1	Calculation of IC ₅₀ value with non-linear regression.....	57
Equation 4.2	Cheng-Prusoff equation to calculate the K_i from the IC ₅₀ value.....	57

LIST OF SYMBOLS AND ABBREVIATIONS

LIST OF SYMBOLS

α	alpha
β	beta
λ	lambda
μ	micro: 10^{-6}
n	nano: 10^{-9}
p	pico: 10^{-12}
e^-	electron
%	percent
$^{\circ}\text{C}$	degrees Celsius
-	negative
+	positive
#	number

LIST OF ABBREVIATIONS

A	
A	adenine
A_{2A}	adenosine receptor, subtype 2
Abs	absorbance
AMP	adenosine monophosphate
ATP	adenosine triphosphate
B	
Br	bromine

List of Symbols and Abbreviations

C	
Cl	chlorine
CNS	central nervous system
CoA	coenzyme A
CoQ	coenzyme Q
COX	cytochrome <i>c</i> oxidase
CPA	cyclopentyl adenosine
CSC	(<i>E</i>)-8-(3-chlorostyryl)caffeine
Cys	cysteine
D	
DA	dopamine
DMF	N,N-dimethylformamide
DMSO	dimethylsulfoxide
DNA	deoxyribonucleic acid
E	
[E]	enzyme concentration
<i>E</i>	<i>trans</i>
e.g.	<i>exempli gratia</i>
EDAC	1-ethyl-3[3-(dimethylamino)propyl]carbodiimide
<i>et al.</i>	<i>et alii</i> : and others
EtOH	ethanol
F	
FAD	flavin adenine dinucleotide
G	
g	gram
<i>g</i>	gravitational force of the earth ($\sim 10 \text{ m.s}^{-1}$)

List of Symbols and Abbreviations

H	
H⁺	hydrogen ion/proton/s
H₂O	water
H₂O₂	hydrogen peroxide
HCl	hydrochloric acid
I	
[I]	inhibitor concentration
i.e.	that is
K	
kb	kilo base pairs (thousand base pairs)
kg	kilogram
K_i	enzyme-inhibitor dissociation constant
L	
M	
M	molar
MAO	monoamine oxidase
mg	milligram
MgCl₂	magnesium chloride
min	minutes
ml	millilitre
mM	millimolar
MMDP⁺	1-methyl-4-(1-methylpyrrol-2-yl)-2,3-dihydropyridinium
MMTP⁺	1-methyl-4-(1-methylpyrrol-2-yl)-1,2,3,6-tetrahydropyridinium
MMP⁺	1-methyl-4-(1-methylpyrrol-2-yl)pyridinium
mp	melting point
MPDP⁺	1-methyl-4-phenyl-2,3-dihydropyridinium
MPP⁺	1-methyl-4-phenylpyridinium
MPTP	1-methyl-4-phenyl-1,2,3,6,-tetrahydropyridine

List of Symbols and Abbreviations

mRNA	messenger ribonucleic acid
MSE	mean square error
N	
n	number
NADH	nicotinamide adenine dinucleotide (reduced)
NMR	nuclear magnetic resonance
O	
O₂	oxygen
O₂⁻	superoxide radical
OH[·]	hydroxyl free radical
ONOO[·]	peroxynitrite
OXPHOS	oxidative phosphorylation
P	
PD	Parkinson's disease
pH	indicates acidity
Q	
R	
RNA	ribonucleic acid
ROS	reactive oxygen species
S	
[S]	substrate concentration
SD	standard deviation
SEM	standard error of mean
SN	Substantia nigra
SNPC	Substantia nigra pars compacta
SNr	Substantia nigra pars reticulata

List of Symbols and Abbreviations

T	
$t_{1/2}$	half life
TCA	tricarboxylic acid
Tris	Tris(hydroxymethyl)aminomethane
Tyr	tyrosine
U	
μl	microlitre
U	units (enzyme activity)
UV	ultraviolet
V	
V_i	initial velocity
V_{max}	maximal velocity
W	
X	
Y	
Z	
Z	<i>cis</i>

Acknowledgements

Completion of this thesis resembles taking a very long journey of self-discipline, dedication and patience while researching, drafting and repeatedly revising the work. Completing such a journey requires any author to seek help and assistance from many people who provide advice and direction along the way. The study presented here was clearly influenced by the inputs of remarkable people. I thank those who supported and encouraged me during my journey. I would like to express my sincere appreciation to the following people and institutions.

- ◆ My promotor, Dr. Petzer, for his guidance, patience and compassion towards me. For being a mentor and role model in all aspects. His valuable advice and encouragement as a supervisor was outstanding!
- ◆ My co-promoters, Prof. Bergh and Prof. Malan, for their valuable insight and inputs in the subject, and for broadening my knowledge in the field of medicinal chemistry.
- ◆ Financial support from the National Research Foundation.
- ◆ Cor Bester and Antoinette Fick at the Animal Research Centre, North-West University, for their assistance during the rat dissections.
- ◆ André Joubert and Johan Jordaan of the SASOL Centre for Chemistry, North-West University for recording NMR and MS spectra.
- ◆ The Laboratory for Applied Molecular Biology at the School of Pharmacy, for the use of the scintillation counter apparatus and support.
- ◆ Last but not least, my Mother (and memory of my Father) for all her guidance, motivation, support, encouragement and love. Both my Mother and sister (Geraldine) have left remarkable footprints throughout my journey of life!

Chapter One

Introduction

1.1 Background

Parkinson's disease (PD) is a neurodegenerative disorder characterised pathologically by a marked loss of dopaminergic nigrostriatal neurons and clinically by disabling movement disorders. Currently, treatment of PD relies on central dopamine replacement with dopamine agonists or the dopamine precursor L-DOPA (Marsden *et al.*, 1982). Even though this approach provides symptomatic relief in the early stages of PD, advanced PD is ultimately associated with poor quality of life and can lead to death (Koller & Hubble, 1990; Koller, 1997).

Drugs that target the mechanism of neuronal cell death and therefore delay or even halt the progression of this disease may offer improved therapeutic approaches for the treatment of PD. The development of neuroprotective agents have focused on identifying compounds that protect against the degenerative processes associated with the exposure to the neurotoxin, 1-methyl-4-phenyl-1,2,3,6-tetrahydropyridine (MPTP). MPTP induces loss of nigrostriatal neurons (Jackson-Lewis *et al.*, 1995) in humans and produces a syndrome that is neurochemically, behaviourally and pathologically similar to that observed in patients diagnosed with PD. The toxic effects of MPTP are reported to be mediated by the pyridinium species, MPP^+ (Markey *et al.*, 1984), a mitochondrial toxin (Nicklas *et al.*, 1985; Ramsay *et al.*, 1991). MPP^+ is formed via the MAO-B catalysed oxidation of the parent tetrahydropyridinyl protoxin which generates the unstable dihydropyridinium intermediate, $MPDP^+$. A second 2-electron oxidation yields MPP^+ (Chiba *et al.*, 1984; Chiba *et al.*, 1985).

Early studies established that (*R*)-deprenyl, an irreversible MAO-B inhibitor and clinically useful anti-parkinsonian agent, is neuroprotective in MPTP-treated animals (Heikkila *et al.*, 1984). Although this neuroprotection may be linked to the blockade of the metabolic bioactivation of MPTP, the neuroprotective properties of (*R*)-deprenyl in MPTP animal models also appear to involve unknown pathways that are independent of the inhibition of MPP⁺ formation (Heikkila *et al.*, 1984; Kupsch *et al.*, 2001; Tatton & Greenwood, 1991; Tatton, 1993; Wu *et al.*, 1993). The inhibition of MPP⁺ formation is reported to ameliorate motor deficits in MPTP-treated animals (Kanda *et al.*, 2000; Grondin *et al.*, 1999; Shiozaki *et al.*, 1999; Ikeda *et al.*, 1999). Recently A_{2A} antagonists have also been shown to possess neuroprotective properties in animal models of PD. Reports of former studies have indicated that the nonselective A₁/A_{2A} antagonist, caffeine, protects against the MPTP induced nigrostriatal neurotoxicity in the mouse model of PD (Chen *et al.*, 2001).

1.2 Problem statement

The enzyme, MAO-B, is of substantial pharmacological importance since it is the principle enzyme that catalyses the oxidation of dopamine in the brain. Inhibitors of MAO-B are commonly used as adjunct therapy for the treatment of Parkinson's disease (PD). The inhibition of the MAO-B catalysed oxidation of dopamine in the central nervous system, results in the concentration of the depleted supply of dopamine and delays the need for levodopa in patients diagnosed with early PD (Rabey *et al.*, 2000). MAO-B inhibitors are also reported to exert a neuroprotective effect by blocking apoptotic cell death (Tatton & Greenwood, 1991), and consequently may be used clinically to postpone the emergence of symptoms that necessitate the initiation of levodopa therapy in PD patients. For these reasons MAO-B is considered to be an attractive target for the treatment of neurodegenerative diseases.

Recently caffeine has also been reported to be neuroprotective in the MPTP mouse model of Parkinsons disease. This action appears to be dependent upon caffeine's ability to

antagonise the adenosine A_{2A} receptor. In accordance with this view, potent A_{2A} receptor antagonists also protect against the MPTP induced neurotoxicity. An A_{2A} receptor antagonist of particular importance is (*E*)-1,2-diethyl-8-(3,4-dimethoxystyryl)-7-methylxanthine (KW-6002) (Shimada *et al.*, 1997), which is currently clinically used as an antiparkinsonian drug. Besides possessing neuroprotective properties, A_{2A} receptor antagonists are also reported to ameliorate the motor deficits associated with Parkinson's disease. Antagonism of the A_{2A} receptor therefore appears to be an attractive target for the development of antiparkinsonian drugs that provides symptomatic relief as well as possible protection against further neurodegeneration.

(*E*)-8-(3-Chlorostyryl)caffeine (CSC) is an A_{2A} receptor antagonist that is frequently used in the pharmacological characterisation of A_{2A} receptors. Recently, CSC has also been reported to be an exceptionally potent reversible inhibitor of MAO-B. This finding has prompted us to investigate the possibility of designing drugs that are both potent A_{2A} receptor antagonists and MAO-B inhibitors. Such drugs may possess enhanced therapeutic value since A_{2A} receptor antagonism and MAO-B inhibition are both considered to be important strategies in the treatment of Parkinson's disease.

1.3 Objective

The principle objective of this study was to synthesise novel C-8 substituted caffeine analogues and to evaluate them as competitive inhibitors of MAO-B as well as antagonists of the adenosine A_{2A} receptor. The structures of the compounds selected for this study are illustrated in Table 1.1. These compounds were expected to be antagonists of the adenosine A_{2A} receptor since they are structurally similar to other known A_{2A} receptor antagonists such as KW-6002 and CSC. We also expected the proposed structures to be reversible inhibitors of MAO-B since preliminary docking studies indicated that the caffeinyl moiety of the structures occupy the active site of MAO-B while the C-8 side chain extends to the entrance cavity. This dual mode of binding is proposed to be responsible for the potency of CSC as an inhibitor of MAO-B.

Table 1.1. Structures of the C-8 substituted caffeine analogues that were investigated for this study: 8-Phenylcaffeine (1a-c), 8-benzylcaffeine (2a-c) and (E,E)-8-(4-phenylbutadien-1-yl)caffeine (3a-g) analogues.

Compound #	Compound structure	R																								
1a 1b 1c		H Cl CF ₃																								
2a 2b 2c		H Cl CF ₃																								
3a 3b 3c 3d 3e 3f 3g		<table border="1"> <thead> <tr> <th>R¹</th> <th>R²</th> <th>R³</th> </tr> </thead> <tbody> <tr> <td>H</td> <td>CH₃</td> <td>CH₃</td> </tr> <tr> <td>Cl</td> <td>CH₃</td> <td>CH₃</td> </tr> <tr> <td>Br</td> <td>CH₃</td> <td>CH₃</td> </tr> <tr> <td>F</td> <td>CH₃</td> <td>CH₃</td> </tr> <tr> <td>H</td> <td>CH₃</td> <td>C₂H₅</td> </tr> <tr> <td>H</td> <td>C₂H₅</td> <td>CH₃</td> </tr> <tr> <td>H</td> <td>C₂H₅</td> <td>C₂H₅</td> </tr> </tbody> </table>	R ¹	R ²	R ³	H	CH ₃	CH ₃	Cl	CH ₃	CH ₃	Br	CH ₃	CH ₃	F	CH ₃	CH ₃	H	CH ₃	C ₂ H ₅	H	C ₂ H ₅	CH ₃	H	C ₂ H ₅	C ₂ H ₅
R ¹	R ²	R ³																								
H	CH ₃	CH ₃																								
Cl	CH ₃	CH ₃																								
Br	CH ₃	CH ₃																								
F	CH ₃	CH ₃																								
H	CH ₃	C ₂ H ₅																								
H	C ₂ H ₅	CH ₃																								
H	C ₂ H ₅	C ₂ H ₅																								

1.4 Concluding remarks

A variety of studies carried out over the last few years support the concept that A_{2A} receptor antagonists can ameliorate motor dysfunction and be relevant in the therapy of Parkinson's disease and possibly other neurodegenerative disorders. A_{2A} receptor antagonism has also been implicated in protection against MPTP-induced neuronal death (Chen *et al.*, 2001). The possibility of developing compounds that act both to antagonise adenosine mediated stimulation of A_{2A} receptors and to inhibit MAO-B catalytic activity,

may offer novel therapeutic benefits in patients diagnosed with PD. During this investigation three classes of C-8 substituted caffeine analogues were prepared and ultimately evaluated as both MAO-B inhibitors and adenosine A_{2A} receptor antagonists.

Methods used in the analysis of data and experimental design are discussed in Chapter One to Four. All results obtained in this study will be presented either graphically or in tabular form followed by short discussions to explain how the results were interpreted. In Chapter Two several related topics are discussed, namely the synthetic design and preparation of the compounds chosen for this investigation, as well as the chemicals and instrumentation utilised during this study. In Chapter Three a description of PD and MAO-B enzymology is given with the enzyme inhibition results and data analysis. Chapter Four describes the adenosine A_{2A} receptor antagonism which include the results and discussion of the competition studies of the selected test compounds. Finally the concluding remarks are presented in Chapter Five.

Chapter Two

Synthesis of the Caffeine Analogues

2.1 Introduction

The principle objective of this study is to discover/design drugs that act as both A_{2A} antagonists and MAO-B inhibitors. Such drugs may find the application in the treatment of Parkinson's disease (PD).

A promising lead compound, (*E*)-8-(3-chlorostyryl)caffeine (CSC) (**4b**), shown in Figure 2.1, was recently found to inhibit MAO-B. CSC is frequently used when examining the *in vivo* pharmacological effects of A_{2A} antagonists (Jacobson *et al.*, 1993; Muller *et al.*, 1997). It was also previously reported that CSC is also a potent reversible inhibitor of monoamine oxidase B (MAO-B) with an enzyme-inhibitor dissociation constant (K_i value) of 128 nM (Chen *et al.*, 2001; Petzer *et al.*, 2003; Vlok *et al.*, 2006).

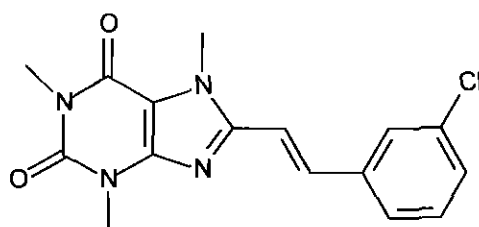


Figure 2.1. (*E*)-8-(3-Chlorostyryl)caffeine (CSC) (**4b**)

In this chapter the synthesis of 8-phenylcaffeine (**1a-c**), 8-benzylcaffeine (**2a-c**), and (*E,E*)-8-(4-phenylbutadien-1-yl)caffeine (**3a-d**) analogues are described. The series of (*E,E*)-8-(4-phenylbutadien-1-yl)caffeine analogues were further expanded with the

synthesis of 3 additional congeners, compounds **3e-g** with ethyl substitution at positions 1, 3 and 7 of the caffeine ring.

2.2 Synthesis of (*E*)-8-styrylxanthinyl derivatives

Since the discovery that introduction of an (*E*)-styryl group in the 8 position of xanthinyl derivatives resulted in compounds that are exceptionally potent and selective antagonists of the A_{2A} receptor (Shimada *et al.*, 1992), numerous derivatives have been synthesised and characterised. Although most exhibit A_{2A} antagonism, very few of these are commercially available. Using standard literature procedures (Suzuki *et al.*, 1993; Jacobson *et al.*, 1993; Müller *et al.*, 1997a) we were able to synthesise fourteen 8-substituted caffeine derivatives.

2.3 Chemistry

The C-8 substituted caffeine analogues (**1a-c**, **2a-c** and **3a-g**) (Figure 2.2) examined in this study, were synthesised in high yield according to the procedure previously reported for the synthesis of (*E*)-8-styrylcaffeine analogues (Suzuki *et al.*, 1993; Vlok *et al.*, 2006). The key starting materials for the procedure, 1,3-dimethyl- (**5a**) or 1,3-diethyl-5,6-diaminouracil (**5b**) (Figure 2.3) (Blicke & Godt, 1954), were allowed to react with the appropriate carboxylic acid in the presence of a carbodiimide activating reagent, N-(3-dimethylaminopropyl)-N'-ethylcarbodiimide hydrochloride (EDAC), (Figure 2.5). The carboxylic acids used were benzoic acids (**10a-c**), phenylacetic acids (**11a-c**) and (*E,E*)-5-phenyl-2,4-pentadienoic acids (**6a-d**) (Figure 2.4) for the preparation of **1a-c**, **2a-c** and **3a-g**, respectively. The resulting amide intermediates underwent ring closure in refluxing aqueous sodium hydroxide to yield the corresponding 1,3-dimethyl-8-substituted-7*H*-xanthinyl analogues (**12**) (Figure 2.5). Without further purification, the crude product thus obtained was selectively 7*N*-alkylated in the presence of an excess of iodomethane (**1a-c**, **2a-c**, **3a-d** and **3f**) or iodoethane (**3e** and **3g**) and potassium carbonate to yield the target compounds **1-3**. Following crystallisation from a suitable solvent the structures and purity of all compounds were verified by mass spectrometry, ¹H-NMR and

^{13}C -NMR. The *trans-trans* geometry about the conjugated ethenyl π -bonds of **3a-g** was confirmed by proton-proton coupling constants in the range of 14.6–15.5 Hz for the olefinic proton signals.

The (*E,E*)-5-phenyl-2,4-pentadienoic acids (**6a-d**) required for the preparation of **3a-g** were conveniently synthesised by allowing the appropriately substituted cinnamylidenemalonic acid (**7a-d**) to react with refluxing acetic anhydride and acetic acid (Gerber, 1960) (Figure 2.4). A solution of the resulting crude 5-phenyl-2,4-pentadienoic acid in chloroform was exposed to ambient light for 5 hours with a crystal of iodine added to the solvent. This converts the *allo*-styryl-acrylic acid into the desired *trans-trans* geometry (Gerber, 1960). Following recrystallisation from benzene, **6a-d** were obtained in good yield and with a high degree of purity. The required cinnamylidenemalonic acids (**7a-d**) were in turn synthesised in high yield from the corresponding cinnamaldehydes (**8a-d**) and malonic acid in pyridine (Kurien *et al.*, 1934). Except for cinnamaldehyde (**8a**), which is commercially available, the other substituted cinnamaldehydes (**8b-d**) (Section 2.5.2) were synthesised by reacting the corresponding benzaldehydes (**9b-d**) with acetaldehyde in basic conditions (Baker & Doll, 1971; Baker *et al.*, 1969). The resulting cinnamaldehydes were purified by neutral aluminium oxide column chromatography.

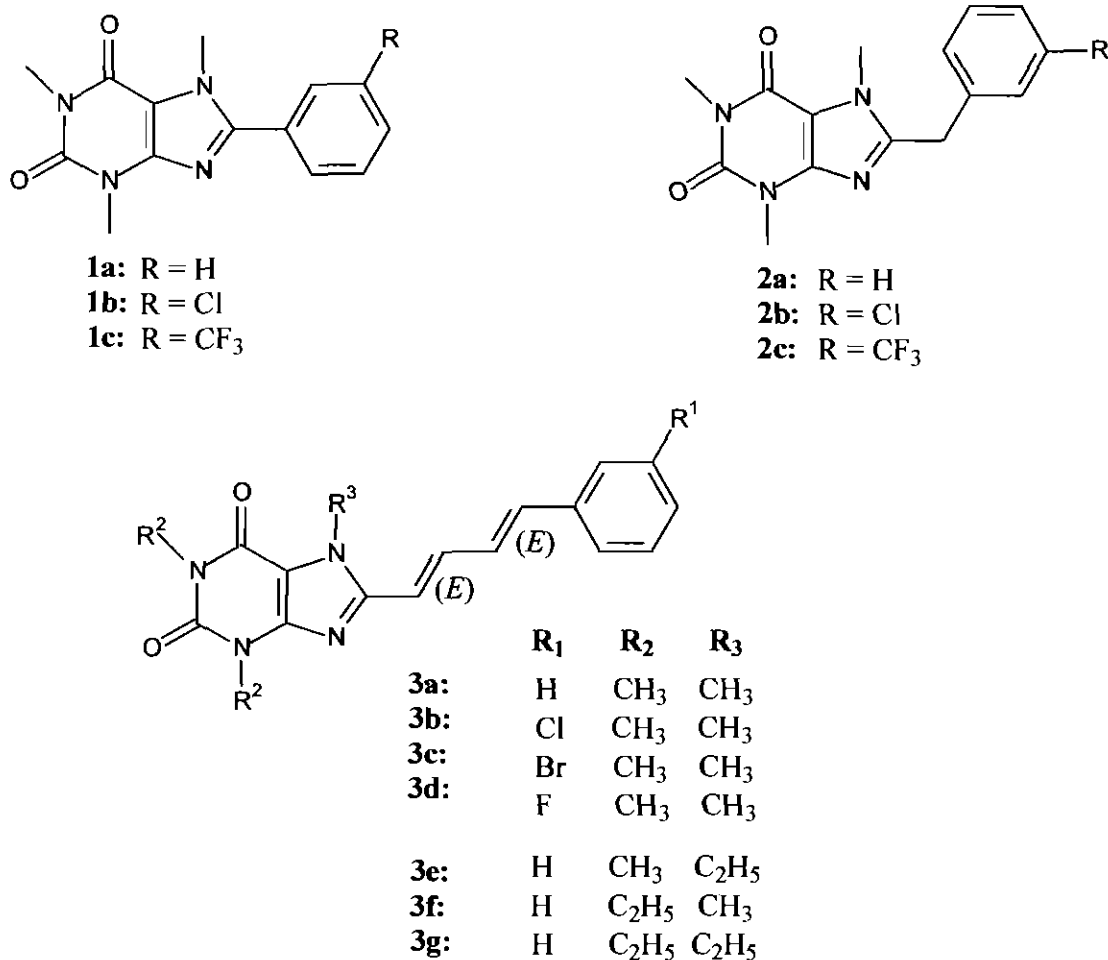


Figure 2.2. The structures of the C-8 substituted caffeine analogues that were investigated in the present study: 8-phenylcaffeine (1a-c), 8-benzylcaffeine (2a-c) and (E,E)-8-(4-phenylbutadien-1-yl)caffeine (3a-g).

2.4 Synthesis of test compounds

2.4.1 Chemicals and instrumentation

All starting materials, unless mentioned elsewhere, were obtained from Sigma-Aldrich and were used without purification. The oxalate salt of MMTP (Bissel *et al.*, 2002), KW-6002 (16) (Suzuki *et al.*, 1993; Petzer *et al.*, 2003), 1,3-dimethyl- (5a) and 1,3-diethyl-5,6-diaminouracil (5b) (Blicke & Godt, 1954) were synthesised according to previously reported procedures. Because of chemical instability, compounds 5a-b were used within 24 hours of preparation. Proton and carbon NMR spectra were recorded on a Varian

Gemini 300 spectrometer. Proton (^1H) spectra were recorded in chloroform (CDCl_3) and dimethyl sulfoxide (DMSO-d_6) at a frequency of 300 MHz and carbon (^{13}C) spectra at 75 MHz. Chemical shifts are reported in parts per million (δ) downfield from the signal of tetramethylsilane added to the deuterated solvent. Spin multiplicities are given as s (singlet), d (doublet), t (triplet), q (quartet), bs (broad singlet) or m (multiplet) and the coupling constants (J) are given in hertz (Hz). Direct insertion electron impact ionisation (EIMS) and high resolution mass spectra (HRMS) were obtained on a VG 7070E mass spectrometer. Melting points (mp) were determined on a Stuart SMP10 melting point apparatus and are uncorrected. UV-Vis spectra were recorded on a Shimadzu UV-2100 double-beam spectrophotometer. Thin layer chromatography (TLC) was carried out with neutral aluminum oxide 60 (Merck) containing UV_{254} fluorescent indicator.

2.5 Preparation of synthetic targets

2.5.1 1,3-Dialkyl-5,6-diaminouracil (5a, b)

The 5,6-diaminouracil derivatives were synthesised according to a general procedure first described by Traube (1900). Symmetric dialkylurea (**A**: 60 mmol) was condensed with cyanoacetic acid (**B**: 60 mmol) in the presence of acetic anhydride (**i**) (7.5 ml) to yield the cyanoacetylurea intermediate (**C**) as indicated in Figure 2.3. On treatment with aqueous sodium hydroxide (10%) (Papesch & Schroeder, 1951) or a metal alkoxide base (**ii**) (Triplett *et al.*, 1978) ring closure takes place to form 1,3-dimethyl-6-aminouracil (**D**). When **D** was treated with sodium nitrite (72.21 mmol) in the presence of an acid (**iii**), 1,3-dimethyl-5-nitroso-6-diaminouracil (**E**) was formed which was reduced to the desired 5,6-diaminouracil (**5a, b**) with sodium hydroxylfite (**iv**) (Blicke & Godt, 1954; Speer & Raymond, 1953).

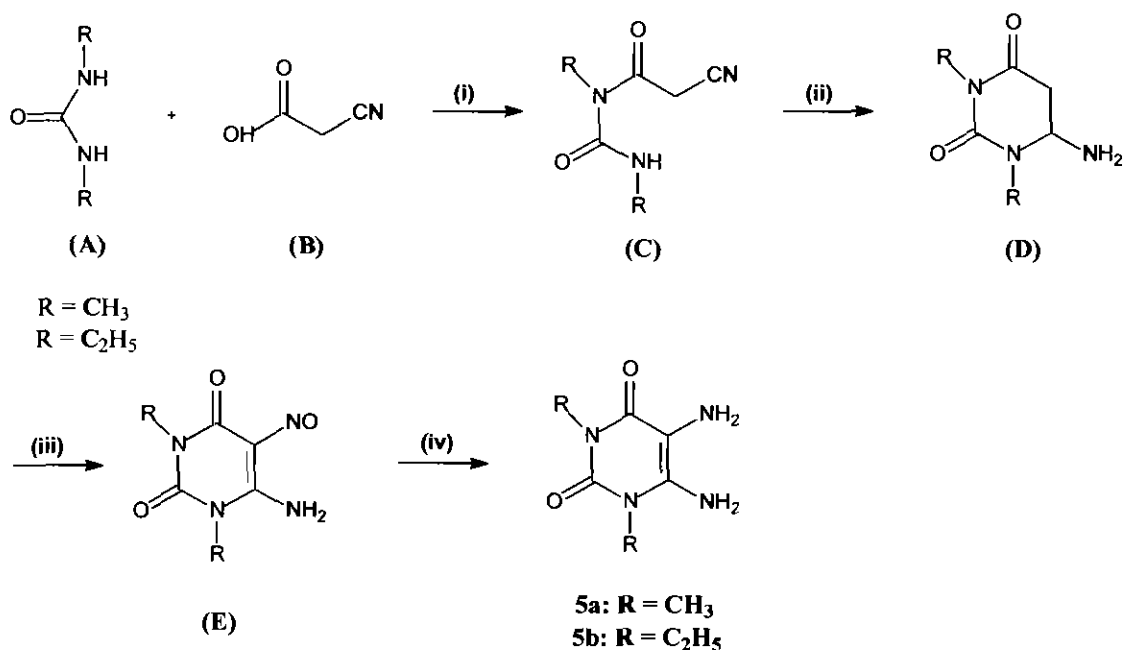


Figure 2.3. Synthetic pathway to substituted 5,6-diaminouracil derivatives (5a,b). Key: (i) acetic anhydride. (ii) NaOH (aq) or NaOEt. (iii). NaNO₂, CH₃CO₂H. (iv) Na₂S₂O₄.

2.5.2 General procedure for the synthesis of (*E,E*)-5-phenyl-2,4-pentadienoic acids (10a-d)

Distilled acetaldehyde (52.35 ml ; 933 mmol) was added to 75 mmol of the substituted benzaldehyde at room temperature. The solution was cooled on ice. A solution of 25% sodium hydroxide in methanol was added slowly and carefully over a period of ten minutes. Stirring continued over an hour on ice and acetic anhydride (43.10 ml ; 456 mmol) was added. This solution was refluxed for an hour at 120 °C after which the solution was cooled on ice and 105 ml distilled water was added. While still on ice 5 N hydrochloric acid (43.8 ml) was added to attain a two phase mixture. Again the solution was heated to 120 °C for 30 minutes and the reaction remained as two separate phases. Following the reaction, an oily residue separated at the bottom of the flask. The reaction was kept overnight at room temperature and the oily residue was collected and the substituted cinnamaldehyde (**8a-d**) was purified by column chromatography (neutral alumina).

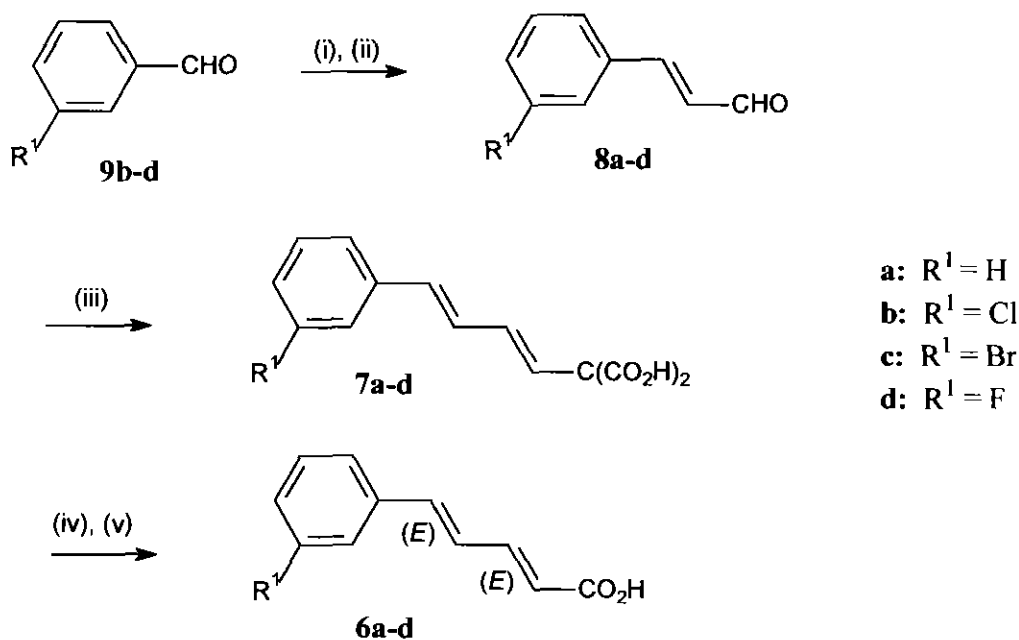


Figure 2.4. Synthetic pathway to the (E,E)-5-phenyl-2,4-pentadienoic acids (6a-e). Key: (i) NaOH, CH₃CHO; (ii) Ac₂O, 120 °C; (iii) CH₂(CO₂H)₂, pyridine, 100 °C; (iv) Ac₂O, CH₃CO₂H, reflux; (v) I₂.

Compounds **6a-d** were synthesised from the corresponding cinnamylidenemalonic acids (**7a-d**) (Kurien *et al.*, 1934) according to the previously described procedure (Gerber, 1960). Cinnamaldehyde (3.5 ml), malonic acid (2.4 g) and pyridine (3 ml) were heated for an hour at 130 °C. Sodium carbonate (140 mmol) was added to the solution. The solution was acidified to pH 4-5 with 4 M of hydrochloric acid after which the product was obtained via filtration. The Cinnamylidenemalonic acid was finally rinsed with ice cold benzene (± 100 ml). Cinnamylidenemalonic acids (**7a-d**) (1 g ; mmol) were allowed to reflux for 60 min with acetic anhydride (5 ml) and acetic acid (3 ml). The reaction was cooled to room temperature and poured into 100 ml water. After 3 hours, the resulting precipitate was collected via filtration. The crude product and a crystal of iodine were dissolved in 20 ml CHCl₃ and incubated in ambient light for 5 hours. The CHCl₃ was removed under reduced pressure and the residue was recrystallised from benzene. For previously described **6a-c** the melting points were recorded as follows: **6a** 194 °C, lit. 178 °C (Gerber, 1960); **6b** 190 °C, lit. 173–174 °C (Werbel *et al.*, 1967); **6c** 187 °C, lit. 179–180 (Crombie *et al.*, 1994).

(*E,E*)-5-(3-Fluorophenyl)-2,4-pentadienoic acid (**6d**) was synthesised from **7d** in a yield of 42%. mp 164 °C; ¹H NMR (DMSO-*d*₆) δ 6.03 (d, 1H, J = 15.0 Hz), 7.10–7.45 (m, 7H) ¹³C NMR (DMSO-*d*₆) δ 112.90, 113.16, 115.33, 123.18, 123.51, 128.09, 130.63, 130.74, 138.19, 143.66, 167.31; EIMS *m/z* 192 (M⁺); HRMS calcd. 192.05866, found 192.05936.

2.5.3 General procedure for the synthesis of caffeine analogues (**1a-c**, **2a-c** and **3a-g**)

For the synthesis of substituted caffeine analogues most literature procedures make use of the 5,6-diaminouracil derivative (**5a, b**) as key starting material (Figure 2.5) (Shimada *et al.*, 1992; Müller *et al.*, 1997; Suzuki *et al.*, 1993). Acylation of uracil (**5a, b**) with a carboxylic acid (**6, 10 and 11**) followed by treatment with aqueous sodium hydroxide gives the corresponding 7H-xanthinyl derivative (**12**) (Shimada *et al.*, 1992). A commercial carbodiimide reagent is used to convert the carboxylic acid to the active acylation agent. The carbodiimide frequently used is N-(3-dimethylaminopropyl)-N'-ethylcarbodiimide hydrochloride (EDAC) (Müller *et al.*, 1997). The amide intermediate can be cyclised by treating with phosphorous oxychloride or aqueous sodium hydroxide (Shimada *et al.*, 1992). The imine product is subsequently subjected to oxidative ring closure using ferric chloride or thienyl chloride. Methylation at the 7-N position is generally required for potent inhibition of the MAO-B enzyme, which is achieved by the addition of iodomethane in the presence of a weak base such as potassium carbonate.

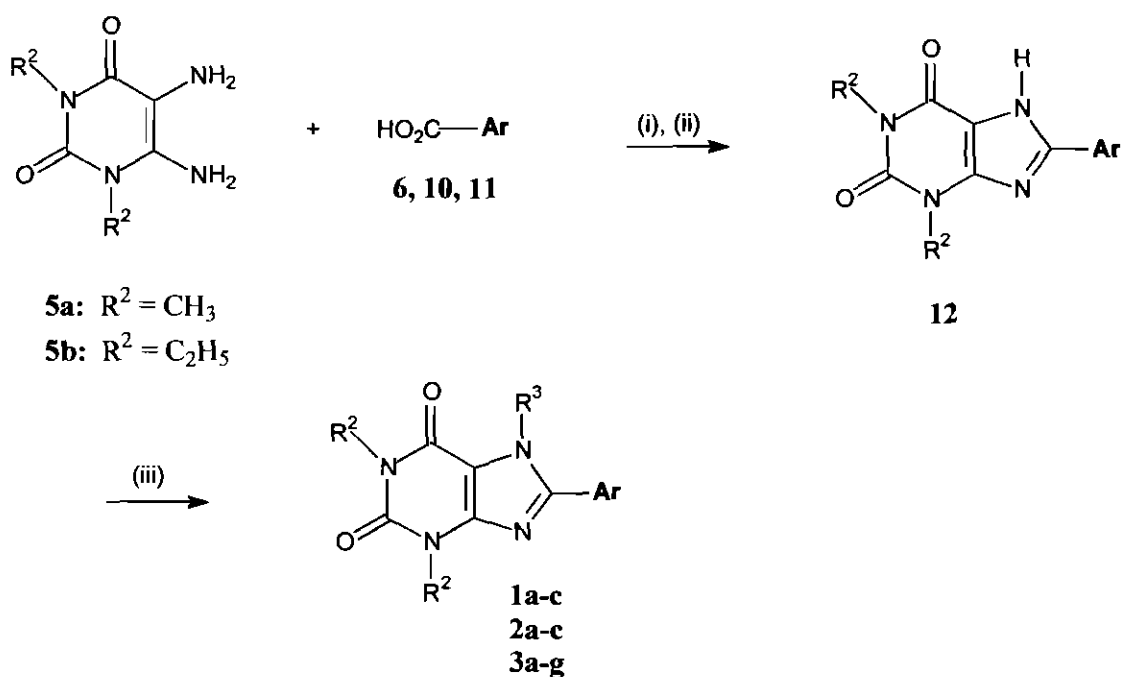


Figure 2.5. Synthetic pathway to the C-8 substituted caffeine analogues **1a-c**, **2a-c** and **3a-g**. Key: (i) EDAC, dioxane/ H_2O ; (ii) NaOH (aq), reflux; (iii) CH_3I or $\text{C}_2\text{H}_5\text{I}$, K_2CO_3 , DMF

The C-8 substituted caffeine analogues were synthesised according to the procedure described in literature (Suzuki *et al.*, 1993). 1,3-Dimethyl- (**5a**) or 1,3-diethyl-5,6-diaminouracil (**5b**) (3.50 mmol) and N-(3-dimethylaminopropyl)-N'-ethylcarbodiimide hydrochloride (EDAC; 5.11 mmol) were dissolved in 40 ml dioxane/ H_2O (1:1) and the appropriate carboxylic acid [benzoic acids (**10a-c**), phenylacetic acids (**11a-c**) or (*E,E*)-5-phenyl-2,4-pentadienoic acids (**6a-d**), 3.81 mmol] was added. A suspension was obtained and the pH was adjusted to 5 with 2 M aqueous hydrochloric acid. The reaction mixture was stirred for an additional 2 hours and then neutralised with 1 M aqueous sodium hydroxide. After cooling to 0 °C, the precipitate that formed was collected by filtration. A solution of this crude amide in 40 ml aqueous sodium hydroxide (1 M)/dioxane (1:1) was heated under reflux for 2 hours, cooled to 0 °C and then acidified to a pH of 4 with 4 M aqueous hydrochloric acid. To obtain **1a-c**, **2a-c** and **3a-e**, the resulting precipitate, 1,3-dimethyl-8-substituted-7*H*-xanthinyl analogue (**12**), was collected by filtration and used in the subsequent reaction without further purification.

For the synthesis of **3f-g**, the resulting precipitate was removed via filtration and the filtrate was extracted to CHCl_3 (2×100 ml). The organic phase was dried over anhydrous MgSO_4 and removed under reduced pressure to yield a yellow oily residue, the 1,3-diethyl-8-substituted-7*H*-xanthinyl analogues (**12**). To a stirred suspension of **12** (0.20 mmol) and potassium carbonate (0.50 mmol) in 5 ml DMF, was added iodomethane (**1a-c**, **2a-c**, **3a-d** and **3f**) or iodoethane (**3e** and **3g**) (0.40 mmol). Stirring was continued at 60 °C for 60 minutes and the insoluble materials were removed by filtration. Sufficient water was added to the filtrate to precipitate the product (**1-3**) which was collected by filtration. Following crystallisation from a mixture of methanol/ethyl acetate (9:1) (**1a-c**, **2a-c**, **3a-e**) or ethanol (**3f-g**), analytically pure samples of the target compounds were obtained. For previously described **1a** and **2a**, we found the melting points to be 180 °C and 165 °C [from methanol/ethyl acetate (9:1)] while the reported melting points are 178 °C (Müller *et al.*, 1997) and 161–163 °C (Cook & Thomas, 1950), respectively.

2.5.4 Characterisation

8-(3-Phenyl)caffeine (**1a**) was synthesised from 1,3-dimethyl-5,6-diaminouracil (**5a**) and benzoic acid (**10a**) in a yield of 84%: mp 180 °C; ^1H NMR (CDCl_3) δ 3.38 (s, 3H), 3.58 (s, 3H), 4.01 (s, 3H), 7.47–7.50 (m, 3H), 7.63–7.67 (m, 2H); ^{13}C NMR (CDCl_3) δ 27.88, 29.68, 33.80, 108.47, 128.36, 128.83, 129.10, 130.28, 148.21, 151.63, 152.01, 155.50; EIMS m/z 304 (M^+); HRMS calcd. 270.11168, found 270.11163.

8-(3-Chlorophenyl)caffeine (**1b**) was synthesised from 1,3-dimethyl-5,6-diaminouracil (**5a**) and 3-chlorobenzoic acid (**10b**) in a yield of 91%: mp 202 °C; ^1H NMR (CDCl_3) δ 3.39 (s, 3H), 3.58 (s, 3H), 4.04 (s, 3H), 7.43–7.48 (m, 2H), 7.53–7.56 (m, 1H), 7.67–7.69 (m, 1H); ^{13}C NMR (CDCl_3) δ 27.97, 29.72, 33.90, 108.73, 127.07, 129.28, 130.10, 130.42, 135.05, 148.16, 150.40, 151.60, 155.51; EIMS m/z 304 (M^+); HRMS calcd. 304.07270, found 304.07108.

8-(3-Trifluoromethylphenyl)caffeine (1c) was synthesised from 1,3-dimethyl-5,6-diaminouracil (**5a**) and 3-trifluoromethylbenzoic acid (**10c**) in a yield of 33.6%: mp 192 °C; ¹H NMR (CDCl₃) δ 3.39 (s, 3H), 3.59 (s, 3H), 4.05 (s, 3H), 7.61–7.67 (m, 1H), 7.73–7.77 (m, 1H), 7.84–7.88 (m, 1H), 7.95–7.96 (m, 1H); ¹³C NMR (CDCl₃) δ 27.97, 29.74, 33.87, 108.84, 121.74, 126.14 (q), 126.93 (q), 129.32, 129.46, 131.62 (q), 132.26, 148.20, 150.23, 151.59, 155.52; EIMS *m/z* 338 (M⁺); HRMS calcd. 338.09906, found 338.09735.

8-3-Benzylcaffeine (2a) was synthesised from 1,3-dimethyl-5,6-diaminouracil (**5a**) and benzoic acid (**11a**) in a yield of 71%: mp 165 °C; ¹H NMR (CDCl₃) δ 3.35 (s, 3H), 3.56 (s, 3H), 3.77 (s, 3H), 4.12 (s, 2H), 7.12–7.30 (m, 5H); ¹³C NMR (CDCl₃) δ 27.77, 29.68, 31.94, 33.40, 107.80, 127.18, 128.16, 128.90, 135.00, 147.85, 151.59, 152.11, 155.26; EIMS *m/z* 304 (M⁺); HRMS calcd. 284.12733, found 284.12745.

8-(3-Chlorobenzyl)caffeine (2b) was synthesised from 1,3-dimethyl-5,6-diaminouracil (**5a**) and 3-chlorophenylacetic acid (**11b**) in a yield of 42%: mp 132 °C; ¹H NMR (CDCl₃) δ 3.36 (s, 3H), 3.56 (s, 3H), 3.79 (s, 3H), 4.10 (s, 2H), 7.02–7.05 (m, 1H), 7.14–7.16 (m, 1H), 7.21–7.24 (m, 2H); ¹³C NMR (CDCl₃) δ 27.83, 29.74, 31.00, 32.96, 107.85, 126.38, 127.54, 128.35, 130.16, 134.84, 137.00, 147.87, 151.20, 151.59, 155.30; EIMS *m/z* 319 (M⁺); HRMS calcd. 318.08835, found 318.08702.

8-(3-Trifluoromethylbenzyl)caffeine (2c) was synthesised from 1,3-dimethyl-5,6-diaminouracil (**5a**) and 3-(trifluoromethyl)phenylacetic acid (**11c**) in a yield of 49%: mp 163 °C; ¹H NMR (CDCl₃) δ 3.36 (s, 3H), 3.55 (s, 3H), 3.81 (s, 3H), 4.18 (s, 2H), 7.34–7.52 (m, 4H); ¹³C NMR (CDCl₃) δ 27.83, 29.72, 31.00, 33.14, 107.86, 122.00, 124.23 (q), 125.08 (q), 125.61, 129.45, 131.37 (q), 131.62, 136.09, 147.90, 151.60, 155.31; EIMS *m/z* 352 (M⁺); HRMS calcd. 352.11471, found 352.11570.

(E,E)-8-(4-Phenylbutadien-1-yl)caffeine (3a) was synthesised from 1,3-dimethyl-5,6-diaminouracil (**5a**) and (*E,E*)-5-phenyl-2,4-pentadienoic acid (**6a**) in a yield of 27%: mp 253 °C; ¹H NMR (CDCl₃) δ 3.37 (s, 3H), 3.58 (s, 3H), 3.96 (s, 3H), 6.44 (d, 1H, J = 15.0

Hz), 6.84–6.95 (m, 2H), 7.24–7.36 (m, 3H), 7.42–7.46 (m, 2H), 7.56 (dd, 1H, $J = 15.0, 10.0$ Hz); ^{13}C NMR (CDCl_3) δ 27.86, 29.66, 31.35, 107.82, 114.46, 126.90, 127.30, 128.65, 128.77, 136.40, 138.14, 138.50, 148.61, 149.98, 151.64, 155.13; EIMS m/z 322 (M^+); HRMS calcd. 322.14298, found 322.14186.

(*E,E*)-8-[4-(3-Chlorophenyl)butadien-1-yl]caffeine (**3b**) was synthesised from 1,3-dimethyl-5,6-diaminouracil (**5a**) and (*E,E*)-5-(3-chlorophenyl)-2,4-pentadienoic acid (**6b**) in a yield of 10%: mp 249 °C; ^1H NMR (CDCl_3) δ 3.39 (s, 3H), 3.59 (s, 3H), 3.99 (s, 3H), 6.49 (d, 1H, $J = 15.0$ Hz), 6.80 (d, 1H, $J = 15.5$ Hz), 7.24–7.31 (m, 4H), 7.44 (d, 1H, $J = 0.41$ Hz), 7.55 (dd, 1H, $J = 14.7, 10.9$ Hz); ^{13}C NMR (CDCl_3) δ 27.92, 29.71, 31.42, 108.01, 115.47, 125.15, 126.61, 128.48, 128.67, 130.01, 134.85, 136.34, 137.87, 138.32, 148.65, 149.72, 151.68, 155.21; EIMS m/z 357 (M^+); HRMS calcd. 356.10400, found 356.10571.

(*E,E*)-8-[4-(3-Bromophenyl)butadien-1-yl]caffeine (**3c**) was synthesised from 1,3-dimethyl-5,6-diaminouracil (**5a**) and (*E,E*)-5-(3-bromophenyl)-2,4-pentadienoic acid (**6c**) in a yield of 40%: mp 246 °C; ^1H NMR (CDCl_3) δ 3.38 (s, 3H), 3.58 (s, 3H), 3.98 (s, 3H), 6.49 (d, 1H, $J = 15.0$ Hz), 6.78 (d, 1H, $J = 15.5$ Hz), 6.95 (dd, 1H, $J = 15.5, 10.9$ Hz), 7.17–7.22 (m, 1H), 7.33–7.40 (m, 2H), 7.55 (dd, 1H, $J = 14.6, 10.9$ Hz), 7.59 (d, 1H, $J = 1.8$ Hz); ^{13}C NMR (CDCl_3) δ 27.91, 29.70, 31.40, 108.00, 115.50, 123.01, 125.58, 128.70, 129.53, 130.27, 131.38, 136.20, 137.82, 138.60, 148.63, 149.70, 151.67, 155.20; EIMS m/z 400, 402 (M^+); HRMS calcd. 400.05349, found 400.05193.

(*E,E*)-8-[4-(3-Fluorophenyl)butadien-1-yl]caffeine (**3d**) was synthesised from 1,3-dimethyl-5,6-diaminouracil (**5a**) and (*E,E*)-5-(3-fluorophenyl)-2,4-pentadienoic acid (**6d**) in a yield of 22.1%: mp 223 °C; ^1H NMR (CDCl_3) δ 3.22 (s, 3H), 3.44 (s, 3H), 3.95 (s, 3H), 6.87 (d, 1H, $J = 15.0$ Hz), 7.01 (d, 1H, $J = 15.4$ Hz), 7.03–7.15 (m, 1H), 7.26 (dd, 1H, $J = 15.4, 11.0$ Hz), 7.35–7.44 (m, 3H), 7.47 (dd, 1H, $J = 14.6, 11.0$ Hz); EIMS m/z 340 (M^+); HRMS calcd. 340.13355, found 340.13367.

(E,E)-1,3-Dimethyl-8-(4-phenylbutadien-1-yl)-7-ethylxanthine (**3e**) was synthesised from 1,3-dimethyl-5,6-diaminouracil (**5a**), (*E,E*)-5-phenyl-2,4-pentadienoic acid (**6a**) and iodoethane in a yield of 6.9%: mp 227 °C; ¹H NMR (CDCl₃) δ 1.46 (t, 3H, J = 7.2 Hz), 3.43 (s, 3H), 3.63 (s, 3H), 4.45 (q, 1H, J = 7.2 Hz), 6.50 (d, 1H, J = 14.9 Hz), 6.92 (d, 1H, J = 15.5 Hz), 7.01 (dd, 1H, J = 15.5, 11.0 Hz), 7.31 (t, 1H, J = 7.3 Hz), 7.38 (t, 2H, J = 7.4 Hz), 7.49 (d, 2H, J = 7.4 Hz), 7.63 (dd, 1H, J = 14.9, 10.9 Hz); ¹³C NMR (CDCl₃) δ 16.65, 28.12, 29.93, 40.18, 107.76, 115.16, 127.73, 128.16, 129.48, 129.63, 137.30, 139.00, 139.40, 149.78, 150.10, 152.69, 155.77; EIMS *m/z* 336 (M⁺); HRMS calcd. 336.15863, found 336.15872.

(E,E)-1,3-Diethyl-8-(4-phenylbutadien-1-yl)-7-methylxanthine (**3f**) was synthesised from 1,3-diethyl-5,6-diaminouracil (**5b**), (*E,E*)-5-phenyl-2,4-pentadienoic acid (**6a**) and iodomethane in a yield of 24%: mp 156–157 °C; ¹H NMR (CDCl₃) δ 1.19 (t, 3H, J = 7.1 Hz), 1.30 (t, 3H, J = 7.0 Hz), 3.93 (s, 3H), 4.01 (q, 2H, J = 6.9 Hz), 4.13 (q, 2H, J = 7.0 Hz), 6.41 (d, 1H, J = 15.0 Hz), 6.84 (d, 1H, J = 15.5 Hz), 6.92 (dd, 1H, J = 15.5, 11.2 Hz), 7.23 (m, 1H), 7.30 (t, 2H, J = 7.4 Hz), 7.40 (d, 2H, J = 7.8 Hz), 7.53 (dd, 1H, J = 14.9, 10.9 Hz); ¹³C NMR (CDCl₃) δ 13.49, 29.90, 31.57, 36.60, 38.68, 108.76, 115.30, 127.73, 128.20, 129.48, 129.64, 137.33, 138.93, 139.38, 149.10, 150.90, 151.70, 156.00; EIMS *m/z* 350 (M⁺); HRMS calcd. 350.17428, found 350.17277.

(E,E)-1,3-Diethyl-8-(4-phenylbutadien-1-yl)-7-ethylxanthine (**3g**) was synthesised from 1,3-diethyl-5,6-diaminouracil (**5b**), (*E,E*)-5-phenyl-2,4-pentadienoic acid (**6a**) and iodoethane in a yield of 21%: mp 177–178 °C; ¹H NMR (CDCl₃) δ 1.19 (t, 3H, J = 7.1 Hz), 1.31 (t, 3H, J = 7.0 Hz), 1.38 (t, 3H, J = 7.2 Hz), 4.01 (q, 2H, J = 7.0 Hz), 4.13 (q, 2H, J = 7.0 Hz), 4.36 (q, 2H, J = 7.2 Hz), 6.41 (d, 1H, J = 14.9 Hz), 6.84 (d, 1H, J = 15.5 Hz), 6.93 (dd, 1H, J = 15.5, 11.0 Hz), 7.22 (m, 1H), 7.29 (t, 2H, J = 7.6 Hz), 7.41 (d, 2H, J = 8.0 Hz), 7.55 (dd, 1H, J = 14.9, 11.0 Hz); ¹³C NMR (CDCl₃) δ 13.47, 16.68, 29.89, 36.62, 38.64, 40.10, 108.00, 115.38, 127.70, 128.26, 129.43, 129.63, 137.37, 138.73, 139.23, 149.33, 149.98, 151.74, 155.57; EIMS *m/z* 364 (M⁺); HRMS calcd. 364.18993, found 364.18904.

2.6 Concluding remarks

Thirteen 8-substituted caffeine derivatives were synthesised successfully. Following recrystallisation from a suitable solvent the structures of the compounds were verified by mass spectrometry, $^1\text{H-NMR}$ and $^{13}\text{C-NMR}$. The *trans-trans* geometry for compounds (**3a-g**) was confirmed by proton-proton coupling constants in the range of 15.0-15.5 Hz for the olefinic proton signals. The $^1\text{H-NMR}$ and $^{13}\text{C-NMR}$ spectra for compounds **1a-c**, **2a-c** and **3a-g** are presented in Appendix A.

Chapter Three

Parkinson's Disease and MAO-B Enzymology

3.1 Introduction

In 1817 James Parkinson described the clinical characteristics of the age-related neurodegenerative disease, which is familiarly known today as Parkinson's disease (PD). The fundamental pathological trait of Parkinson's disease was established to be the loss of neurons in the substantia nigra pars compacta (SNpc), after which research has accelerated dramatically when Arvid Carlsson discovered dopamine (DA) in the mammalian brain in 1958. Shortly after this discovery it was found that SNpc neurons form part of the nigrostriatal dopaminergic pathway, where two conclusions were reached (Przedborski & Dauer, 2003):

- Loss of SNpc neurons leads to striatal DA deficiency, which is responsible for the major symptoms of Parkinson's disease.
- Replenishment of striatal DA through the oral administration of the DA precursor levodopa (L-3,4-dihydroxyphenylalanine), alleviates most of these symptoms. (Przedborski & Dauer, 2003).

The discovery of levodopa transformed the treatment of PD. It was soon established that after several years of treatment most patients develop involuntary movements also known as "dyskinesias" which are hard to control and impair the quality of life dramatically. Recent research is aimed at prevention of dopaminergic neuron degeneration. Unfortunately, all current treatments are symptomatic and none will stop the progress of, or delay dopaminergic neuron degeneration (Chalmers-Redman & Tatton, 1996).

3.2 Clinical presentation and disease cause

Parkinson's disease is a progressive disease with a mean age of onset at 55, and the incidence increases markedly with age, from 20/100 000 overall to 120/100 000 at age 70. In about 95% of the PD cases, there is no apparent genetic linkage, however in the remaining cases, the disease is inherited. As time passes, symptoms worsen. Most PD patients suffer substantial motor disability after 5-10 years of disease; even with proper medical treatment (Table 3.1). Clinically, any disease that includes striatal DA deficiency or direct striatal damage may lead to "parkinsonism", a syndrome characterised by a tremor at rest, rigidity, slowness or absence of voluntary movement, postural instability, and freezing. PD is the most common cause of parkinsonism, accounting for approximately 80% of cases. (Hely *et al.*, 1989; Morgante *et al.*, 2000; Levy *et al.*, 2002; Przedborski & Dauer, 2003).

PD tremor occurs at rest but decreases with voluntary movement, so it typically does not impair activities of daily living. Some of the clinical manifestations of PD are given in Table 3.1.

Table 3.1 Clinical manifestations of Parkinson's disease

PD deficiency	Symptom description
Rigidity	Increased resistance to passive movement of patient's limbs (stiffness)
Bradykinesia	Slowness of movement
Hypokinesia	Reduction in movement amplitude
Akinesia <ul style="list-style-type: none"> • Hypomimia • Hypophonia • Drooling • Micrographia 	Absence of normal unconscious movements, <i>e.g.</i> arm swing in walking. <ul style="list-style-type: none"> • Paucity of normal facial expression. • Decreased voice volume • Failure to swallow • Decreased size, speed of handwriting, and decreased stride length during walking.
Freezing	Inability to begin a voluntary movement such as walking
Bradyphrenia	Cognitive processes are slowed

Bradykinesia may significantly impair the quality of life because it takes much longer to perform everyday tasks such as dressing or eating. PD patients also typically develop a stooped posture and may lose normal postural reflexes, leading to falls and, even confinement to a wheelchair. Depression is common, and dementia is significantly more frequent in PD, especially in older patients (Adapted from Przedborski & Dauer, 2003).

3.3 Oxidative stress and modelling of PD in animals

3.3.1 Oxidative stress

Oxidative stress can broadly be defined as a condition in which there is an elevated concentration of reactive oxygen species (Bauman *et al.*, 1991). There are two fundamental ways to produce oxidative stress:

- (1) Increase the production of reactive oxygen species.
- (2) Induce oxidative stress by decreasing the defence systems involved in protection against reactive oxygen species.

Causes of oxidative stress have been associated with several clinical conditions. Reactive oxygen species (ROS) are continually produced in tissues by the action of the mitochondrial electron transport system and of reduced nicotinamide adenine dinucleotide phosphate (NADH) oxidase (Wakeyama *et al.*, 1982; Cadenas & Davies, 2000).

Oxidative stress refers to cytological consequences of a variance between the production of free radicals or ROS (generated by mitochondria and produced as by-products of normal oxidative metabolism) and the ability and capacity of the cell to defend against these hazardous chemical species (Robinson, 1998). The oxygen molecule accepts an additional electron to generate superoxide, a more reactive form of oxygen, probably produced by a non-enzymatic mechanism in the mitochondria (Raha & Robinson, 2001).

Oxidative stress transpires as the production of ROS increases, when scavenging of free radicals or repair of oxidatively modified macromolecules decreases, or both, (Zhou *et al.*, 2003). ROS could damage proteins, lipids, nucleic acids, and other biological macromolecules that result in the impairment of the function of various organs (Zhou *et al.*, 2003).

A genetic defect may lead to altered oxidative metabolism which is induced by defective synthesis of the nuclear or mtDNA encoded subunits of the enzymatic complexes of the respiratory chain (Chance *et al.* 1979; Wallace, 1999). Ubisemiquinone generated in the course of the electron transport reaction in the respiratory chain donates electrons to oxygen and provides a constant source of superoxide. It has been estimated that the fate of 1-2% of all electrons passing down the electron transport chain is to be diverted into the formation of superoxide radicals. Superoxide can attack iron sulphur centres in enzymes such as aconitase, succinate dehydrogenase, and mitochondrial NADH:ubiquinone oxidoreductase, releasing iron and destroying catalytic function. Superoxide is therefore rapidly removed by conversion to hydrogen peroxide (H_2O_2) in a reaction catalysed by superoxide dismutase. Three superoxide dismutases exist in mammalian systems: cytosolic CuZn superoxide dismutase (CuZnSOD), intramitochondrial superoxide dismutase (MnSOD) and extracellular CuZn superoxide dismutase (Robinson, 1998; Raha & Robinson, 2001; Wallace, 1999).

Hydrogen peroxide can, in the presence of cupric or ferric ions (Cu^+ or Fe^{2+}), produce the highly reactive hydroxyl radical, which can cause damage to proteins, lipids and DNA as illustrated in Figure 3.1. The formation of H_2O_2 by either MnSOD or CuZnSOD can be processed by glutathione peroxidase (GPX) to water. Molecular oxygen is a vital element of life, yet limited reduction of oxygen to water during normal aerobic metabolism generates ROS which pose a serious threat to all aerobic organisms (Dalton *et al.*, 1999).

Complex I and complex III are the respiratory chain complexes responsible for the generation of superoxide in the mitochondria (Raha and Robinson, 2001; Wallace, 1999).

Reduced complex I activity has been found in platelets from PD patients (Parker *et al.*, 1989). Mitochondria-related energy failure may disrupt vesicular storage of DA, causing the free cytosolic concentration of DA to rise and allowing harmful DA-mediated reactions to damage cellular macromolecules. DA may be crucial in rendering SNpc dopaminergic neurons susceptible to oxidative attack.

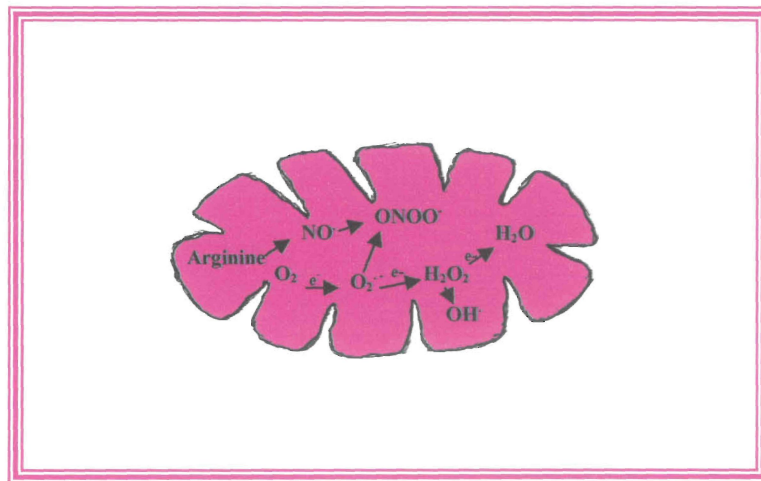


Figure 3.1. Representation of the production of ROS from molecular oxygen. Superoxide anion is converted to hydrogen peroxide by SOD. Hydrogen peroxide, if not broken down to water, can be converted to hydroxyl radicals that cause damage to lipids, membranes and ultimately to DNA. (With permission of the Mitochondrial Research Laboratory, North West University).

3.3.2 Toxin-induced models of PD

Environmental toxins (Table 3.2) are responsible for the production of oxidative stress and cause multiple diseases such as the neurodegenerative PD. Pathologic and genetic animal models of PD are summarised with a specific focus on the MPTP toxin-induced model, as this model is best characterised to date. There is a striking similarity between PD and individuals intoxicated with MPTP. Only non-human primates accurately mimic the motor symptoms of PD and has proven to be the only suitable model for such investigations.

Table 3.2. Toxin based models

Toxin	Characteristic traits
6-Hydroxydopamine (6-OHDA)	<ul style="list-style-type: none"> • Selective for monoaminergic neurons • Cannot cross the blood brain barrier
Paraquat	<ul style="list-style-type: none"> • Structural similarity to MPP⁺ • Does not easily penetrate the blood brain barrier
Rotenone	<ul style="list-style-type: none"> • Potent member of rotenoids • Highly lipophilic • Crosses biological membranes easily • Independent of transporters • Causes complex I inhibition • Exerts a diffuse neurotoxicity
MPTP (1-methyl-4-phenyl-1,2,3,6 tetrahydropyridine)	<ul style="list-style-type: none"> • Produces an irreversible and severe parkinsonian syndrome characterized by all the features of PD • Highly lipophilic • Crosses the blood brain barrier within minutes • Damages dopaminergic pathway • Selective for dopaminergic neurons • Depend on dopamine transporters to gain access to the neurons • Causes cell loss in the SNpc

(Luthman et al., 1989; Sirinathsinghji et al., 1992; Talpade et al., 2000; Shimizu et al., 2001; Greenamyre, 2003)

3.4 Enzymology

3.4.1 Monoamine oxidase-B (MAO-B)

Monoamine oxidases (MAOs) are flavine adenine dinucleotide (FAD) dependant enzymes bound to the mitochondrial outer membrane, and are responsible for the metabolism of neurotransmitters such as dopamine, serotonin, adrenaline and noradrenaline. MAO also plays a role in the inactivation of exogenous arylalkyl amines

(Shih, *et al.*, 1999). Thus, MAO-A and MAO-B catalyse the oxidation of primary, secondary, and a number of tertiary amines to their corresponding protonated imines with concomitant reduction of oxygen to hydrogen peroxide. Both MAO-A and MAO-B enzymes received attention in pharmacological research due to the reversible and irreversible inhibitors of both enzymes that have been utilised clinically in the treatment of age related neurological disorders. These two enzymes have distinct and overlapping qualities and share ~70% sequence identity (Shih, *et al.*, 1999). MAO-A mainly deaminates serotonin, norepinephrine, and epinephrine (Waldmeier, 1987), is irreversibly inhibited by low concentrations of chlorgyline and exists in catecholaminergic neurons. MAO-B (EC 1.4.3.4), which is found in serotonergic neurons and glial cells, mainly deaminates β -phenylethylamine and benzylamine and is irreversibly inhibited by (*R*)-deprenyl, (Figure 3.2) (Grimsby *et al.*, 1990). MAO-A and MAO-B are encoded by different nuclear genes located on the X chromosome (Xp11.23), and consist of 15 exons with identical intron-exon organisation, suggesting that these enzymes are derived from a common ancestral gene (Nagatsu, 2004).

Monoamine oxidases are involved in various physiological and pathological processes making these enzymes important targets in the development of new drugs. Interest is directed at the particular involvement of MAO-B in Parkinson's disease and the role inhibitors of this enzyme have as a treatment strategy (Calne, 1993; Jankovik, 2000). Since MAO-B metabolises dopamine, inhibition of this enzyme in the brain may help conserve the depleted supply of dopamine and delay the need for levodopa in patients diagnosed with early PD. In patients with advanced PD, who experience levodopa response fluctuations, MAO-B inhibition may potentiate and prolong its effects and permit a lower levodopa dose (Rabey *et al.*, 2000). Inhibitors that have been demonstrated to be of clinical value include irreversible inhibitors such as (*R*)-deprenyl (The Parkinson Study Group, 1989) and rasagiline (Rabey *et al.*, 2000) as well as reversible inhibitors such as lazabemide (The Parkinson Study Group, 1996) and safinamide (Chazot, 2001) (Figure 3.2).

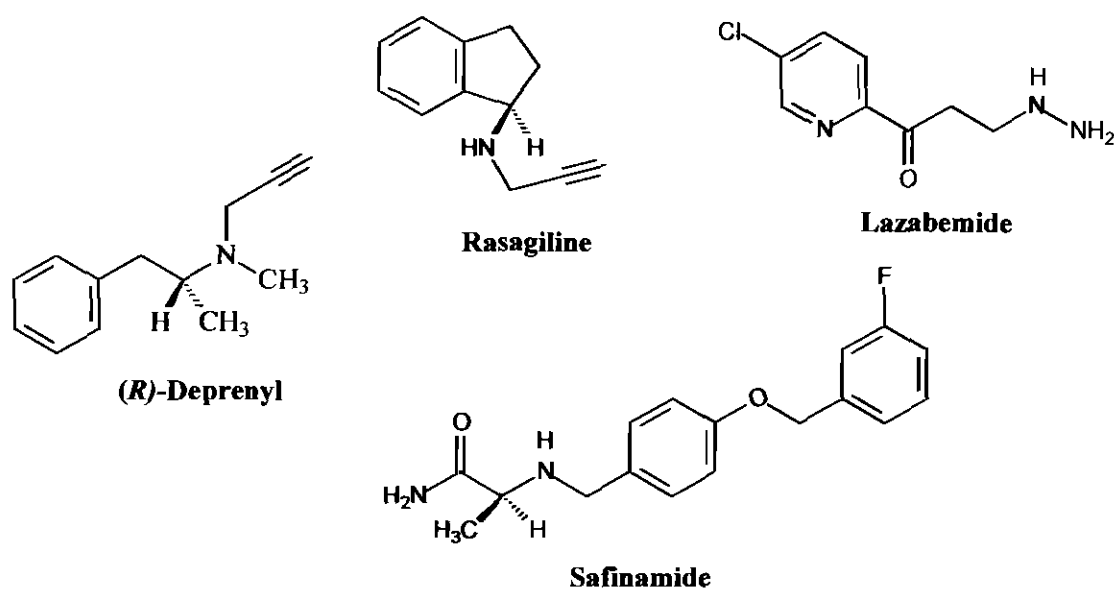


Figure 3.2. Structures of MAO-B inhibitors, (*R*)-deprenyl, rasagiline, lazabemide and safinamide.

3.5 The role of MAO-B in Parkinson's disease

MAO plays a major role in metabolising dopamine. Inhibition of the isoenzyme B blocks the metabolism of dopamine, subsequently enhancing the endogenous dopamine level and also dopamine produced from exogenously administered precursor levodopa (L-DOPA) (Foley, *et al.*, 2000; Yamada & Yasuhara, 2004). Inhibition of dopamine degradation by MAO-B inhibitors combined with the supplementation of dopamine by L-DOPA have been shown to be successful in the treatment of Parkinson's patients (Palhagen, *et al.*, 2006).

To date MAO-B has been recognised as the principle enzyme responsible for the metabolic activation of the proneurotoxin, 1-methyl-4-phenyl-1,2,3,6-tetrahydropyridine (MPTP), in the brains of humans and mammals (Chiba *et al.*, 1984). MPTP selectively damages nigrostriatal neurons which inherently induce a parkinsonian syndrome in mammals, and humans (Heikkila *et al.*, 1984). Monoamine oxidases catalyse the

α -carbon oxidation of amines to imines and iminiums with a simultaneous reduction of the covalently bound FAD cofactor. The enzyme is regenerated by reoxidation of the reduced FAD with simultaneous reduction of molecular oxygen to hydrogen peroxide.

MAO-B catalyses the α -carbon oxidation of the parent tetrahydropyridinyl protoxin to the corresponding dihydropyridinium intermediate, MPDP⁺, that undergoes a second 2-electron oxidation to yield MPP⁺ as indicated in Figure 3.3. Competitive inhibitors and mechanism based inactivators of MAO-B protect experimental animals against the neurotoxic effects of MPTP (Chiba *et al.*, 1985; Castagnoli, *et al.*, 1999; Castagnoli, *et al.*, 2001; Heikkila, *et al.*, 1984).

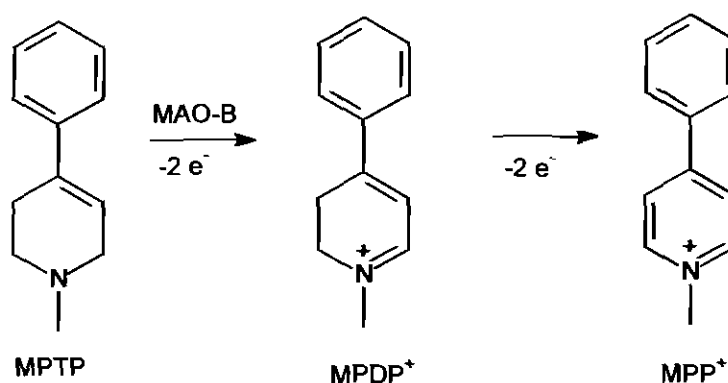


Figure 3.3. The oxidation of MPTP by MAO-B.

3.6 MMTP as a substrate

The K_i value for competitive inhibition of MAO-B may be calculated by means of measuring the extent to which various concentrations of the inhibitory compounds decreases the rate of α -carbon oxidation of MMTP (13) to the corresponding dihydropyridinium metabolite, the 1-methyl-4-(1-methylpyrrol-2-yl)-2,3-dihydropyridinium, MMDP⁺ (14) (Nimkar *et al.*, 1996). MMDP⁺ concentration is measured spectropotometrically at 420 nm, a wavelength that is apart from the chromophores of both substrate and inhibitors investigated (Petzer *et al.*, 2003). The

chemical stability of MMDP^+ (14) obviates the need to monitor the formation of the 1-methyl-4-(1-methylpyrrol-2-yl)pyridinium species MMP^+ (15).

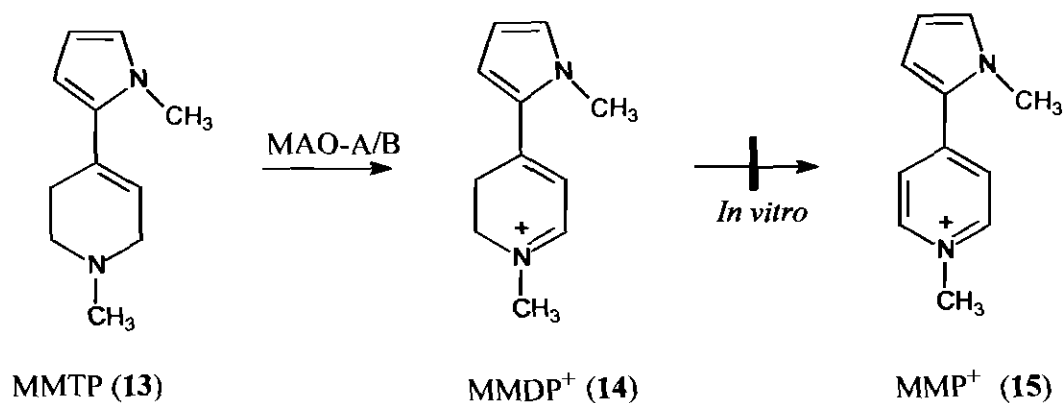


Figure 3.4. The MAO catalysed oxidation of MMTP (13) to the corresponding dihydropyridinium species (14) Further oxidation of MMDP^+ to pyridinium species MMP^+ (15) is not observed (Petzer et al., 2003).

3.7 Experimental objectives and procedures

3.7.1 Molecular Docking

Molecular docking consists of a procedure where one molecule is fitted onto another molecule. This procedure may consist of coupling two types of molecules or fitting a ligand into the active cavity of another molecule or protein. Many types of interactions occur between a ligand and a macromolecule. Interactions between atoms or subunits within the molecule such as dispersion interaction, hydrogen bonding, hydrophobic interactions, electrostatic interactions, ionic bonding, ion-dipole interactions, dipole-dipole interactions, ion induced dipole interactions, charge transfer and covalent bonding may occur. The Molecular docking software programme that had been used during this study was the ligand fit module of Discovery Studio[®] suite of programs.

MAO-B is dimeric, and each monomer consists of a globular domain anchored to the membrane by the C-terminal helix (Binda *et al.*, 2002). MAO-B contains two cavities in

the enzyme. A small entrance cavity situated with an opening to the exterior of the enzyme which is connected to the substrate cavity. Isoleucine 199 (Ile 199) serves as a “gate” between these two cavities. Rotation of the side chains allows for either fusion or separation of the two cavities. Tyr 435, FAD and Tyr 398 form an aromatic cage wherein the ligands bind. The substrate cavity is further surrounded by Tyr 326, Phe 343, Leu 171, Ile 199, Cys 172 and Ile 198 (Binda *et al.*, 2003) (Figure 3.5).

By utilising a molecular modeling program it is possible to establish possible sites for ligand binding. For these studies we used the MAO-B crystal structure (PDB:2BK3). 2BK3 is a PDB file that contains the coordinates for the MAO-B enzyme co-crystallised with the inhibitor farnesol. FAD (magenta) is bound to MAO-B via a single covalent bond at Cys 397. FAD is situated in a hydrophobic surrounding within MAO-B with specific interactions dominated by hydrogen bonding to either side chains or the peptide backbone of the protein. A large part of the substrate cavity is hydrophobic, which allows for the tight binding of apolar substrates and inhibitors. Diagrammatic presentations of, 8-benzylcaffeine, 8-phenylcaffeine, and (*E,E*)-8-(4-phenylbutadien-1-yl)caffeine analogues docked in the enzyme are displayed Figures 3.5a-d. These inhibitors all form hydrogen bonds with Tyr 435. This and further hydrogen bonding to the xanthinyl moiety and the conformation of the side chain was found to be favourable for the interaction with the MAO-B enzyme. Molecular docking score results for these compounds are shown in Tables 3.3-3.5.

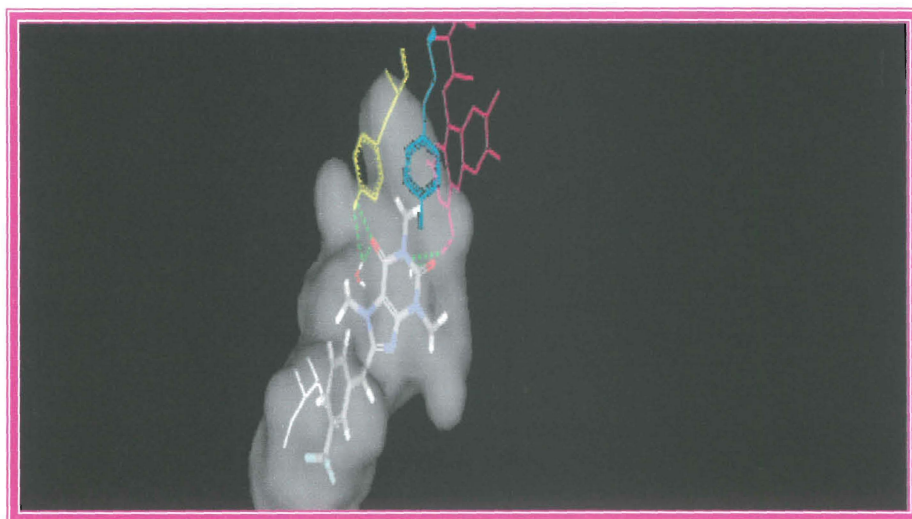


Figure 3.5 a. 8-(3-Trifluoromethylbenzyl)caffeine analogue. Nitrogens are shown in blue and oxygens in red. Tyr 398 forms part of the cage = cyan. Tyr 435 forms part of the cage = yellow. Ile 199 forms part of the gate = white. Hydrogen bonds are indicated in green dashed lines.

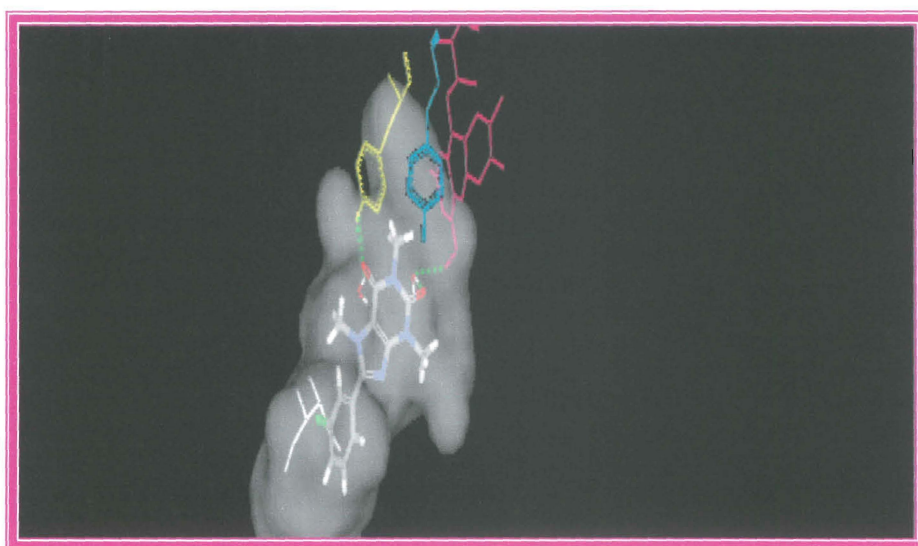


Figure 3.5 b. 8-(3-Chlorophenyl)caffeine analogue. Nitrogens are shown in blue and oxygens in red. Tyr 398 forms part of the cage = cyan. Tyr 435 forms part of the cage = yellow. Ile 199 forms part of the gate = white. Hydrogen bonds are indicated in green dashed lines.

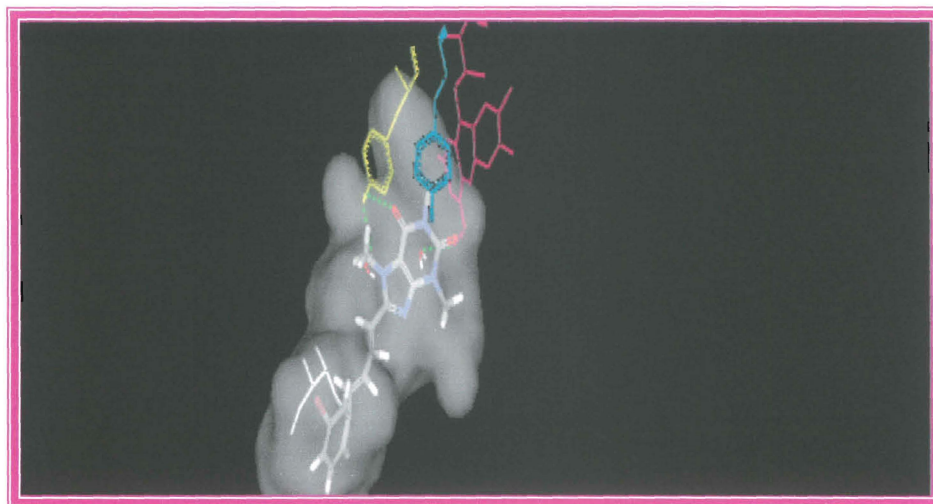


Figure 3.5 c. *(E,E)*-8-[4-(3-Bromophenylbutadien-1-yl)]caffeine analogue. Nitrogens are blue and oxygens in red. Tyr 398 forms part of the cage = cyan. Tyr 435 forms part of the cage = yellow. Ile 199 forms part of the gate = white. Hydrogen bonds are indicated in green dashed lines.

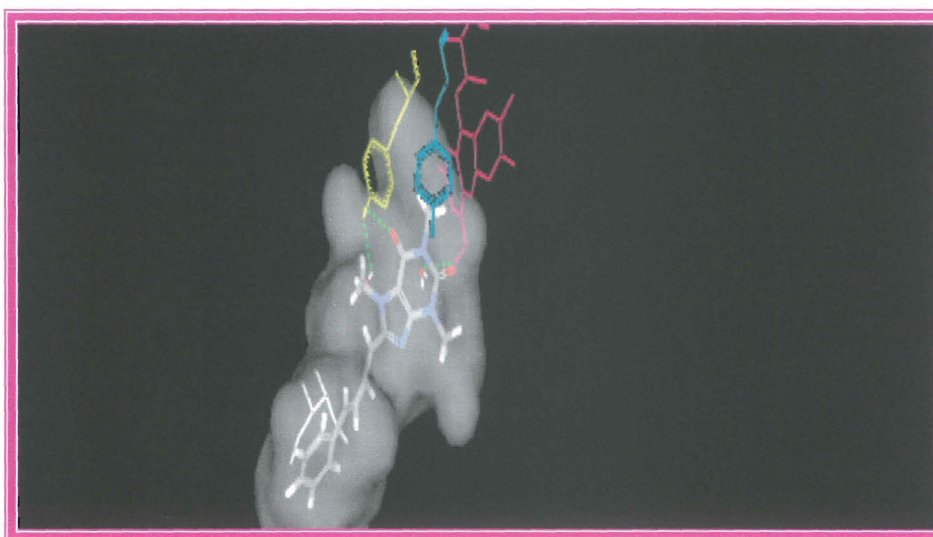


Figure 3.5 d. *(E,E)*-8-(4-Phenylbutadien-1-yl)caffeine analogue. Nitrogens are shown in blue and oxygens in red. Tyr 398 forms part of the cage = cyan. Tyr 435 forms part of the cage = yellow. Ile 199 forms part of the gate = white. Hydrogen bonds are indicated in green dashed lines.

Comparing the inhibitor activity and the individual docking scores for the inhibitors, reasonable good correlations were obtained (Tables 3.3-3.5). For the 8-phenylcaffeine analogues, the lowest scoring congener (**1c**) also proved to be the weakest MAO-B

inhibitor. Similarly, for the 8-benzylcaffeine analogues, the lowest scoring congener (**2a**) also indicated to have the weakest MAO-B inhibitor activity. For the (*E,E*)-8-(4-phenylbutadien-1-yl)caffeine analogues, the three weakest inhibitors (**3e-g**) also indicated the weakest inhibition potencies. Therefore, a good indication of binding within the cavity can be obtained with this method, and weak inhibitors can be separated from potent inhibitors within a series of compounds.

3.7.2 Enzyme kinetics: K_m determination

If the concentration of an enzyme substrate [S] is increased while all other conditions are kept constant, the initial velocity (V_i , the velocity when very little substrate has been consumed) of an enzymatic reaction increases to a maximum value, V_{max} . At this point the enzyme is saturated with substrate and V_i is unaffected by further increases in substrate concentration. The substrate concentration [S] that produces half-maximal velocity ($V_{max}/2$), termed the K_m value or Michaelis constant, is determined experimentally by graphing V_i vs. [S] (Figure 3.6). The K_m value may approximate, with certain assumptions, a binding constant (K_d) for the enzyme-substrate complex. Since the affinity of an enzyme for its substrate is equal to the inverse of K_d , a numerically small K_m indicates a high affinity of the substrate for the enzyme. The behaviour of many enzymes under the influence of varied substrate concentrations is described by the Michaelis-Menten equation (Equation 3.1).

Equation 3.1. Michaelis-Menten

$$V_i = \frac{V_{max} \times [S]}{K_m + [S]}$$

The Michaelis-Menten equation describes the behaviour of an enzyme under the influence of varied substrate concentrations.

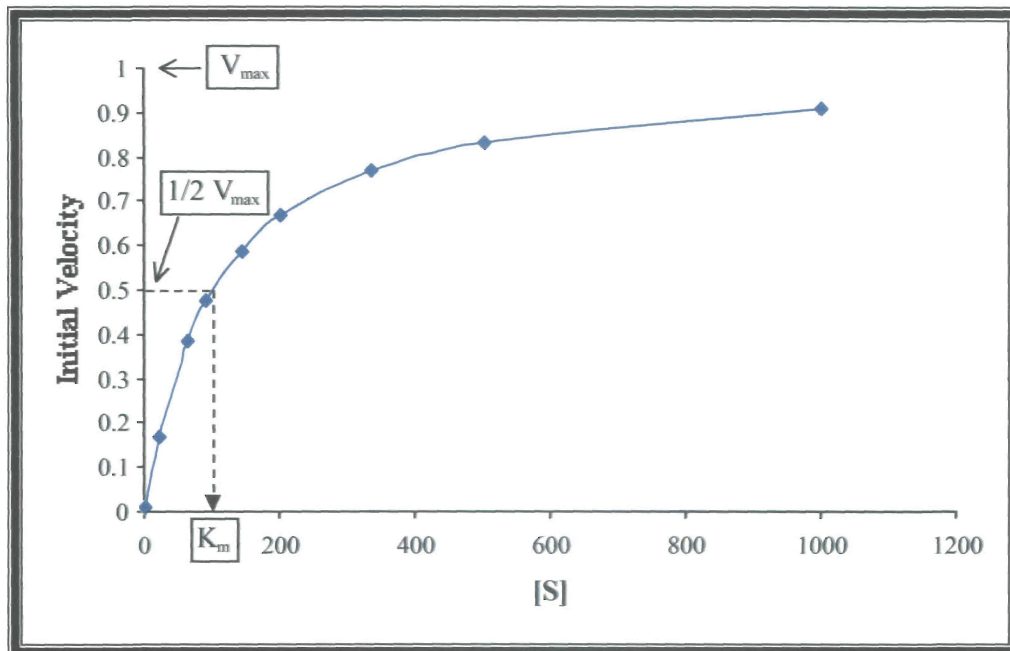


Figure 3.6. Graphical representation of the Michaelis-Menten equation (V_i versus $[S]$).

Many enzymes give saturation curves that do not readily permit accurate measurement of V_{\max} (and therefore K_m) when V_i is plotted vs $[S]$. By inversion of the Michaelis-Menten equation (Equation 4.2) and graphing the inverse of the initial velocity ($1/V_i$) as a function of the inverse of substrate concentration ($1/[S]$), a straight line is obtained. This plot is called a double reciprocal plot or Lineweaver-Burke plot (Figure 3.7). The K_m and V_{\max} values can be easily obtained from this plot since the y-axis intercept is equal to $1/V_{\max}$ and the slope is K_m/V_{\max} . The x-axis intercept is equal to $-1/K_m$ (Segel, 1993).

Equation 3.2. Lineweaver-Burke

$$\frac{1}{V_i} = \left(\frac{K_m}{V_{\max}} \right) \times \left(\frac{1}{[S]} \right) + \frac{1}{V_{\max}}$$

Inversion of the Michaelis-Menten equation describes the double reciprocal plot or Lineweaver-Burke plot.

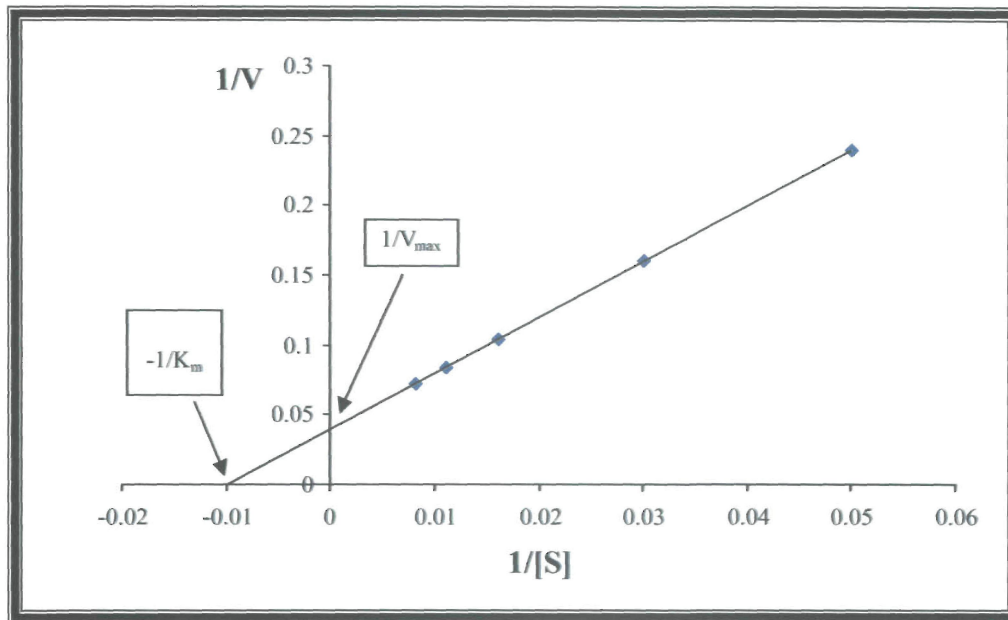


Figure 3.7. An example of the Lineweaver-Burke plot ($1/V_i$ versus $1/[S]$).

When $[S]$ is approximately equal to K_m , V_i is very responsive to changes in substrate concentrations and the presence of inhibitors. Therefore, when examining the effects inhibitors on MAO-B catalytic rate, substrate concentrations that bracket the reported apparent K_m value are used.

3.7.3 K_i and IC_{50} determination

The affinity of an inhibitor for the active site of an enzyme is described by the K_i value of a competitive inhibitor. For a series of competitive inhibitors, those with lowest K_i values will cause the greatest degree of inhibition at a fixed concentration of inhibitor $[I]$. The dissociation constant for the reaction between the enzyme $[E]$ and inhibitor $[I]$ is K_i , where;

Equation 3.3. K_i determination

$$K_i = \frac{[E][I]}{[EI]}$$

In the present study we have, for selected inhibitors, experimentally obtained K_i values as well as IC_{50} values (concentration of inhibitor producing 50% inhibition) for reversible interaction with MAO-B. The relationship between K_i and IC_{50} of a competitive inhibitor of a monosubstrate reaction is described by the Cheng-Prusoff equation: $K_i = IC_{50}/(1 + [S]/K_m)$ (Cheng & Prusoff, 1973).

We are therefore able to comment on the validity of using this equation to convert experimentally determined IC_{50} values to K_i values for the competitive inhibition of MAO-B (Morón *et al.*, 2000).

3.7.4 MAO-B inhibition studies

During this study, we investigated the theory that the synthetic C-8 substituted caffeine analogues (**1a-c**, **2a-c** and **3a-g**) may act as inhibitors of MAO-B. Enzyme activity measurements were based on the MAO-B catalysed oxidation of 1-methyl-4-(1-methylpyrrol-2-yl)-1,2,3,6-tetrahydropyridine (MMTP) to the corresponding dihydropyridinium metabolite (MMDP⁺) (Inoue *et al.*, 1999). MMDP⁺ conveniently absorbs light maximally at a wavelength of 420 nm, making it possible to measure the rate of MMDP⁺ production spectrophotometrically. Neither the substrate nor the test inhibitors absorb light at this wavelength and therefore do not interfere with the accuracy of the MMDP⁺ concentration measurements. As enzyme source we have employed the mitochondrial fraction obtained from baboon liver tissue. Even though MMTP is a MAO-A/B mixed substrate, its oxidation by baboon liver mitochondria can be exclusively attributed to the action of the MAO-B isoform, since baboon liver tissue exhibits a high degree of MAO-B catalytic activity while MAO-A activity is negligible (Inoue *et al.*, 1999). Also, the interaction of reversible inhibitors with MAO-B obtained from baboon liver tissue appears to be similar to the interaction with the human form of the enzyme since inhibitors such as CSC are approximately equipotent with both enzyme sources (Vlok *et al.*, 2006). For the purpose of this study we have chosen the incubation time of the enzyme catalysed reaction to be 10 minutes since the MMTP oxidation was found to

be linear (Figure. 3.7) for at least 10 minutes at all substrate concentrations used in the inhibition studies (30–120 μM). Also, from Lineweaver-Burke plots in the absence of inhibitor, we have estimated the K_m value for the oxidation of MMTP by baboon liver MAO-B to be 68.3 μM , which is slightly lower than the reported value of 60.8 μM (Inoue *et al.*, 1999). This K_m was used in the studies where K_i values for the inhibition of MAO-B were calculated from the corresponding IC_{50} values (see below).

The mitochondrial fraction of baboon liver tissue was isolated as described previously (Salach & Weyler, 1987) and stored at $-70\text{ }^\circ\text{C}$. Following addition of an equal volume of sodium phosphate buffer (100 mM, pH 7.4) containing glycerol (50%, w/v) to the mitochondrial isolate, the protein concentration was determined by the method of Bradford using bovine serum albumin as reference standard (Bradford, 1976). MMTP ($K_m = 68.3\text{ }\mu\text{M}$ for baboon liver MAO-B) (Inoue *et al.*, 1999), served as substrate for the inhibition studies. The enzymatic reactions were prepared in sodium phosphate buffer (100 mM, pH 7.4) and contained MMTP (30–120 μM), the mitochondrial isolate (0.15 mg protein/ml) and various concentrations of the test inhibitors. The final incubation volume was 500 μl . For the IC_{50} determinations, a fixed substrate concentration of 50 μM was used and the inhibitor concentrations spanned at least three orders of a magnitude (3–1000 μM). The stock solutions of the inhibitors were prepared in DMSO and were added to the incubation mixtures to yield a final DMSO concentration of 4% (v/v). DMSO concentrations higher than 4% are reported to inhibit MAO-B (Gnerre *et al.*, 2000). The reactions were incubated at $37\text{ }^\circ\text{C}$ for 10 min and then terminated by the addition of 10 μl perchloric acid (70%). The MAO-B catalysed production of MMDP^+ was found to be linear for the first 10 minutes of incubation under these conditions. The samples were centrifuged at $16,000 \times g$ for 10 minutes, and the concentrations of the MAO-B generated product, MMDP^+ , were measured spectrophotometrically at 420 nm ($\epsilon = 25,000\text{ M}^{-1}$) in the supernatant fractions (Inoue *et al.*, 1999). For the K_i determinations, the initial rates of oxidation at four different substrate concentrations (30–120 μM) in the absence and presence of three different concentrations of the inhibitors were used to construct Lineweaver-Burke plots. The slopes of the Lineweaver-Burke plots were plotted *versus* the inhibitor concentration and the K_i values were determined from the abscissa intercept

(intercept = $-K_i$). Linear regression analysis was performed using the SigmaPlot software package (Systat Software Inc.). Each K_i value reported here is representative of a single determination where the correlation coefficient (R^2 value) of the replot of the slopes *versus* the inhibitor concentrations was at least 0.98. The IC_{50} values were determined by plotting the initial rates of oxidation versus the logarithm of the inhibitor concentrations to obtain a sigmoidal dose-response curve. This kinetic data were fitted to the one site competition model incorporated into the Prism software package (GraphPad Software Inc.). The IC_{50} values were determined in duplicate and are expressed as mean \pm standard error of the mean (S.E.M).

3.8 Results and discussion

For the purpose of this study we have chosen the incubation time of the enzyme catalysed reaction to be 10 minutes since the MMTP oxidation was found to be linear (Figure 3.8) for at least 10 minutes at all substrate concentrations used in the inhibition studies (30–120 μ M). Also, from Lineweaver–Burke plots in the absence of inhibitor, we have estimated the K_m value for the oxidation of MMTP by baboon liver MAO-B to be 68.3 ± 1.60 μ M which is slightly higher than the reported value of 60.8 μ M (Inoue *et al.*, 1999). This K_m was used in the studies where K_i values for the inhibition of MAO-B were calculated from the corresponding IC_{50} values

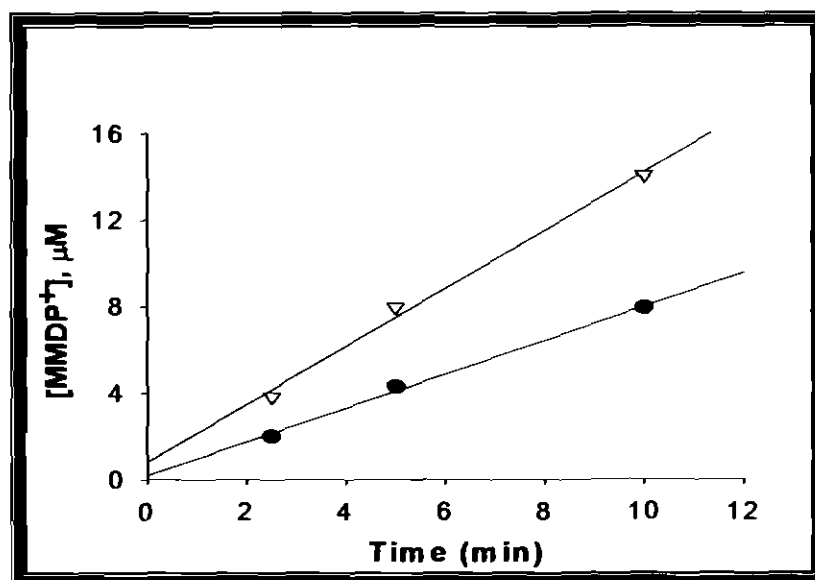


Figure 3.8. Linearity in the oxidation of MMTP by baboon liver MAO-B (0.15 mg protein/ml of the mitochondrial preparation). The concentration of MMDP⁺ produced was measured spectrophotometrically following termination of the enzyme catalyzed reaction at time points of 2.5, 5 and 10 minutes. The concentrations of MMTP used in this study were 30 μM (filled circles) and 120 μM (open triangles).

All of the C-8 substituted caffeine analogues tested were found to be inhibitors of MAO-B. As demonstrated for example with (*E,E*)-8-(4-phenylbutadien-1-yl)caffeine (**3a**) (Figure. 3.9), the lines of the Lineweaver–Burke plots intersected at the y-axis, indicating the mode of inhibition to be competitive. Competitive inhibition were observed with (*E*)-8-styrylcaffeine analogues in previous studies (Petzer *et al.*, 2003; Vlok *et al.*, 2006; Van den Berg *et al.*, 2007). The enzyme–inhibitor dissociation constants (K_i values) for the inhibition of MAO-B by the test compounds are presented in Tables 3.3-3.5.

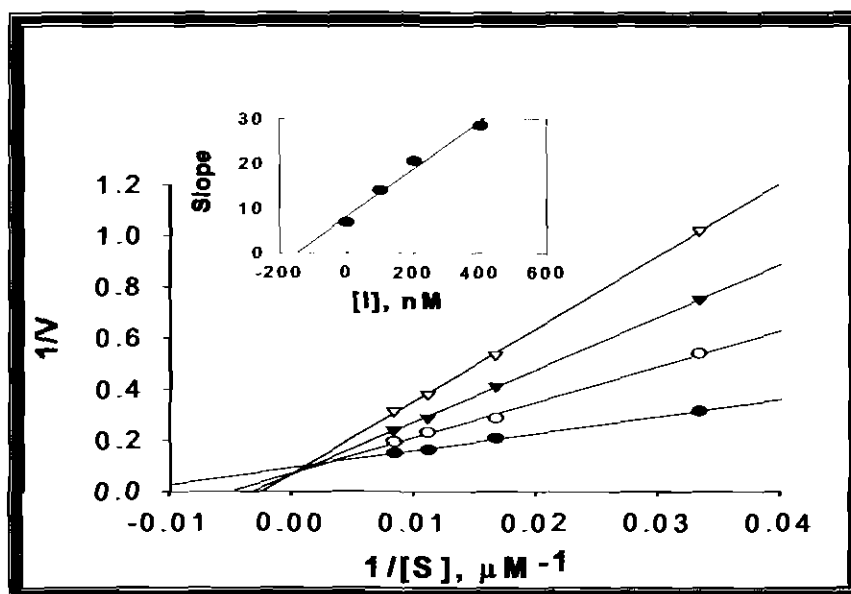


Figure 3.9 Lineweaver–Burke plots of the oxidation of MMTP by baboon liver MAO-B in the absence (filled circles) and presence of various concentrations of **6a** (open circles, 0.1 μM ; filled triangles, 0.2 μM ; open triangles, 0.4 μM). The concentration of the baboon liver mitochondrial preparation was 0.15 mg/ml and the rates are expressed as nmoles.mg protein⁻¹.min⁻¹ of MMDP¹ formed. The inset is the replot of the slopes versus the inhibitor concentrations.

For the (*E,E*)-8-(4-phenylbutadien-1-yl)caffeine analogues (**3a-e**) we also measured the IC_{50} values for the inhibition of MAO-B. An example of the data routinely obtained for the IC_{50} determinations is illustrated for (*E,E*)-8-[4-(3-chlorophenyl)butadien-1-yl]caffeine (**3b**) (Figure. 3.10). Considering that the substrate concentration used for the IC_{50} determinations was 50 μM and the K_m value of MMTP oxidation by baboon liver mitochondrial MAO-B is 68.3 μM , we have also calculated the K_i values from the measured IC_{50} values. As mentioned earlier, the relationship between K_i and IC_{50} of a competitive inhibitor of a monosubstrate reaction is described by the Cheng-Prusoff equation: $K_i = \text{IC}_{50}/(1 + [\text{S}]/K_m)$ (Cheng & Prusoff, 1973). As shown in Table 3.5, the calculated K_i values closely approximate those that were experimentally determined, and the differences are within the range expected for experimental error. For example, the K_i value for the reversible interaction of **3a** with MAO-B was measured as 148.6 nM, while the value calculated from the IC_{50} was found to be 221.1 nM. The same trend is observed for (*E*)-8-styrylcaffeine analogues **4b-d** (Table 3.6) where the experimentally determined K_i value of CSC (**4b**), for example, was 80.6 nM while the value calculated from the corresponding IC_{50} was 84.3 nM. It should be noted that the accuracy of an IC_{50}

determination is dependent upon adequately defining the sigmoid curve (obtained from plotting the MAO-B catalysed MMTP oxidation rate versus the logarithm of the inhibitor concentration) at both low and high inhibitor concentrations. For relatively weak inhibitors such as **4a**, the limit of solubility in the aqueous incubation solvent prevents the definition of the curve at higher inhibitor concentrations (maximal inhibition) and an accurate IC_{50} determination is therefore not possible.

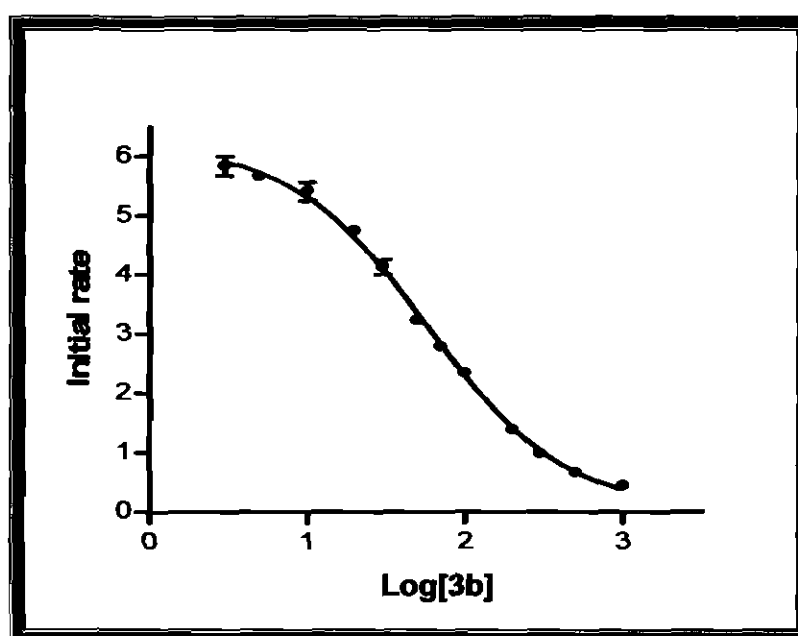
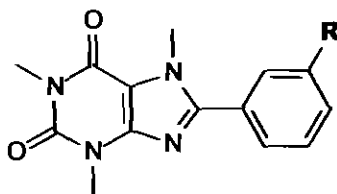


Figure 3.10. The sigmoidal dose-response curve of the initial rates of oxidation of MMTP versus the logarithm of concentration of inhibitor **3b** (expressed in nM). The IC_{50} value (96.3 nM) was determined by fitting the data, using nonlinear least-squares regression analysis, to the one site competition model incorporated into the Prism software package (GraphPad Software Inc.). The concentration of the baboon liver mitochondrial preparation was 0.15 mg/ml, the rates are expressed as nmoles.mg protein⁻¹.min⁻¹ of MMDP¹ formed and the concentration of MMTP used was 50 μ M.

3.8.1 8-Phenylcaffeine analogues

The 8-phenylcaffeine analogues (**1a-c**) (Table 3.3) were found to be relatively weak inhibitors, with K_i values ranging from 36.0 to 86.2 μ M. Compound **1c** was found to be a particularly weak inhibitor with only 24.0% inhibition at a concentration of 1000 μ M. Molecular docking scores calculated for this compound ranged from 34-43.

Table 3.3. The K_i values for the inhibition of MAO-B by 8-phenylcaffeine analogues (1a–c).



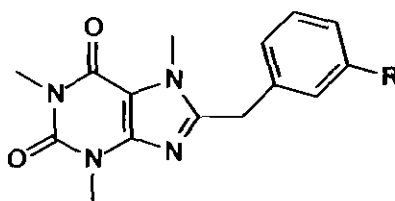
	R	K_i value (μM) ^a	Dock Score
1a	H	86.2	42.911
1b	Cl	36.0	44.270
1c	CF ₃	24.0% ^b	34.089

^aThe enzyme source used was baboon liver mitochondrial MAO-B ^bPercentage inhibition at a concentration of 1000 μM Due to limited solubility in the aqueous incubation solvent, higher concentrations were not tested

3.8.2 8-Benzylcaffeine analogues

The 8-benzylcaffeine (2a-c) (Table 3.4) analogues were also found to be relatively weak inhibitors, with K_i values ranging from 54.6 to 97.6 μM . Compound 2a was found to be a particularly weak inhibitor with only 18.0% inhibition at a concentration of 1000 μM . Molecular docking scores calculated for this compound ranged from 12-50.

Table 3.4. The K_i values for the inhibition of MAO-B by 8-benzylcaffeine analogues (2a–c).



	R	K_i value (μM) ^a	Dock Score
2a	H	18.0% ^b	12.317
2b	Cl	54.6	27.278
2c	CF ₃	97.6	49.467

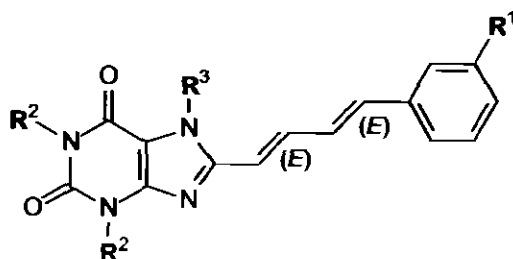
^aThe enzyme source used was baboon liver mitochondrial MAO-B. ^bPercentage inhibition at a concentration of 1000 μM . Due to limited solubility in the aqueous incubation solvent, higher concentrations were not tested.

3.8.3 (*E,E*)-8-(4-Phenylbutadien-1-yl)caffeine analogues

The (*E,E*)-8-(4-phenylbutadien-1-yl)caffeine analogues (3a–d) (Table 3.5) exhibited exceptionally potent MAO-B inhibition activities. The most potent inhibitor was found to be (*E,E*)-8-[4-(3-bromophenyl)butadien-1-yl]caffeine (3c) with a K_i value of 17.2 nM, approximately 3.6 times more potent than that of the corresponding (*E*)-8-(3-bromostyryl)caffeine analogue (4c) (Table 3.6) (Van den Berg *et al.*, 2007). The second most potent inhibitor was (*E,E*)-8-[4-(3-chlorophenyl)butadien-1-yl]caffeine (3b) with a K_i value of 42.1 nM. This is approximately 2–3 times more potent than that of the corresponding (*E*)-8-(3-chlorostyryl)caffeine analogue (CSC) (4b) which has a reported K_i value for the inhibition of baboon liver MAO-B of 128 nM (Vlok *et al.*, 2006) and a K_i value measured here of 80.6 nM (Table 3.6). This trend also exists for the other (*E,E*)-8-(4-phenylbutadien-1-yl)caffeine analogues (3a and 3d) that were examined here, with 3a (K_i = 148.6 nM) remarkably being 19 times more potent than (*E*)-8-styrylcaffeine (4a) (K_i = 2864 nM) (Vlok *et al.*, 2006). Considering the exceptional MAO-B inhibition potencies

of the **3a-d**, we have expanded the series with the preparation of **3e-g**. With these compounds the effect that ethyl substitution at positions 1, 3 and 7 of the caffeine ring has on the potencies of MAO-B inhibition and A_{2A} antagonism, were investigated. As shown in Table 3.5, compounds **3e-g** were much weaker MAO-B inhibitors than the caffeine analogues **3a-d**. For example, **6e** inhibited MAO-B with a K_i value of 1712 nM, which is approximately 11 times less potent than the corresponding caffeine analogue **3a**. Similarly, at a relatively high concentration of 30 μ M, **3f** and **3g** exhibited only 32.7% and 14.6% MAO-B inhibition, respectively. Molecular docking scores calculated for these compounds ranged from 27-47.

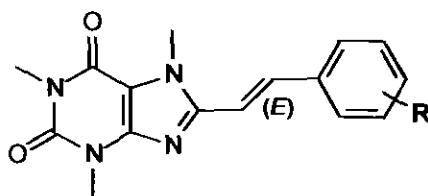
Table 3.5. The K_i and IC_{50} values for the inhibition of MAO-B by (*E,E*)-8-(4-phenylbutadien-1-yl)caffeine analogues (3a-g).



	R ¹	R ²	R ³	Exp. K_i (nM) ^a	Exp. IC_{50} (nM) ^{a,b}	Calcd. K_i (nM) ^c	Dock Score
3a	H	CH ₃	CH ₃	148.6	383 ± 5.65	221.1	46.738
3b	Cl	CH ₃	CH ₃	42.1	96.3 ± 22.2	55.6	38.346
3c	Br	CH ₃	CH ₃	17.2	37.9 ± 7.42	21.9	34.141
3d	F	CH ₃	CH ₃	46.4	89.0 ± 6.20	51.4	31.819
3e	H	CH ₃	C ₂ H ₅	1712	2371 ± 42.5	1369	28.403
3f	H	C ₂ H ₅	CH ₃	–	32.7% ^d	–	27.102
3g	H	C ₂ H ₅	C ₂ H ₅	–	14.6% ^d	–	27.987

^aThe enzyme source used was baboon liver mitochondrial MAO-B. ^bThe IC_{50} values were experimentally determined by fitting the rate data to the one site competition model incorporated into the Prism software package. ^cThe K_i values were calculated from the experimental IC_{50} values according to the equation by Cheng and Prusoff: $K_i = IC_{50}/(1 + [S]/K_m)$ with $[S] = 50 \mu\text{M}$ and K_m (MMTP) = 68.3 μM (Cheng & Prusoff, 1973). ^dPercentage inhibition at a concentration of 30 μM . Due to limited solubility in the aqueous incubation solvent, higher concentrations were not tested, and K_i values were not determined.

Table 3.6. The K_i and IC_{50} values for the inhibition of MAO-B by (*E*)-8-styrylcaffeine analogues (4a–d).



	R	Exp. K_i (nM) ^a	Exp. IC_{50} (nM) ^{a,b}	Calcd. K_i (nM) ^c
4a	H	2864 ^d	Not determined ^e	–
4b	3-Cl	80.6 ± 1.96; 128 ^d	146 ± 1.42	84.3
4c	3-Br	62.7 ± 2.73; 83 ^f	107 ± 4.59	61.8
4d	3,4-Cl ₂	18.9 ± 0.89; 36 ^f	28.4 ± 1.07	16.4

^aThe enzyme source used was baboon liver mitochondrial MAO-B. ^bThe IC_{50} values were experimentally determined by fitting the rate data to the one site competition model incorporated into the Prism software package. ^cThe K_i values were calculated from the experimental IC_{50} values according to the equation by Cheng and Prusoff: $K_i = IC_{50}/(1 + [S]/K_m)$ with $[S] = 50 \mu M$ and K_m (MMTP) = 68.3 μM (Cheng & Prusoff, 1973). ^dValue obtained from Ref. (Vlok et al., 2006). ^eFor weak inhibitors limits of aqueous solubility prevents accurate IC_{50} determination. ^fValue obtained from Ref. (Van den Berg et al., 2007).

3.9 Concluding remarks

In this study the caffeine analogues synthesised were evaluated as potential MAO-B inhibitors. The K_i values for the inhibition of MAO-B by these analogues were determined spectrophotometrically. All of the C-8 substituted analogues were found to be inhibitors of MAO-B. 8-Phenylcaffeine (1a–c) and 8-benzylcaffeine (2a–c) analogues were found to be relatively weak inhibitors in contrast to the exceptional potent inhibition of the (*E,E*)-8-(4-phenylbutadien-1-yl)caffeine analogues (3a–d). Compounds 3e–g were much weaker inhibitors of MAO-B suggesting that ethyl substitution C-1, C-2 and C-7

leads to weaker MAO-B inhibition potency. Molecular docking were performed to establish possible sites for ligand binding. The obtained docking scores provided an indication of ligand binding and reasonable correlations between docked scores and MAO-B inhibition activity of members within a series were obtained. The docking studies indicated that the caffeinyl ring is located within the substrate cavity, while the C-8 side chain exerts towards the entrance cavity.

Chapter Four

Adenosine A_{2A} Receptor Antagonism

4.1 Introduction

Adenosine is formed from the purine base adenine and a ribose moiety. Adenosine is present in all tissues in the mammalian organism, where it performs a variety of vital physiological functions. It is allied to phosphate groups to form ATP, which plays an integral part of the cellular energy system. At synapses, adenosine is a mediator in many biological systems and as a neuromodulator acts through the stimulation of specific receptors (adenosine receptors), located on cell membranes. Adenosine receptors belong to the family of G protein-coupled receptors (Baraldi *et al.*, 1996; Ongini *et al.*, 1997).

Approximately eight decades ago, Drury & Szent-György (1929) reported that adenosine can influence circulation, respiration and gastrointestinal motility in whole animals. Electrical stimulation was found to increase accumulation of adenosine-3',5'-cyclic monophosphate (cAMP) in brain slices (Kakiuchi *et al.*, 1968). This was blocked by methylxanthines, which also blocked the cAMP elevating effects of adenosine (Sattin & Rall, 1970).

The generation of adenosine takes place both intra- and extracellularly. The intracellular production is mediated either by an intracellular 5'-nucleotidase, that dephosphorylates AMP or by hydrolysis of *S*-adenosyl-homocysteine (Scuhbert *et al.*, 1979; Broch & Ueland, 1980). The levels of adenosine in the basal forebrain, striatum, hippocampus and thalamus are significantly higher during wakefulness than during sleep (Huston *et al.*, 1996).

4.1.1 Adenosine receptors

The idea that methylxanthine-sensitive adenosine receptors are coupled to the formation of cAMP was well established approximately four decades ago (Afonso & O'Brien, 1970). It was found that adenosine derivatives, with different order of potencies, were able to increase or decrease intracellular cAMP, and the occurrence of two distinct adenosine receptors was suggested. The receptors that inhibited adenylyl cyclase were classified as A_1 or R_i receptors, and those that stimulated adenylyl cyclase as A_2 or R_a receptors. Both receptor subtypes were found to be highly expressed in the central nervous system (CNS) (Londos *et al.*, 1980). To date, four adenosine receptors have been cloned and characterised, A_1 , A_{2A} , A_{2B} and A_3 . The foremost intracellular signalling pathways are through the formation of cyclic AMP, with A_1 and A_3 causing inhibition of adenylyl cyclase, whereas A_{2A} and A_{2B} activate it (Olah & Stiles, 2000; Fredholm *et al.*, 1998).

Several studies, based on autoradiography using radiolabeled ligands, *in situ* hybridization and reverse transcription polymerase chain reaction have indicated that A_1 receptors are widely distributed in the brain, while A_{2A} receptors are abundant in discrete brain regions such as the striatum. The distribution and density of A_{2B} and A_3 receptors are less clear. A_{2A} receptors are located on membranes of several cell types, which include, amongst others, elements of the circulating blood such as platelets, neutrophils and lymphocytes on smooth muscle cells, cardiac myocytes, mast cells, and within the CNS, on neurons and glial cells. The distribution of these receptors has important implications in pharmacology, as most drugs producing their action through receptors located in the CNS can also interact with receptors in the periphery that may also contribute to the overall biological activity (Ongini & Fredholm, 1996; Gessi *et al.*, 2000). In the caudate putamen, adenosine A_{2A} receptors are localized in several neurons and are thought to modulate neurotransmission mediated by γ -aminobutyric acid (GABA), acetylcholine, and glutamate. These actions of the A_{2A} adenosine receptor could contribute to motor behaviour, as it has been indicated that adenosine A_{2A} antagonists

prevent the motor disturbances of dopamine D₂ receptor null mice (Ochi *et al.*, 2000; Kuwana *et al.*, 1999; Aoyama *et al.*, 2000).

The ability of adenosine to stimulate adenylyl cyclase, divided A₂ receptors into two subforms; A_{2A} with a high affinity for adenosine (0.1-1.0 μM), and A_{2B}, with a lower affinity (≥ 10 μM). This subclassification was strongly supported by an extensive characterisation of the binding properties of [³H]5'-N-ethylcarboxamidoadenosine ([³H]NECA), a non-selective adenosine agonist, and its displacement by several non-labeled adenosine agonists and antagonists in striatal membranes (Bruns *et al.*, 1986).

Characterisation of rat, mouse and human A_{2A} receptor genes has revealed the presence of two exons and a 6-7.2 kb (kilo base pairs) long intron between the regions encoding transmembrane segments 3 and 4 that correspond to the intracellular loop of the receptor (Peterfreund *et al.*, 1996; Chu *et al.*, 1996). It has been established that the location of the human A_{2A} receptor gene is on chromosome 22q13 (MacCollin *et al.*, 1994; Peterfreund *et al.*, 1996). Reverse transcriptase PCR revealed mRNA encoding A_{2A} receptors in all examined areas of the rat brain (Dixon *et al.*, 1996). Northern blots from rat tissue showed high expression of A_{2A} receptor mRNA in the striatum (Fink *et al.*, 1992).

Of the four subtypes of central adenosine receptors, the A_{2A} receptor has been linked most closely to dopaminergic neurotransmission and convincing evidence has accumulated that the A_{2A} receptor plays an important role in CNS controlled motor activity (Morelli *et al.*, 1994). For instance, it has been demonstrated that A_{2A} receptor agonists induce catalepsy in experimental animals (Kanda *et al.*, 1994) while antagonists ameliorate catalepsy induced by haloperidol, a potent dopamine receptor antagonist (Shimada *et al.*, 1997). Also, motor stimulation induced by dopamine agonists is potentiated by adenosine antagonists (Jiang *et al.*, 1993) and inhibited by adenosine agonists (Ferré *et al.*, 1991). Consistent with these views, xanthinyl analogues that are potent A_{2A} antagonists have been found to stimulate motor activity in experimental animal models of PD (Kanda *et al.*, 2000; Shiozaki *et al.*, 1999). In contrast to the widespread distribution of the other adenosine receptors in the brain, the A_{2A} receptor

subtype is virtually limited to the striatum, nucleus accumbens and olfactory tubercle as demonstrated in the rat and human by Northern blotting analyses (Peterfreund *et al.*, 1996), *in situ* hybridization (Schiffman *et al.*, 1991) and autoradiographic (Jarvis & Williams, 1989) studies. Also, in the striatum the A_{2A} receptors are co-expressed on the same neurons as those bearing dopamine D_2 receptors (Pollack *et al.*, 1993).

The distinctive distribution of A_{2A} receptors in the brain and the observation that A_{2A} antagonists potentiate the function of dopamine in the striatum, led to the identification of the A_{2A} receptor as a potential target for the development of drugs to treat motor deficits such as those encountered in PD (Shimada & Suzuki, 2000; Ongini *et al.*, 1997; Ongini *et al.*, 2001). Moreover, A_{2A} binding sites are preserved in the striatum of humans diagnosed with PD (Martinez-Mir *et al.*, 1991) reaffirming the relevance of the A_{2A} receptor as a potential therapeutic target for this disease.

4.2 Adenosine A_{2A} receptor antagonists

Several structurally diverse antagonists have been recognised. This includes the methylxanthines, caffeine and theophylline. Substitutions at position 8 of the caffeine ring, with cycloalkyl groups have led to potent and selective A_1 receptor antagonists. On the other hand, substitution at position 8 with styryl groups leads to potent and selective A_{2A} antagonists. Recently, evaluation of the A_{2A} receptor antagonist, KW-6002 (**16**), showed that it exhibits antiparkinsonian activity in the parkinsonian monkey model without producing hyperactivity and provoking dyskinesia. This indicates that A_{2A} receptor antagonists can be utilised as a new class of antisymptomatic drugs for Parkinson's disease. Various selective A_{2A} adenosine receptor antagonists have been developed, using purine as a template (Kanda *et al.*, 2000; Baraldi *et al.*, 2002). In patients diagnosed with PD these compounds may provide a novel therapeutic approach to overcome PD related motor deficits.

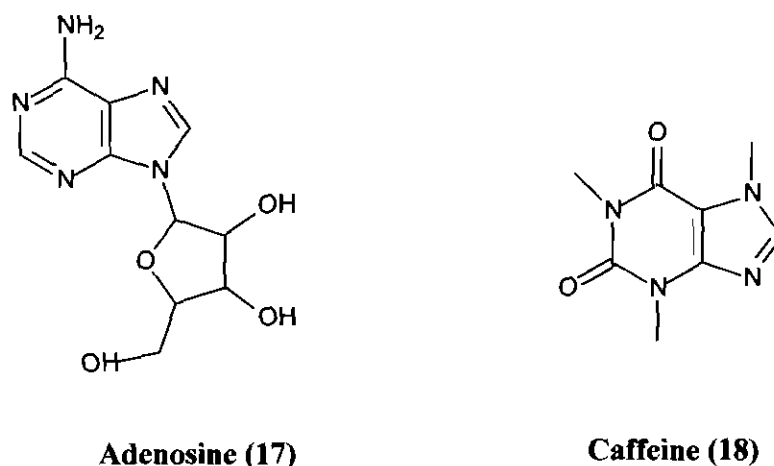


Figure 4.1. Structures of adenosine (17) and caffeine (18) indicating structural comparison in the purine and purine-2,6-dione moieties respectively.

A_{2A} antagonists may be categorised into compounds derived from methylxanthines and non-xanthine heterocycles, which is discussed in section 4.2.1 and 4.2.2. On the basis of affinity for adenosine receptors, A_{2A} antagonists may be labeled selective or non-selective. Selective A_{2A} antagonists exhibit preferential binding to the A_{2A} receptor, as opposed to the A_1 receptor.

4.2.1 (*E*)-8-Styrylxanthinyl derivatives

Caffeine (18) is widely consumed as a psychoactive dietary component (Fredholm *et al.*, 1999). While caffeine exhibits only moderate A_{2A} antagonism properties with practically no selectivity between the A_1 and A_{2A} receptor subtypes (Müller *et al.*, 1997a), it provided a model for the development of the first selective A_{2A} receptor antagonists. A selection of synthetic substitutions on the xanthine moiety of caffeine led to the introduction of an (*E*)-styryl group at the 8 position of xanthines which resulted in compounds that are remarkably potent and selective antagonists of the A_{2A} receptor (Figure 4.2) (Shimada *et al.*, 1992). Therefore, the majority of reported A_{2A} antagonists are 1,3-dimethyl, 1,3-diethyl or 1,3-dipropyl substituted xanthinyl analogs bearing an (*E*)-8-styryl moiety modified on the phenyl ring.

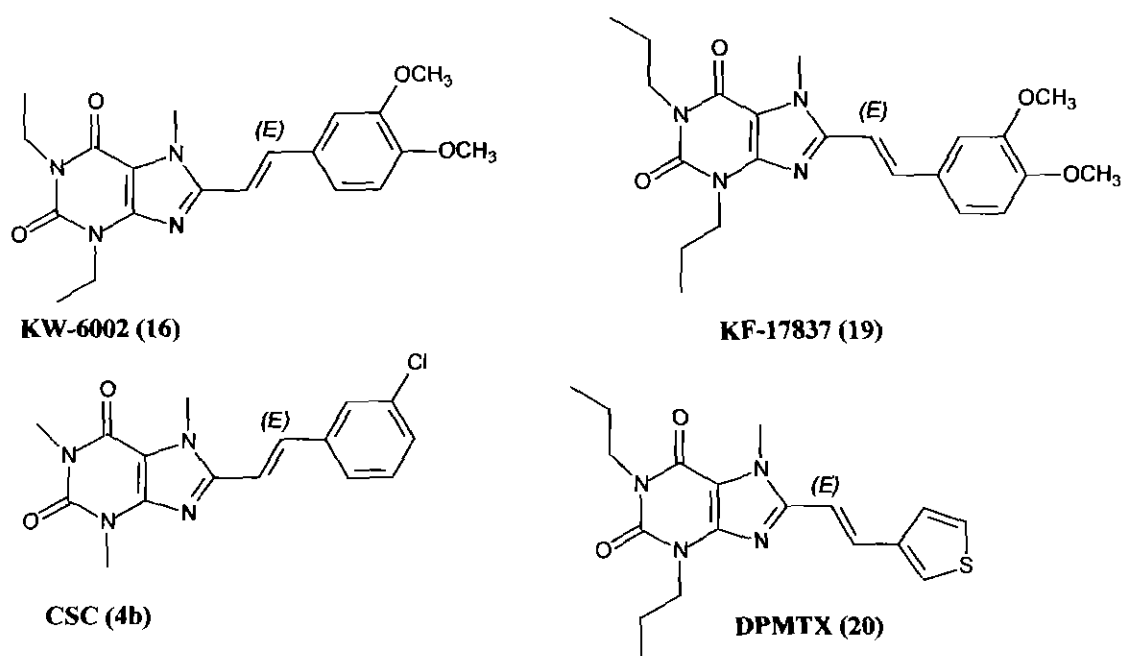


Figure 4.2. Xanthinyl type adenosine receptor antagonists.

Of particular importance is (*E*)-1,3-diethyl-8-(3,4-dimethoxystyryl)-7-methylxanthine [KW-6002 (**16**)] (Shimada *et al.*, 1997), a compound that ameliorates motor deficits in mice as well as in sub-human primate models of PD (Grondin *et al.*, 1999; Shiozaki *et al.*, 1999; Kanda *et al.*, 1998; Kanda *et al.*, 2000). KW-6002 is currently undergoing clinical trials as a novel, non-dopaminergic agent for the treatment of PD (Grondin *et al.*, 1999; Shiozaki *et al.*, 1999). This compound was derived from the prototype (*E*)-1,3-dipropyl-8-(3,4-dimethoxystyryl)-7-methylxanthine [KF-17837 (**19**)] (Suzuki *et al.*, 1993) and demonstrated superior bioavailability after oral administration (Shimada *et al.*, 1997). KF-17837 is also documented as a compound that ameliorates motor deficits in experimental animals by virtue of antagonizing A_{2A} receptors (Kanda *et al.*, 1994). Another xanthine derivative, (*E*)-8-(3-chlorostyryl)caffeine [CSC (**4b**)] is commercially available and is used extensively as a reference A_{2A} antagonist in pharmacological studies. (Jacobson *et al.*, 1993; Müller *et al.*, 1997a). Replacement of the styryl phenyl group with a heterocycle as in the case of (*E*)-1,3-dipropyl-7-methyl-8-[2-(3-thienyl)ethenyl]xanthine [DPMTX (**20**)] also produced a series of potent and selective A_{2A} antagonists (Del Giudice *et al.*, 1996).

4.2.2 Non-xanthinyl heterocycles

Among the number of non-xanthinyl heterocycles reported to antagonize A_{2A} receptors are several compounds having receptor affinity in the low nanomolar range (Figure 4.3). Synthetic efforts by Baraldi *et al.* (1994; 1996) led to a series of interesting compounds whose prototype, 5-amino-2-(7-phenylmethyl)-2-(2-furyl)pyrazolo[2,3-e]-1,2,4-triazolo[1,5-c]pyrimidine or SCH 58261 (**21**), is widely used as a tool for characterizing the A_{2A} receptor subtype (Zocchi *et al.*, 1996a; Zocchi *et al.*, 1996b). Consistent with its A_{2A} antagonism properties, SCH 58261 reverses haloperidol induced catalepsy in experimental animals (Impagnatiello *et al.*, 2000). A related class of compounds, having a bicyclic instead of the tricyclic ring structure is also of interest. The prototype of these derivatives, 4-[2-[[7-amino-2-(2-furyl)[1,2,4]-triazolo[2,3-a][1,3,5]triazin-5-yl]amino]ethyl]phenol or ZM 241385 (**22**), has been developed as a more hydrophilic A_{2A} antagonist (Keddie *et al.*, 1996; Poucher *et al.*, 1995). Both of these compounds have been derived from 5-amino-9-chloro-2-(2-furyl)-1,2,4-triazolo[1,5-c]quinazoline or CGS 15943 (**23**), which is reported to be a nonselective A_1/A_{2A} receptor antagonist (Francis *et al.*, 1988).

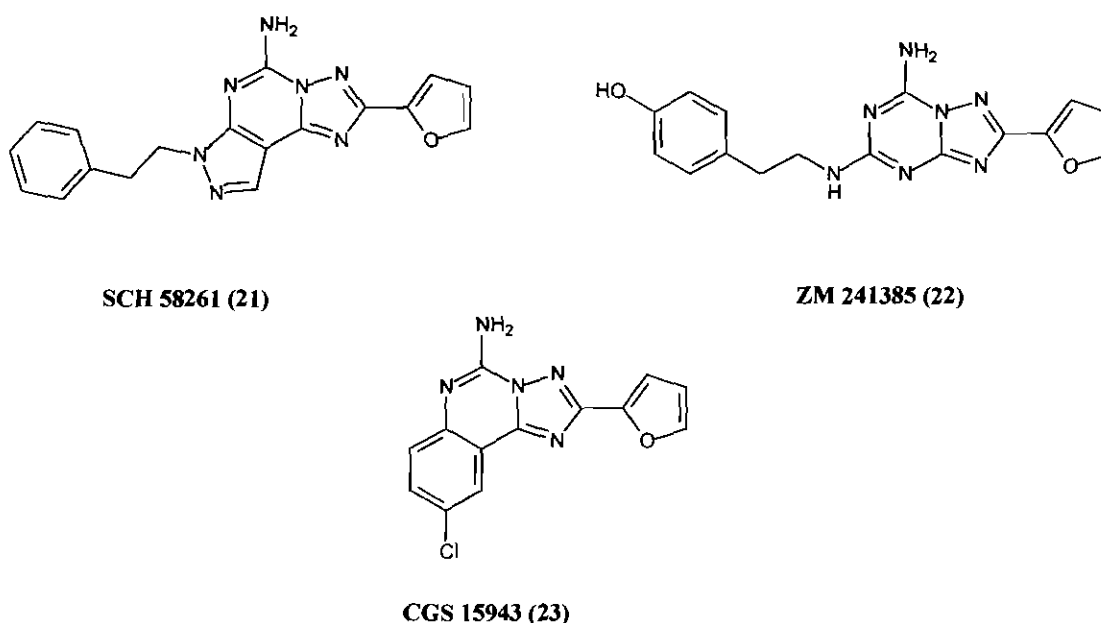


Figure 4.3. Non-xanthinyl heterocyclic adenosine receptor antagonists.

4.3 Experimental design and procedures

4.3.1 Tissue preparations

The adenosine A_{2A} receptor binding studies were carried out according to the procedure described in literature (Bruns *et al.*, 1986). Approval for the collection of the tissues was obtained from the Research Ethics Committee of the North-West University (05D04). Rat striata from 500 g male Sprague Dawley rats ($n = 40$) were dissected and obtained from the Animal Research Centre of the North West University, Potchefstroom Campus, and it was immediately snap frozen with liquid nitrogen and stored at $-70\text{ }^{\circ}\text{C}$. The striatum (90 mg) was disrupted in 10 ml of ice-cold 50 mM Tris HCl at pH 7.7, $25\text{ }^{\circ}\text{C}$, for 30 seconds with a Polytron PT-10 homogeniser (Brinkman) at a setting of 5. The suspension was centrifuged at $50,000 \times g$ for 10 minutes. Thereafter, the supernatant was discarded and the pellet was resuspended in 10 ml of ice-cold Tris HCl, after which the disruption procedure was repeated. The suspension was yet again centrifuged under the same conditions as mentioned above. Finally, to the pellet, ice-cold Tris HCl was added to yield 5 mg/0.79 ml. These membrane suspensions were aliquoted and stored in plastic vials at $-70\text{ }^{\circ}\text{C}$. When needed the tissue was thawed at room temperature, and kept on ice until use.

4.3.2 Incubation conditions

Cell membranes (5 mg/0.79) ml expressing rat adenosine A_{2A} receptors were incubated with different concentrations of the test antagonists described in Chapter Two and shown in Table 4.2.

Incubations were carried out for 60 minutes at room temperature ($25\text{ }^{\circ}\text{C}$). Assays were performed in 6 ml polyethylene vials which had been pre-treated with sigma-cote and left overnight to dry. These assays were done in duplicate. The tubes consisted of 5 mg of the original tissue weight of the rat striatal membranes, 4 nM [^3H]NECA, 50 nM CPA to

eliminate A₁ receptor binding, 10 mM MgCl₂, 0.1 unit/ml of adenosine deaminase and 1% dimethyl sulfoxide (DMSO). The stock solutions of the compounds to be tested as well as that of CPA were prepared in DMSO.

CPA was dissolved at 10 mM in DMSO and diluted to 500 nM in Tris the day of the experiment. The test antagonist for the competition study was dissolved at 10 μM in DMSO and diluted to 100 times the final incubation concentration. Control incubations received an equal volume (10 μl) of DMSO, as DMSO had no effect on specific binding (Bruns *et al.*, 1986). [³H]NECA was diluted to 40 nM in Tris. To the membrane suspension (5 mg/0.79 ml) sufficient MgCl₂ (10 mM) and adenosine deaminase (0.1 unit/ml) were added. These competition reactions were performed in a total volume of 1000 μl in miniature polyethylene sigma-coted tubes, and consisted of the following components:

- Test compound (Inhibitor) 10 μl
- CPA [500 nM] 100 μl
- [³H]NECA 100 μl
- Membrane mixture 790 μl

Components for the non-specific binding consisted of:

- CPA [10 mM] 10 μl
- CPA [500 nM] 100 μl
- [³H]NECA 100 μl
- Membrane mixture 790 μl

After addition, the rack of tubes was vortexed and the tubes were then incubated for 60 minutes at 25 °C in a shaking water bath. The rack of tubes was vortexed for a second time halfway through the incubation experiment. Incubations were terminated with rapid filtration through Whatman[®] GF/B 25 filters (25 mm diameter) fitted on a Hoffeler vacuum system. The filters were washed three times with 4 ml ice cold Tris buffer (4 °C).

The damp filters were put into scintillation vials and 4 ml of scintillation fluid were added and the vials were left overnight. The radioactivity retained on the filters were counted with a Packard Tri-CARB 2100 TR scintillation counter.

The IC₅₀ values were determined by plotting the count values versus the logarithm of the inhibitor concentrations to obtain a sigmoidal dose-response curve. This kinetic data were fitted to the one site competition model incorporated into the Prism software package (GraphPad Software Inc.). The K_i values for the competitive inhibition of [³H]NECA (K_d = 15.3 nM) binding by the test compounds were calculated according to the Cheng and Prusoff equation (Cheng & Prusoff, 1973). All incubations were carried out in duplicate and the K_i values are expressed as mean ± S.E.M. An estimate of the nonspecific binding was obtained from binding studies in the presence of 100 μM CPA. To determine the IC₅₀ value for the sigmoid plot, a non-linear regression equation was used as indicated in Equation 4.1.

Equation 4.1. Calculation of IC₅₀ value with non-linear regression

$$Y = \text{Bottom} \times \frac{\text{Top} - \text{Bottom}}{1 + 10^{x - \log IC_{50}}}$$

On a sigmoid curve the X-axis is the logarithm of the concentration of the unlabeled compound, and the Y-axis is the percentage of control where the control is the cpm bound in the absence of the unlabeled compound. Y = the amount of cpm bound. X = the concentration of the unlabeled ligand. "Top" represents the top part of the sigmoid curve and "Bottom" the bottom part of the sigmoid curve.

Using the known concentration of the radio labelled ligand in the incubations, the IC₅₀ value can be converted into a K_i value for the unlabeled ligand. The K_i value is the equilibrium dissociation constant of the unlabeled ligand for the receptor. The K_i value can be obtained from the IC₅₀ value using the Cheng-Prusoff equation indicated below in Equation 4.2.

Equation 4.2. Cheng-Prusoff equation to calculate the K_i from the IC_{50} value

$$K_i = \frac{IC_{50}}{1 + \frac{D}{K_d}}$$

D = concentration of the radio ligand. *K_d* = affinity of the radio ligand for the receptor under the equal conditions used with the competition experiment.

Table 4.1 summarises the reagents and materials utilised for this study as well as the companies where it has been obtained from.

Table 4.1. Description of materials and suppliers of reagents and materials utilised for the A_{2A} assay

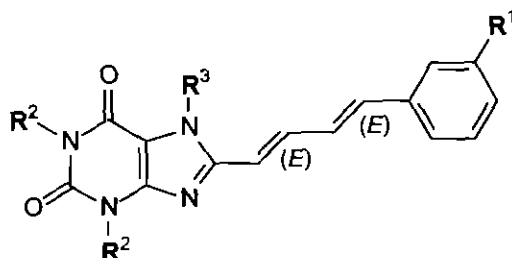
Materials	Company
25 Ci/mmol (250 μ Ci) [3 H] 5'- <i>N</i> -ethylcarboxamide-adenosine [3 H]NECA	Amersham Biosciences
Adenosine deaminase (250 units) E.C. 3.5.4.4	Sigma Aldrich
N^6 -Cyclopentyladenosine (CPA)	Sigma Aldrich
Magnesium chloride anhydrous	Sigma Aldrich
Silicone solution (Sigma-cote)	Sigma Aldrich
Whatman [®] GF/B 25 mm diameter filters	Merck
Filtercount scintillation fluid	Sepsi
Dimethyl sulfoxide (DMSO)	Riedel-de Haën
Trizma [®] Hydrochloride	Fluka
Trizma [®] Base	Fluka

4.4 Results and discussion

Since the goal of the present study was to identify promising dual-acting compounds that potentially block both the adenosine A_{2A} receptor and the catalytic function of MAO-B, we have selected the (*E,E*)-8-(4-phenylbutadien-1-yl)caffeine analogues (**3a-g**) for further evaluation as potential antagonists of the adenosine A_{2A} receptor. The potencies by which

the test compounds antagonise A_{2A} receptors were determined by the radioligand binding procedure described in literature (Bruns *et al.*, 1986). Binding to the A_{2A} receptors was performed with N-[3H]ethyladenosin-5'-uronamide (3H]NECA) in rat striatal membranes in the presence of N^6 -cyclopentyladenosine (CPA) to eliminate the adenosine A_1 receptor binding component of 3H]NECA. This procedure is frequently used to identify compounds that exhibit high affinity binding to A_{2A} receptors (Suzuki *et al.*, 1993; Jacobson *et al.*, 1993; Müller *et al.*, 1997). For comparison with the literature we have used this procedure to determine the equilibrium dissociation constant (K_i value) of the reference A_{2A} antagonists, CSC (**4b**) and KW-6002 (**16**), for the A_{2A} receptor. As shown in Table 4.2, a K_i value of 30.2 ± 5.40 nM has been recorded for CSC, while the literature values are 36 ± 6 nM (Müller *et al.*, 1997) and 54 ± 19 nM (Jacobson *et al.*, 1993). For KW-6002 (**16**), a K_i value of 4.46 ± 1.13 nM was measured, while the reported value is 2.2 ± 0.34 nM (Shimada *et al.*, 1997). The similarity in range of the K_i values determined here with those reported testifies to the validity of the competition data generated here.

Table 4.2. The K_i values for the competitive inhibition of [^3H]NECA binding to rat striatal adenosine A_{2A} receptors by selected caffeine analogues.



	R ¹	R ²	R ³	K_i value (nM) ^a
3a	H	CH ₃	CH ₃	153 ± 5.40
3b	Cl	CH ₃	CH ₃	104 ± 1.50
3c	Br	CH ₃	CH ₃	59.1 ± 15.8
3d	F	CH ₃	CH ₃	114 ± 14.2
3e	H	CH ₃	C ₂ H ₅	13.5 ± 4.87
3f	H	C ₂ H ₅	CH ₃	2.74 ± 0.35
3g	H	C ₂ H ₅	C ₂ H ₅	7.73 ± 2.80
16	KW-6002			4.46 ± 1.13; (2.2) ^b
4b	CSC			30.2 ± 5.40; (36) ^c ; (54) ^d

^aThe IC_{50} values were determined by fitting the data, using nonlinear least-squares regression analysis, to the one site competition model incorporated into the Prism software package. The K_i values for the competitive inhibition of [^3H]NECA ($K_d = 15.3$ nM) binding was subsequently calculated according to the Cheng-Prusoff equation (Cheng & Prusoff, 1973). ^bValue obtained from Ref. (Shimada et al., 1997). ^cValue obtained from Ref. (Müller et al., 1997). ^dValue obtained from Ref. (Jacobson et al., 1993).

As shown in Table 4.2 all of the (*E,E*)-8-(4-phenylbutadien-1-yl)caffeine analogues (**3a-g**) tested were found to be potent antagonists of the A_{2A} receptor. The dose-inhibition curves for the test compounds versus [^3H]NECA that were routinely observed are illustrated by example with **3f** (Fig. 4.4). The most potent antagonist was found to be **3f** with a K_i value of 2.74 ± 0.35 nM. Since all of the ethyl substituted compounds, **3e-g**, were approximately 11-55 times more potent than the caffeine analogue **3a**. It is evident that ethyl substitution C-1, C-2 and C-7 of the xanthine ring leads to enhanced A_{2A} antagonism potency compared to 1,3-dimethyl substitution.

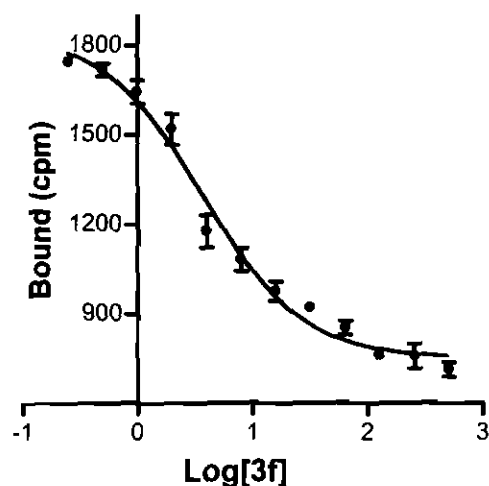


Figure 4.4. Competition study between [3f] and the radio labelled ligand. The sigmoidal dose-response curve for the inhibition of [^3H]NECA binding to rat striatal A_{2A} receptors by antagonist 3f (expressed in nM). The IC_{50} value was determined by fitting the data, using nonlinear least-squares regression analysis, to the one site competition model incorporated into the Prism software package (GraphPad Software Inc.). The K_i value (2.74 nM) for the competitive inhibition of [^3H]NECA ($K_d = 15.3$ nM) binding was calculated with the Cheng-Prusoff equation (Cheng & Prusoff, 1973). In this experiment the non-saturable, nonspecific binding was 623 cpm.

4.5 Concluding remarks

Test compounds synthesised were evaluated as adenosine A_{2A} receptor antagonists with a radioligand binding procedure. All the (*E,E*)-8-(4-phenylbutadien-1-yl)caffeine analogues (**3a-g**) were found to be relatively potent A_{2A} antagonists. In contrast to its effect on MAO-B inhibition potency, ethyl substitution at positions 1, 3 and 7 of the caffeine ring had a positive effect on the potency of A_{2A} antagonism.

Chapter Five

Conclusion

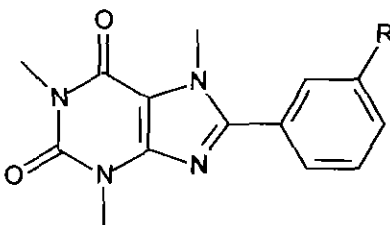
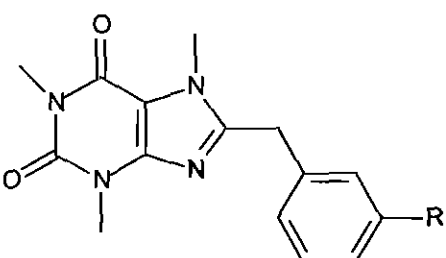
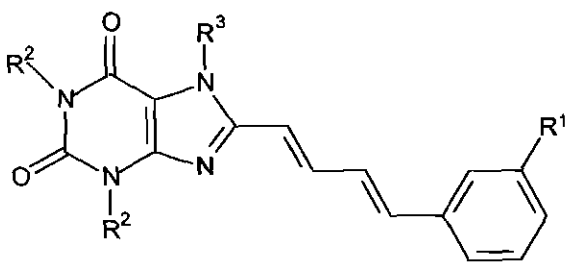
5.1 Discussion

Several (*E*)-8-styrylcaffeines act as potent reversible inhibitors of MAO-B (Petzer *et al.*, 2003; Vlok *et al.*, 2006; Van den Berg *et al.*, 2007). (*E*)-8-Styrylcaffeines have also been shown to be antagonists of adenosine A_{2A} receptors (Suzuki *et al.*, 1993; Jacobson *et al.*, 1993; Müller *et al.*, 1997). During this investigation, using (*E*)-8-styrylcaffeine as lead compound, we have attempted to identify additional dual-target-directed compounds, possibly with enhanced MAO-B inhibition and A_{2A} antagonism potencies. This study elucidated the structural requirements of C-8 substituted caffeine analogues to act as dual inhibitors of MAO-B and antagonists of the adenosine A_{2A} receptor. Since caffeine (**18**) is a weak inhibitor of MAO-B (Chen *et al.*, 2001) and only a moderately potent adenosine A_{2A} antagonist (Müller *et al.*, 1997), it can be concluded that the (*E*)-styryl group at C-8 plays an important role in the dual-action of (*E*)-8-styrylcaffeines. In this study we have prepared 3 additional classes of C-8 substituted caffeine analogues: the 8-phenylcaffeine (**1a-c**), 8-benzylcaffeine (**2a-c**) and (*E,E*)-8-(4-phenylbutadien-1-yl)caffeine (**3a-d**) analogues (Table 5.1).

The aim was to identify additional C-8 substituents which may, similar to the (*E*)-styryl functional group, confer dual-action to the caffeine scaffold. The series of (*E,E*)-8-(4-phenylbutadien-1-yl)caffeine analogues (**3a-d**) were further expanded with the synthesis of 3 additional members, **3e-g**. With these compounds we investigated the effect that ethyl substitution at positions 1, 3 and 7 of the caffeine ring has on the potencies of MAO-B inhibition and A_{2A} antagonism.

The results of MAO-B inhibition studies have shown that the 8-phenylcaffeine (**1a-c**) and 8-benzylcaffeine (**2a-c**) analogues were weak inhibitors of MAO-B while the (*E,E*)-8-(4-phenylbutadien-1-yl)caffeine analogues (**3a-d**) were found to be exceptionally potent inhibitors. The (*E,E*)-8-(4-phenylbutadien-1-yl)caffeine analogue (**3b**) substituted with chlorine at C-3 of the phenyl ring ($K_i = 42.1$ nM) was approximately 855 and 1269 times more potent as a MAO-B inhibitor than the corresponding C-3 chlorine substituted 8-phenylcaffeine (**1b**) ($K_i = 36.0$ μ M) and 8-benzylcaffeine (**2b**) ($K_i = 54.6$ μ M) analogues, respectively. The (*E,E*)-8-(4-phenylbutadien-1-yl)caffeine analogues (**3a-d**) were also more potent inhibitors than the corresponding (*E*)-8-styrylcaffeines (**4a-c**). For example, the C-3 chlorine substituted **3b** ($K_i = 42.1$ nM) was approximately 1.9 times more potent than CSC (**4b**) ($K_i = 80.6$ nM) while the unsubstituted (*E,E*)-8-(4-phenylbutadien-1-yl)caffeine, **3a** ($K_i = 148.6$ nM), was found to be remarkably 19 times more potent than the corresponding unsubstituted (*E*)-8-styrylcaffeine (**4a**) ($K_i = 2864$ nM). Compounds **3e-g** were found to be relatively weak inhibitors of MAO-B, indicating that ethyl substitution at positions 1, 3 and 7 of the caffeine ring has a negative effect on the potency of MAO-B inhibition. For (*E*)-8-styrylcaffeines, 1,3-diethyl substitution of the caffeine ring has also been shown to reduce the MAO-B inhibition potency compared to 1,3-dimethyl substitution (Petzer *et al.*, 2003).

Table 5.1. Structures of the C-8 substituted caffeine analogues that were investigated for this study: 8-Phenylcaffeine (1a–c), 8-benzylcaffeine (2a–c) and (*E,E*)-8-(4-phenylbutadien-1-yl)caffeine (3a–g) analogues.

Compound #	Compound structure	R																								
1a 1b 1c		H Cl CF ₃																								
2a 2b 2c		H Cl CF ₃																								
3a 3b 3c 3d 3e 3f 3g		<table border="1"> <thead> <tr> <th>R¹</th> <th>R²</th> <th>R³</th> </tr> </thead> <tbody> <tr> <td>H</td> <td>CH₃</td> <td>CH₃</td> </tr> <tr> <td>Cl</td> <td>CH₃</td> <td>CH₃</td> </tr> <tr> <td>Br</td> <td>CH₃</td> <td>CH₃</td> </tr> <tr> <td>F</td> <td>CH₃</td> <td>CH₃</td> </tr> <tr> <td>H</td> <td>CH₃</td> <td>C₂H₅</td> </tr> <tr> <td>H</td> <td>C₂H₅</td> <td>CH₃</td> </tr> <tr> <td>H</td> <td>C₂H₅</td> <td>C₂H₅</td> </tr> </tbody> </table>	R ¹	R ²	R ³	H	CH ₃	CH ₃	Cl	CH ₃	CH ₃	Br	CH ₃	CH ₃	F	CH ₃	CH ₃	H	CH ₃	C ₂ H ₅	H	C ₂ H ₅	CH ₃	H	C ₂ H ₅	C ₂ H ₅
R ¹	R ²	R ³																								
H	CH ₃	CH ₃																								
Cl	CH ₃	CH ₃																								
Br	CH ₃	CH ₃																								
F	CH ₃	CH ₃																								
H	CH ₃	C ₂ H ₅																								
H	C ₂ H ₅	CH ₃																								
H	C ₂ H ₅	C ₂ H ₅																								

Since the series of (*E,E*)-8-(4-phenylbutadien-1-yl)caffeine analogues were found to be exceptionally potent reversible MAO-B inhibitors, they were selected for further evaluation as potential antagonists of the adenosine A_{2A} receptor. All the (*E,E*)-8-(4-phenylbutadien-1-yl)caffeine analogues (3a–g) were found to be relatively potent A_{2A} antagonists. In contrast to its effect on MAO-B inhibition potency, ethyl substitution at positions 1, 3 and 7 of the caffeine ring had a positive effect on the potency of A_{2A} antagonism. For example, the 1,3-diethyl substituted 3f ($K_i = 2.74$ nM) was

approximately 55 times more potent than the corresponding 1,3-dimethyl substituted **3a** ($K_i = 153$ nM).

5.2 Concluding remarks

It can be concluded that the (*E,E*)-8-(4-phenylbutadien-1-yl)caffeines, **3a-d**, are promising lead compounds for the discovery of dual-target-directed compounds that block both at MAO-B and at A_{2A} receptors. 1,3-Ethyl substitution of C-1, C-3 and C-7 of the caffeine ring (**3f-g**), leads to enhanced potency of A_{2A} antagonism, but has the opposite effect on MAO-B inhibition potency, and is therefore an unsuitable structural modification where dual-action is desired. The A_{2A} receptor may provide a novel target for long-term medication of PD because blockade of this receptor exerts both antisymptomatic and chronic neuroprotective activities. The antiparkinsonian potential of A_{2A} antagonism has been boosted by preclinical evidence that A_{2A} antagonists might favourably alter the course as well as symptoms of the disease.

MAO-B inhibitors are also useful for the treatment of PD since it delays the initiation levodopa therapy, by blocking the central metabolism of dopamine. Furthermore, MAO-B inhibitors may also protect against further neurodegeneration by blocking H_2O_2 formation as a result of dopamine oxidation, and therefore reduces oxidative stress in the CNS.

References

1. Afonso, S., O'Brien, G.S. 1970. Inhibition of cardiovascular metabolic and hemodynamic effects of adenosine by aminophylline. *American journal of physiology*. 219: 1672-1674.
2. Aoyama, S., Kase, H., Borrelli, E. 2000. Rescue of locomotor impairment in dopamine D₂ receptor deficient mice by an adenosine A_{2A} receptor antagonist. *Journal of neuroscience*. 20: 5848-5852.
3. Baker, B.R., Janson, E.E., Vermeulen, N.M.J. 1969. Irreversible enzyme inhibitors. CLX. Some factors in cell wall transport of active-site-directed irreversible inhibitors of dihydrofolic reductase derived from 4,6-diamino-1,2-dihydro-2,2-dimethyl-1-(phenylalkylphenyl)-s-triazines *Journal of medicinal chemistry*. 12: 898-902.
4. Baker, B.R., Doll, M.H. 1971. Inhibitors of guinea pig compliment derived by quaternization of phenylalkylpyridines with α -Bromomethylbenzenesulfonyl fluorides. *Journal of medicinal chemistry*. 14: 793-799.
5. Baraldi, P.G., Cacciari, B., Romagnoli, R., Spalluto, G., Monopoli, A., Ongini, E., Varani, K., Borea, P.A. 2002. 7-Substituted 5-Amino-2-(2-furyl)pyrazolo[4,3-e]-1,2,4-triazolo[1,5-c]pyrimidines as A_{2A} adenosine receptor antagonists: A study on the importance of modifications at the side chain on the activity and solubility. *Journal of medicinal chemistry*. 45: 115-126.
6. Baraldi, P.G., Cacciari, B., Spalluto, G., Pineda de las Infants Y Villatoro, M.J., Zocchi, C., Dionsotti, S., Ongini, E. 1996. Pyrazolo[4,3-e]-1,2,4-triazolo[1,5-c]pyrimidine derivatives: potent and selective A_{2A} adenosine antagonists. *Journal of medicinal chemistry*. 39: 1164-1171.

References

7. Baraldi, P.G., Manfredini, S., Simoni, D., Zappaterra, L., Zocchi, C., Dionsotti, S., Ongini, E. 1994. Synthesis and activity of new Pyrazolo[4,3-e]-1,2,4-triazolo[1,5-c]pyrimidine and 1,2,3-triazolo[4,5-e]1,2,4-triazolo[1,5-c]pyrimidine displaying potent and selective activity as A_{2A} adenosine receptor antagonists. *Bioorganic & medicinal chemistry letters*. 4: 2539-2544.
8. Bauman, J.W., Lui, J., Lui, P., Klaassen, C.D. 1991. Increase in metallothionein produced by chemicals that induce oxidative stress. *Toxicology and applied pharmacology*. 110: 347-354.
9. Binda, C., Li, M., Hubalek, F., Restelli, N., Edmonson, D.E., Mettevi, A. 2003. Insights into the model of inhibition of human mitochondrial monoamine oxidase B from high-resolution crystal structures. 2003. *Proceedings of the national academy of sciences of the United States of America*. 100: 9750-9755.
10. Binda, C., Newton-Vinson, P., Hubalek, F., Edmonson, D.E., Mattevi, A. 2002. Structure of human monoamine oxidase B, a drug target for the treatment of neurological disorders. *Nature structural & molecular biology*. 9: 22-26.
11. Bissel, P., Bigley, M.C., Castagnoli, K., Castagnoli, Jr. N. 2002. Synthesis and biological evaluation of MAO-A selective 1,4-disubstituted-1,2,3,6-tetrahydropyridinyl substrates *Bioorganic & medicinal chemistry*. 10: 3031-3041.
12. Blicke, F.F., Godt, H.C., Jr. 1954. Reactions of 1,3-dimethyl-5,6-diaminouracil. *Journal of the American chemical society*. 76: 2798-2800.
13. Bradford, M.M. 1976. A rapid and sensitive method for the quantification of microgram quantities of protein utilizing the principle of protein-dye binding. *Analytical biochemistry*. 72: 247-254.
14. Broch, O.J., Ueland, P.M. 1980. Regional and subcellular distribution of S-adenosylhomocysteine hydrolase in the adult rat brain. *Journal of neurochemistry*. 35: 484-488.

References

15. Bruns, R.F., Lu, G.H., Pugsley, T.A. 1986. Characterization of the A₂ adenosine receptor labeled by [³H]-NECA in rat striatal membranes. *Molecular pharmacology*. 29: 331-346.
16. Cadenas, E., Davies, K.J.A. 2000. Mitochondrial free radical generation, oxidative stress and aging. *Free radical biology and medicine*. 29: 222-230.
17. Calne, D.B. 1993. Treatment of Parkinson's disease. *New England journal of medicinal chemistry*. 329: 1021-1027.
18. Castagnoli, K., Palmer, S., Castagnoli, Jr. N. 1999. Neuroprotection by (R)-deprenyl and 7-nitroindazole in the MPTP C57BL/6 mouse model of neurotoxicity. *Neurobiology*. 7: 135-149.
19. Castagnoli, K.P., Steyn, S.J., Petzer, J.P., Van der Schyf, C.J., Castagnoli, Jr. N. 2001. Neuroprotection in the MPTP parkinsonian C57BL/6 mouse model by a compound isolated from tobacco. *Chemical research in toxicology*. 14: 523-527.
20. Chalmers-Redmen, R.M., Tatton, W.G. 1996. Modulation of gene expression rather than monoamine oxidase inhibition: (-)-deprenyl-related compounds in controlling neurodegeneration. *Neurology*. 47: 171-183.
21. Chance, B., Sies, H., Boveris, A. 1979. Hydroperoxide metabolism in mammalian organs. *Physiological reviews*. 59: 527-605.
22. Chazot, P.L. 2001. Safinamide (Newton Pharmaceuticals). *Current opinion in investigational drugs*. 2: 809-813.
23. Chen, J.-F., Xu, K., Petzer, J.P., Staal, R., Xu, Y.-H., Beilstein, M., Sonsalla, P.K., Castagnoli, K., Castagnoli, Jr., N., Schwarzchild, M.A. 2001. Neuroprotection by caffeine and A_{2A} adenosine receptor inactivation in a model of Parkinson's disease. *Journal of neuroscience*. 21: RC143.
24. Cheng, Y., Prusoff, W.H. 1973. Relationship between the inhibition constant and the concentration of inhibitor which causes 50 percent inhibition of an enzymatic reaction. *Biochemical pharmacology*. 22: 3099-3108.
25. Chiba, K., Peterson, L.A., Castagnoli, K.P., Trevor, A.J., Castagnoli, Jr. N. 1985. Studies in the molecular mechanism of bioactivation of the selective

- nigrostriatal toxin 1-methyl-4-phenyl-1,2,3,6-tetrahydropyridine (MPTP). *Drug metabolism and disposition*. 13: 342-347.
26. Chiba, K., Trevor, A.J., Castagnoli, Jr. N. 1984. Metabolism of the neurotoxic tertiary amine, MPTP, by brain monoamine oxidase. *Biochemical and biophysical research communications*. 120: 574-578.
27. Chu, Y.Y., Tu, K.H., Lee, Y.C., Kuo, Z.J., Lai, H.L., Chern, Y. 1996. Characterization of the rat A_{2a} adenosine receptor gene. *DNA Cellular biology*. 15: 329-337.
28. Cook, A. H., Thomas, G. H. 1950. Studies in the azole series. Part XXIX. The preparation of some natural xanthines and related purines. *Journal of the chemical society*. 1884-1888.
29. Crombie, L., Crombie, W. M. L. 1994 Stereochemistry of thermolytic base-catalysed decarboxylation to form conjugated diene-acids: synthesis using ethyldenemalonic ester condensation. *Journal of the chemical society. Perkin transactions*. 10: 1267.
30. Dalton, T.P., Shertzer, H.G., Alvaro, P. 1999. Regulation of gene expression by reactive oxygen. *Pharmacology toxicology*. 39: 67-101.
31. Del Giudice, M.R., Borioni, S., Mustazza, C., Gatta, F., Dionisotti, S., Zocchi, E., Ongini, E. 1996. (E)-1-(Heterocyclyl or cyclohexyl)-2-[1,3,7-trisubstituted(xanthin-8-yl)]ethenes as A_{2A} adenosine receptor antagonists. *European journal of medicinal chemistry*. 69: 1771-1773.
32. Dixon, A.K., Gubitz, A.K., Sirinathsingji, D.J., Richardson, P.J., Freeman, T.C. 1996. Tissue distribution of adenosine receptor mRNA's in the rat. *British journal of pharmacology*. 118: 1461-1468.
33. Drury, A.N., Szent-György, A. 1929. The physiological activity of adenine compounds with especial reference to their action upon mammalian heart. *Journal of physiology. (London)*. 68: 213-237.
34. Ferré, S., Herrera-Marschitz, M., Grabowska-Andén, M., Ungerstedt, U., Casa, M., Andén, N.-E. 1991. Postsynaptic dopamine/adenosine interaction: I. adenosine analogues inhibit dopamine D₂-mediated behavior in short-term reserpinized mice. *European journal of pharmacology*. 192: 25-30.

35. Fink, J.S., Weaver, D.R., Rivkees, S.A., Peterfeund, R.A., Pollack, A.E., Adler, E.M., Reppert, S.M. 1992. Molecular cloning of the rat A₂ adenosine receptor: selective co-expression with D₂ dopamine receptors in rat striatum. *Molecular brain research*. 14: 186-195.
36. Foley, P., Gerlach, M., Youdim, M.B.H., Riederer, P. 2000. MAO-B inhibitors: multiple roles in the therapy of neurodegenerative disorders. *Parkinsonism related disorders*. 6: 25-47.
37. Francis, J.E., Cash, W.D., Psychoyos, S., Ghai, G., Wenk, P., Friedmann, R.C., Atkins, C., Warren, V., Furness, P., Huyn, J.L. 1988. Structure-activity profile of a series of novel triazoloquiazoline adenosine antagonists. *Journal of medicinal chemistry*. 31: 1014-1020.
38. Fredholm, B.B., Bättig, K., Holmén, J., Nehlig, A., Zvartau, E.E. 1999. Actions of caffeine in the brain with special reference to factors that contribute to its widespread use. *Pharmacology reviews*. 51: 83-133.
39. Fredholm, B.B., Ljzerman, A.P., Jacobson, K.A., Linden, J., Stiles, G.L. 1998. Adenosine receptors, in: IUPHAR compendium of receptor characterisation and classification. *IUPHAR Media, London*. pp. 48-57.
40. Gerber, N.N. 1960. Synthesis of bridged hydrofluorenes. *Journal of the American chemical society*. 82: 5216-5218.
41. Gessi, S., Varani, K., Merighi, S., Ongini, E., Borea, P.A. 2000. A_{2A} adenosine receptors in human peripheral blood cells. *British journal of pharmacology*. 129: 2-11.
42. Gnerre, C., Catt, M., Leonetti, F., Weber, P., Carrupt, P.-A., Altomare, C., Carotti, A., Testa, B. 2000. Inhibition of monoamine oxidases by functionalized coumarin derivatives: biological activities, QSAR, and 3D-QSARs. *Journal of medicinal chemistry*. 43: 4747-4758.
43. Greenamyre, J.T., Sherer T.B., Betarbet R., Panov A.V. 2003. Complex I and Parkinson's disease. *IUBMB Life*. 52: 135-141.
44. Grimsby, J., Lan, N. C., Neve, R., Chen, K., Shih, J.C. 1990. Tissue distribution of human oxidase A and B mRNA. *Journal of neurochemistry*. 55: 1166-1169.

45. Grondin, R., Bedard, P.J., Tahar, A.H., Gregoire, L., Mori, A., Kase, H. 1999. Antiparkinsonian effect of a new selective adenosine A_{2A} receptor antagonist in MPTP-treated monkeys. *Neurology*. 52: 1673-1677.
46. Heikkila, R.E. Manzano, L., Cabbat, F.S., Duvoisin, R.C. 1984. Protection against the dopaminergic neurotoxicity of 1-methyl-4-phenyl-1,2,5,6-tetrahydropyridine by monoamine oxidase inhibitors. *Nature*. 311: 467-469.
47. Heikkila, R.E., Hess, A., Duvoisin, R.C. 1984. Dopaminergic neurotoxicity of 1-methyl-4-phenyl-1,2,5,6-tetrahydropyridine in mice. *Science*. 224:1451-1453.
48. Hely, M.A., Morris, J.G., Rail, D., Reid, W.G., O'Sullivan, D.J., Williamson, P.M., Genge, S., Broe, G.A. 1989. The Sydney Multicentre Study of Parkinson's disease: a report on the first 3 years. *Journal of neurology, neurosurgery & psychiatry*. 52: 324-328.
49. Huston, J.P., Haas, H.L., Boix, F., Pfister, M., Decking, U., Schrader, J., Schwarting, R.K. 1996. Extracellular adenosine levels in neostriatum and hippocampus during rest and activity periods of rats. *Neuroscience*. 73: 99-107.
50. Ikeda, K., Kurokawa, M., Aoyama, S., Kuwana, Y. 2002. Neuroprotection by adenosine A_{2A} receptor blockade in experimental models of Parkinson's disease. *Journal of neurochemistry*. 80: 262-270.
51. Impagnatiello, F., Bastia, E., Ongini, A. 2000. Adenosine receptors in neurological disorders. *Emerging therapeutic targets*. 4: 635-664.
52. Inoue, H., Castagnoli, K., van der Schyff, C., Mabic, S., Igarashi, K., Castagnoli, Jr. N. 1999. Species-Dependant differences in monoamine oxidase A and B-catalyzed oxidation of various substituted 1-methyl-4-phenyl-1,2,3,6-tetrahydropyridinyl derivatives. *Journal of pharmacology and experimental therapeutics*. 291: 856-864.
53. Jackson-Lewis, V., Jokowec, M., Burke, R.E., Przedborski, S. 1995 Time course and morphology of dopaminergic neuronal death caused by 1-methyl-4-phenyl-1,2,3,6-tetrahydropyridine. *Neurodegeneration*. 4: 257-269.

54. Jacobson, K.A., Gallo-Rodriguez, C., Melman, N., Fischer, B., Mailard, M., Van Bergen, A., Van Galen, P.J.M., Karton, Y. 1993. Structure-activity relationships of 8-styrylxanthines as A₂-selective adenosine antagonists. *Journal of medicinal chemistry*. 36: 1333-1342.
55. Jankovik, J. 2000. Parkinson's disease therapy: Tailoring choices for early and late disease, young and old patients. *Clinical neurology*. 23: 252-261.
56. Jarvis, M.F., Williams, M. 1989. Direct autoradiographic localization of adenosine A₂ receptors in the rat brain using the A₂-selective agonist, [³H]-CGS 21680. *European journal of pharmacology*. 168: 243-246.
57. Jiang, H., Jackson-Lewis, V., Muthane, U., Dollison, A., Ferreira, M., Espinosa, A., Parsons, B., Przedborski, S. 1993. Adenosine receptor antagonists potentiate dopamine receptor agonist-induced rotational behaviour in 6-hydroxydopamine-lesioned rats. *Brain research*. 613: 347-351.
58. Kakiuchi, S., Rall, T.W., McIlwain, H. 1968. The effect of electrical stimulation upon the accumulation of adenosine 3',5'-phosphate in isolate cerebral tissue. *Journal of neurochemistry*. 16: 485-491.
59. Kanda, T., Jackson, M.J., Smith, L.A., Pearce, R.K.B., Nakamura, J., Kase, H., Kuwana, Y. and Jenner, P. 2000. Combined use of the adenosine A_{2A} antagonist, KW-6002 with L-DOPA or with selective D1 or D2 dopamine agonists increases antiparkinsonian activity but not dyskinesia in MPTP-treated monkeys. *Experimental neurology*. 162: 321-327
60. Kanda, T., Jackson, M.J., Smith, L.A., Pearce, R.K.B., Nakamura, J., Kase, H., Kuwana, Y., Jenner, P. 1998. Adenosine A_{2A} antagonist: a novel antiparkinsonian agent that does not provoke dyskinesia in parkinsonian monkeys. *Annals of neurology*. 43: 507-513.
61. Kanda, T., Shiozaki, S., Shimada, J., Suzuki, F., Nakamura, J. 1994. KF 17837: a novel selective adenosine A_{2A} receptor antagonist with anticataleptic activity. *European journal of medicinal pharmacology*. 256: 263-268.

62. Keddie, J.R., Poucher, S.M., Shaw, G.R., Brooks, R., Collins, M.G. 1996. *In vivo* characterization of ZM 241385, a selective adenosine A_{2A} receptor antagonist. *European journal of pharmacology*. 301: 107-113.
63. Koller, W.C. 1997. Neuroprotective therapy for Parkinson's disease. *Experimental neurology*. 144: 24-28.
64. Koller, W.C., Hubble, J.P. 1990. Levodopa therapy in Parkinson's disease. *Neurology*. 40: 58-61.
65. Kupsch, A., Sautter, J., Gotz, M.E., Breithaupt, W., Schwarz, J., Youdim, M.B., Riederer, P., Gerlach, M., Oertel, W.H. 2001. Monoamine oxidase-inhibition and MPTP-induced neurotoxicity in the non-human primate: comparison of rasagiline (TVP 1012) with selegiline. *Journal of neural transmission*. 108: 985-1009.
66. Kurien, P.N., Pandya, K.C., Surange, V.R. 1934. The condensation of aldehydes with malonic acid in the presence of organic bases. Part I. In the presence of pyridine alone. *Journal of the Indian chemistry society*. 11: 823-826.
67. Kuwana, Y., Shiozaki, S., Kanda, T., Kurokawa, M., Koga, K., Ochi, M., Ikeda, K., Kase, H., Jackson, M.J., Smith, L.A., Pearce, R.K.B. and Jenner, P.G., 1999. Antiparkinsonian activity of adenosine A_{2A} antagonists in experimental models. *Advanced neurology*. 80: 121-123
68. Levy, G., Tang, M.X., Louis, E.D., Cote, L.J., Alfaró, B., Mejia, H., Stern, Y., Marder, K. 2002. The association of incident dementia with mortality in PD. *Neurology*. 59: 1708-1713.
69. Londos, C., Cooper, D.M., Wolff, J. 1980. Subclasses of external adenosine receptors. *Proceedings of the national academy of sciences of the United States of America*. 77: 2551-2554.
70. Luthman, J., Fredriksson, A., Sundstorm, E., Jonsson, G., Archer, T. 1989. Selective lesion of central dopamine or noradrenaline neuron systems in the neonatal rat: motor behavior and monoamine alterations at adult stage. *Behav. Brain Research*. 33: 267-277.

71. MacCollin, M., Peterfreund, R., MacDonald, M., Fink, J.S., Gusella, J. 1994. Mapping of a human A_{2a} adenosine receptor (ADORA2) to chromosome 22. *Genomics*. 20: 332-333.
72. Markey, S.P., Johannessen, J.N., Chiueh, C.C., Burns, R.S., Herkenham, M.A. 1984. Intra-neuronal generation of pyridinium metabolite may cause drug-induced parkinsonism. *Nature*. 31: 464-469.
73. Marsden, C.D., Perkes, J.D., Quinn, N. 1982. Fluctuations in disability in Parkinson's disease: clinical aspects. In: *Marsden, C.D., Fahn, S. Eds; Butterworth Scientific: NY, USA. Movement disorders*. p 96-122.
74. Martinez-Mir, M.I., Probst, A., Palacios, J.M. 1991. Adenosine A₂ receptors selective localization in the human basal ganglia and alterations with disease. *Neuroscience*. 42: 697-706.
75. Morelli, M., Fenu, S., Pinna, A., Di Chiara, G. 1994. Adenosine A₂ receptors interact negatively with dopamine D₁ and D₂ receptors unilaterally 6-hydroxydopamine-lesioned rats. *European journal of pharmacology*. 251: 21-25.
76. Morgante, L., Salemi, G., Meneghini, F., Di Rosa, A.E., Epifanio, A., Grigoletto, F., Ragonese, P., Patti, F., Reggio, A., Di Perri, R., Savettieri, G. 2000. Parkinson's disease survival: a population based study. *Arch. neurology*. 57: 507-512.
77. Morón, J.A., Campillo, M., Perez, V., Unzeta, M., Pardo, L. 2000. Molecular Determinants of MAO Selectivity in a Series of Indolylmethylamine Derivatives: Biological Activities, 3D-QSAR/CoMFA Analysis, and Computational Simulation of Ligand Recognition *Journal of medicinal chemistry*. 43: 1684-1691.
78. Müller, C.E., Geis, U., Hipp, J., Schobert, U., Frobenius, W., Pawlowski, M., Suzuki, F., Sandoval-Ramirez, J. 1997. Synthesis and structure-activity relationships of 3,7-dimethyl-1-propargylxanthine derivatives, A_{2A}-selective adenosine receptor antagonists. *Journal of medicinal chemistry*. 40: 4396-4405.

79. Müller, C.E., Schobert, U., Hipp, J., Geis, U., Frobenius, W., Pawłowski, M. 1998. Configurationally stable analogs of styrylxanthines as A_{2A} adenosine receptor antagonists. *European journal of medicinal chemistry*. 32: 709-719.
80. Nagatsu, T. 2004. Progress in monoamine oxidase (MAO) research in relation to genetic engineering. *Neurotoxicology*. 25: 11-20.
81. Nicklas, W.J., Vyas, I., Heikkila, R.E. 1985. Inhibition of NADH-linked oxidation in brain mitochondria by 1-methyl-4-phenylpyridine, a metabolite of the neurotoxin 1-methyl-4-phenyl-1,2,3,6-tetrahydropyridine. *Life sciences*. 36: 2503-2508.
82. Nimkar, S.K., Anderson, A., Rimoldi, J.M., Stanton, J.M., Castagnoli, K.P., Mabic, S., Wang, Y.-X., Castagnoli, Jr. N. 1996. Synthesis and monoamine oxidase B catalyzed oxidation of C-4 heteroaromatic substituted 1,2,3,6-tetrahydropyridine derivatives. *Chemical research in toxicology*. 9: 1013-1022.
83. Ochi, M., Koga, K., Kurokawa, M., Kase, H., Nakamura, J. and Kuwana, Y., 2000. Systemic administration of adenosine A_{2A} receptor antagonist reverses increased GABA release in the globus pallidus of unilateral 6-hydroxydopamine-lesioned rats: a microdialysis study. *Neuroscience* 100: 53-62.
84. Olah, M., Stiles, G.L. 2000. The role of receptor structure in determining adenosine receptor activity. *Pharmacology & therapeutics*. 85: 55-75.
85. Ongini, E., Adami, M., Ferri, C., Bertorelli, R. 1997. Adenosine A_{2A} receptors and neuroprotection. *Annals of the New York academy of science*. 825: 30-48.
86. Ongini, E., Fredholm, B.B. 1996. Pharmacology of adenosine A_{2A} receptors. *Trends in pharmacological sciences*. 17: 364-372.
87. Ongini, E., Monopoli, A. Cacciari, B., Baraldi, P.G. 2001. Selective adenosine A_{2A} receptor antagonists. *Il farmaco*. 56: 87-90.
88. Palhagen, S., Heinonen, E., Hägglund, J., Kaugesaar, T., Mäki-Ikola, O., Palm, R. 2006. Selegiline slows the progression of the symptoms of Parkinson disease. *Neurology*. 66: 1200-1206.

89. Papesch, V., Schroeder, E.F. 1951. Synthesis of 1-mono- and 1,3-disubstituted 6-aminouracils. Diuretic activity. *Journal of organic chemistry*. 16: 1879-1890.
90. Parker, W.D., Jr., Boyson, S.J., Parks, J.K. 1989. Abnormalities of the electron transport chain in idiopathic Parkinson's disease. *Annals of neurology*. 26: 719-723.
91. Peterfreund, R.A., MacCollin, M., Gusella, J., Fink, J.S. 1996. Characterization and expression of the human A_{2a} adenosine receptor gene. *Journal of neurochemistry*. 66: 362-368.
92. Petzer, J.P., Steyn, S., Castagnoli, K.P., Chen, J.-F., Schwarzschild, M.A., Van der Schyf, C.J., Castagnoli, N. 2003. Inhibition of monoamine oxidase B by selective adenosine A_{2A} receptor antagonists. *Bioorganic & medicinal chemistry*. 11: 1299-1310.
93. Poacher, S.M., Keddie, J.R., Singh, P., Stoggall, S.M., Caulkett, P.W.R., Jones, G., Collins, M.G. 1995. The *in vitro* pharmacology of ZM 241385, a potent, non xanthine, A_{2A} selective adenosine receptor antagonist. *British journal of pharmacology*. 115: 1096-1102.
94. Pollack, A.E., Harrison, M.B., Wooten, F.G., Fink, S.J. 1993. Differential localization of A_{2A} adenosine receptor mRNA with D₁ and D₂ dopamine receptor mRNA in striatal output pathways following a selective lesion of striato-nigral neurons. *Brain research*. 115: 1096-1102.
95. Przedborski, S., Dauer, W. 2003. Parkinson's disease: Mechanisms and Models. *Neuron*. 39: 889-909.
96. Rabey, J.M., Sagi, L., Huberman, M., Melamed, E., Korezyn, A., Giladi, M., Inzeberg, R., Djaldetti, R., Klein, C., Berecz, G. 2000. Rasagiline mesylate, a new MAO-B inhibitor for the treatment of Parkinson's disease: a double-blind study as adjunctive therapy to levodopa. *Clinical neuropharmacology*. 23: 324-330.
97. Raha, S., and Robinson, B.H. 2001. Mitochondria, oxygen free radicals, and apoptosis. *American journal of medical genetics*. 106: 62-70.

98. Ramsay, R.R., Krueger, M.J., Youngster, S.K., Gluck, M.R., Casuda, J.E., Singer, T.P. 1991. Interaction of 1-methyl-4-phenylpyridinium ion (MPP⁺) and its analogs with the rotenone/piericidin binding site of NADH dehydrogenase. *Journal of neurochemistry*. 56: 1184-1190.
99. Robinson, B.H. 1998. Human Complex I deficiency: Clinical spectrum and involvement of oxygen free radicals in the pathogenicity of the defect. *Biochemica et biophysica acta*, 1364: 271-286.
100. Salach, J., Weyler, J. 1987. Preparation of the flavin-containing aromatic amine oxidases of human placenta and beef liver. *Methods in enzymology*. 142: 627-637.
101. Sattin, A., & Rall, T.W. 1970. The effects of adenosine and adenine nucleotides on the cyclic adenosine 3', 5' phosphate content of guinea pig cerebral cortex slices. *Molecular pharmacology*. 6: 13-23.
102. Schiffman, S.N., Libert, F., Vassart, G., Vanderhaegen, J.-J. 1991. Distribution of adenosine A₂ receptor mRNA in the human brain. *Neuroscience letters*. 130: 177-180.
103. Schubert, P., Komp, W., Kreutzberg, G.W. 1979. Correlation of 5'-nucleotidase activity and selective transneuronal transfer of adenosine in the hippocampus. *Brain research*. 168: 419-424.
104. Segel, I. H. 1993. *Enzyme kinetics*. Wiley, New York. Pp. 100-125.
105. Shih, J.C., Chen, K., Ridd, M.J. 1999. Monoamine oxidase: From genes to behavior. *Annual review of neuroscience*. 22: 197-217.
106. Shimada, J., Koike, N., Nonaka, H., Shiozaki, S., Yanagawa, K., Kanada, T., Kobayashi, H., Fumio, S. 1997. Adenosine A_{2A} antagonists with potent anti-cataleptic activity. *Bioorganic & medicinal chemistry letters*. 7: 2349-2352.
107. Shimada, J., Suzuki, F. 2000. Medicinal chemistry of adenosine receptors in brain periphery. Chapter 3. 31-48.
108. Shimada, J., Suzuki, F., Nonaka, H., Ishii, A. 1992. 8-Polycycloalkyl-1,3-dipropylxanthines as potent and selective antagonists for A₁-adenosine receptors. *Journal of medicinal chemistry*. 35: 924-930.

References

109. Shimizu, K., Ohtaki, K., Matsubara, K., Aoyama, K., Uezono, T., Saito, O., Suno, M., Ogawa, K., Hayase, N., Kimura, K., Shiono, H. 2001. Carrier-mediated processes in blood-brain barrier penetration and neural uptake of paraquat. *Brain research*. 906: 135-142.
110. Shiozaki, S., Ichikawa, S., Nakamura, J., Kitamura, S., Yamada, K., Kuwana, Y. 1999. Actions of adenosine A_{2A} receptor antagonist KW-6002 on drug-induced catalepsy and hypokinesia caused by reserpine or MPTP. *Psychopharmacology*. 147: 90-95.
111. Sirinthsinghji, D.J., Kupsch, A., Mayer, E., Zivin, M., Pufal, D., Oertel, W.H. 1992. Cellular localization of tyrosine hydroxylase mRNA and cholecystokinin mRNA-containing cells in the ventral mesencephalon of the common marmoset: effects of 1-methyl-4-phenyl-1,2,3,6-tetrahydropyridine. *Molecular brain research*. 12:267-274.
112. Speer, J.H., Raymond, A.L., 1953. Some alkyl homologues of theophylline. *Journal of the American chemical society*. 75: 114-115.
113. Suzuki, F., Shimada, J., Shiozaki, S., Ichikawa, S., Ishii, A., Nakamura, J., Nonaka, H., Kobayashi, H., Fuse, E. 1993. Adenosine A₁ antagonists. 3. Structure-activity relationships on amelioration against scopolamine- or N⁶-(R-phenylisopropyl)adenosine-induced cognitive disturbance. *Journal of medicinal chemistry*. 36: 2508-2518.
114. Talpade, D.J., Greene, J.G., Higgins, D.S., Jr., Greenamyre, J.T. 2000. *In vivo* labeling of mitochondrial complex I (NADH:ubiquinone oxidoreductase) in rat brain using [(3)H]dihydrorotenone. *Journal of neurochemistry*. 75: 2611-2621.
115. Tatton, W.G. 1993. Selegiline can mediate neuronal rescue rather than neuronal protection. *Movement disorders*. 8:20-30.
116. Tatton, W.G., Greenwood, C.E. 1991. Rescue of dying neurons a new action of deprenyl in MPTP parkinsonism. *Journal of neuroscience research*. 30: 666-667.
117. The Parkinson Study Group. 1989. Effect of lazabemide on the progression of disability in early Parkinson's disease. *Annals of neurology*. 40: 99-107

118. Traube, W. 1900. Der synthetische aufbau der harnsäure, des xanthines, theobromins, theophyllins und caffeïns aus der cyanessigsäure. *Chemische Berichte*. 33: 3035-3056.
119. Triplett, J.W., Mack, S.W., Smith, S.L., Digenis, G.A. 1978. Synthesis of carbon-13 labeled uracil,6,7-dimethylumzaine, and lumichrome, via a common intermediate: cyanoacetylurea. *Journal of labeled compounds and radiopharmaceuticals*. 14: 35-41.
120. Van den Berg, D., Zoellner, K. R., Ogunrombi, M.O., Malan, S.F., Terre'Blanche, G., Castagnoli, Jr., N., Bergh, J.J., Petzer, J.P. 2007. Inhibition of monoamine oxidase B by selected benzimidazole and caffeine analogues. *Bioorganic & medicinal chemistry*. 15: 3692-3702.
121. Vlok, N., Malan, S.F., Castagnoli, Jr., N., Bergh, J.J., Petzer, J.P. 2006. Inhibition of monoamine oxidase B by analogues of the adenosine A_{2A} receptor antagonist (*E*)-8-(3-chlorostyryl)caffeine (CSC). *Bioorganic & medicinal chemistry*. 14: 3512-3521.
122. Wakeyama, H., Takeshige, K., Takayanagi, R., Minakami, S. 1982. Superoxide- forming NADPH oxidase preparation of pig polymorphnuclear leukocytes. *Biochemical journal*. 205: 593-601.
123. Waldmeier, P.C. 1987. Amine oxidases and their endogenous substrates. *Journal of neural transmission*. 22: 55-72.
124. Wallace, D.C., 1999. Mitochondrial disease in man and mouse. *Science*. 283:1482-1488.
125. Werbel, L. M., Headen, M., Elslager, E.F. 1967. 5-Phenyl-2,4-pentadienamides as Potential Antimalarial Agents. *Journal of medicinal chemistry*. 10: 366-370.
126. Wu, R.M., Chieuh, C.C., Pert, A., Murphy, D.L. 1993. Apparent antioxidant effect of L-deprenyl on hydroxyl radical formation and nigral injury elicited by MPP⁺ in vivo. *European journal of pharmacology*. 243: 241-247.
127. Yamada, M., Yasuhara, H. 2004. Clinical pharmacology of MAO inhibitors: safety and future. *Neurotoxicology*. 25: 215-221.

References

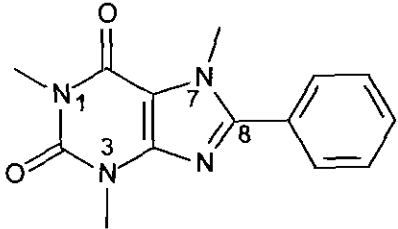
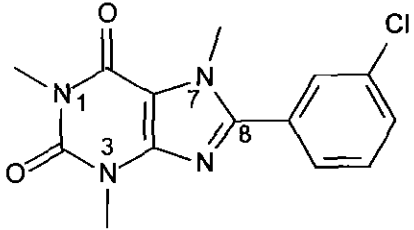
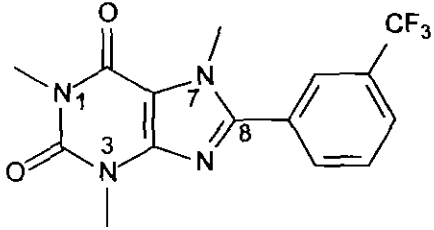
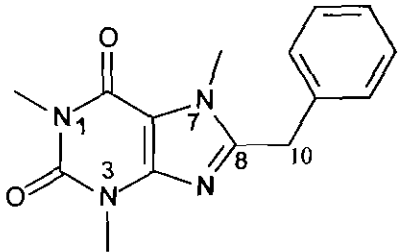
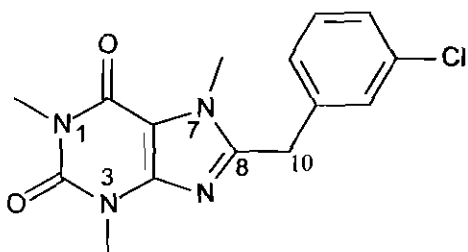
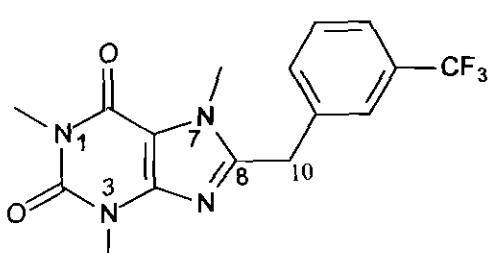
128. Zhou, Z., Ding, H., Qin, F., Lui, L., Cheng, S. 2003. Effect of Zn²⁺-metallothionein on oxidative stress in liver of rats with severe thermal injury. *Acta pharmacologica sinica*. 24: 764-770.
129. Zocchi, C., Ongini, E., Conti, A., Monopoli, A., Negretti, A., Baraldi, P.G., Dionisotti, S. 1996. The non xanthine heterocyclic compound SCH 58261 is a new potent and selective A_{2A} adenosine receptor antagonist. *Journal of pharmacology and experimental therapeutics*. 276: 398-404.
130. Zocchi, C., Ongini, E., Ferrara, S., Baraldi, P.G., Dionisotti, S. 1996. Binding of the radioligand [³H]-SCH 58261, a new non xanthine A_{2A} adenosine receptor antagonist, to rat striatal membranes. *British journal of pharmacology*. 117: 1381-1386.

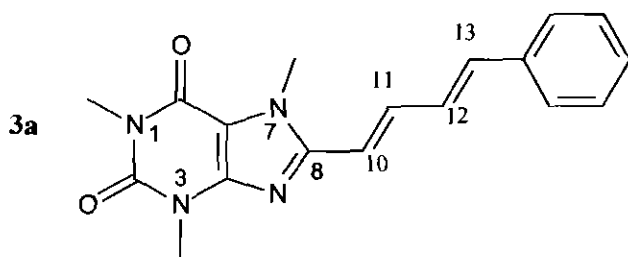
Appendix A

$^1\text{H-NMR}$ and $^{13}\text{C-NMR}$

- a) $^1\text{H-NMR}$ 8-phenylcaffeine (**1a**)
- b) $^{13}\text{C-NMR}$ 8-phenylcaffeine (**1a**)
- c) $^1\text{H-NMR}$ 8-(3-Chlorophenyl)caffeine (**1b**)
- d) $^{13}\text{C-NMR}$ 8-(3-Chlorophenyl)caffeine (**1b**)
- e) $^1\text{H-NMR}$ 8-(3-Trifluoromethylphenyl)caffeine (**1c**)
- f) $^{13}\text{C-NMR}$ 8-(3-Trifluoromethylphenyl)caffeine (**1c**)
- g) $^1\text{H-NMR}$ 8-benzylcaffeine (**2a**)
- h) $^{13}\text{C-NMR}$ 8-benzylcaffeine (**2a**)
- i) $^1\text{H-NMR}$ 8-(3-Chlorobenzyl)caffeine (**2b**)
- j) $^{13}\text{C-NMR}$ 8-(3-Chlorobenzyl)caffeine (**2b**)
- k) $^1\text{H-NMR}$ 8-(3-Trifluorobenzyl)caffeine (**2c**)
- l) $^{13}\text{C-NMR}$ 8-(3-Trifluorobenzyl)caffeine (**2c**)
- m) $^1\text{H-NMR}$ (E,E)-8-(4-Phenylbutadien-1-yl)caffeine (**3a**)
- n) $^{13}\text{C-NMR}$ (E,E)-8-(4-Phenylbutadien-1-yl)caffeine (**3a**)
- o) $^1\text{H-NMR}$ (E,E)-8-[4-(3-Chlorophenylbutadien-1-yl)]caffeine (**3b**)
- p) $^{13}\text{C-NMR}$ (E,E)-8-[4-(3-Chlorophenylbutadien-1-yl)]caffeine (**3b**)
- q) $^1\text{H-NMR}$ (E,E)-8-[4-(3-Bromophenylbutadien-1-yl)]caffeine (**3c**)
- r) $^{13}\text{C-NMR}$ (E,E)-8-[4-(3-Bromophenylbutadien-1-yl)]caffeine (**3c**)
- s) $^1\text{H-NMR}$ (E,E)-8-[4-(3-Fluorophenylbutadien-1-yl)]caffeine (**3d**)
- t) $^{13}\text{C-NMR}$ (E,E)-8-[4-(3-Fluorophenylbutadien-1-yl)]caffeine (**3d**)
- u) $^1\text{H-NMR}$ (E,E)-1,3-Dimethyl-8-(4-phenylbutadien-1-yl)-7-ethylxanthine (**3e**)
- v) $^{13}\text{C-NMR}$ (E,E)-1,3-Dimethyl-8-(4-phenylbutadien-1-yl)-7-ethylxanthine (**3e**)
- w) $^1\text{H-NMR}$ (E,E)-1,3-Diethyl-8-(4-phenylbutadien-1-yl)-7-methylxanthine (**3f**)
- x) $^{13}\text{C-NMR}$ (E,E)-1,3-Diethyl-8-(4-phenylbutadien-1-yl)-7-methylxanthine (**3f**)
- y) $^1\text{H-NMR}$ (E,E)-1,3-Diethyl-8-(4-phenylbutadien-1-yl)-7-ethylxanthine (**3g**)
- z) $^{13}\text{C-NMR}$ (E,E)-1,3-Diethyl-8-(4-phenylbutadien-1-yl)-7-ethylxanthine (**3g**)

Table A.1 A summary of the $^1\text{H-NMR}$.

Structure	$^1\text{H-NMR}$ signal assignment
<p>1a</p> 	<p>a. Methyl groups at N-1, N-3 and N-7 – singlets at 3.38, 3.58 and 4.01 ppm.</p> <p>b. Aromatic protons – multiplets at 7.47–7.50 (3H) and 7.63–7.67 (2H) ppm.</p>
<p>1b</p> 	<p>a. Methyl groups at N-1, N-3 and N-7 – singlets at 3.39, 3.58 and 4.04 ppm.</p> <p>b. Aromatic protons – multiplets at 7.43–7.48 (2H), 7.53–7.56 (1H) and 7.67–7.69 (1H) ppm.</p>
<p>1c</p> 	<p>a. Methyl groups at N-1, N-3 and N-7 – singlets at 3.39, 3.59 and 4.05 ppm.</p> <p>b. Aromatic protons – multiplets at 7.61–7.67 (1H), 7.73–7.77 (1H), 7.84–7.88 (1H) and 7.95–7.96 (1H) ppm.</p>
<p>2a</p> 	<p>a. Methyl groups at N-1, N-3 and N-7 – singlets at 3.35, 3.56 and 3.77 ppm.</p> <p>b. Methylene group at C-10 – singlet at 4.12 ppm.</p> <p>c. Aromatic protons – multiplet at 7.12–7.30 ppm (5H).</p>
<p>2b</p> 	<p>a. Methyl groups at N-1, N-3 and N-7 – singlets at 3.36, 3.56 and 3.79 ppm.</p> <p>b. Methylene group at C-10 – singlet at 4.10 ppm.</p> <p>c. Aromatic protons – multiplets at 7.02–7.15 (1H), 7.14–7.16 (1H) and 7.21–7.24 (2H) ppm.</p>
<p>2c</p> 	<p>a. Methyl groups at N-1, N-3 and N-7 – singlets at 3.36, 3.55 and 3.81 ppm.</p> <p>b. Methylene group at C-10 – singlet at 4.18 ppm.</p> <p>c. Aromatic protons – multiplet at 7.34–7.52 ppm (4H).</p>

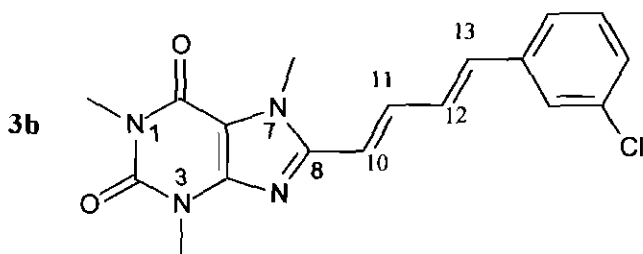


a. Methyl groups at N-1, N-3 and N-7 – singlets at 3.37, 3.58 and 3.96 ppm.

b. Methinyl proton at C-10/13 – doublet at 6.44 ppm. Trans geometry – $J = 15.0$ Hz.

c. Methinyl proton at C-11/12 – doublet of doublets at 7.56 ppm. Trans geometry – $J = 15.0$ Hz.

d. Aromatic protons and other two methinyl protons – multiplets at 6.84–6.95 (2H), 7.24–7.36 (3H), 7.42–7.46 (2H) ppm.



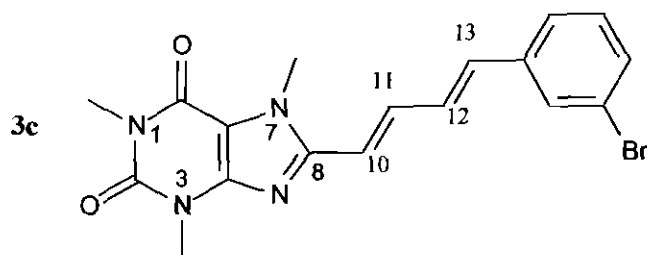
a. Methyl groups at N-1, N-3 and N-7 – singlets at 3.39, 3.59 and 3.99 ppm.

b. Methinyl proton at C-10/13 – doublet at 6.49 ppm. Trans geometry – $J = 15.0$ Hz.

c. Methinyl proton at C-10/13 – doublet at 6.80 ppm. Trans geometry – $J = 15.5$ Hz.

d. Methinyl proton at C-11/12 – doublet of doublets at 7.55 ppm. Trans geometry – $J = 14.7$ Hz.

e. Aromatic protons and other methinyl proton at C-11/12 – multiplets at, 7.24–7.31 (4H), doublet at 7.44 (1H) ppm.



a. Methyl groups at N-1, N-3 and N-7 – singlets at 3.38, 3.58 and 3.98 ppm.

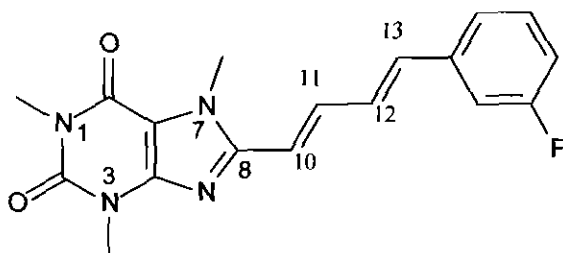
b. Methinyl proton at C-10/13 – doublet at 6.49 ppm. Trans geometry – $J = 15.0$ Hz.

c. Methinyl proton at C-10/13 – doublet at 6.78 ppm. Trans geometry – $J = 15.5$ Hz.

d. Methinyl proton at C-11/12 – doublet of doublets at 6.95 ppm. Trans geometry – $J = 15.5$ Hz.

e. Methinyl proton at C-11/12 – doublet

3d



of doublets at 7.55 ppm. Trans geometry
– J = 14.6 Hz.

f. Aromatic protons – multiplets at 7.17–
7.22 (1H), 7.33–7.40 (2H), doublet at
7.59 (1H) ppm.

a. Methyl groups at N-1, N-3 and N-7 –
singlets at 3.22, 3.44 and 3.95 ppm.

b. Methinyl proton at C-10/13 – doublet
at 6.87 ppm. Trans geometry – J = 15.0
Hz.

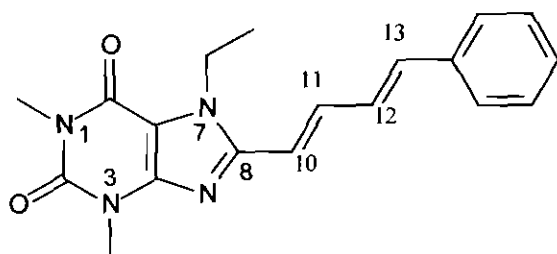
c. Methinyl proton at C-10/13 – doublet
at 7.01 ppm. Trans geometry – J = 15.4
Hz.

d. Methinyl proton at C-11/12 – doublet
of doublets at 7.26 ppm. Trans geometry
– J = 15.0 Hz.

e. Methinyl proton at C-11/12 – doublet
of doublets at 7.47 ppm. Trans geometry
– J = 14.6 Hz.

f. Aromatic protons – multiplets at 7.03–
7.15 (1H) and 7.35–7.44 (3H) ppm.

3e



a. Methyl group at N-7 – triplet at 1.46
ppm.

b. Methyl groups at N-1 and N-3 –
singlets at 3.43 and 3.63 ppm.

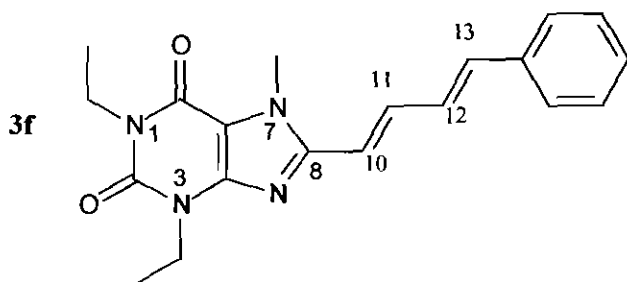
c. Methylene groups at N-7 – quartet at
4.45 ppm.

d. Methinyl proton at C-10/13 – doublet
at 6.50 ppm. Trans geometry – J = 14.9
Hz.

e. Methinyl proton at C-10/13 – doublet
at 6.92 ppm. Trans geometry – J = 15.5
Hz.

f. Methinyl proton at C-11/12 – doublet
of doublets at 7.01 ppm. Trans geometry
– J = 15.5 Hz.

g. Methinyl proton at C-11/12 – doublet
of doublets at 7.63 ppm. Trans geometry



- J = 14.9 Hz.

h. Aromatic protons – triplets at 7.31 (1H) and 7.38 (2H) and doublet at 7.49 (2H) ppm.

a. Methyl groups at N-1/3 – triplets at 1.19 and 1.30 ppm.

b. Methyl groups at N-7 – singlet at 3.93 ppm.

c. Methylene groups at N-1/3 – quartets at 4.01 and 4.13 ppm.

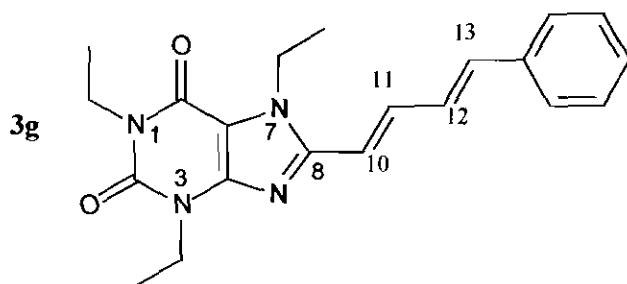
d. Methinyl proton at C-10/13 – doublet at 6.41 ppm. Trans geometry – J = 15.0 Hz.

e. Methinyl proton at C-10/13 – doublet at 6.84 ppm. Trans geometry – J = 15.5 Hz.

f. Methinyl proton at C-11/12 – doublet of doublets at 6.92 ppm. Trans geometry – J = 15.5 Hz.

g. Methinyl proton at C-11/12 – doublet of doublets at 7.53 ppm. Trans geometry – J = 14.9 Hz.

h. Aromatic protons – multiplet at 7.23 (1H), triplet at 7.30 (2H) and doublet at 7.40 (2H) ppm.



a. Methyl groups at N-1/3 – triplets at 1.19 and 1.31 ppm.

b. Methyl groups at N-7 – triplet at 1.38 ppm.

c. Methylene groups at N-1/3 – quartets at 4.01 and 4.13 ppm.

c. Methylene groups at N-7 – quartet at 4.36 ppm.

d. Methinyl proton at C-10/13 – doublet at 6.41 ppm. Trans geometry – J = 14.9 Hz.

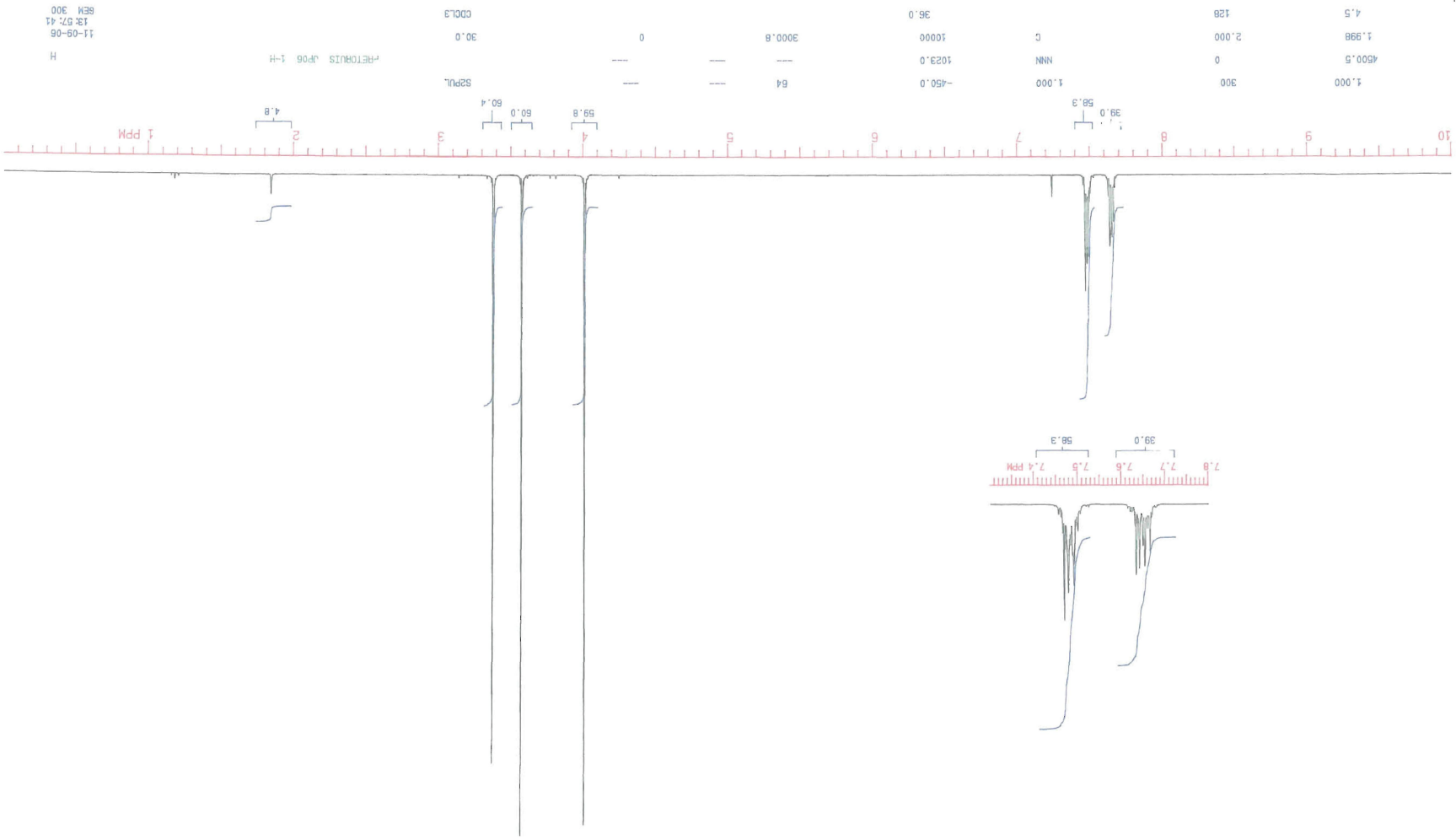
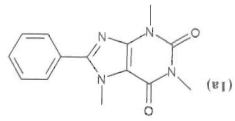
e. Methinyl proton at C-10/13 – doublet at 6.84 ppm. Trans geometry – J = 15.5

Hz.

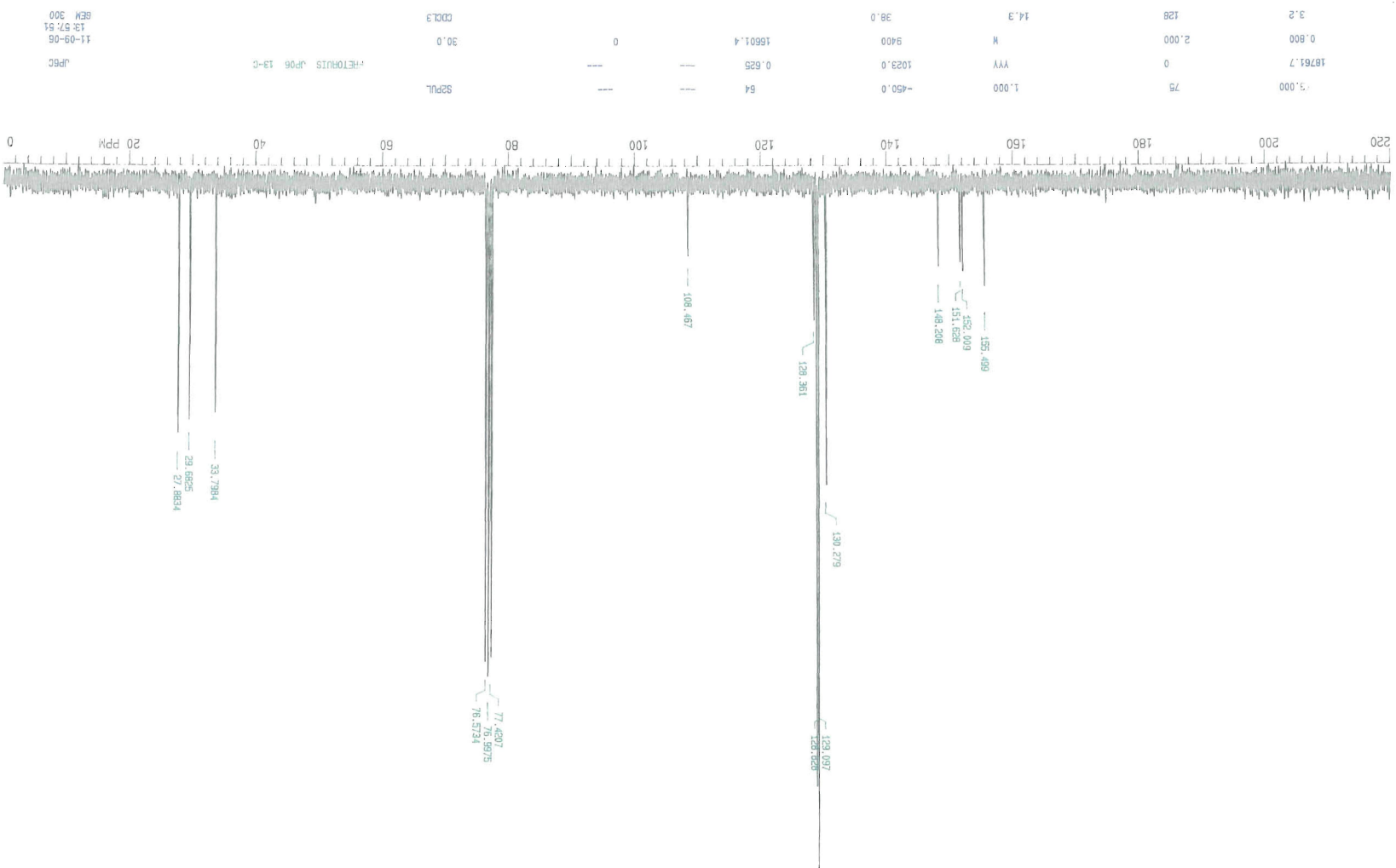
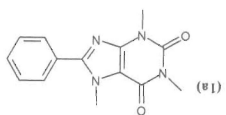
f. Methinyl proton at C-11/12 – doublet of doublets at 6.93 ppm. Trans geometry – J = 15.5 Hz.

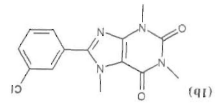
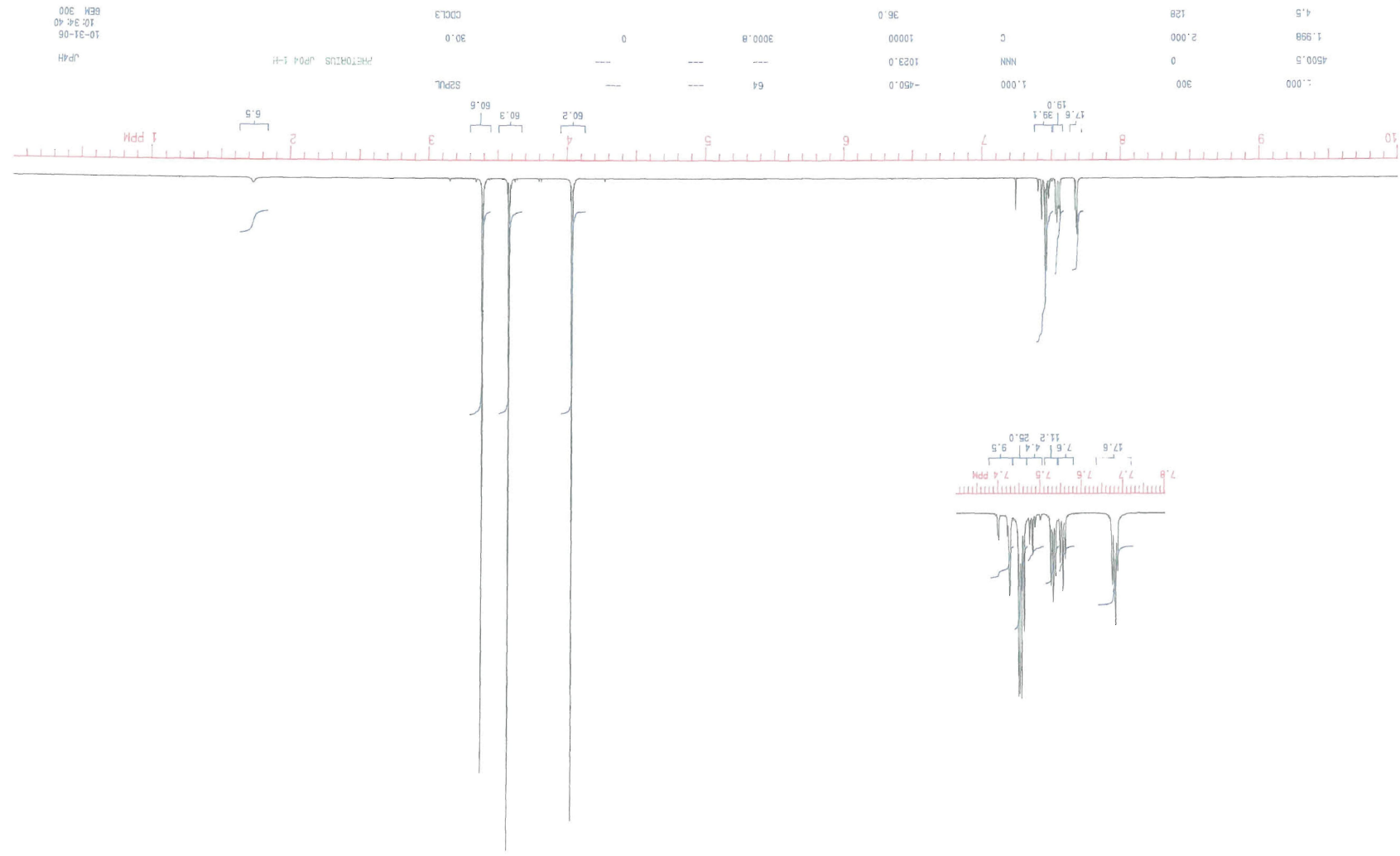
g. Methinyl proton at C-11/12 – doublet of doublets at 7.55 ppm. Trans geometry – J = 14.9 Hz.

h. Aromatic protons – multiplet at 7.22 (1H), triplet at 7.29 (2H) and doublet at 7.41 (2H) ppm.

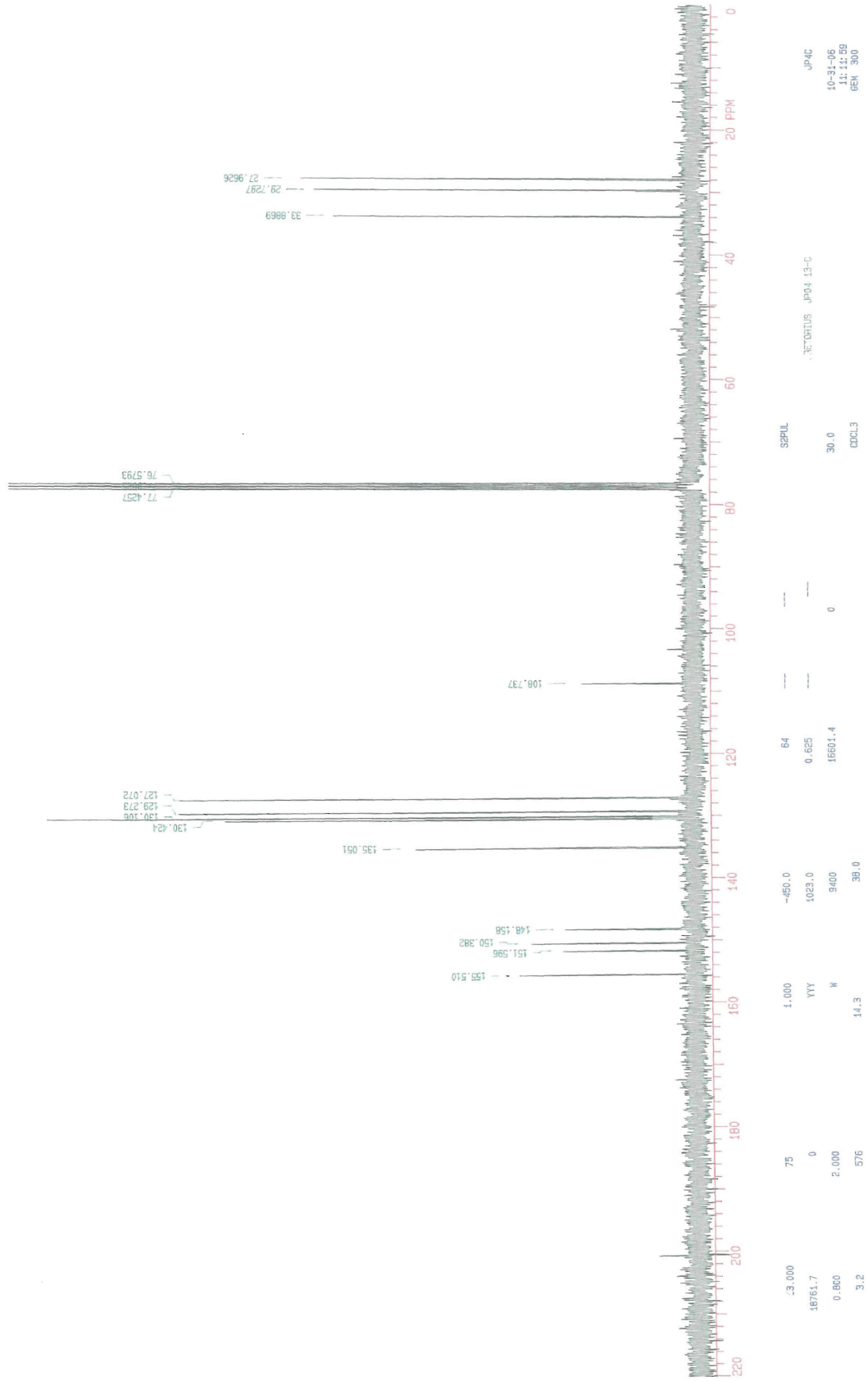
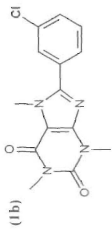


Appendix A

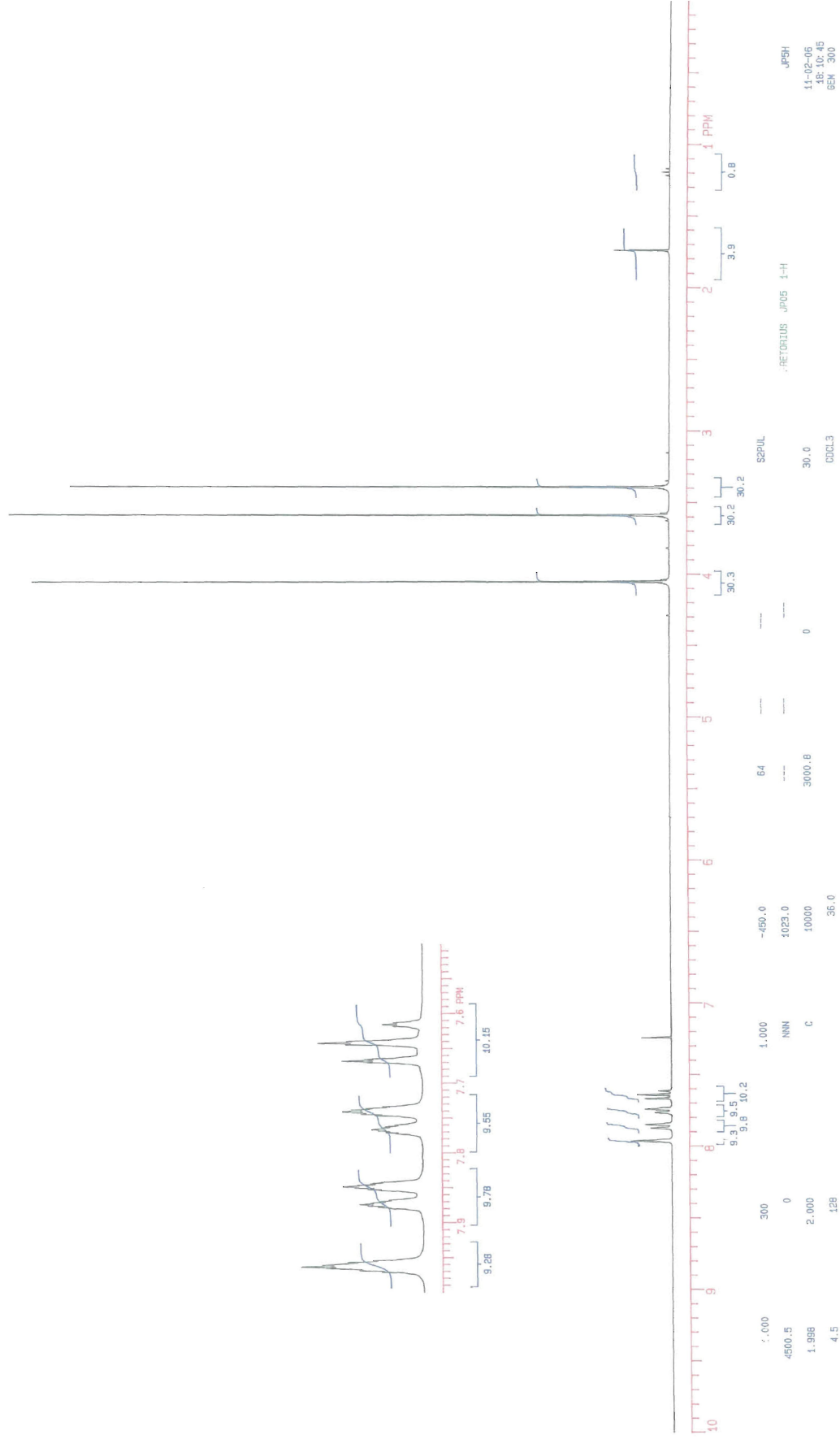
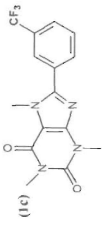




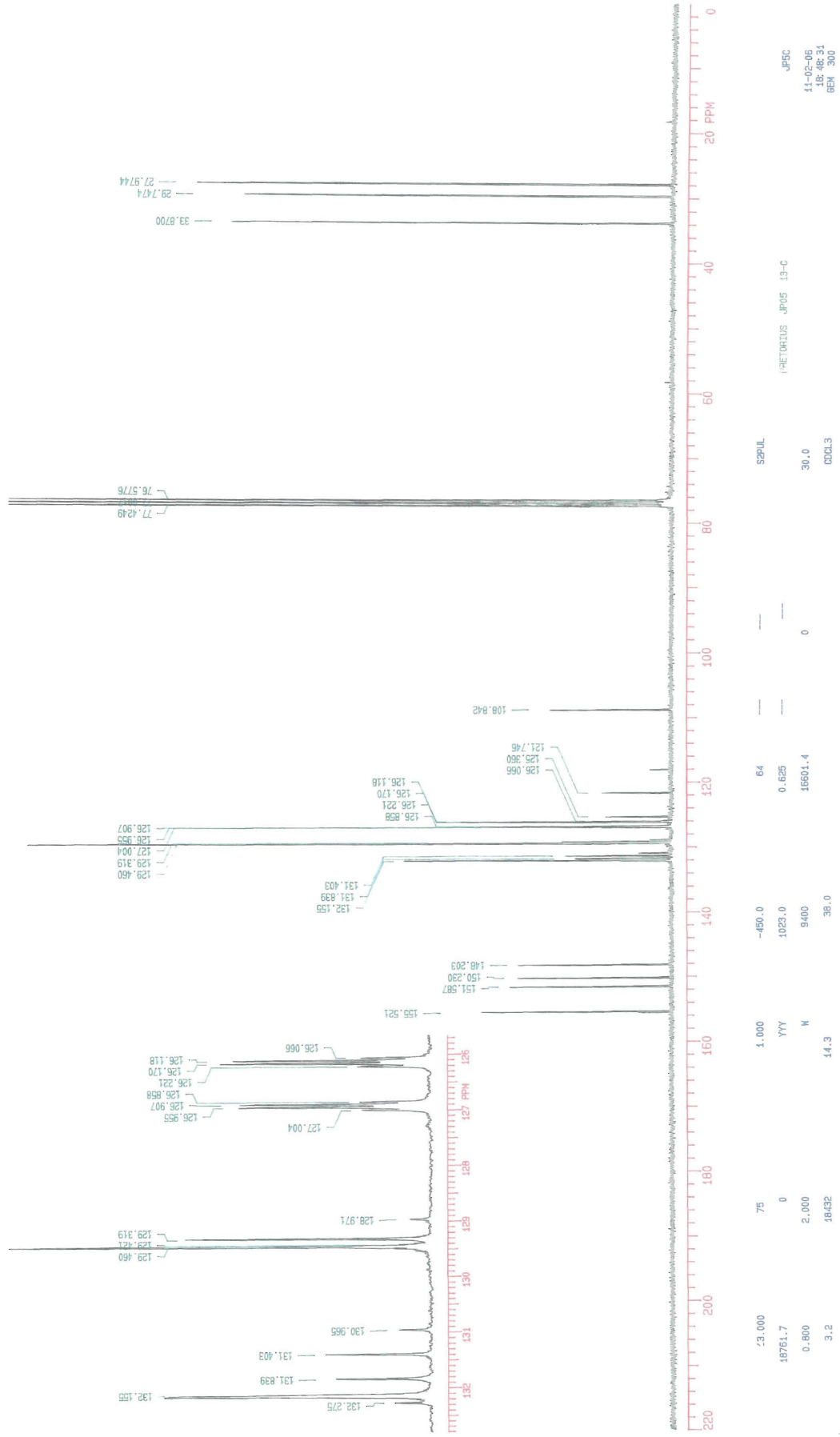
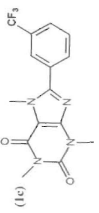
Appendix A



Appendix A



Appendix A



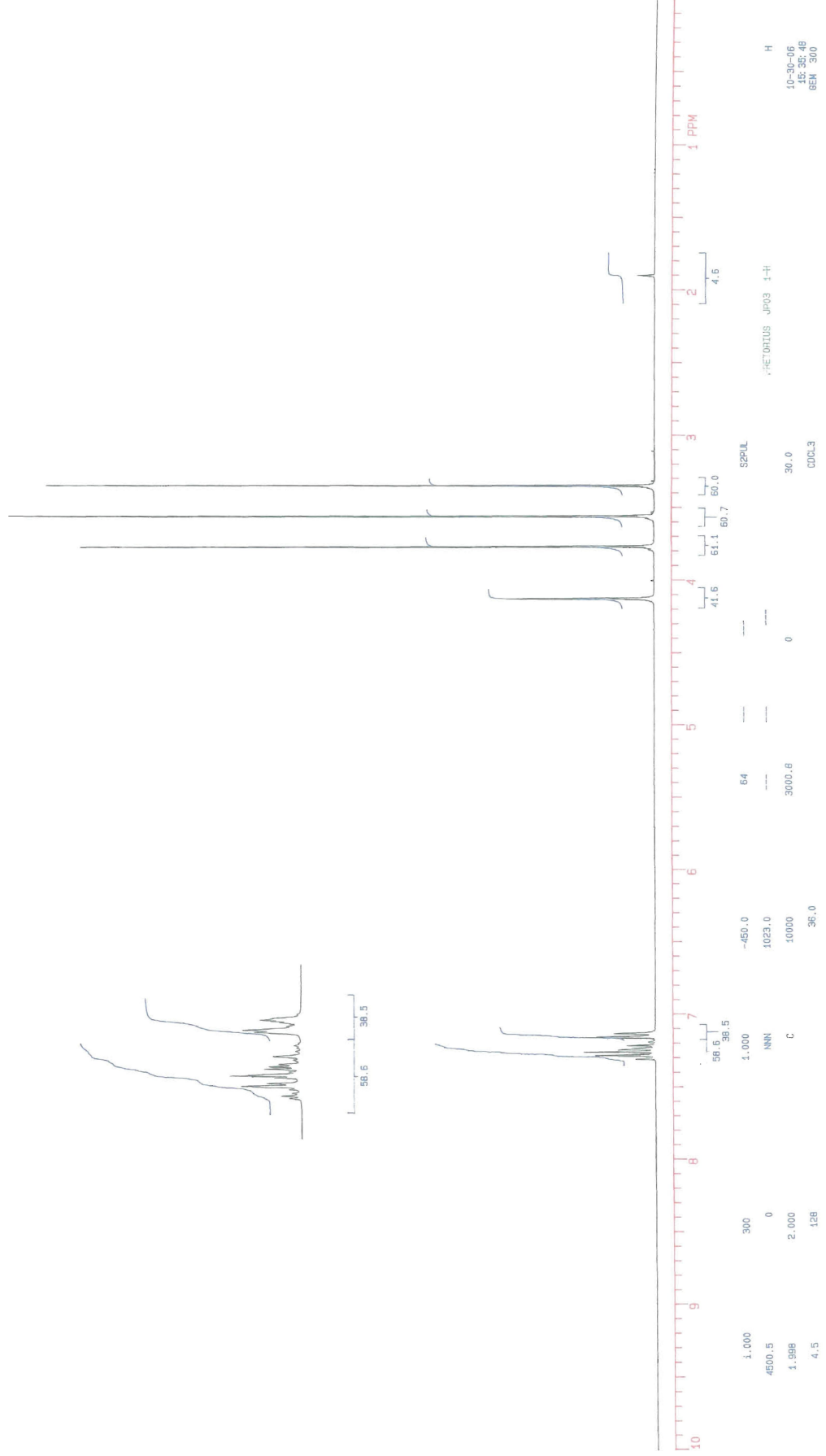
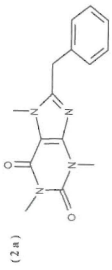
JPSC
14-02-05
18/03/1
GEN 300

RETORTIUS JP05 13-C
30.0
CDCl3

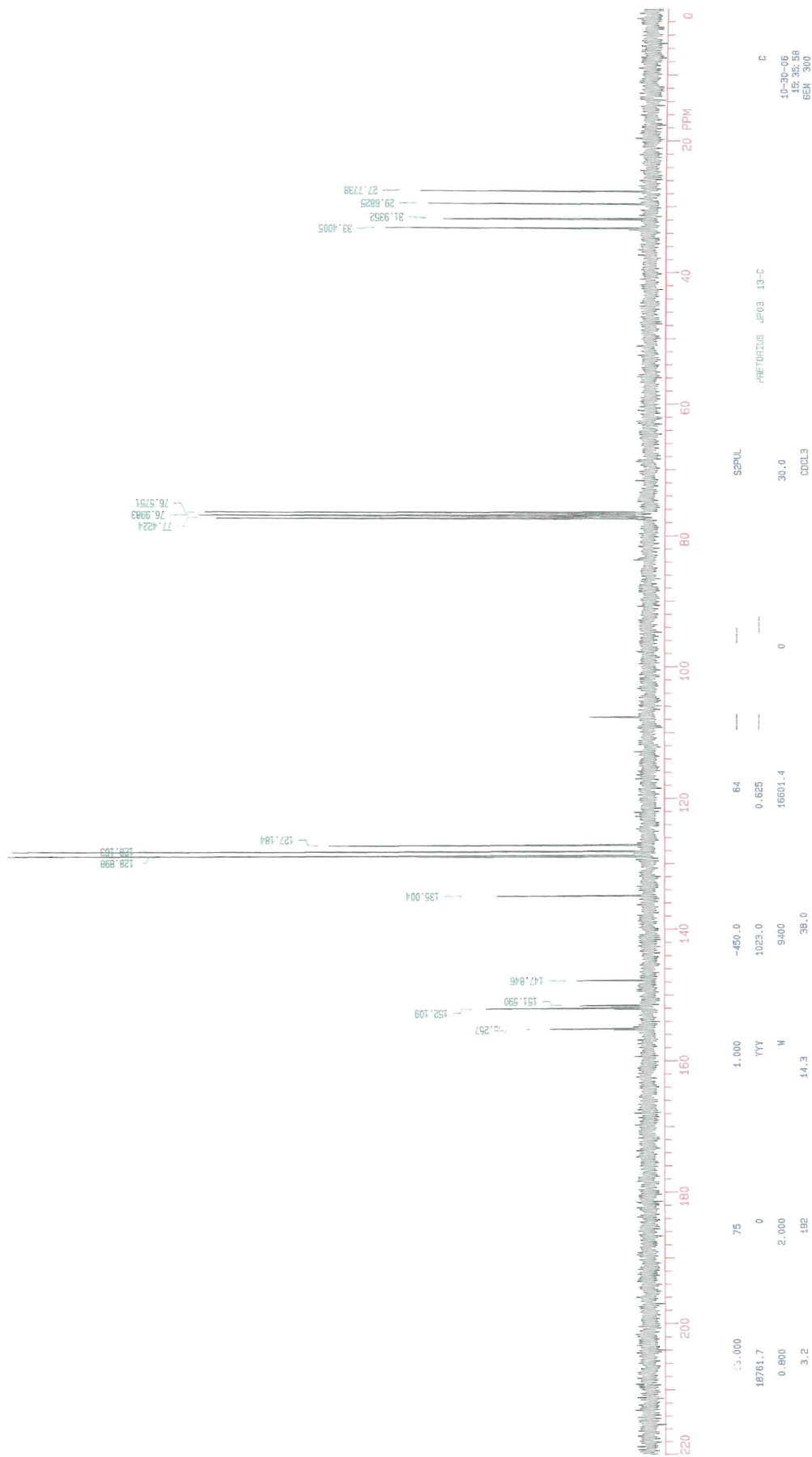
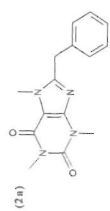
64
0.625
16501.4

1.000
YYY
W
14.3

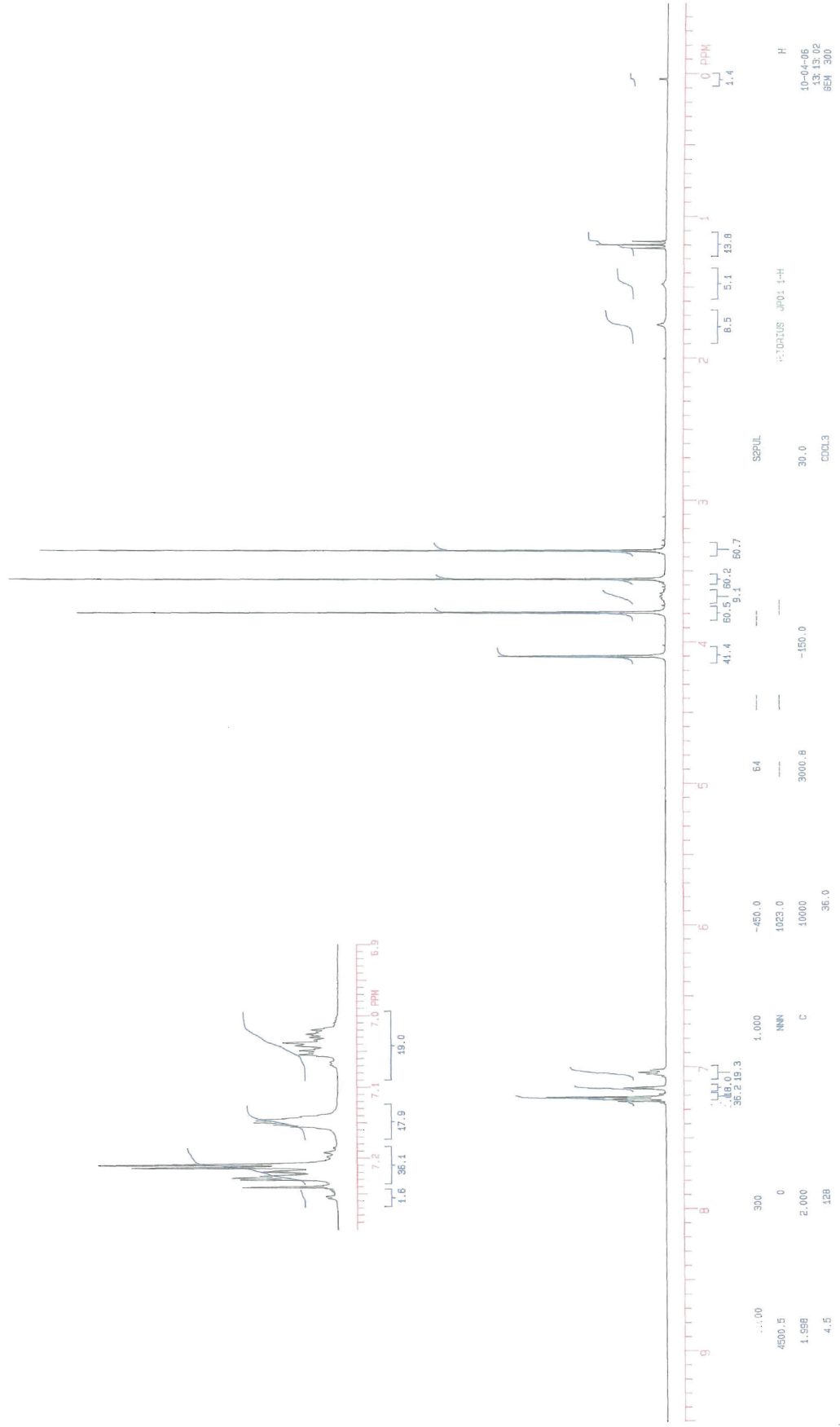
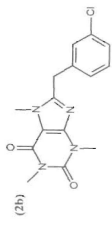
Appendix A



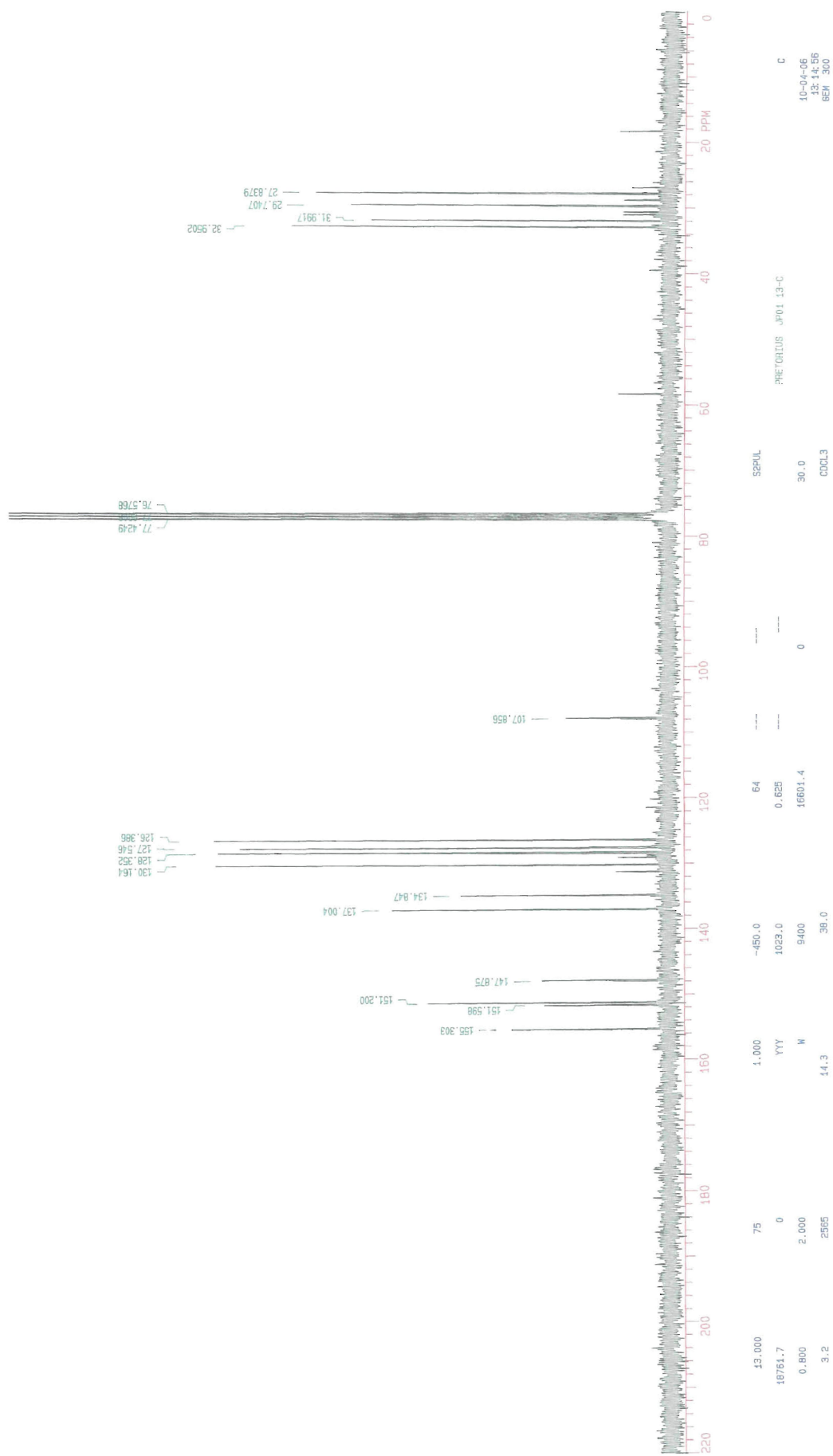
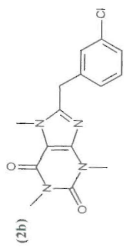
Appendix A



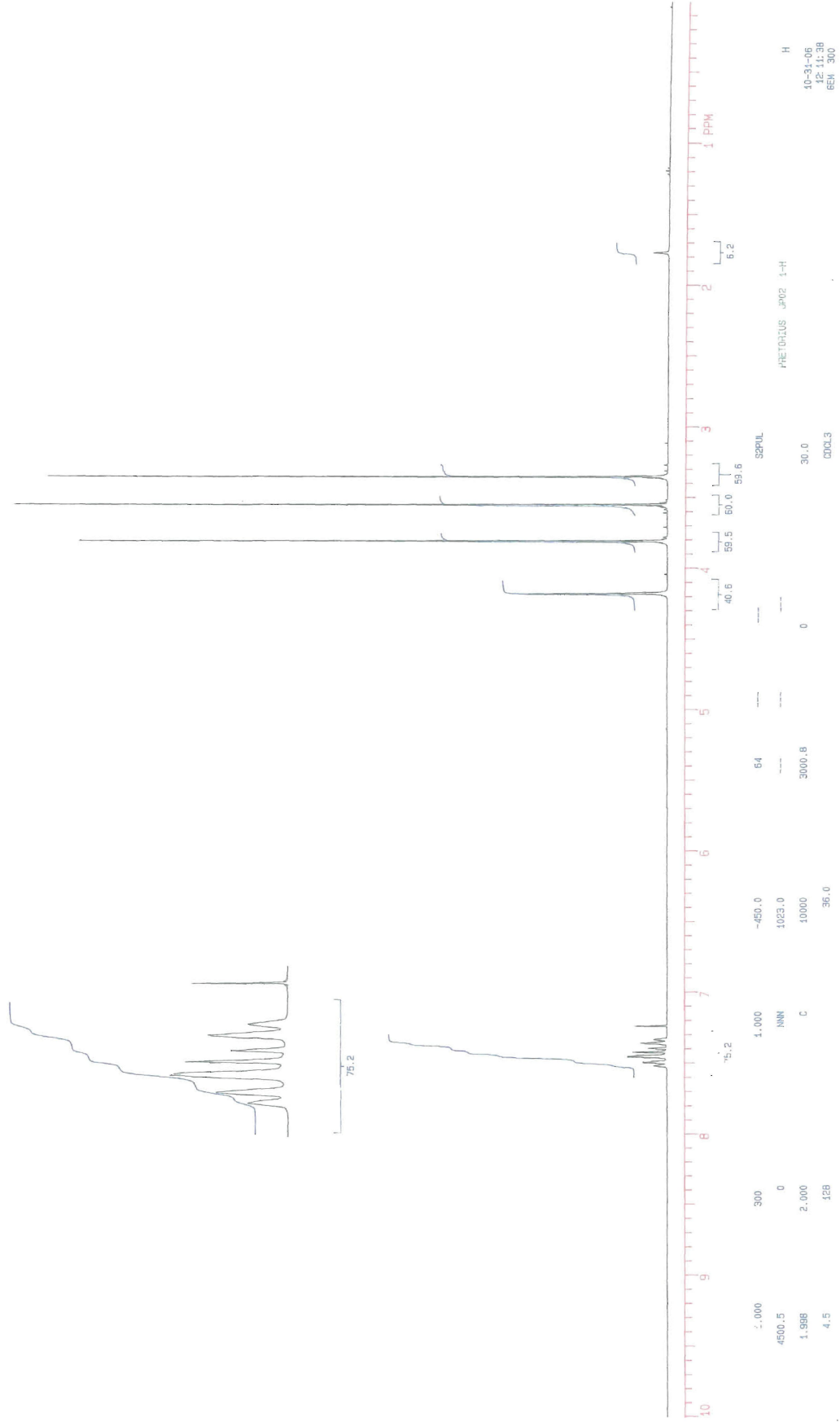
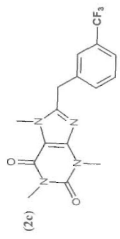
Appendix A



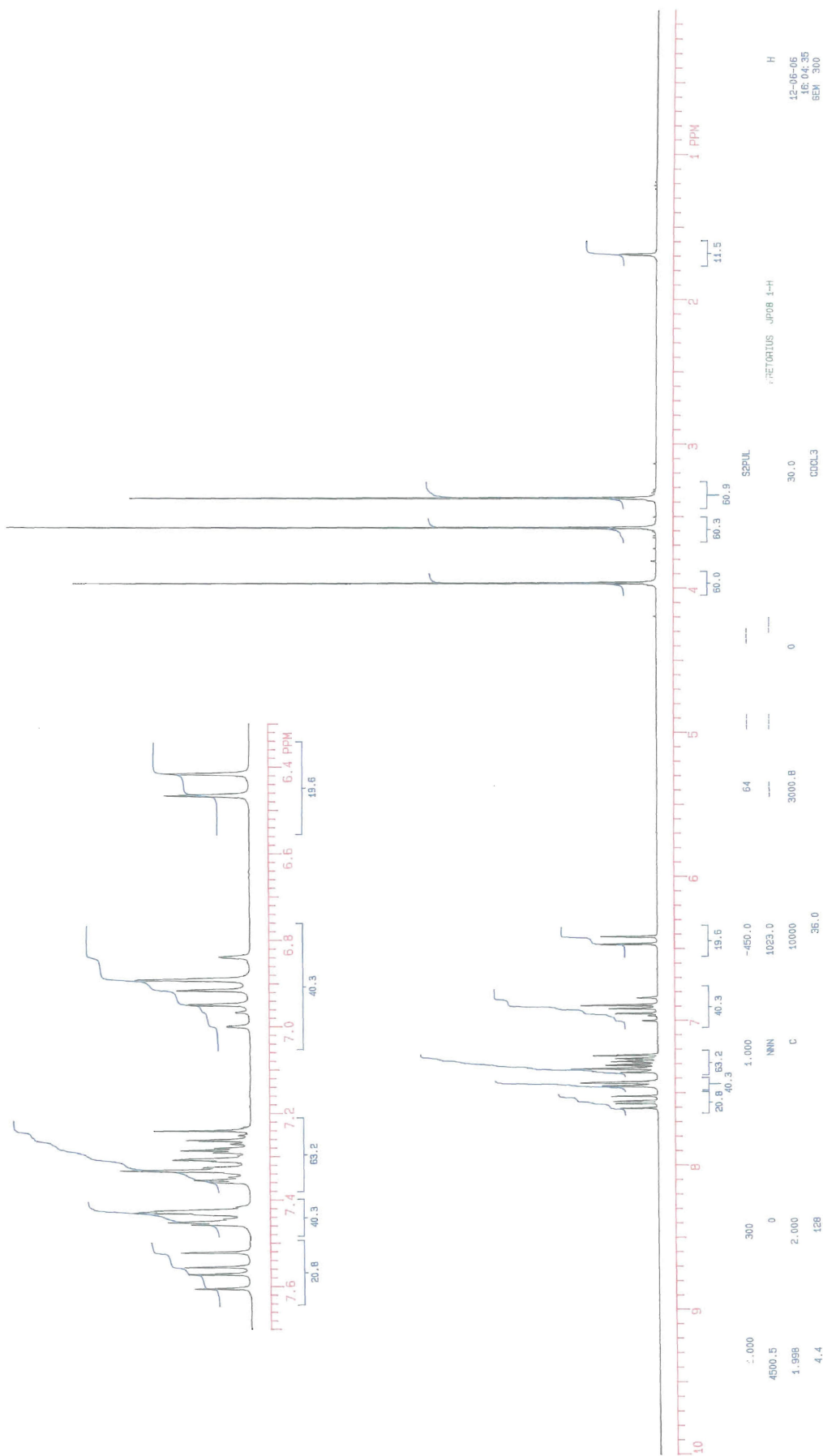
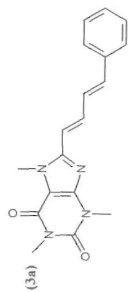
Appendix A



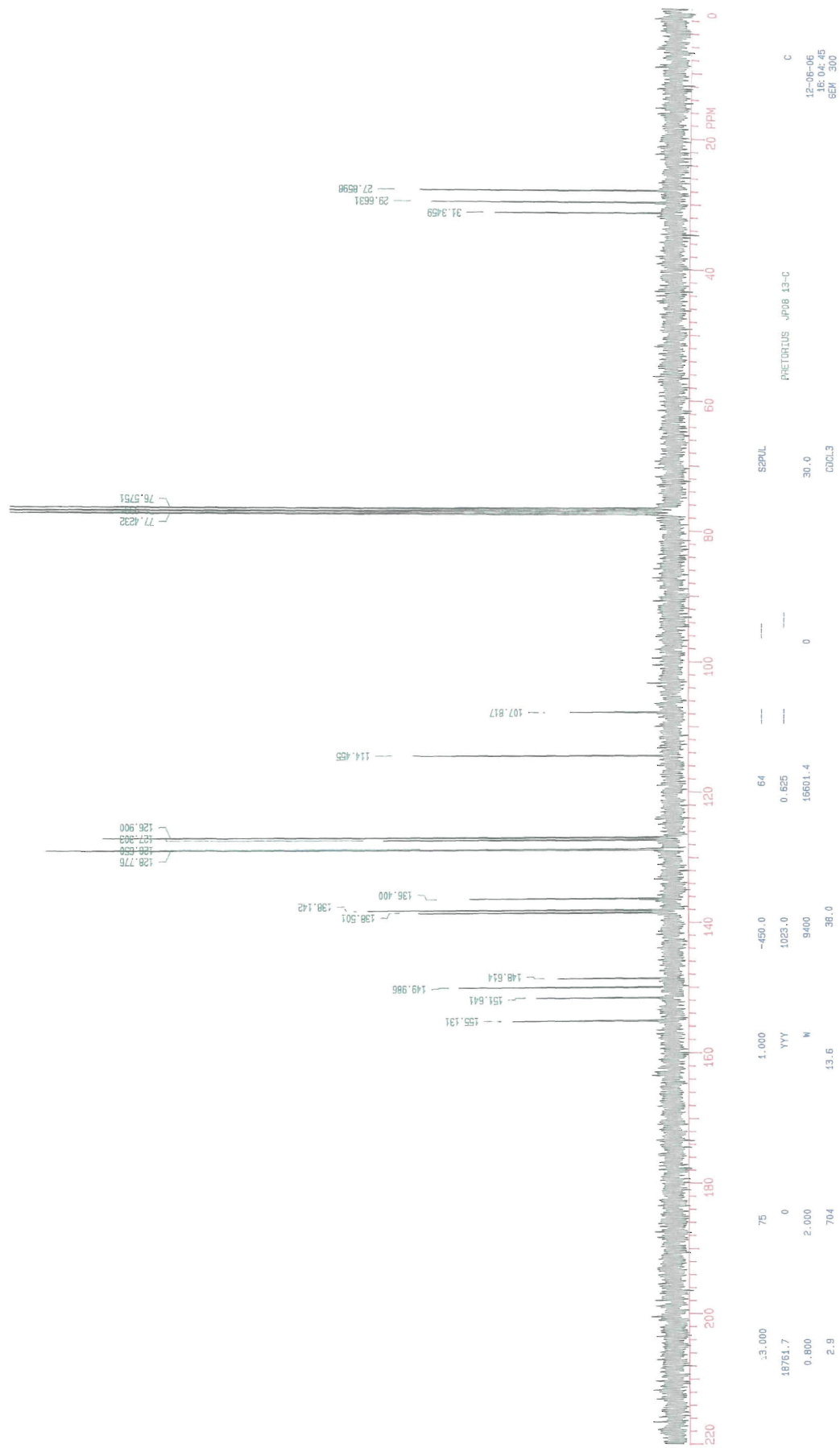
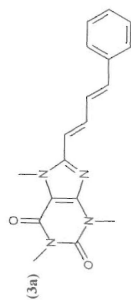
Appendix A



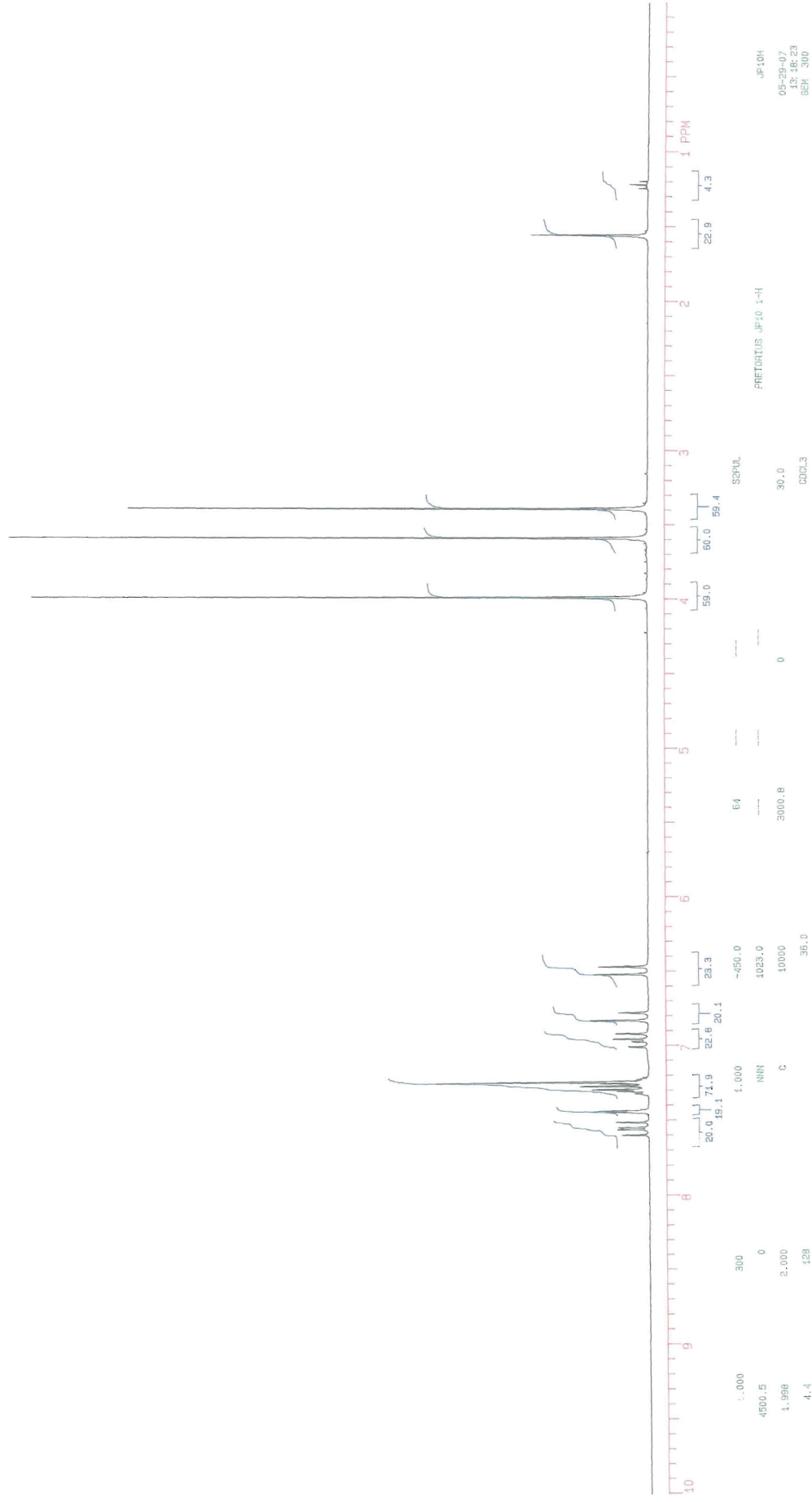
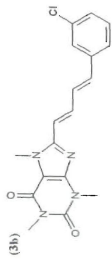
Appendix A



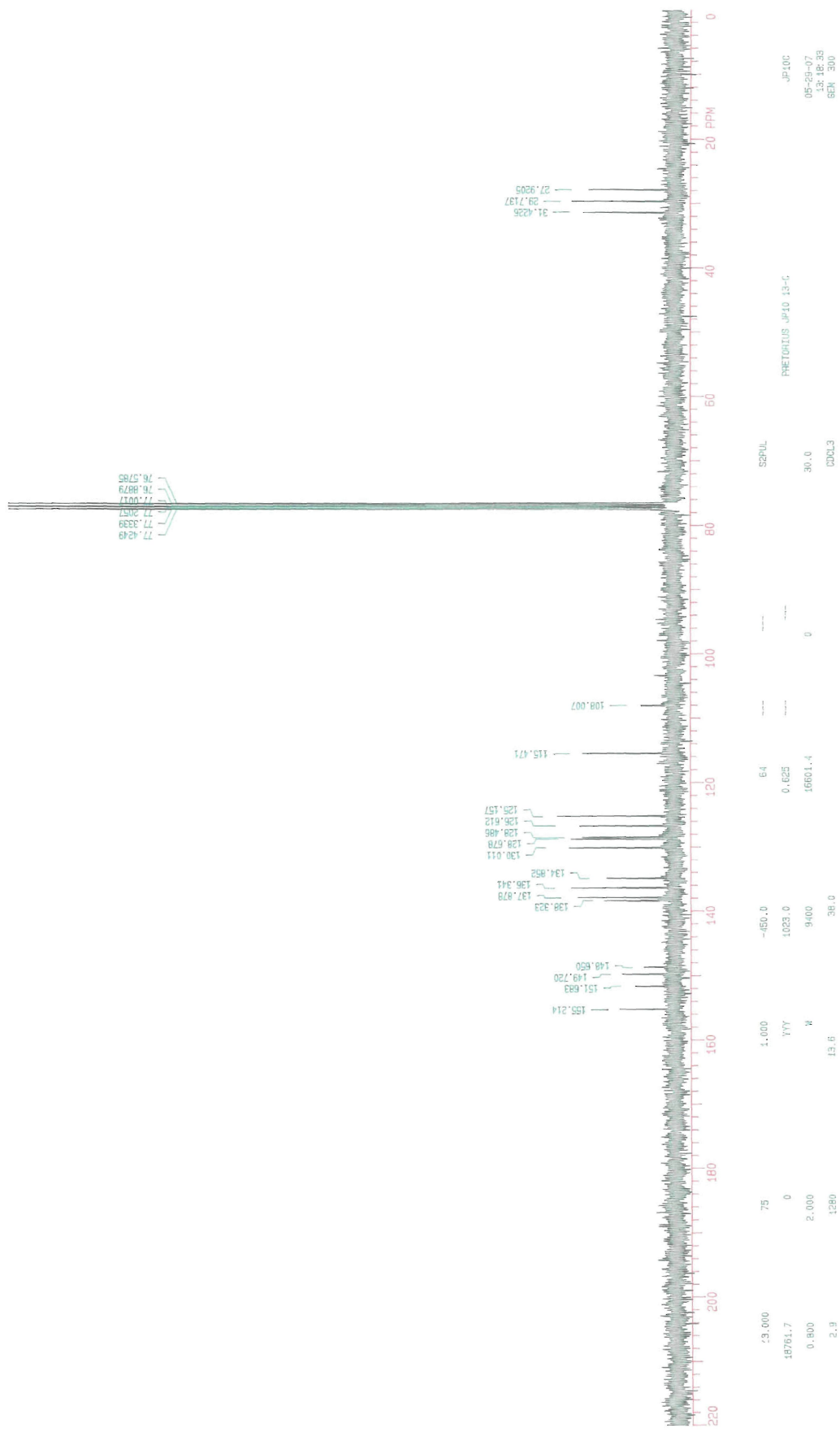
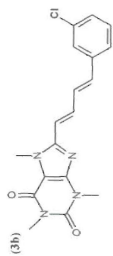
Appendix A



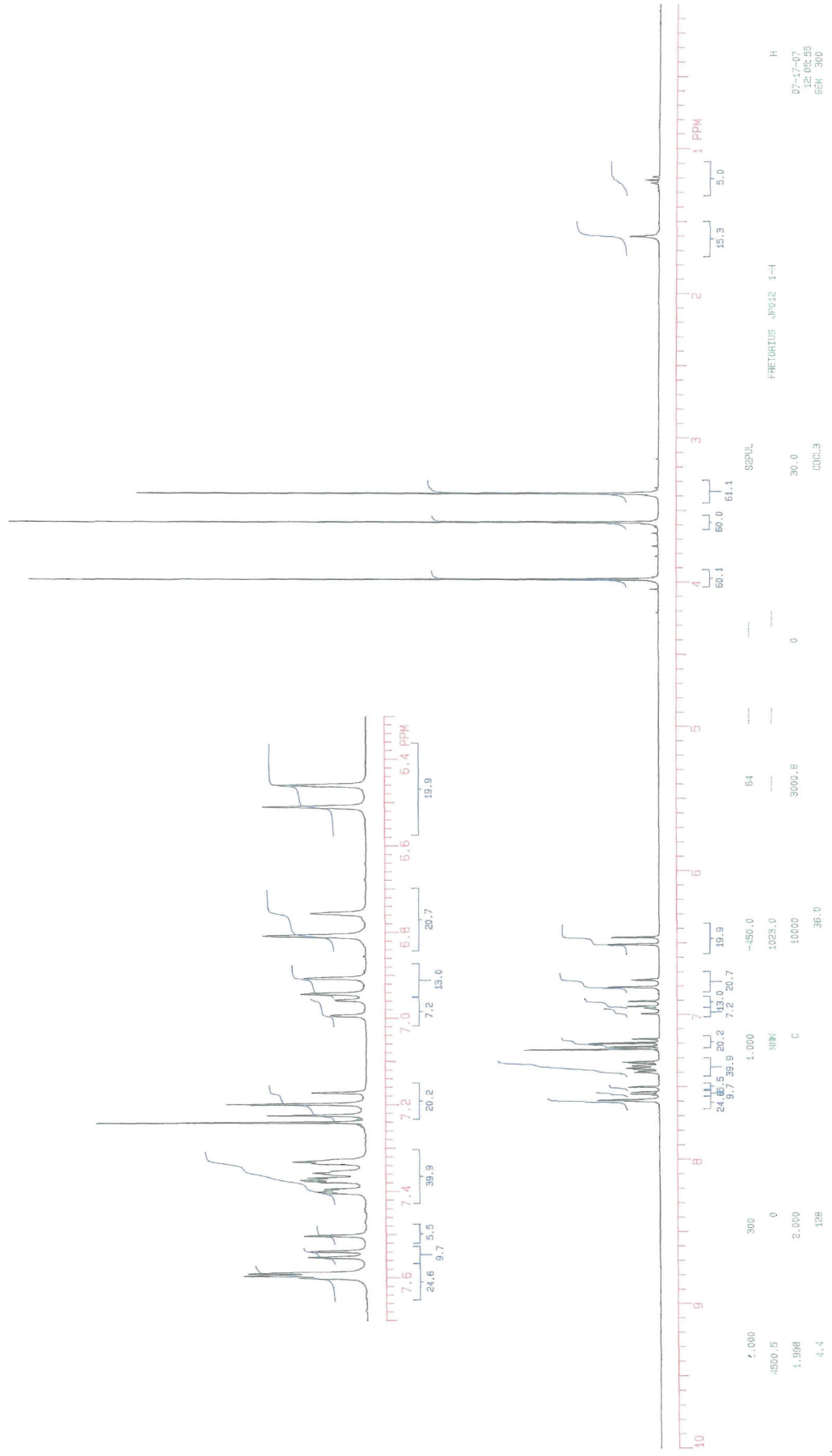
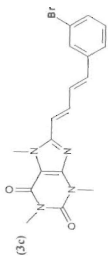
Appendix A



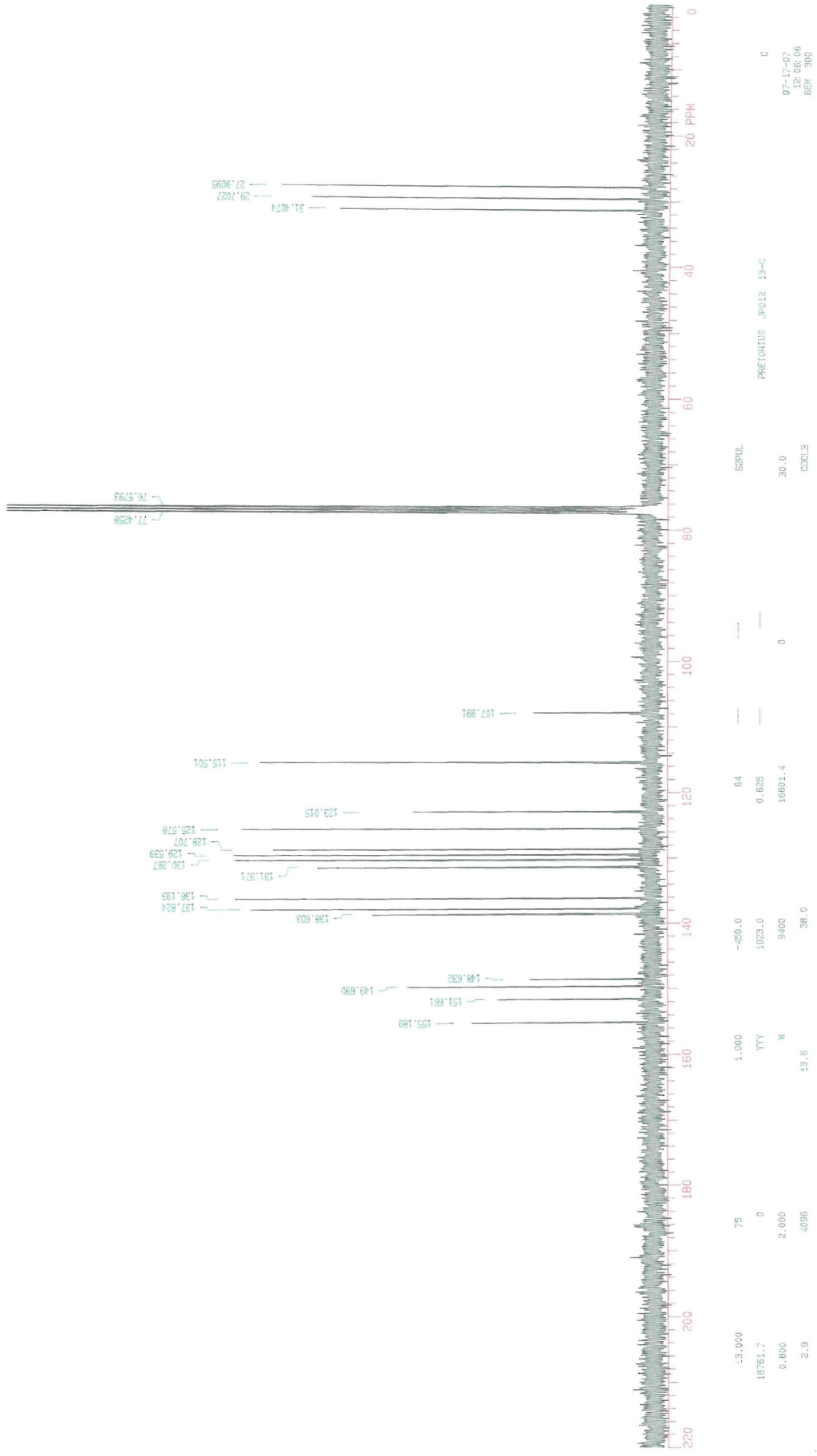
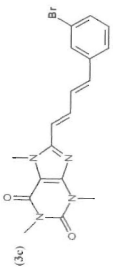
Appendix A



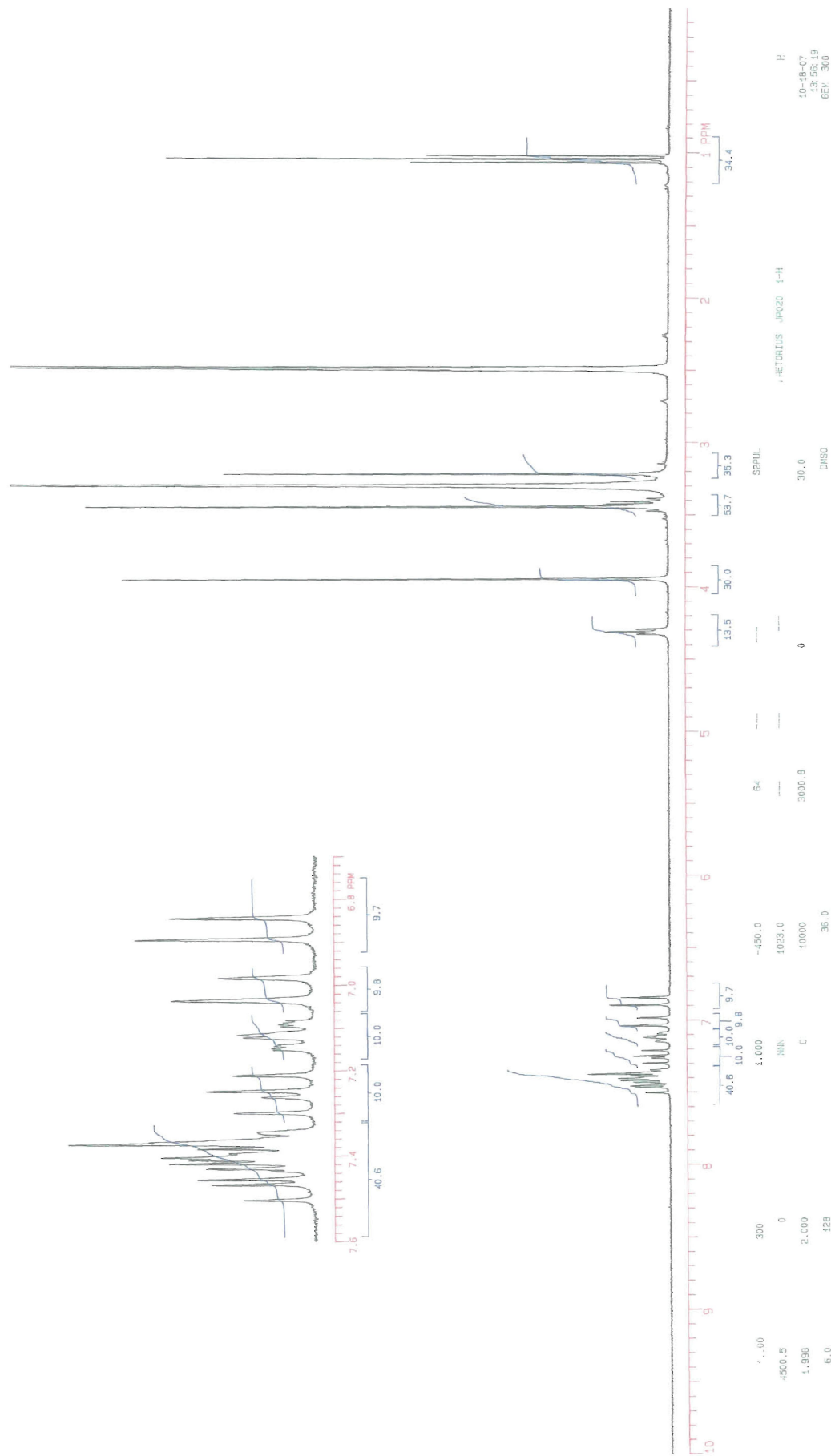
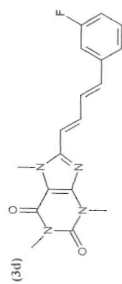
Appendix A



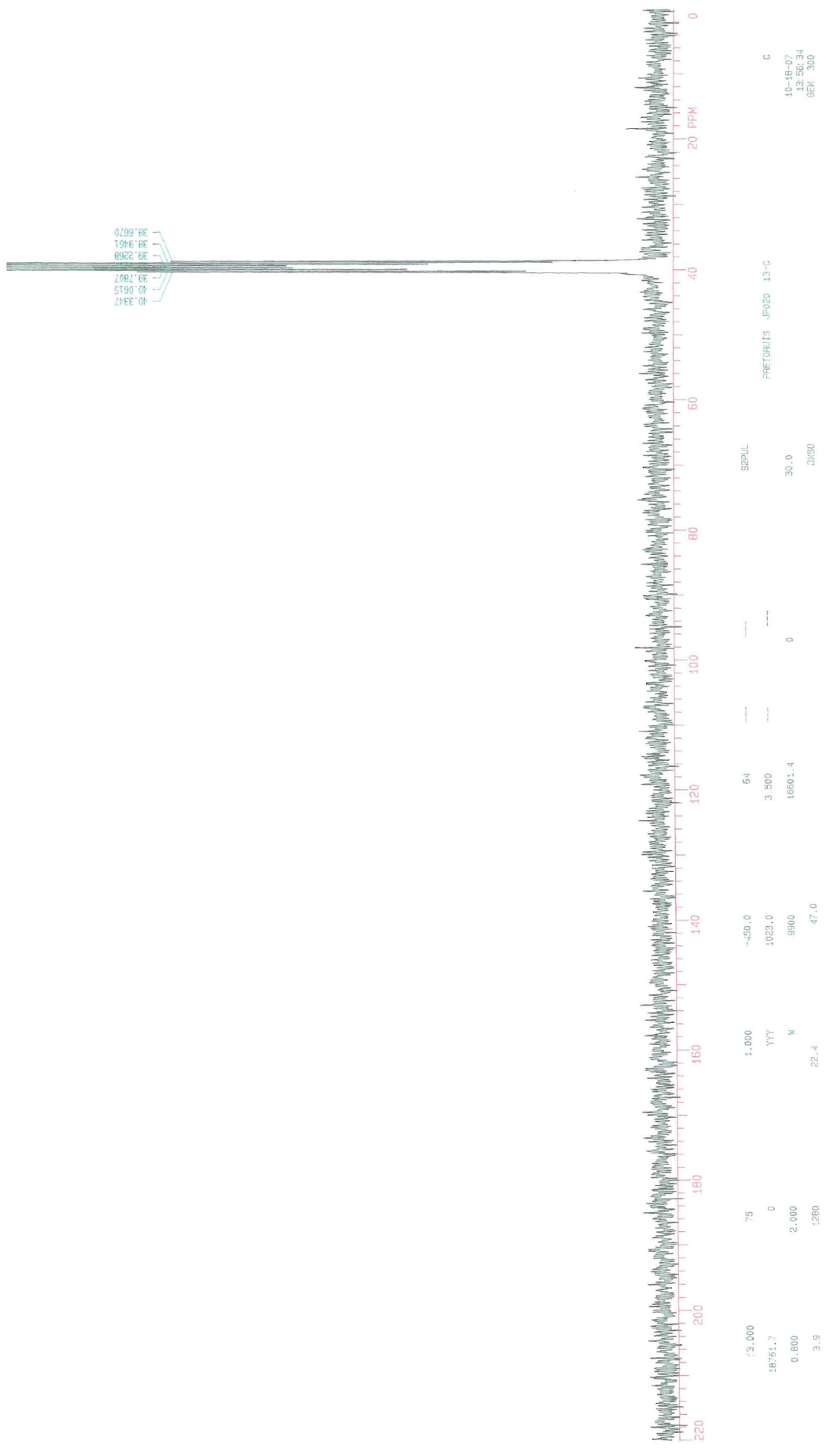
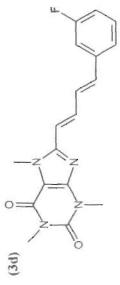
Appendix A



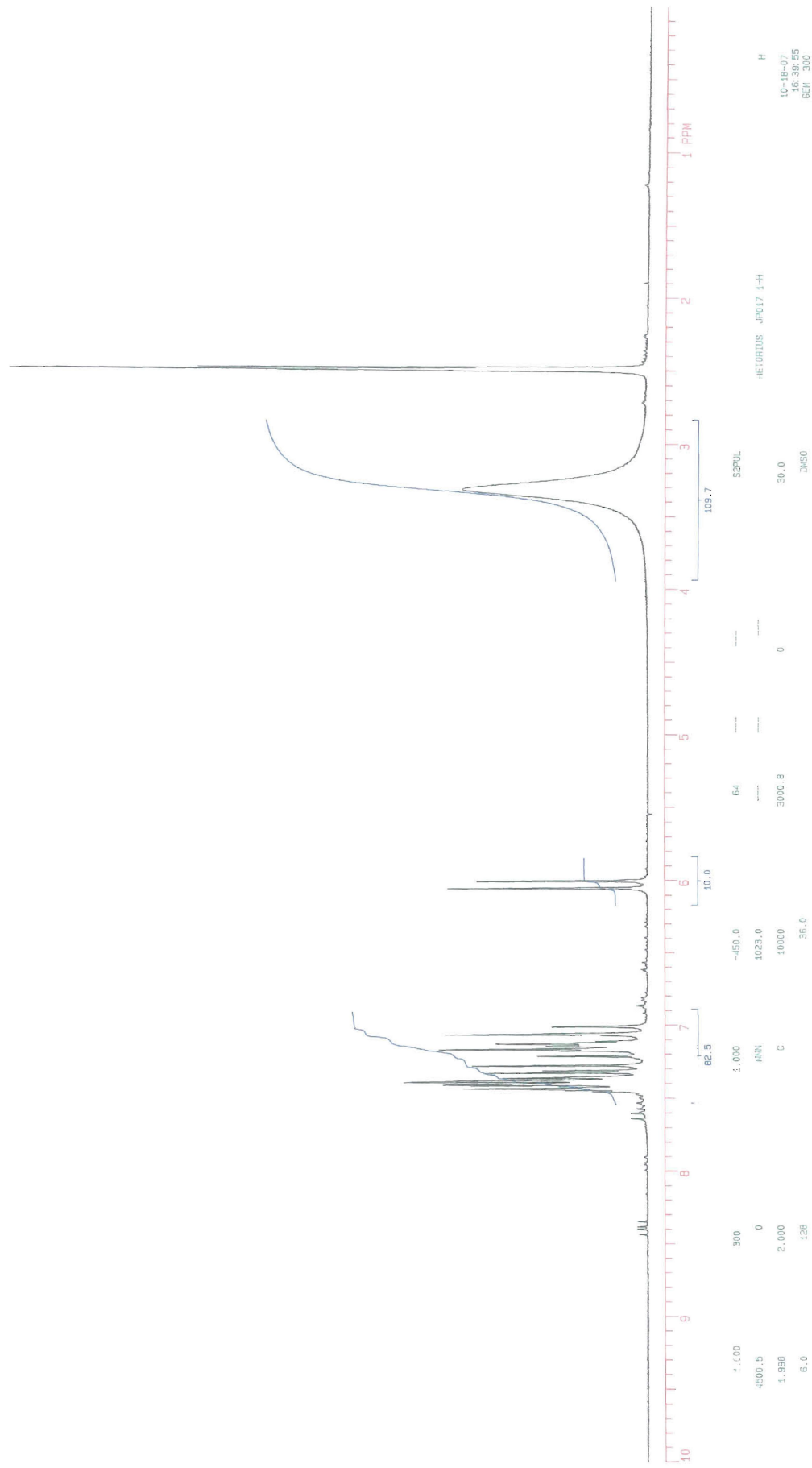
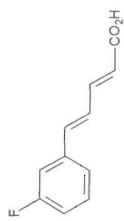
Appendix A



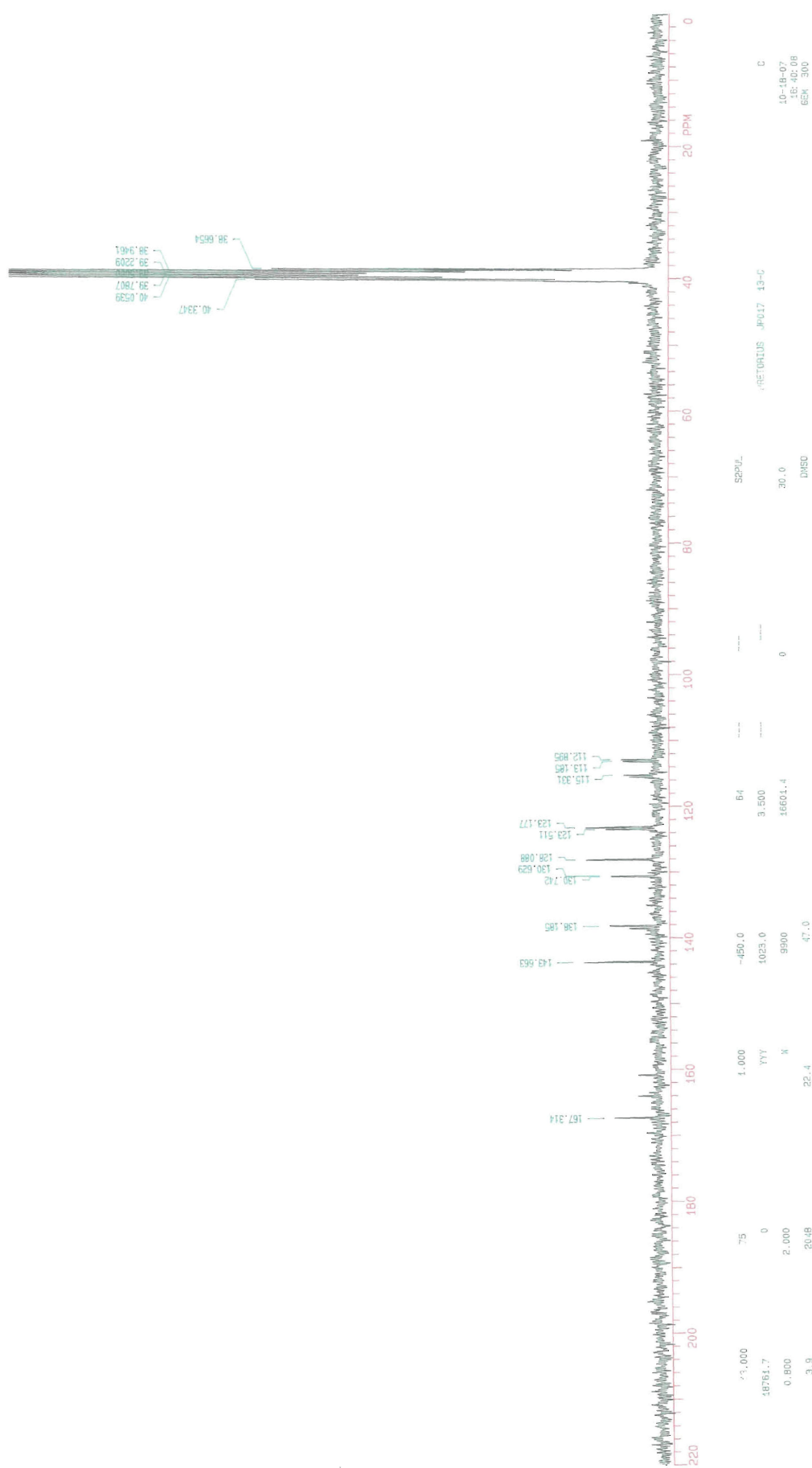
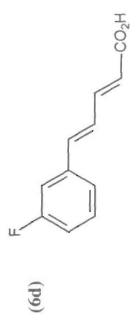
Appendix A

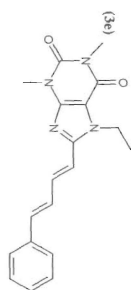


Appendix A

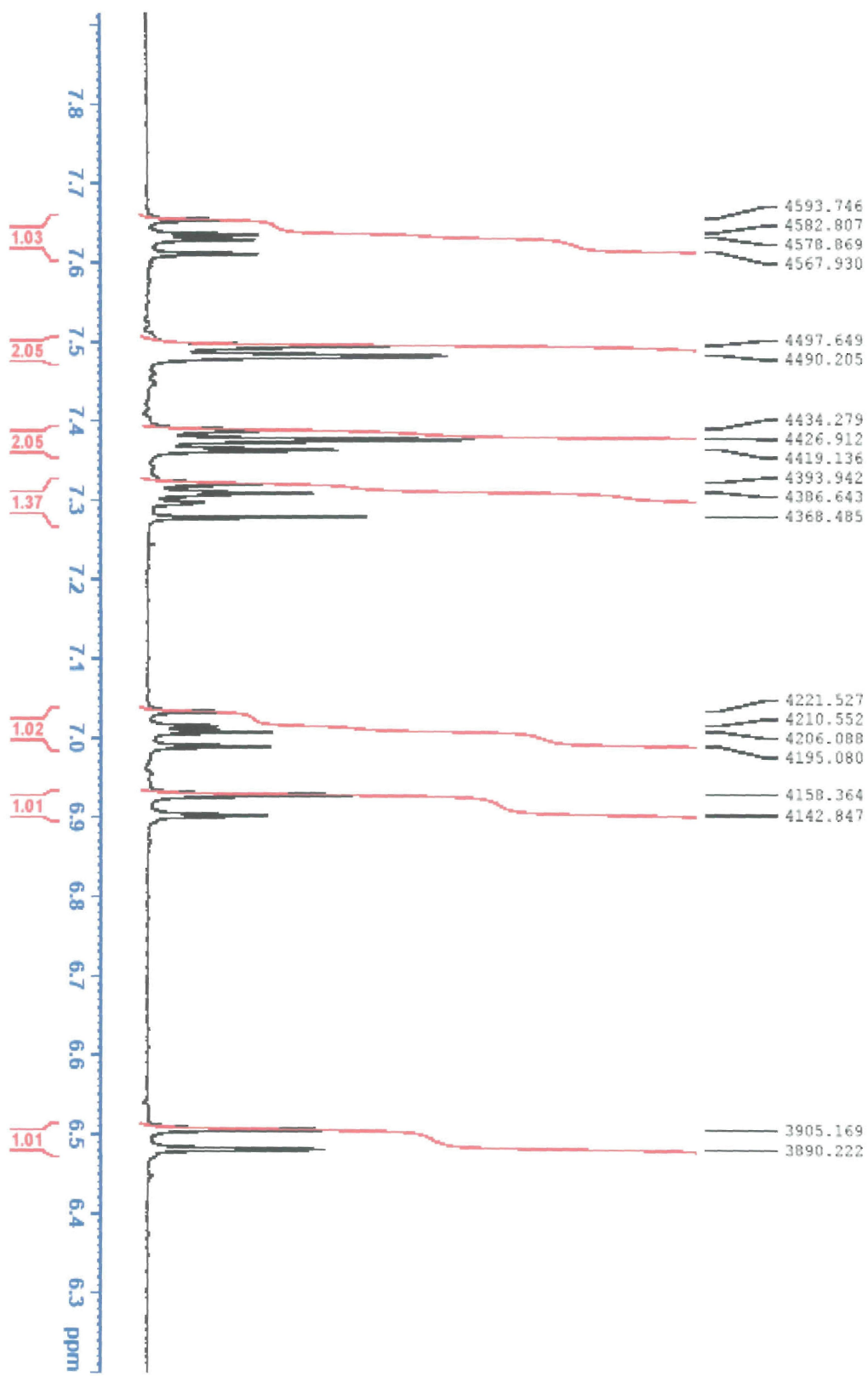


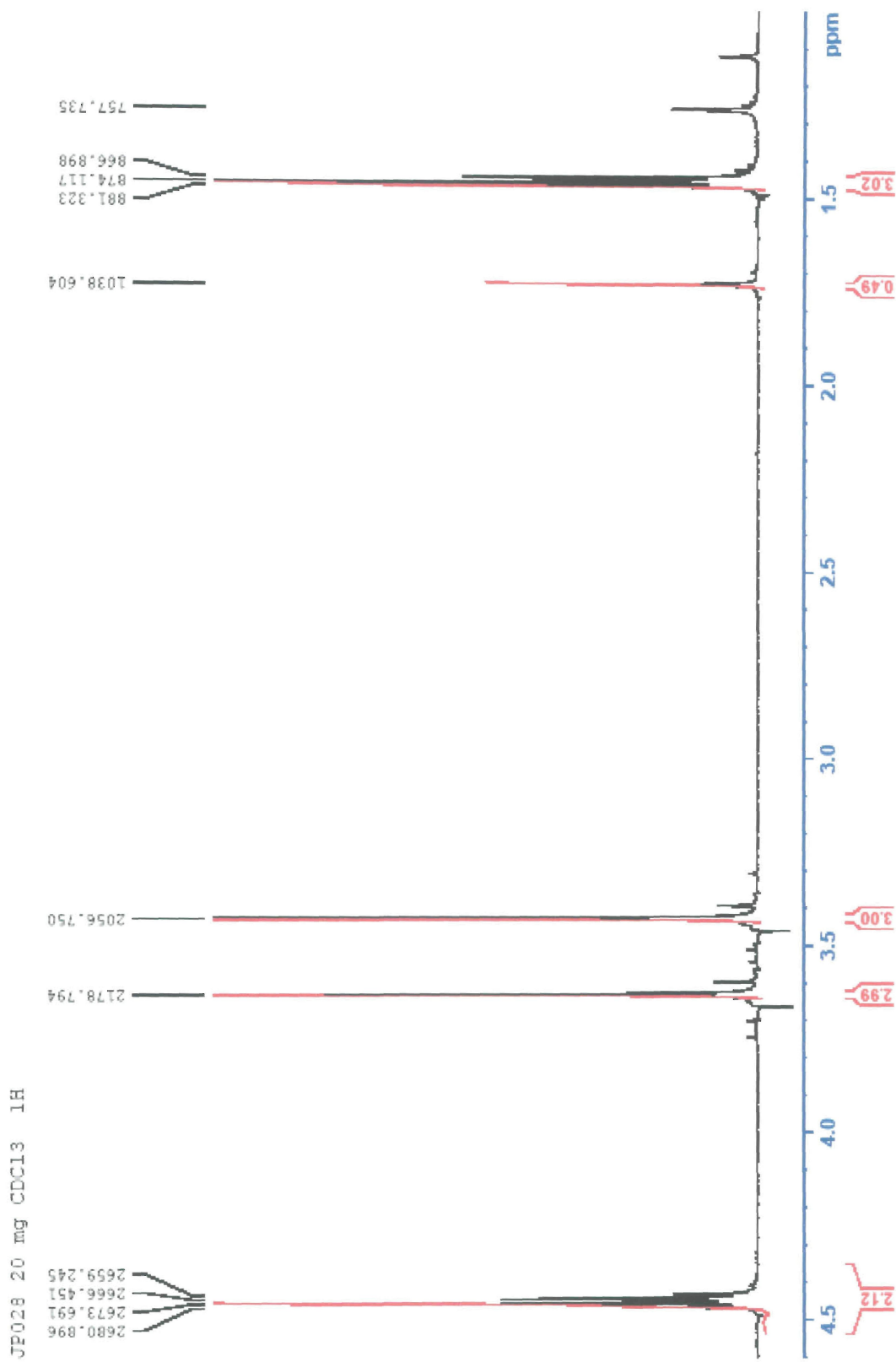
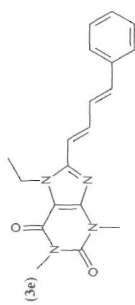
Appendix A



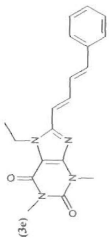


JP028 20 mg CDCl₃ 1H

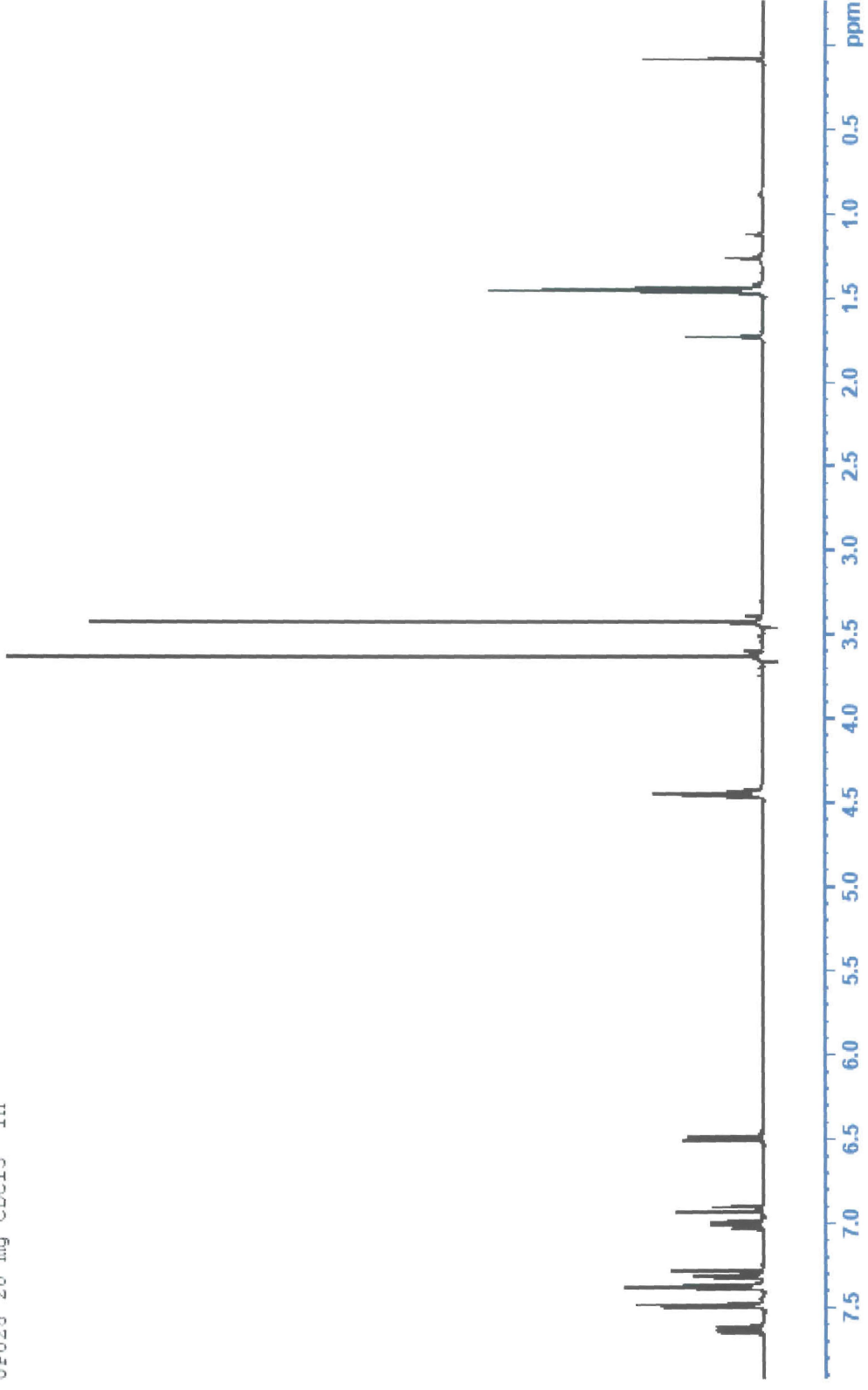


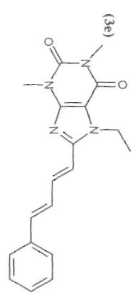


Appendix A

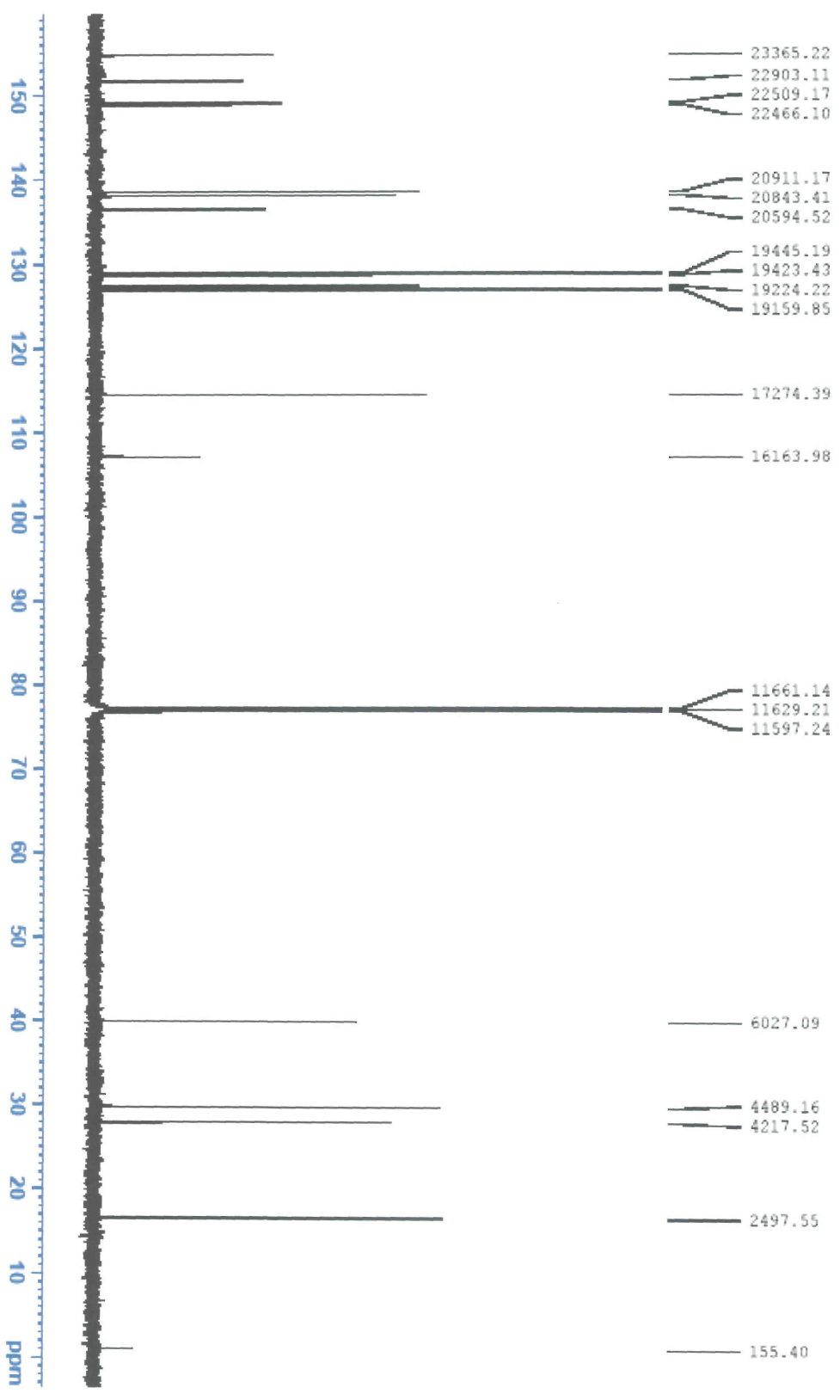


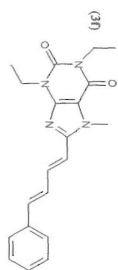
JP028 20 mg CDCl₃ 1H



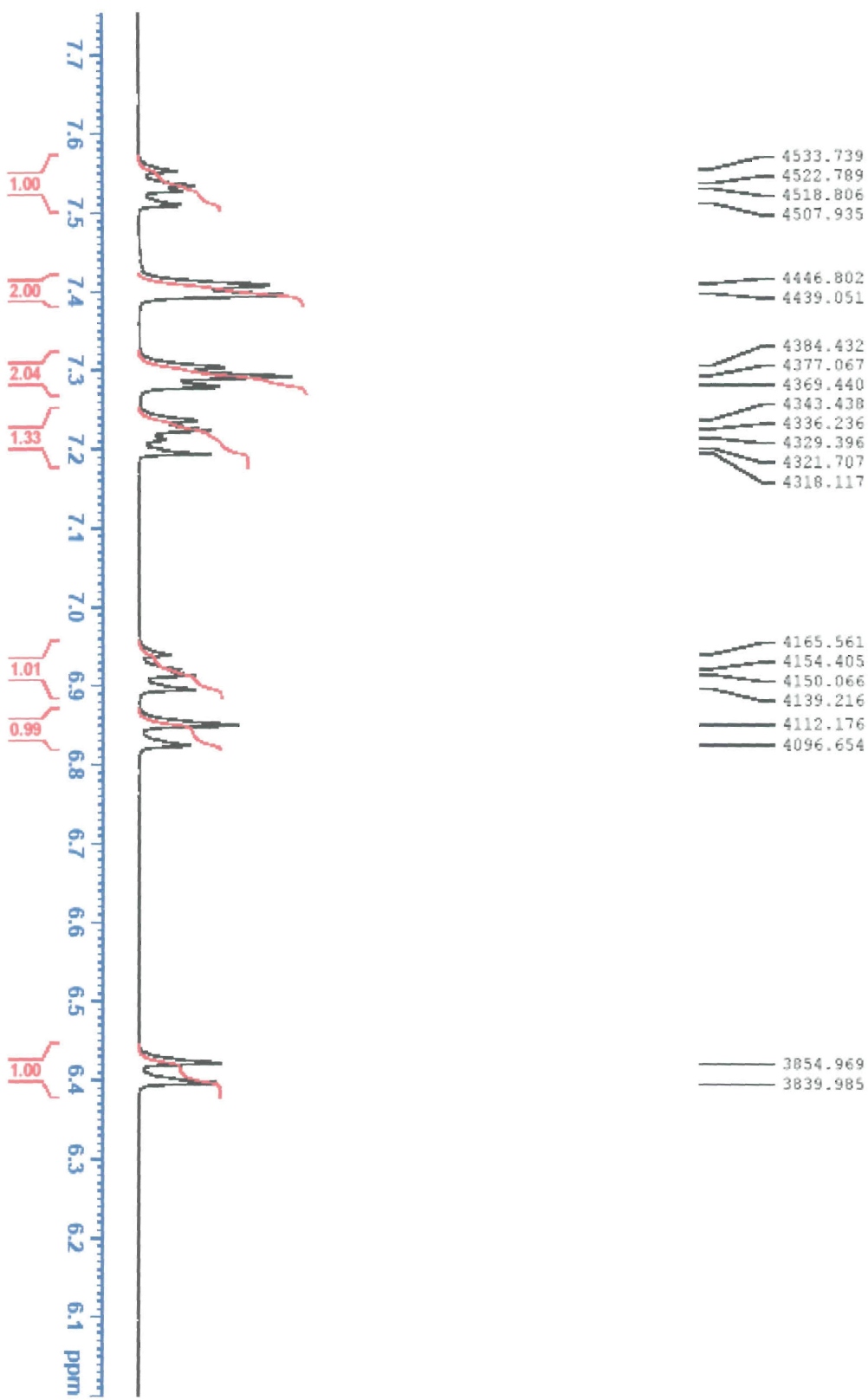


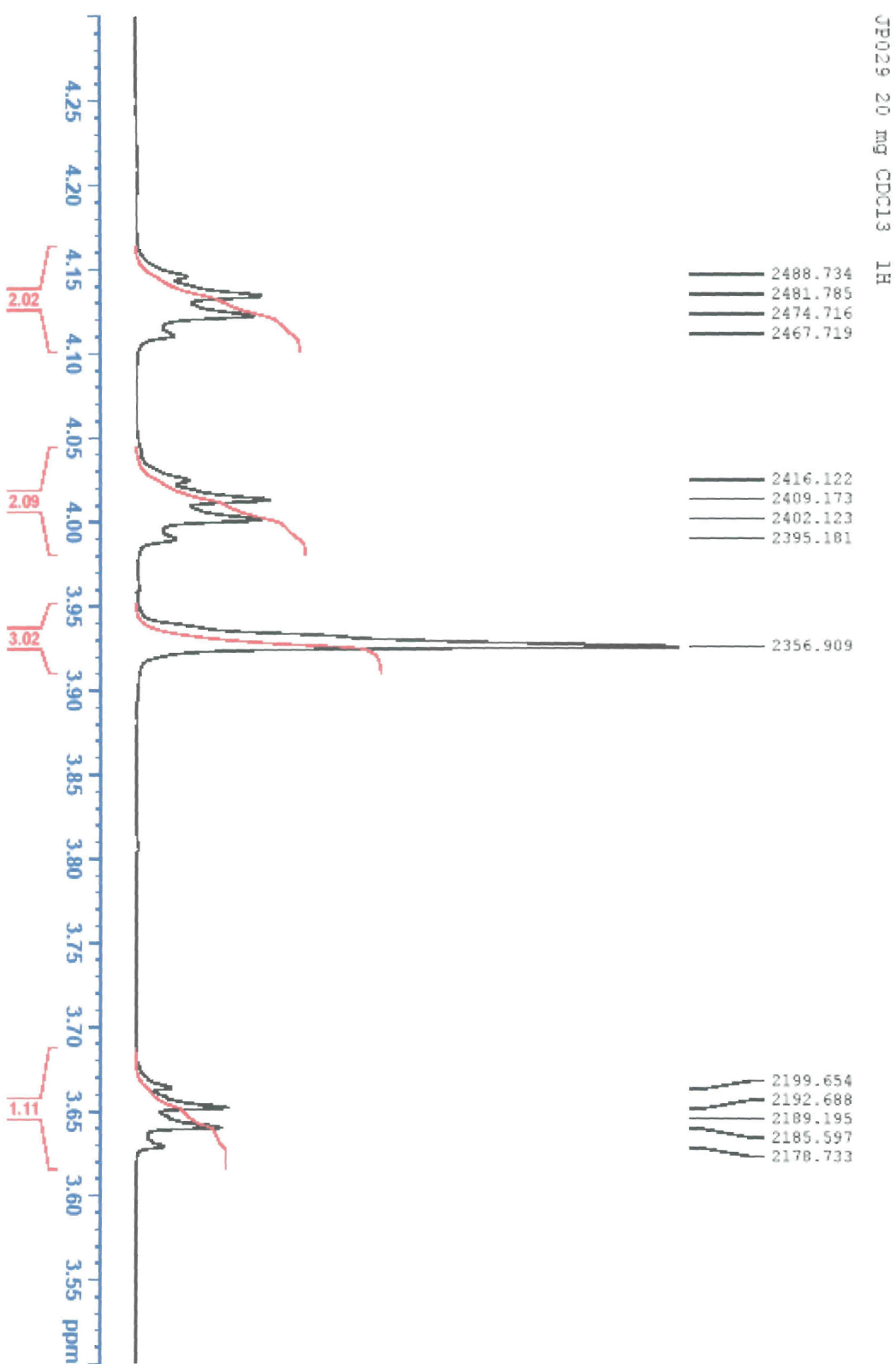
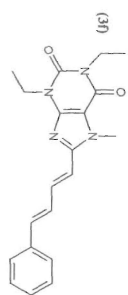
JP028 20 mg CDCl3 13C



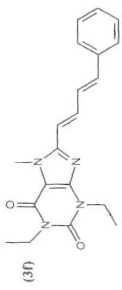


JP029 20 mg CDCl₃ 1H

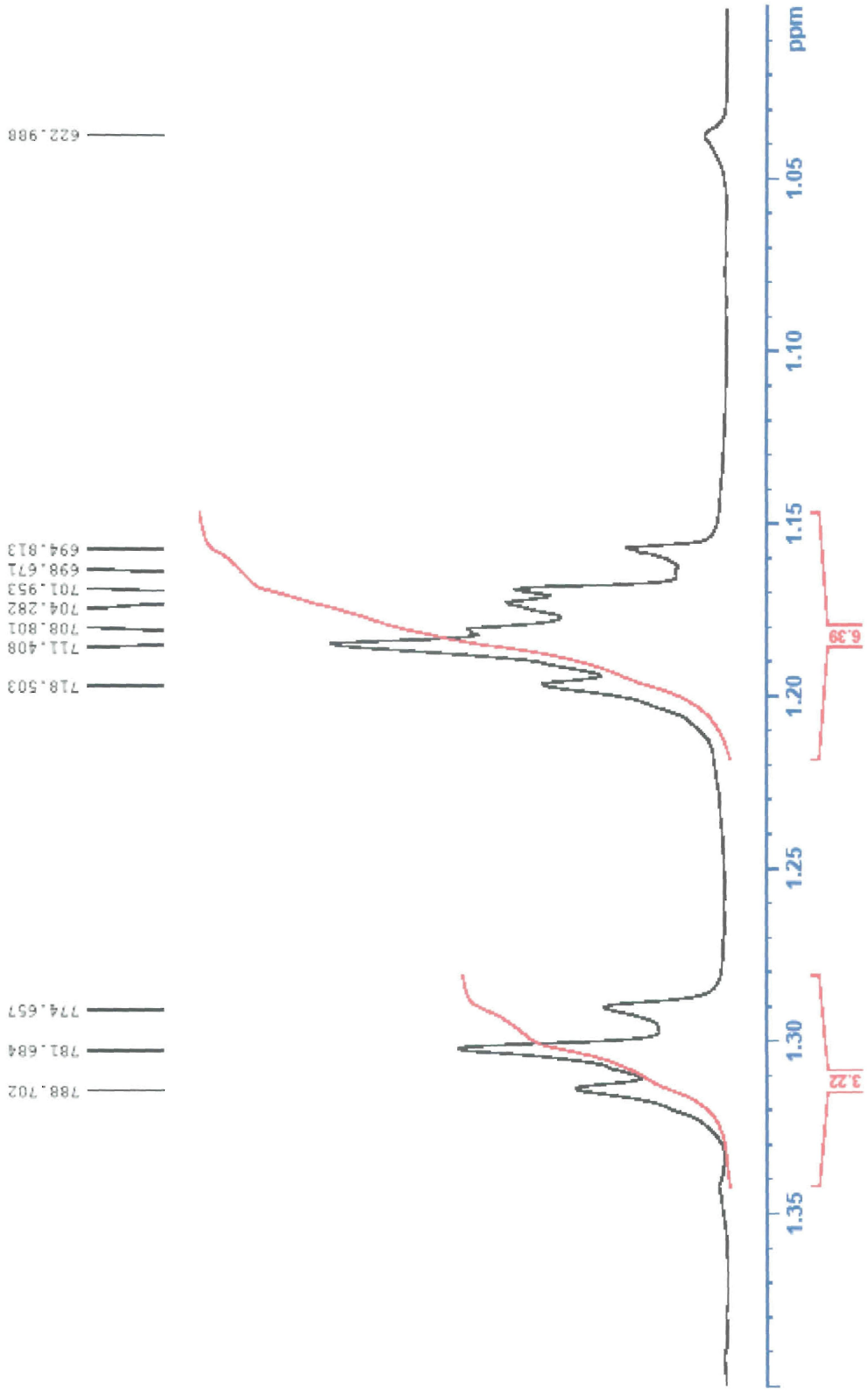




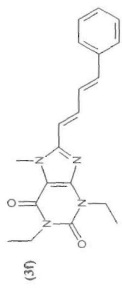
Appendix A



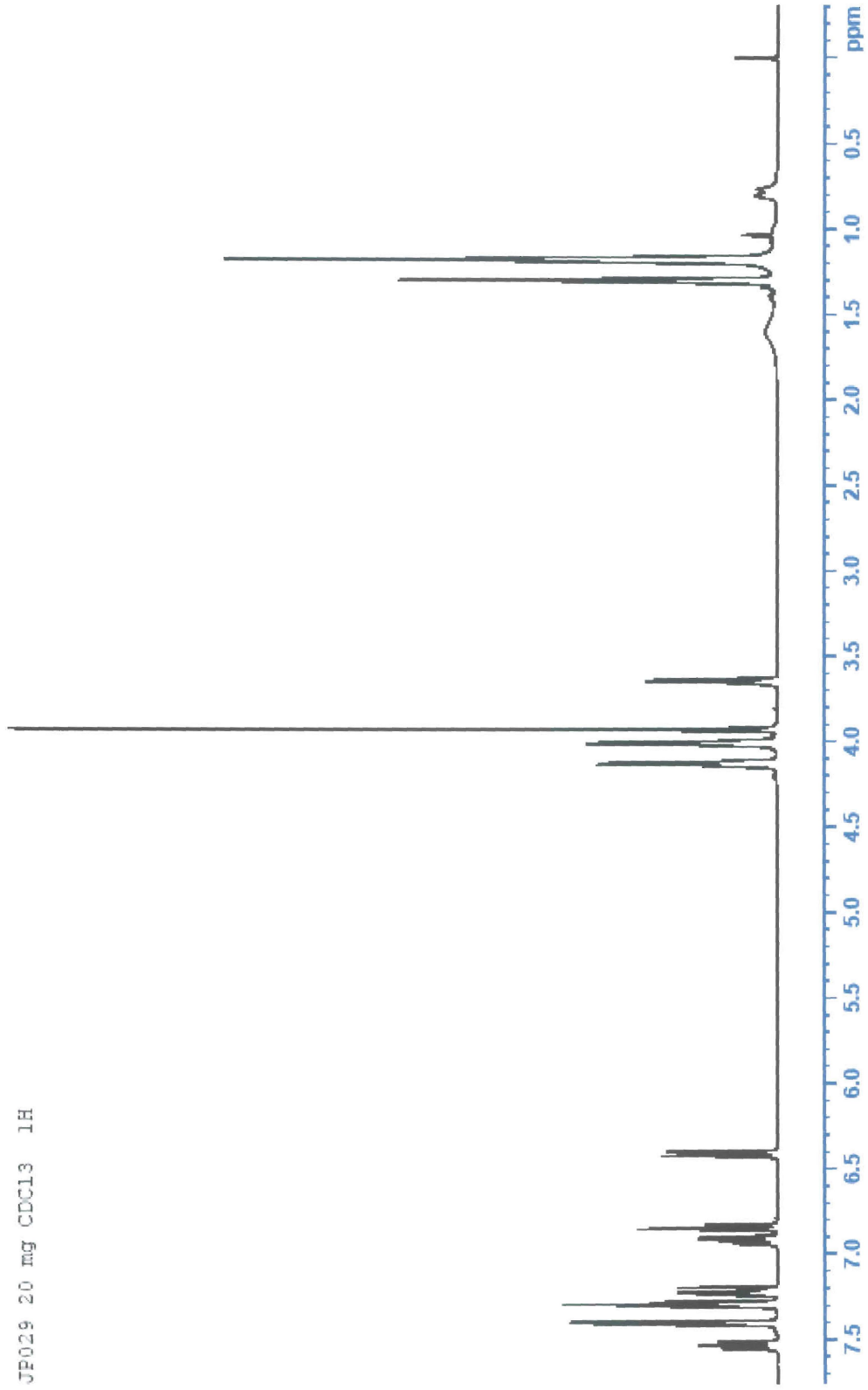
JP029 20 mg CDCl3 1H

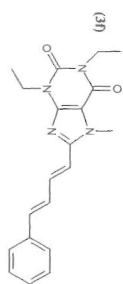


Appendix A

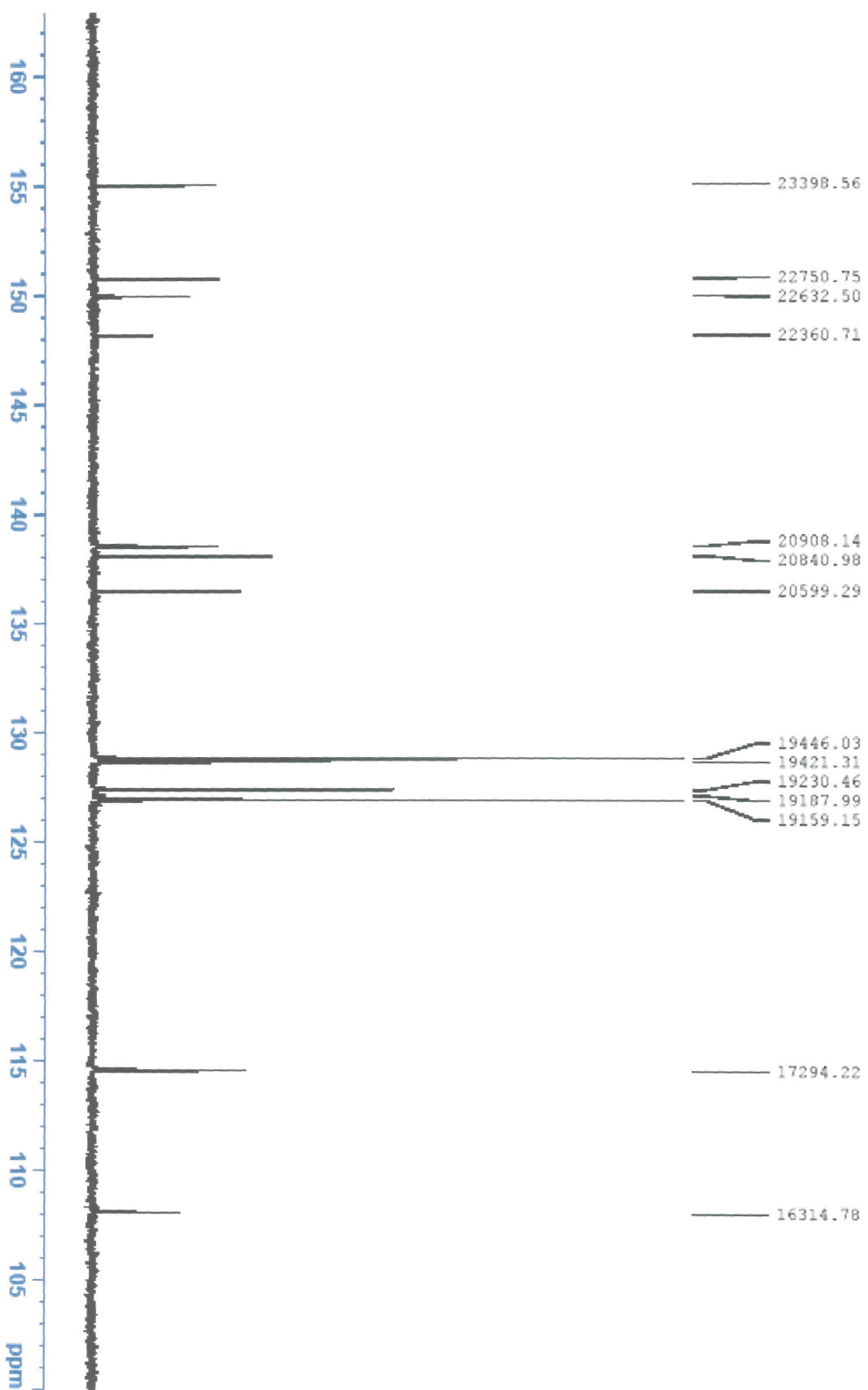


JP029 20 mg CDCl₃ 1H

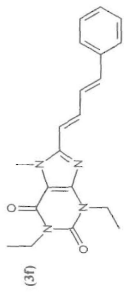




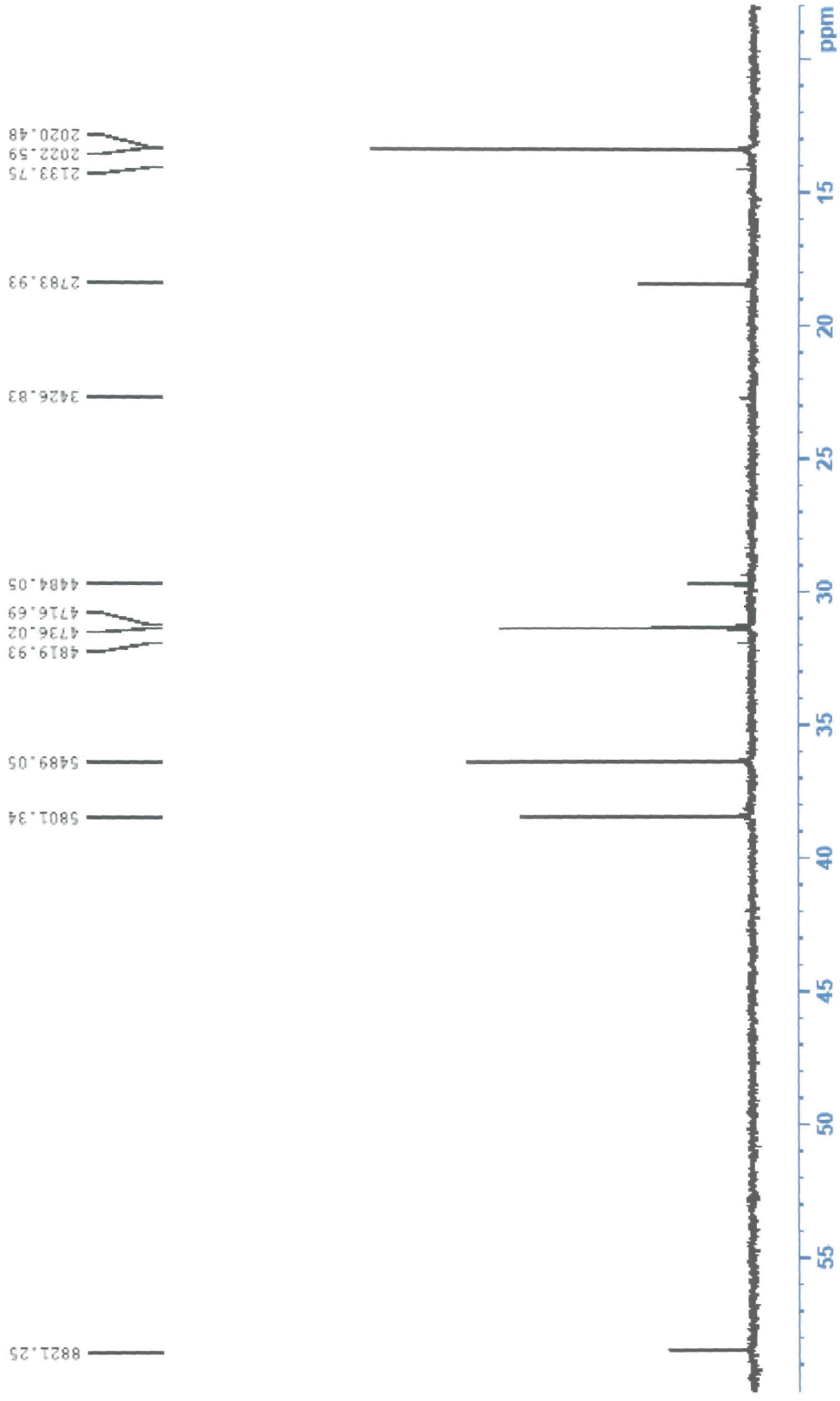
JP029 20 mg CDCl₃ 13C



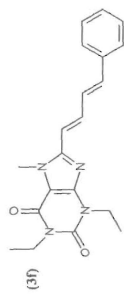
Appendix A



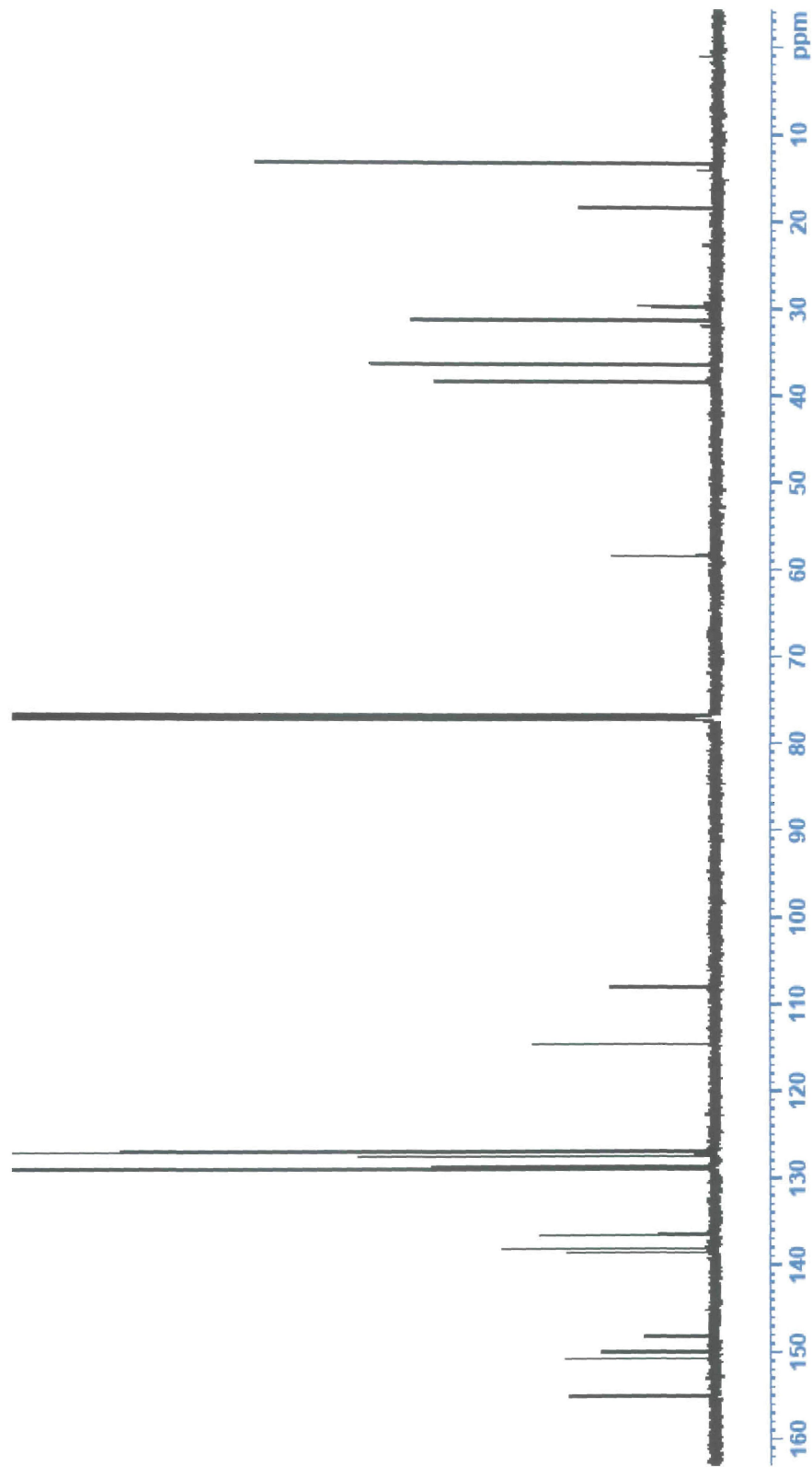
JP029 20 mg CDCl3 13C

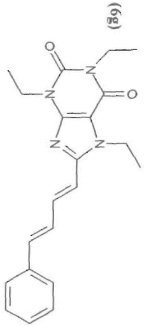


Appendix A

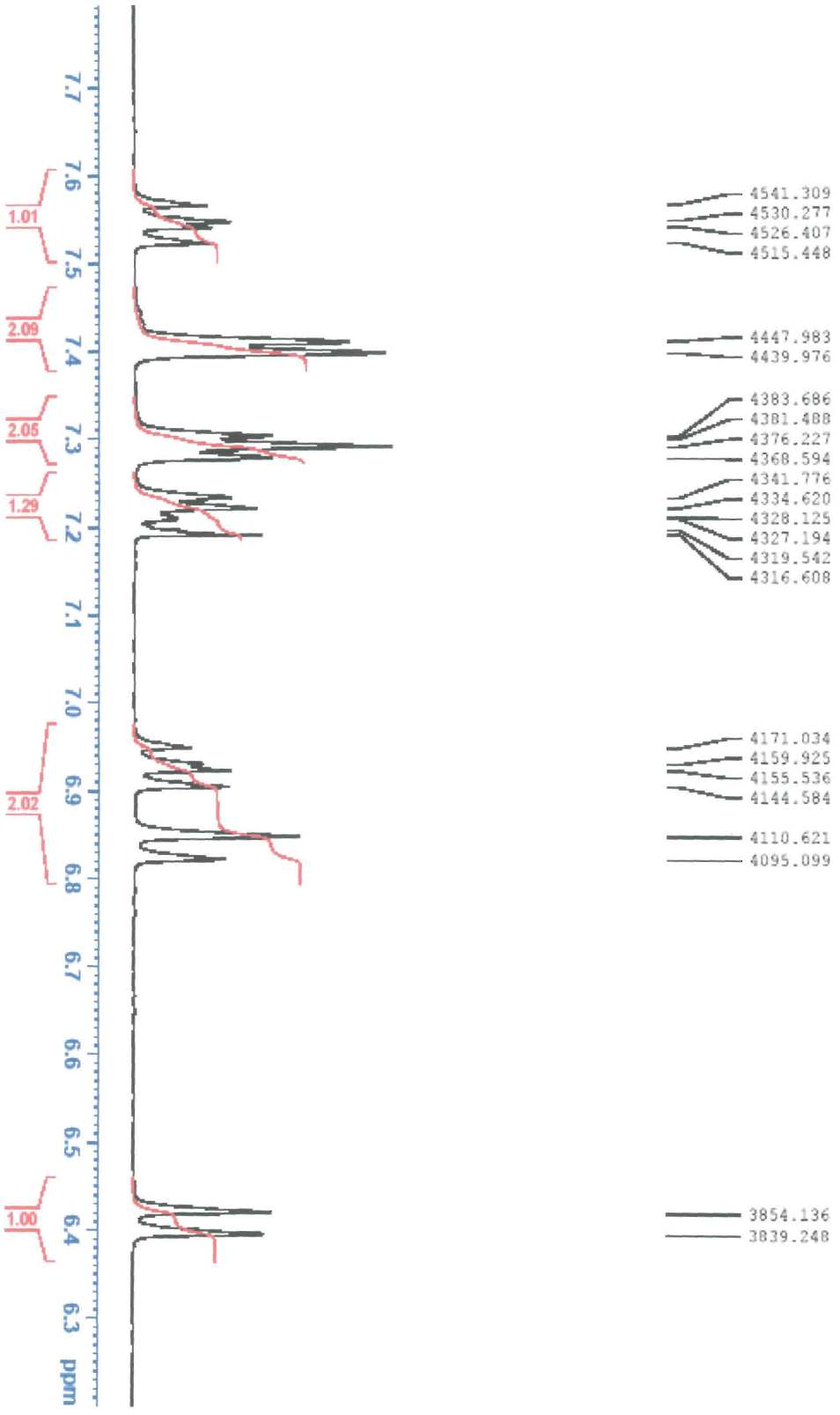


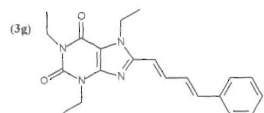
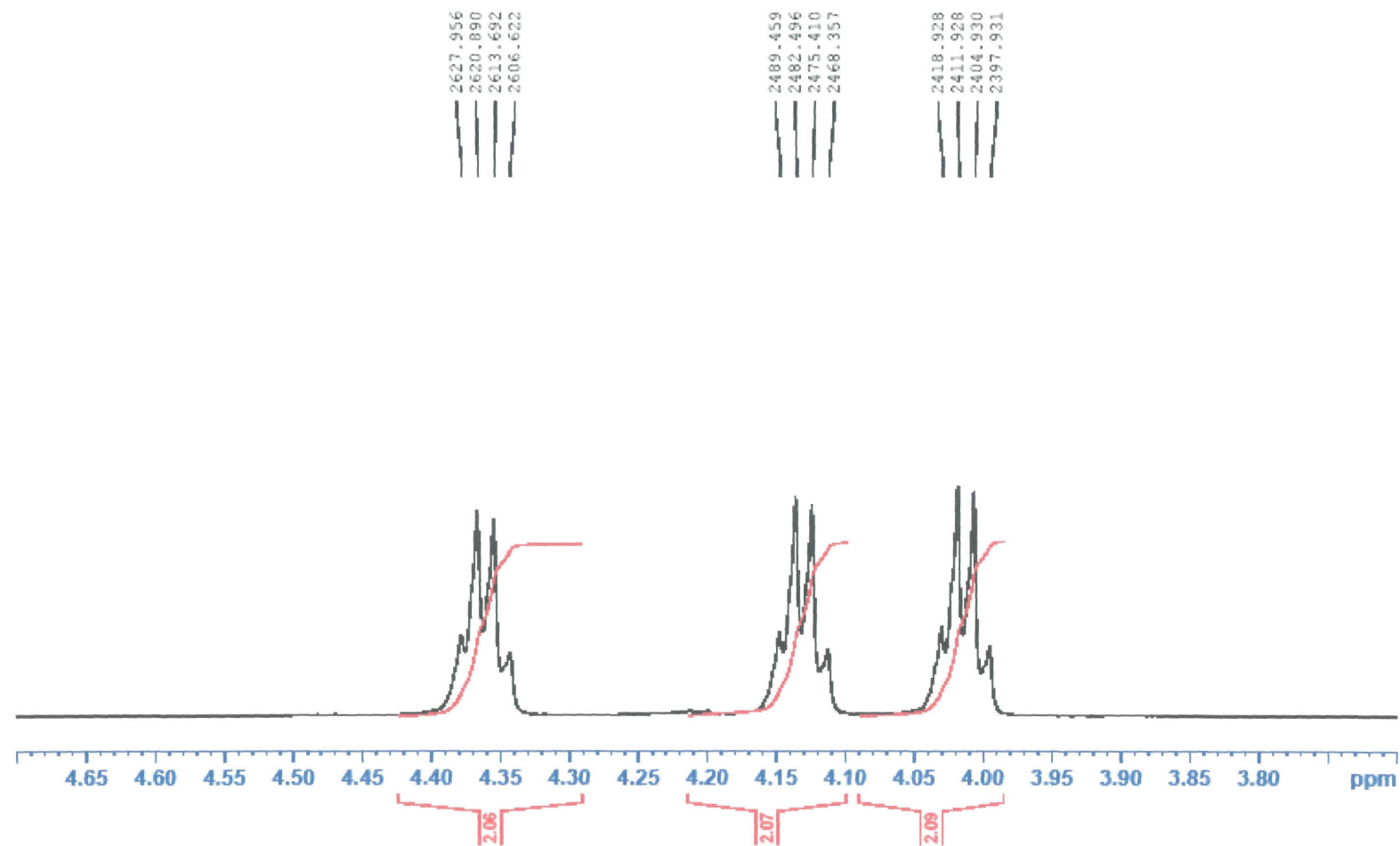
JP029 20 mg CDCl₃ 13C



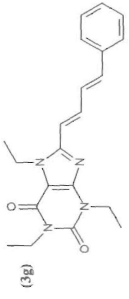


JP030a 20 mg CDCl3 1H

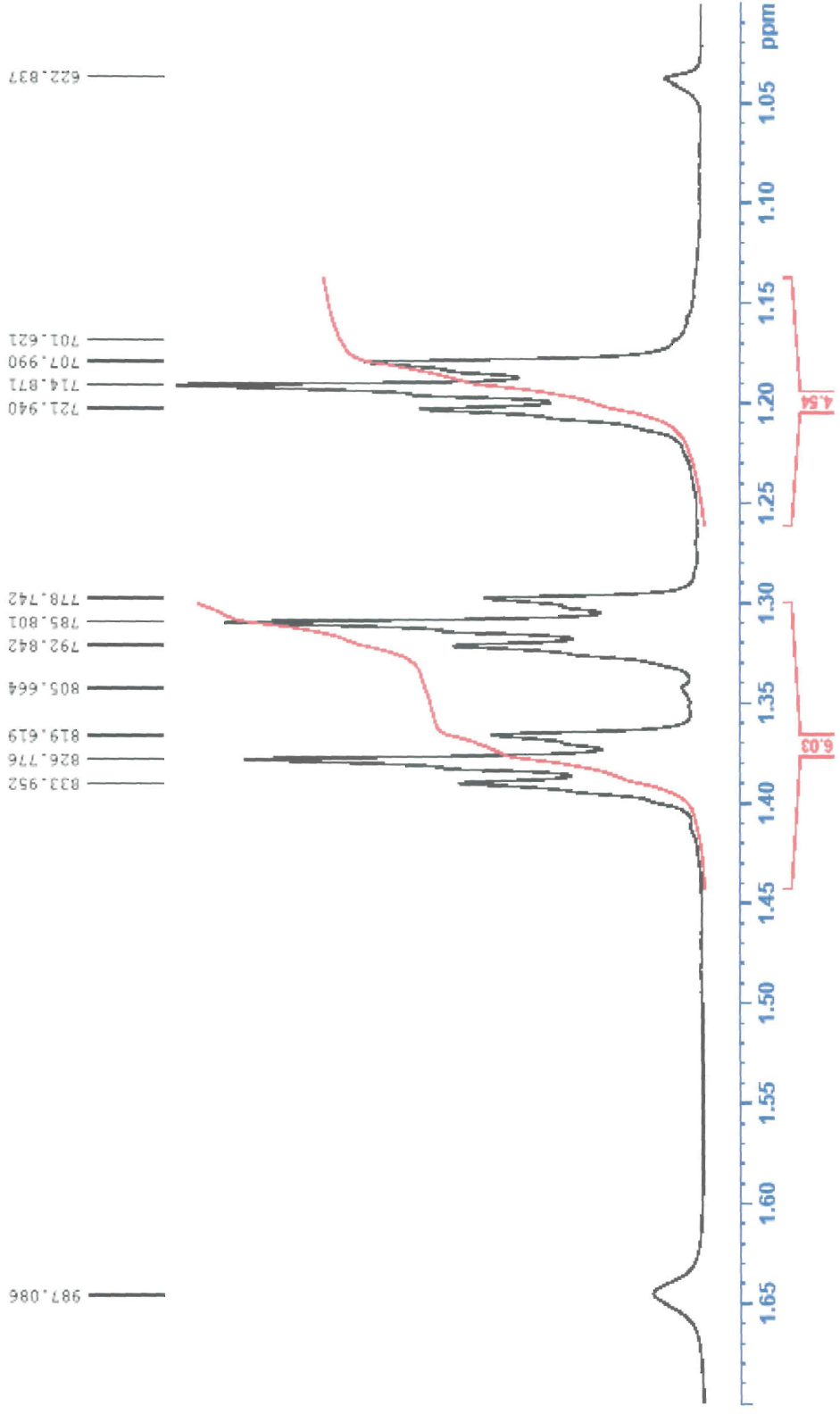


JP030a 20 mg CDCl₃ 1H

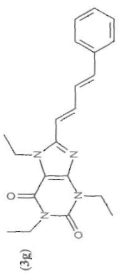
Appendix A



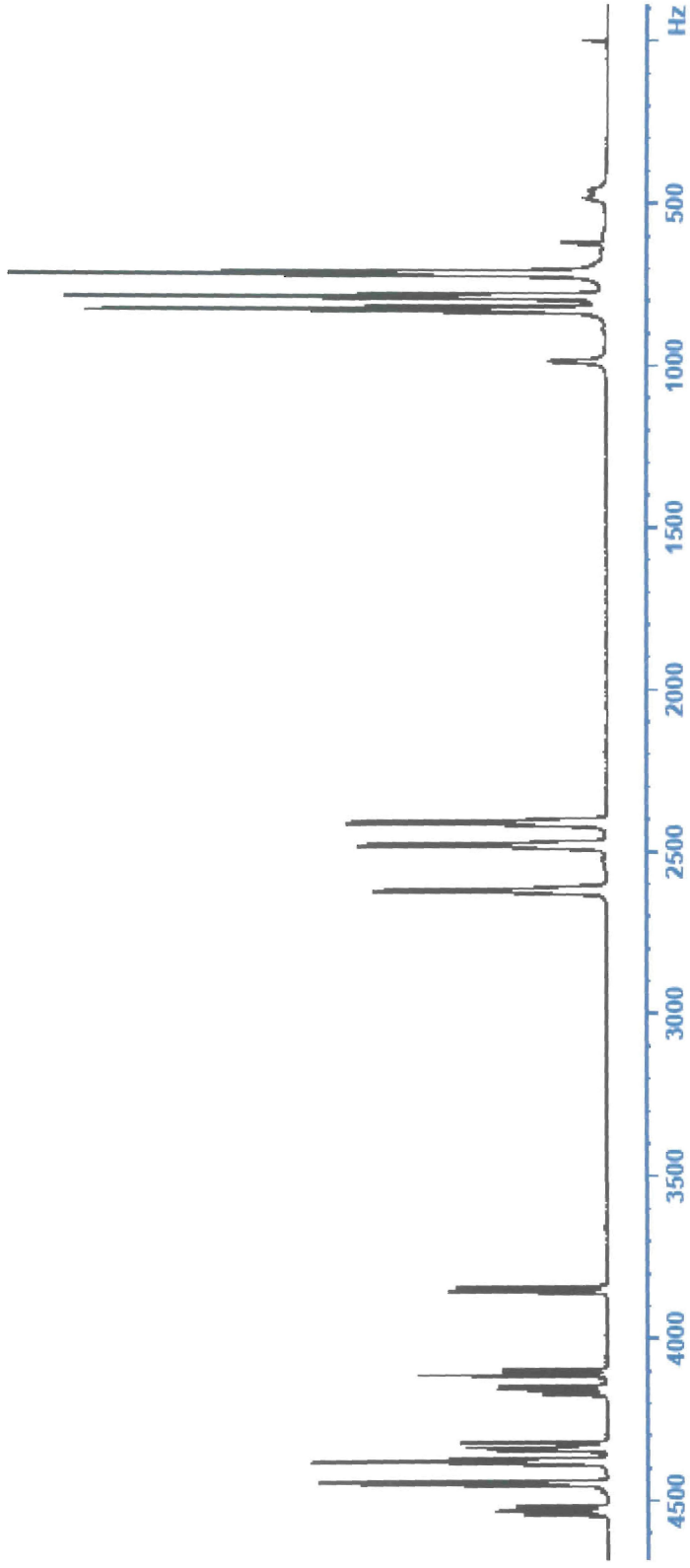
JP030a 20 mg CDCl3 1H



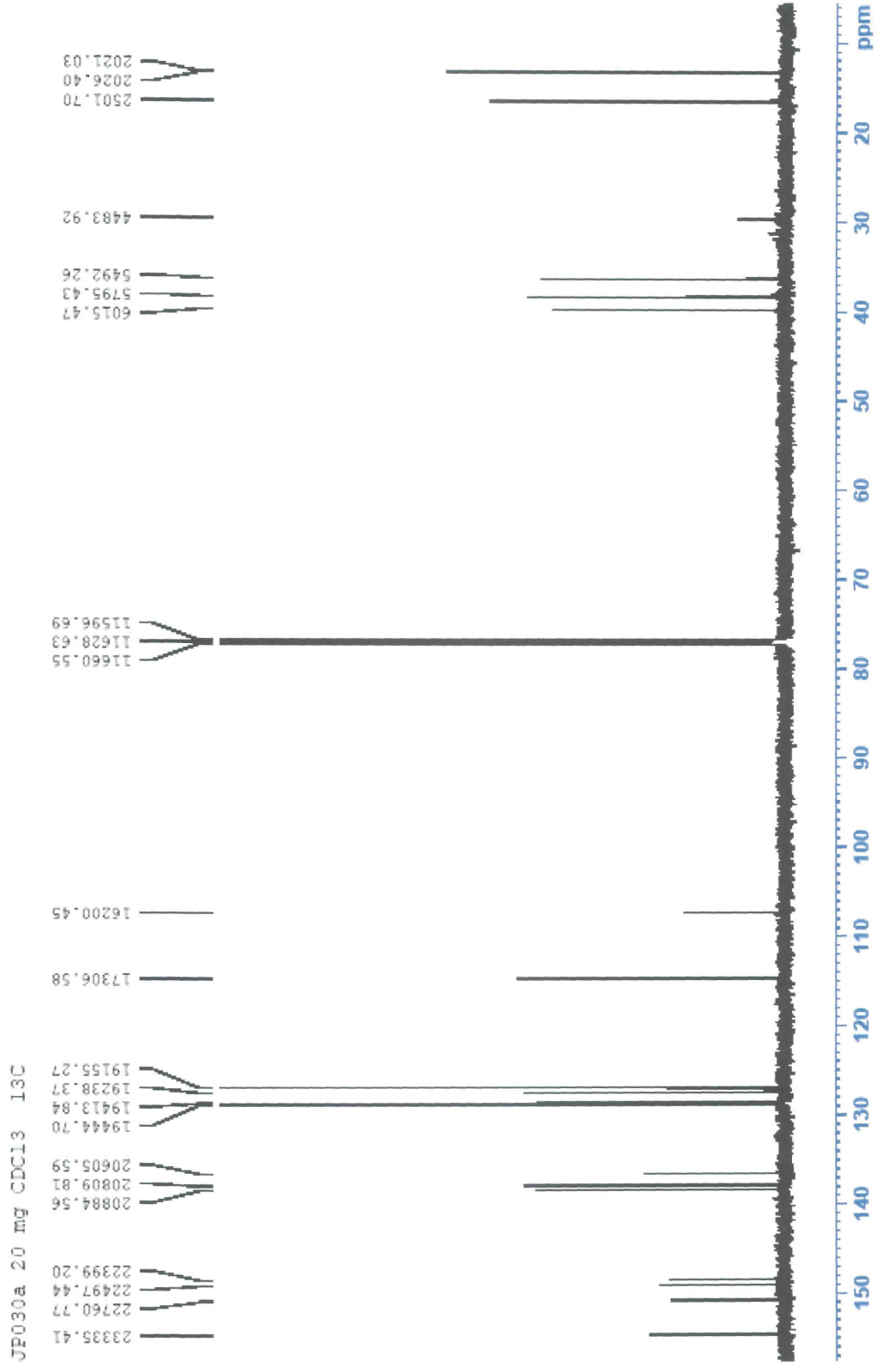
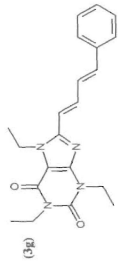
Appendix A



JP030a 20 mg CDCl₃ 1H



Appendix A





Dual inhibition of monoamine oxidase B and antagonism of the adenosine A_{2A} receptor by (*E,E*)-8-(4-phenylbutadien-1-yl)caffeine analogues

Judey Pretorius^a, Sarel F. Malan^a, Neal Castagnoli Jr.^b, Jacobus J. Bergh^a, Jacobus P. Petzer^{a,*}

^a Pharmaceutical Chemistry, School of Pharmacy, North-West University, Private Bag X6001, Potchefstroom 2520, South Africa

^b Department of Chemistry, Virginia Tech and Edward Via College of Osteopathic Medicine, Blacksburg, VA 24061, USA

ARTICLE INFO

Article history:

Received 20 June 2008

Revised 29 July 2008

Accepted 30 July 2008

Available online 5 August 2008

Keywords:

Monoamine oxidase B

Adenosine A_{2A} receptor

Reversible inhibition

Antagonism

Dual-target-directed drug

Caffeine

ABSTRACT

The adenosine A_{2A} receptor has emerged as an attractive target for the treatment of Parkinson's disease (PD). Evidence suggests that antagonists of the A_{2A} receptor (A_{2A} antagonists) may be neuroprotective and may help to alleviate the symptoms of PD. We have reported recently that several members of the (*E*)-8-styrylcaffeine class of A_{2A} antagonists also are potent inhibitors of monoamine oxidase B (MAO-B). Since MAO-B inhibitors are known to possess anti-parkinsonian properties, dual-target-directed drugs that block both MAO-B and A_{2A} receptors may have enhanced value in the management of PD. In an attempt to explore this concept further we have prepared three additional classes of C-8 substituted caffeinyl analogues. The 8-phenyl- and 8-benzylcaffeinyl analogues exhibited relatively weak MAO-B inhibition potencies while selected (*E,E*)-8-(4-phenylbutadien-1-yl)caffeinyl analogues were found to be exceptionally potent reversible MAO-B inhibitors with enzyme-inhibitor dissociation constants (K_i values) ranging from 17 to 149 nM. Furthermore, these (*E,E*)-8-(4-phenylbutadien-1-yl)caffeines acted as potent A_{2A} antagonists with K_i values ranging from 59 to 153 nM. We conclude that the (*E,E*)-8-(4-phenylbutadien-1-yl)caffeines are a promising candidate class of dual-acting compounds.

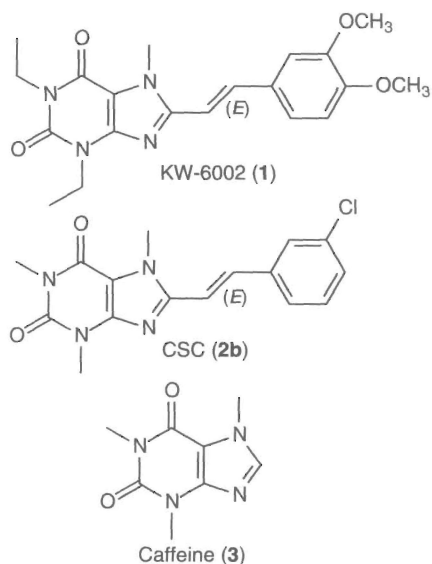
© 2008 Elsevier Ltd. All rights reserved.

1. Introduction

Currently, the therapy of Parkinson's disease (PD) is largely focused on dopamine replacement strategies with the dopamine precursor levodopa and dopamine agonist drugs.¹ Although these strategies are highly effective in controlling the early stages of the disease, long-term treatment is associated with drug-related complications such as a loss of drug efficacy, the onset of dyskinesias and the occurrence of psychosis and depression.^{2,3} The inadequacies of dopamine replacement therapy have prompted the search for alternative drug targets. The adenosine A_{2A} receptor has emerged as one such target and antagonists of this receptor (A_{2A} antagonists) are considered promising agents for the symptomatic treatment of PD.⁴ Additionally, evidence suggests that A_{2A} antagonists may slow the course of the disease by protecting against the underlying neurodegenerative processes^{5,6} and may prevent the development of dyskinesias that are normally associated with levodopa treatment.⁷ Furthermore, since the symptomatic relief conferred by A_{2A} antagonists are additive to the effect produced by dopamine replacement therapy, it may be possible to reduce the dose of the dopaminergic drugs and therefore the occurrence of side effects.^{2,8} A_{2A} antagonists are therefore a promising adjunctive to dopamine replacement therapy.⁹

A particularly well-characterized A_{2A} antagonist, (*E*)-1,3-diethyl-8-(3,4-dimethoxystyryl)-7-methylxanthine (KW-6002; **1**) (Scheme 1), is currently undergoing clinical trials for the treatment of the motor symptoms associated with PD.¹⁰ Another A_{2A} antagonist and structural analogue of KW-6002, (*E*)-8-(3-chlorostyryl)caffeine (CSC; **2b**) (Scheme 1), is frequently used when examining the in vivo pharmacological effects of A_{2A} antagonists.^{11,12} We have previously reported that CSC is also a potent reversible inhibitor of monoamine oxidase B (MAO-B) with an enzyme-inhibitor dissociation constant (K_i value) of 128 nM.^{5,13,14} Inhibitors of MAO-B also are considered to be useful for the treatment of age-related neurodegenerative diseases such as Alzheimer's disease and PD.^{15,16} Since MAO-B appears to be predominantly responsible for dopamine metabolism in the basal ganglia,^{17,18} inhibition of this enzyme in the brain may conserve the depleted supply of dopamine. MAO-B inhibitors are used in combination with levodopa as dopamine replacement therapy in patients diagnosed with early PD.¹⁹ MAO-B inhibitors have been shown to elevate dopamine levels in the striatum of primates treated with levodopa.²⁰ Furthermore, for each mole of dopamine oxidized by MAO-B, one mole of hydrogen peroxide (H₂O₂) is produced. H₂O₂ may interact with free iron to form highly reactive hydroxyl radicals that may contribute to neurodegenerative processes.²¹ Inhibition of MAO-B, therefore, may also exert a protective effect by reducing H₂O₂ production in the brain.²² These effects of MAO-B inhibitors are especially relevant when considering that the brain shows an age-related increase in MAO-B activity.^{23,24} This increase

* Corresponding author. Tel.: +27 18 2992206; fax: +27 18 2994243.
E-mail address: jacques.petzer@nwu.ac.za (J.P. Petzer).



Scheme 1. The structures of the adenosine A_{2A} receptor antagonists KW-6002 (**1**), CSC (**2b**), and caffeine (**3**).

may be attributed to glial cell proliferation, since central MAO-B is predominantly located in glial cells.²⁵ In the aged parkinsonian brain, inhibition of MAO-B may, therefore, counter the effects of increased MAO-B activity and protect against further neurodegeneration.²⁶

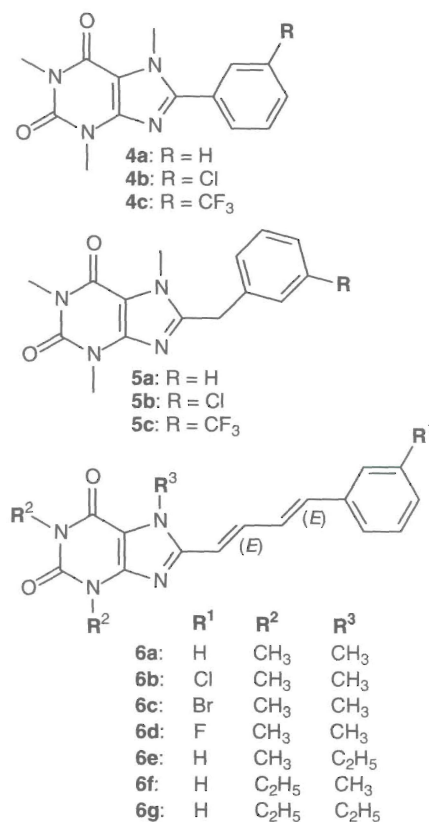
Based on these observations, dual-target-directed drugs, compounds that inhibit MAO-B and antagonize A_{2A} receptors, may have enhanced value in the management of PD. Using CSC as a lead compound we have, in the present study, attempted to identify additional dual-acting compounds, possibly with enhanced MAO-B inhibition and A_{2A} antagonism potencies. Such compounds may deepen our understanding of the structural requirements of C-8 substituted caffeinyl analogues to act as dual inhibitors of MAO-B and antagonists of the A_{2A} receptor. The (*E*)-styryl group at C-8 appears to be critical for the dual-action of CSC since caffeine (**3**) is only a moderate A_{2A} antagonist ($K_i = 22 \mu\text{M}$)¹² and a weak MAO-B inhibitor.⁵ In this study, we further investigate the importance of the (*E*)-styryl functional group for dual-action by preparing and evaluating three additional classes of C-8 substituted caffeinyl analogues. These are the 8-phenylcaffeinyl analogues **4a–c**, the 8-benzylcaffeinyl analogues **5a–c** and the (*E,E*)-8-(4-phenylbutadien-1-yl)caffeinyl analogues **6a–d** (Scheme 2). The particularly potent series of (*E,E*)-8-(4-phenylbutadien-1-yl)caffeinyl analogues **6a–d** was expanded to include the ethyl homologs, **6e–g**. The MAO-B inhibition properties of the test compounds were first investigated, and the most potent inhibitors were then further evaluated for binding at the A_{2A} receptor.

As part of this effort we have measured both the K_i and IC_{50} values (concentration of inhibitor producing 50% inhibition) for the inhibition of MAO-B of a subset of the test compounds. The results have provided an opportunity to examine the validity of the relationship between K_i and IC_{50} of a competitive inhibitor of a mono-substrate reaction that is described by the Cheng-Prusoff equation, $K_i = \text{IC}_{50}/(1 + [S]/K_m)$,²⁷ by comparing experimentally determined K_i values to those calculated from the IC_{50} values.²⁸

2. Results

2.1. Chemistry

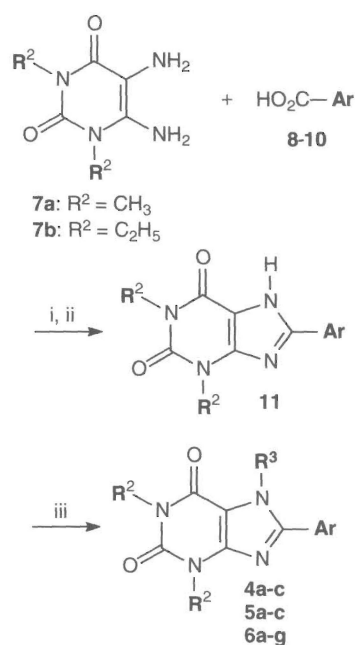
The C-8 substituted caffeinyl analogues **4a–c**, **5a–c**, and **6a–g** (Scheme 2) were prepared in high yield according to the procedure



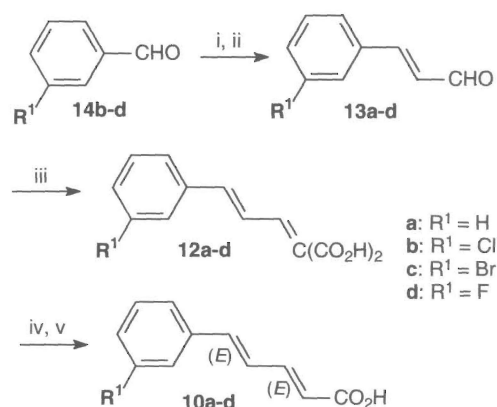
Scheme 2. The structures of the C-8 substituted caffeinyl analogues that were investigated in the present study: 8-phenylcaffeinyl analogues **4a–c**, 8-benzylcaffeinyl analogues **5a–c**, and (*E,E*)-8-(4-phenylbutadien-1-yl)caffeinyl analogues **6a–g**.

previously reported for the preparation of (*E*)-8-styrylcaffeinyl analogues.^{29,14} The key starting materials for the procedure, 1,3-dimethyl- (**7a**) and 1,3-diethyl-5,6-diaminouracil (**7b**),³⁰ were allowed to react with the appropriate carboxylic acid in the presence of the carbodiimide activating reagent *N*-(3-dimethylamino-propyl)-*N'*-ethylcarbodiimide hydrochloride (EDAC) (Scheme 3). The commercially available benzoic acids **8a–c**, phenylacetic acids **9a–c**, and newly synthesized (*E,E*)-5-phenyl-2,4-pentadienoic acids **10a–d** (see below) were used for the preparation of **4a–c**, **5a–c**, and **6a–g**, respectively. The resulting amidyl intermediates underwent ring closure when heated under reflux in aqueous sodium hydroxide to yield the corresponding 1,3-dialkyl-8-substituted-7*H*-xanthinyl analogues (**11**). Without further purification, the crude xanthinyl intermediates were selectively 7*N*-alkylated with an excess of iodomethane (**4a–c**, **5a–c**, **6a–d**, and **6f**) or iodoethane (**6e** and **6g**) and potassium carbonate to yield the target compounds **4–6**. Following crystallization from a suitable solvent, the structures and purity of all compounds were verified by mass spectrometry, ¹H NMR and ¹³C NMR. The *trans–trans* geometry about the conjugated ethenyl π -bonds of **6a–g** was confirmed by proton–proton coupling constants in the range of 14.6–15.5 Hz for the olefinic proton signals.

The (*E,E*)-5-phenyl-2,4-pentadienoic acids (**10a–d**) required for the preparation of **6a–g** were conveniently prepared by allowing the appropriately substituted cinnamylidenemalonamic acid (**12a–d**) to react with refluxing acetic anhydride and acetic acid (Scheme 4).³¹ A solution of the resulting crude 5-phenyl-2,4-pentadienoic acids in chloroform containing a crystal of iodine was exposed to ambient light for 5 h. This photochemical reaction converts the *allo*-styryl-acrylic acid into the desired *trans–trans* geometry.³¹



Scheme 3. Synthetic pathway to the C-8 substituted caffeinyl analogues **4a–c**, **5a–c**, and **6a–g**. Reagents and conditions: (i) EDAC, dioxane/H₂O; (ii) NaOH (aq), reflux; (iii) CH₃I or C₂H₅I, K₂CO₃, DMF.



Scheme 4. Synthetic pathway to the (*E,E*)-5-phenyl-2,4-pentadienoic acids (**10a–d**). Reagents and conditions: (i) NaOH, CH₃CHO; (ii) Ac₂O, 120 °C; (iii) CH₂(CO₂H)₂, pyridine, 100 °C; (iv) Ac₂O, CH₃CO₂H, reflux; (v) I₂, light.

Following recrystallization from benzene, **10a–d** were obtained in good yield and with a high degree of purity. The required cinnamylidene malonic acids (**12a–d**) were in turn prepared in high yield from the corresponding cinnamaldehydes (**13a–d**) and malonic acid in pyridine.³² Except for cinnamaldehyde (**13a**), which is commercially available, the other substituted cinnamaldehydes (**13b–d**) were prepared by reacting the corresponding benzaldehydes (**14b–d**) with acetaldehyde under basic conditions.^{33,34} The resulting cinnamaldehydes were purified by neutral aluminum oxide column chromatography.

2.2. MAO-B inhibition studies

Enzyme activity measurements were based on the MAO-B catalyzed oxidation of 1-methyl-4-(1-methylpyrrol-2-yl)-1,2,3,6-tetrahydropyridine (MMTP) to the corresponding dihydropyridinium metabolite (MMDP⁺).³⁵ MMDP⁺ absorbs light maximally at a wavelength of 420 nm. Since neither MMTP nor the test inhibitors

absorb light at this wavelength, it is possible to measure the rates of substrate oxidation spectrophotometrically. We have employed baboon liver mitochondrial preparations as the enzyme source. Even though MMTP is a MAO-A/B mixed substrate, its oxidation by baboon liver mitochondria is exclusively attributed to the action of MAO-B since baboon liver tissue exhibits a high degree of MAO-B catalytic activity while MAO-A activity is negligible.³⁵ Also, the interaction of reversible inhibitors with MAO-B obtained from baboon liver tissue appears to be similar to the interaction with the human form of the enzyme, since inhibitors such as CSC are approximately equipotent with both enzyme sources.¹⁴ The incubation time of the enzyme catalyzed reaction was 10 min since the rate of MMTP oxidation was found to be linear (Fig. 1) for at least 10 min at all substrate concentrations (30–120 μM) used in the inhibition studies. From Lineweaver–Burke plots generated from data obtained in the absence of inhibitor, we have estimated the *K_m* value for the oxidation of MMTP by baboon liver MAO-B to be 68.3 ± 1.60 μM, a value consistent with the reported value of 60.8 μM.³⁵ This *K_m* was used in the studies where *K_i* values for the inhibition of MAO-B were calculated from the corresponding IC₅₀ values (see below).

All of the C-8 substituted caffeinyl analogues tested were found to be inhibitors of MAO-B. As demonstrated with (*E,E*)-8-(4-phenylbutadien-1-yl)caffeine (**6a**) (Fig. 2), the lines of the Lineweaver–Burke plots intersected at the y-axis, indicating the mode of inhibition to be competitive. Competitive inhibition has also been observed with (*E*)-8-styrylcaffeinyl analogues.^{13,14,36} The enzyme–inhibitor dissociation constants (*K_i* values) for the inhibition of MAO-B by the test compounds are presented in Tables 1–3. The 8-phenylcaffeinyl analogues **4a–c** (Table 1) and 8-benzylcaffeinyl analogues **5a–c** (Table 2) were found to be relatively weak inhibitors with *K_i* values ranging from 36.0 to 97.6 μM. Compounds **4c** and **5a** were especially weak inhibitors with only 24.0% and 18.0% inhibition at a concentration of 1000 μM. In contrast, the (*E,E*)-8-[4-(3-phenylbutadien-1-yl)caffeinyl] analogues **6a–d** (Table 3) were exceptionally potent MAO-B inhibitors. The most potent inhibitor was (*E,E*)-8-[4-(3-bromophenyl)butadien-1-yl]caffeine (**6c**) with a *K_i* value of 17.2 nM, approximately 3.6 times more potent than that of the corresponding (*E*)-8-(3-bromostyryl)caffeinyl analogue **2c** (Table 4).³⁶ The second most potent inhibitor was (*E,E*)-8-[4-(3-chlorophenyl)butadien-1-yl]caffeine (**6b**) with a *K_i* value of 42.1 nM. This is approximately 2.5 times more potent than that of the corresponding (*E*)-8-(3-chlorostyryl)caffeinyl analogue

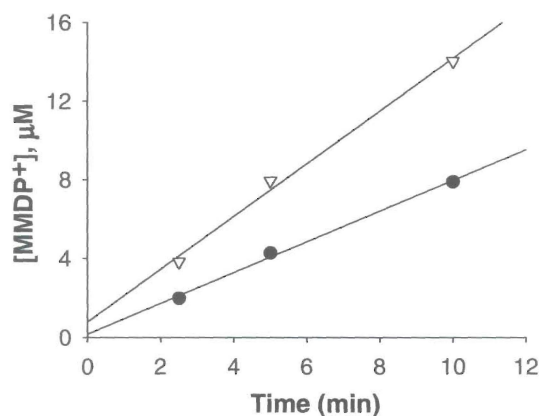


Figure 1. Linearity in the oxidation of MMTP by baboon liver MAO-B (0.15 mg protein/mL of the mitochondrial preparation). The concentration of MMDP⁺ produced was measured spectrophotometrically following termination of the enzyme catalyzed reaction at time points of 2.5, 5, and 10 min. The concentrations of MMTP used in this study were 30 μM (filled circles) and 120 μM (open triangles).

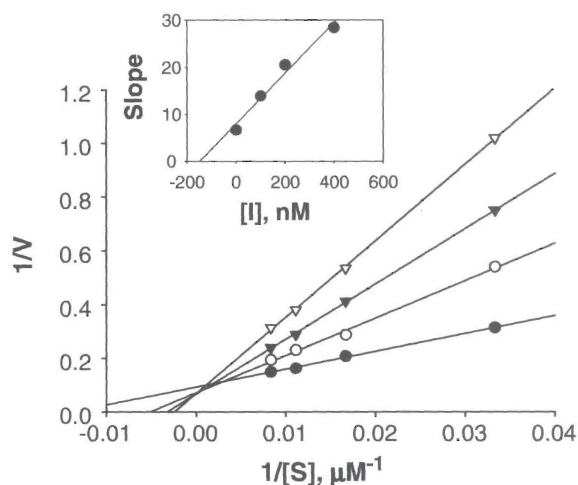


Figure 2. Lineweaver–Burke plots of the oxidation of MMTP by baboon liver MAO-B in the absence (filled circles) and presence of various concentrations of **6a** (open circles, 0.1 μM ; filled triangles, 0.2 μM ; open triangles, 0.4 μM). The concentration of the baboon liver mitochondrial preparation was 0.15 mg protein/mL, and the rates are expressed as nmol of MMDP⁺ formed/mg protein/min. The inset is the replot of the slopes versus the inhibitor concentrations.

Table 1

The K_i values for the inhibition of MAO-B by 8-phenylcaffeinyl analogues **4a–c**

	R	K_i value ^a (μM)
4a	H	86.2
4b	Cl	36.0
4c	CF ₃	24.0% ^b

^a The enzyme source used was baboon liver mitochondrial MAO-B.

^b Percentage inhibition at an inhibitor concentration of 1000 μM . Due to limited solubility in the aqueous incubation solvent, higher concentrations were not tested.

Table 2

The K_i values for the inhibition of MAO-B by 8-benzylcaffeinyl analogues **5a–c**

	R	K_i value ^a (μM)
5a	H	18.0% ^b
5b	Cl	54.6
5c	CF ₃	97.6

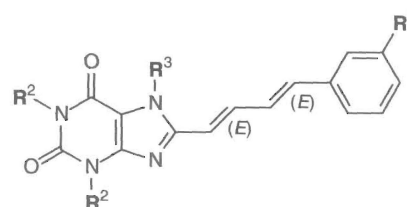
^a The enzyme source used was baboon liver mitochondrial MAO-B.

^b Percentage inhibition at an inhibitor concentration of 1000 μM . Due to limited solubility in the aqueous incubation solvent, higher concentrations were not tested.

CSC (**2b**) that has a reported K_i value for the inhibition of baboon liver MAO-B of 128 nM.¹⁴ The K_i value for CSC determined in this study is 80.6 nM (Table 4). This trend also exists for the other (*E,E*)-8-(4-phenylbutadien-1-yl)caffeinyl analogues **6a** and **6d** with the most dramatic difference in activities found with **6a** ($K_i = 148.6$ nM) that is 19 times more potent than (*E*)-8-styrylcaf-

Table 3

The K_i and IC_{50} values for the inhibition of MAO-B by (*E,E*)-8-(4-phenylbutadien-1-yl)caffeinyl analogues **6a–g**



	R1	R2	R3	Exp. K_i^a (nM)	Exp. $\text{IC}_{50}^{a,b}$ (nM)	Calcd K_i^c (nM)
6a	H	CH ₃	CH ₃	148.6	383 \pm 5.65	221.1
6b	Cl	CH ₃	CH ₃	42.1	96.3 \pm 22.2	55.6
6c	Br	CH ₃	CH ₃	17.2	37.9 \pm 7.42	21.9
6d	F	CH ₃	CH ₃	46.4	89.0 \pm 6.20	51.4
6e	H	CH ₃	C ₂ H ₅	1712	2371 \pm 42.5	1369
6f	H	C ₂ H ₅	CH ₃	–	32.7% ^d	–
6g	H	C ₂ H ₅	C ₂ H ₅	–	14.6% ^d	–

^a The enzyme source used was baboon liver mitochondrial MAO-B.

^b The IC_{50} values were experimentally determined by fitting the rate data to the one site competition model incorporated into the Prism software package.

^c The K_i values were calculated from the experimental IC_{50} values according to the equation by Cheng and Prusoff: $K_i = \text{IC}_{50}/(1 + [S]/K_m)$ with $[S] = 50$ μM and K_m (MMTP) = 68.3 \pm 1.60 μM .²⁷

^d Percentage inhibition at an inhibitor concentration of 30 μM . Due to limited solubility in the aqueous incubation solvent, higher concentrations were not tested, and K_i values were not determined.

Table 4

The K_i and IC_{50} values for the inhibition of MAO-B by (*E*)-8-styrylcaffeinyl analogues **2a–d**

	R	Exp. K_i^a (nM)	Exp. $\text{IC}_{50}^{a,b}$ (nM)	Calcd K_i^c (nM)
2a	H	2864 ^d	Not determined ^e	–
2b	3-Cl	80.6 \pm 1.96; 128 ^d	146 \pm 1.42	84.3
2c	3-Br	62.7 \pm 2.73; 83 ^f	107 \pm 4.59	61.8
2d	3,4-Cl ₂	18.9 \pm 0.89; 36 ^f	28.4 \pm 1.07	16.4

^a The enzyme source used was baboon liver mitochondrial MAO-B.

^b The IC_{50} values were experimentally determined by fitting the rate data to the one site competition model incorporated into the Prism software package.

^c The K_i values were calculated from the experimental IC_{50} values according to the equation by Cheng and Prusoff: $K_i = \text{IC}_{50}/(1 + [S]/K_m)$ with $[S] = 50$ μM and K_m (MMTP) = 68.3 \pm 1.60 μM .²⁷

^d Value obtained from Ref. 14.

^e For weak inhibitors limits of aqueous solubility prevents accurate IC_{50} determinations.

^f Value obtained from Ref. 36.

feine (**2a**) with a reported K_i value of 2864 nM.¹⁴ In view of the exceptional MAO-B inhibition potencies of **6a–d**, we have expanded the series to include the ethyl homologs **6e–g**. These compounds provided an opportunity to examine the effects that homologation at positions 1, 3, and 7 of the caffeinyl ring would have on MAO-B inhibition potency and A_{2A} antagonism activity. As shown in Table 3, **6e–g** proved to be much weaker MAO-B inhibitors than the corresponding methyl analogues **6a–d**. For example, the K_i value for the inhibition of MAO-B by **6e** (1712 nM) was over 10 times higher than the corresponding value for **6a**. Similarly, at a relatively high concentration of 30 μM , **6f** and **6g** exhibited only 32.7% and 14.6% MAO-B inhibition, respectively.

For the (*E,E*)-8-(4-phenylbutadien-1-yl)caffeinyl analogues **6a–e** we have also measured the IC_{50} values for the inhibition of

MAO-B. An example of the data routinely obtained for the IC_{50} determinations is illustrated by (*E,E*)-8-[4-(3-chlorophenyl)butadien-1-yl]caffeine (**6b**) (Fig. 3). Considering that the substrate concentration used for the IC_{50} determinations was $50 \mu\text{M}$ and the K_m value of MMTP oxidation by baboon liver mitochondrial MAO-B is $68.3 \pm 1.60 \mu\text{M}$, we have also calculated the K_i values from the measured IC_{50} values. As mentioned in the introduction, the relationship between K_i and IC_{50} of a competitive inhibitor of a monosubstrate reaction is described by the Cheng–Prusoff equation: $K_i = IC_{50}/(1 + [S]/K_m)$.²⁷ As shown in Table 3, the calculated K_i values closely approximate those that were experimentally determined, and the differences are within the range expected for experimental error. For example, the K_i value for the reversible interaction of **6a** with MAO-B was measured as 148.6 nM , while the value calculated from the IC_{50} was found to be 221.1 nM . The same trend is observed for (*E*)-8-styrylcaffeine analogues **2b–d** (Table 4) where the experimentally determined K_i value of CSC (**2b**), for example, was 80.6 nM while the value calculated from the corresponding IC_{50} was 84.3 nM . It should be noted that the accuracy of an IC_{50} determination is dependent upon adequately defining the sigmoid curve (obtained from plotting the MAO-B catalyzed MMTP oxidation rate versus the logarithm of the inhibitor concentration) at both low and high inhibitor concentrations. For relatively weak inhibitors such as **2a**, the limit of solubility in the aqueous incubation solvent prevents the definition of the curve at higher inhibitor concentrations (maximal inhibition) and an accurate IC_{50} determination is therefore not possible.

2.3. Adenosine A_{2A} receptor antagonism studies

The (*E,E*)-8-(4-phenylbutadien-1-yl)caffeine analogues **6a–g** were selected for further evaluation as potential antagonists of the adenosine A_{2A} receptor. The potencies by which the test compounds antagonize A_{2A} receptors were determined by the radioligand binding procedure described in lit.³⁷ Binding to the A_{2A} receptors was evaluated with N -[^3H]ethyladenosin-5'-uronamide ([^3H]NECA) in rat striatal membranes in the presence of N^6 -cyclo-pentyladenosine (CPA) to minimize the adenosine A_1 receptor binding component of [^3H]NECA. This procedure is frequently used to identify compounds that exhibit high binding affinity and selectivity to A_{2A} receptors.^{11,12,29} As positive controls we included the

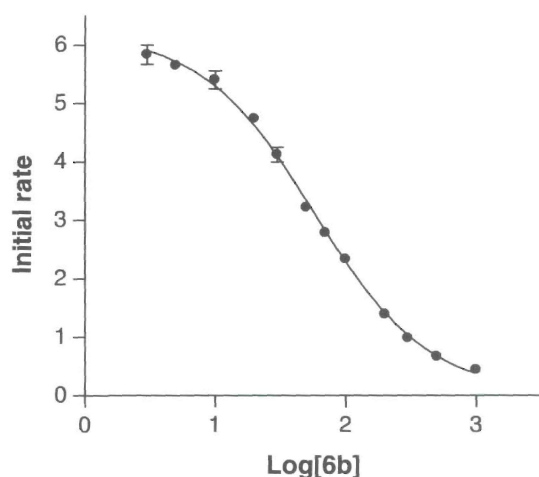


Figure 3. The sigmoidal dose–response curve of the initial rates of oxidation of MMTP versus the logarithm of concentration of inhibitor **6b** (expressed in nM). The concentration of the baboon liver mitochondrial preparation was $0.15 \text{ mg protein/mL}$; the rates are expressed as nmol MPDP^+ formed/ mg protein/min ; the concentration of MMTP used was $50 \mu\text{M}$. The determinations were carried out in duplicate and the values are expressed as mean \pm SEM.

known A_{2A} antagonists CSC (**2b**) and KW-6002 (**1**). As reported in Table 5, a K_i value of $30.2 \pm 5.40 \text{ nM}$ was observed for CSC. This value corresponds well with the lit. values of $36 \pm 6 \text{ nM}$ ¹² and $54 \pm 19 \text{ nM}$.¹¹ The K_i value obtained for KW-6002 (**1**) was $4.46 \pm 1.13 \text{ nM}$ that compares favorably with the lit. value of $2.2 \pm 0.34 \text{ nM}$.¹⁰

As shown in Table 5 all of the (*E,E*)-8-(4-phenylbutadien-1-yl)caffeine analogues (**6a–g**) tested were found to be potent antagonists of the A_{2A} receptor. The dose–inhibition curves for the test compounds versus [^3H]NECA that were routinely observed are illustrated by example with **6f** (Fig. 4). This analogue was found to be the most potent antagonist with a K_i value of $2.74 \pm 0.35 \text{ nM}$. Since **6f** is approximately 55 times more potent than the corresponding caffeine analogue **6a**, 1,3-diethyl substitution of the xanthinyl ring leads to enhanced A_{2A} antagonism potency compared to 1,3-dimethyl substitution.

3. Discussion

We have recently reported that several (*E*)-8-styrylcaffeines act as potent reversible inhibitors of MAO-B.^{13,14,36} (*E*)-8-Styrylcaffeines have also been shown to be antagonists of adenosine A_{2A} receptors.^{11,12,29} In the present study, using (*E*)-8-styrylcaffeine as the lead compound, we have attempted to identify additional dual-target-directed compounds, possibly with enhanced MAO-B inhibition and A_{2A} antagonism potencies. This study also served to elucidate the structural requirements of C-8 substituted caffeine analogues to act as dual inhibitors of MAO-B and antagonists of the adenosine A_{2A} receptor. Since caffeine (**3**) is a weak inhibitor of MAO-B⁵ and only a moderately potent adenosine A_{2A} antagonist,¹² it can be concluded that the (*E*)-styryl group at C-8 plays an important role in the dual-action of (*E*)-8-styrylcaffeines. In this study we have prepared three additional classes of C-8 substituted caffeine analogues **4**, **5**, and **6**. The series of (*E,E*)-8-(4-phenylbutadien-1-yl)caffeine analogues **6a–d** was expanded to include the ethyl homologs **6e–g** that provided additional insight into the ste-

Table 5
The K_i values for the competitive inhibition of [^3H]NECA binding to rat striatal adenosine A_{2A} receptors by selected caffeine analogues

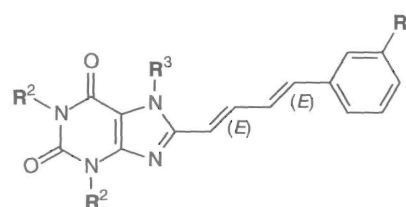
	R ¹	R ²	R ³	K_i value ^a (nM)
6a	H	CH ₃	CH ₃	153 ± 5.40
6b	Cl	CH ₃	CH ₃	104 ± 1.50
6c	Br	CH ₃	CH ₃	59.1 ± 15.8
6d	F	CH ₃	CH ₃	114 ± 14.2
6e	H	CH ₃	C ₂ H ₅	13.5 ± 4.87
6f	H	C ₂ H ₅	CH ₃	2.74 ± 0.35
6g	H	C ₂ H ₅	C ₂ H ₅	7.73 ± 2.80
1	KW-6002			4.46 ± 1.13 ; (2.2) ^b
2b	CSC			30.2 ± 5.40 ; (36) ^c ; (54) ^d

^a The K_i values for the competitive inhibition of [^3H]NECA ($K_d = 15.3 \text{ nM}$) binding was calculated from the corresponding IC_{50} values according to the Cheng–Prusoff equation.²⁷ The IC_{50} values were in turn determined by fitting the data, using nonlinear least-squares regression analysis, to the one site competition model incorporated into the Prism software package.

^b Value obtained from Ref. 10.

^c Value obtained from Ref. 12.

^d Value obtained from Ref. 11.



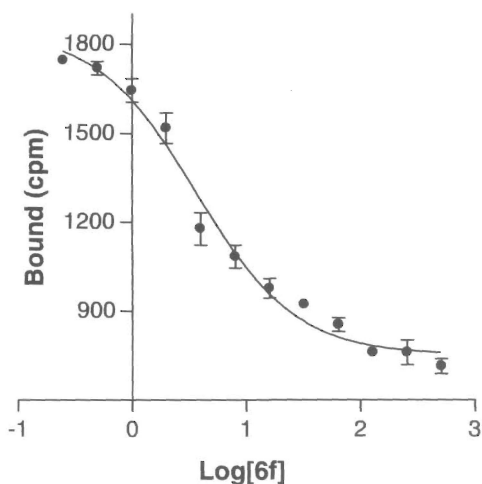


Figure 4. The sigmoidal dose–response curve for the inhibition of [³H]NECA binding to rat striatal A_{2A} receptors by antagonist **6f** (expressed in nM). The IC₅₀ value was determined by fitting the data, using nonlinear least-squares regression analysis, to the one site competition model incorporated into the Prism software package (GraphPad Software Inc.). The K_i value (2.74 nM) for the competitive inhibition of [³H]NECA (K_d = 15.3 nM) binding was calculated with the Cheng–Prusoff equation.²⁷ In this experiment the non-saturable, nonspecific binding was 623 cpm. The determinations were carried out in duplicate and the values are expressed as mean ± SEM.

ric features associated with the potencies of MAO-B inhibition and A_{2A} antagonism.

The results of MAO-B inhibition studies have shown that the 8-phenylcaffeinyll (**4a–c**) and 8-benzylcaffeinyll (**5a–c**) analogues were weak inhibitors of MAO-B while the (*E,E*)-8-(4-phenylbutadien-1-yl)caffeinyll analogues **6a–d** were found to be exceptionally potent inhibitors. For example, the (*E,E*)-8-(4-phenylbutadien-1-yl)caffeinyll analogue **6b** substituted with chlorine at C-3 of the phenyl ring (K_i = 42.1 nM) was approximately 855 and 1269 times more potent as an MAO-B inhibitor than was the corresponding C-3 chlorine substituted 8-phenylcaffeinyll analogue **4b** (K_i = 36.0 μM) and 8-benzylcaffeinyll analogue **5b** (K_i = 54.6 μM), respectively. The (*E,E*)-8-(4-phenylbutadien-1-yl)caffeinyll analogues **6a–d** were also more potent inhibitors than the corresponding (*E*)-8-styrylcaffeinyll analogues **2a–c**. For example, chloro substituted analogue **6b** (K_i = 42.1 nM) was approximately 1.9 times more potent than CSC (**2b**) (K_i = 80.6 nM) while the unsubstituted (*E,E*)-8-(4-phenylbutadien-1-yl)caffeinyll analogue **6a** (K_i = 148.6 nM) was almost 20 times more potent than the corresponding unsubstituted (*E*)-8-styrylcaffeinyll analogue **2a** (K_i = 2864 nM). Compounds **6e–g** were found to be relatively weak inhibitors of MAO-B indicating that ethyl substitution at positions 1, 3, and 7 of the caffeinyll ring has a negative effect on the potency of MAO-B inhibition. This result suggests that 1, 3, and 7 methyl substitution is probably optimal for the design of xanthine-based reversible MAO-B inhibitors. In the case of (*E*)-8-styrylcaffeinyls, 1,3-diethyl substitution of the caffeine ring has also been shown to reduce the MAO-B inhibition potency compared to 1,3-dimethyl substitution.¹³

Since the series of (*E,E*)-8-(4-phenylbutadien-1-yl)caffeinyll analogues was found to include exceptionally potent reversible MAO-B inhibitors, they were selected for further evaluation as potential antagonists of the adenosine A_{2A} receptor. All the (*E,E*)-8-(4-phenylbutadien-1-yl)caffeinyll analogues **6a–g** were found to be relatively potent A_{2A} antagonists. In contrast to its effect on MAO-B inhibition potency, ethyl substitution at positions 1, 3, and 7 of the caffeinyll ring had a positive effect on the potency of A_{2A} antagonism. For example, the 1,3-diethyl analogue **6f** (K_i = 2.74 nM) was approximately 55 times more potent than the

corresponding 1,3-dimethyl analogue **6a** (K_i = 153 nM). Although functional antagonism has not been demonstrated, it is reasonable to assume caffeine derived structures would act in an antagonistic manner since caffeine analogues are well-known antagonists of the adenosine A_{2A} receptor.

We conclude that the (*E,E*)-8-(4-phenylbutadien-1-yl)caffeinyls, **6a–d**, are promising lead compounds for the development of dual-target-directed compounds that inhibit MAO-B and antagonize A_{2A} receptors. Although 1,3-diethyl substitution of the caffeinyll ring leads to enhanced potency of A_{2A} antagonism, the opposite effect was observed on MAO-B inhibition potency.

In the second part of this study it was shown that for potent inhibitors, the K_i values for competitive interaction with MAO-B could be accurately calculated from the corresponding IC₅₀ values using the Cheng–Prusoff equation. This would facilitate the comparison of IC₅₀ and K_i values from different lit. sources and the employment of the inhibitors in QSAR studies.

4. Experimental

Caution: MMTP is a structural analogue of the nigrostriatal neurotoxin, 1-methyl-4-phenyl-1,2,3,6-tetrahydropyridine (MPTP), and should be handled using disposable gloves and protective eye-wear. Procedures for the safe handling of MPTP have been described previously.³⁸

4.1. Chemicals and instrumentation

All starting materials, unless mentioned elsewhere, were obtained from Sigma–Aldrich and were used without purification. The oxalate salt of MMTP,³⁹ KW-6002 (**1**),^{13,29} compounds **2b–2d**,^{14,36} 1,3-dimethyl- (**7a**) and 1,3-diethyl-5,6-diaminouracil (**7b**)³⁰ were prepared according to previously reported procedures. Because of chemical instability, compounds **7a–b** were used within 24 h of preparation. Proton and carbon NMR spectra were recorded on a Varian Gemini 300 spectrometer. Proton (¹H) spectra were recorded in CDCl₃ or DMSO-*d*₆ at a frequency of 300 MHz and carbon (¹³C) spectra at 75 MHz. Chemical shifts are reported in parts per million (δ) downfield from the signal of tetramethylsilane added to the deuterated solvent. Spin multiplicities are given as s (singlet), d (doublet), t (triplet), q (quartet), dd (doublet of doublets), or m (multiplet) and the coupling constants (*J*) are given in hertz (Hz). Direct insertion electron impact ionization (EIMS) and high resolution mass spectra (HRMS) were obtained on a VG 7070E mass spectrometer. Melting points (mp) were determined on a Stuart SMP10 melting point apparatus and are uncorrected. UV–vis spectra were recorded on a Shimadzu UV-2100 double-beam spectrophotometer. Thin layer chromatography (TLC) was carried out with neutral aluminum oxide 60 (Merck) containing UV₂₅₄ fluorescent indicator. [³H]NECA was obtained from Amersham (specific activity 25 Ci/mmol), while adenosine deaminase (type X from calf spleen) and CPA were from Sigma–Aldrich. Counting of radio activities was performed using a Packard Tri-Carb 2100 TR liquid scintillation counter.

4.2. General procedure for the synthesis of (*E,E*)-5-phenyl-2,4-pentadienoic acids (**10a–d**)

Compounds **10a–d** were prepared from the corresponding cinnamylidenemalonic acids (**12a–d**)³² according to the previously described procedure.³¹ Cinnamylidenemalonic acids (**12a–d**) (1 g) were allowed to reflux for 60 min with acetic anhydride (5 mL) and acetic acid (3 mL). The reaction was cooled to room temperature and poured into 100 mL water. After 3 h, the resulting precipitate was collected by filtration. The crude product and a crystal of iodine were dissolved in 20 mL CHCl₃ and incubated in

ambient light for 5 h. The CHCl_3 was removed under reduced pressure and the residue was recrystallized from benzene. For previously described **10a–c**, the melting points were recorded as follows: **10a** 194 °C, lit. 178 °C³¹; **10b** 190 °C, lit. 173–174 °C⁴⁰; **10c** 187 °C, lit. 179–180.⁴¹

4.2.1. (*E,E*)-5-(3-Fluorophenyl)-2,4-pentadienoic acid (**10d**)

The title compound was prepared from **12d** in a yield of 42%. Mp 164 °C; ¹H NMR (DMSO-*d*₆) δ 6.03 (d, 1H, *J* = 15.0 Hz), 7.10–7.45 (m, 7H) ¹³C NMR (DMSO-*d*₆) δ 112.90, 113.16, 115.33, 123.18, 123.51, 128.09, 130.63, 130.74, 138.19, 143.66, 167.31; EIMS *m/z* 192 (*M*⁺); HRMS calcd 192.05866; found: 192.05936.

4.3. General procedure for the synthesis of caffeinyl analogues (**4a–c**, **5a–c**, and **6a–g**)

The C-8 substituted caffeinyl analogues examined in this study were prepared according to the procedure described in lit.²⁹ 1,3-Dimethyl- (**7a**) or 1,3-diethyl-5,6-diaminouracil (**7b**) (3.50 mmol) and *N*-(3-dimethylaminopropyl)-*N'*-ethylcarbodiimide hydrochloride (EDAC; 5.11 mmol) were dissolved in 40 mL dioxane/H₂O (1:1) and the appropriate carboxylic acid [benzoic acids (**8a–c**), phenylacetic acids (**9a–c**), or (*E,E*)-5-phenyl-2,4-pentadienoic acids (**10a–d**), 3.81 mmol] was added. A suspension was obtained and the pH was adjusted to 5 with 2 M aqueous hydrochloric acid. The reaction mixture was stirred for an additional 2 h and then neutralized with 1 M aqueous sodium hydroxide. After cooling to 0 °C, the precipitate that formed was collected by filtration. A solution of this crude amide in 40 mL aqueous sodium hydroxide (1 M)/dioxane (1:1) was heated under reflux for 2 h, cooled to 0 °C and then acidified to a pH of 4 with 4 M aqueous hydrochloric acid. For the preparation of **4a–c**, **5a–c**, and **6a–e**, the resulting precipitate, the corresponding 1,3-dimethyl-8-substituted-7*H*-xanthinyl analogue (**11**), was collected by filtration and used in the subsequent reaction without further purification. For the preparation of **6f–g**, the resulting precipitate was removed via filtration and the filtrate was extracted to CHCl_3 (2 × 100 mL). The organic phase was dried over anhydrous MgSO_4 and removed under reduced pressure to yield a yellow oily residue, the 1,3-diethyl-8-substituted-7*H*-xanthinyl analogues (**11**). To a stirred suspension of **11** (0.20 mmol) and potassium carbonate (0.50 mmol) in 5 mL DMF was added iodomethane (**4a–c**, **5a–c**, **6a–d**, and **6f**) or iodoethane (**6e** and **6g**) (0.40 mmol). Stirring was continued at 60 °C for 60 min, and the insoluble materials were removed by filtration. Sufficient water was added to the filtrate to precipitate the product (**4–6**) which was collected by filtration. Following crystallization from a mixture of methanol/ethyl acetate (9:1) (**4a–c**, **5a–c**, and **6a–e**) or ethanol (**6f–g**), analytically pure samples of the target compounds were obtained. For previously described **4a** and **5a**, we found the melting points to be 180 and 165 °C [from methanol/ethyl acetate (9:1)] while the reported melting points are 178 °C¹² and 161–163 °C,⁴² respectively.

4.3.1. 8-(3-Chlorophenyl)caffeine (**4b**)

The title compound was prepared from 1,3-dimethyl-5,6-diaminouracil (**7a**), 3-chlorobenzoic acid (**8b**), and iodomethane in a yield of 91%; mp 202 °C; ¹H NMR (CDCl_3) δ 3.39 (s, 3H), 3.58 (s, 3H), 4.04 (s, 3H), 7.43–7.48 (m, 2H), 7.53–7.56 (m, 1H), 7.67–7.69 (m, 1H); ¹³C NMR (CDCl_3) δ 27.97, 29.72, 33.90, 108.73, 127.07, 129.28, 130.10, 130.42, 135.05, 148.16, 150.40, 151.60, 155.51; EIMS *m/z* 304 (*M*⁺); HRMS calcd 304.07270; found: 304.07108.

4.3.2. 8-(3-Trifluoromethylphenyl)caffeine (**4c**)

The title compound was prepared from 1,3-dimethyl-5,6-diaminouracil (**7a**), 3-trifluoromethylbenzoic acid (**8c**), and iodomethane

in a yield of 33.6%; mp 192 °C; ¹H NMR (CDCl_3) δ 3.39 (s, 3H), 3.59 (s, 3H), 4.05 (s, 3H), 7.61–7.67 (m, 1H), 7.73–7.77 (m, 1H), 7.84–7.88 (m, 1H), 7.95–7.96; ¹³C NMR (CDCl_3) δ 27.97, 29.74, 33.87, 108.84, 121.74, 126.14 (q), 126.93 (q), 129.32, 129.46, 131.62 (q), 132.26, 148.20, 150.23, 151.59, 155.52; EIMS *m/z* 338 (*M*⁺); HRMS calcd 338.09906; found: 338.09735.

4.3.3. 8-(3-Chlorobenzyl)caffeine (**5b**)

The title compound was prepared from 1,3-dimethyl-5,6-diaminouracil (**7a**), 3-chlorophenylacetic acid (**9b**) and iodomethane in a yield of 42%; mp 132 °C; ¹H NMR (CDCl_3) δ 3.36 (s, 3H), 3.56 (s, 3H), 3.79 (s, 3H), 4.10 (s, 2H), 7.02–7.05 (m, 1H), 7.14–7.16 (m, 1H), 7.21–7.24 (m, 2H); ¹³C NMR (CDCl_3) δ 27.83, 29.74, 31.00, 32.96, 107.85, 126.38, 127.54, 128.35, 130.16, 134.84, 137.00, 147.87, 151.20, 151.59, 155.30; EIMS *m/z* 319 (*M*⁺); HRMS calcd 318.08835; found: 318.08702.

4.3.4. 8-(3-Trifluoromethylbenzyl)caffeine (**5c**)

The title compound was prepared from 1,3-dimethyl-5,6-diaminouracil (**7a**), 3-(trifluoromethyl)phenylacetic acid (**9c**), and iodomethane in a yield of 49%; mp 163 °C; ¹H NMR (CDCl_3) δ 3.36 (s, 3H), 3.55 (s, 3H), 3.81 (s, 3H), 4.18 (s, 2H), 7.34–7.52 (m, 4H); ¹³C NMR (CDCl_3) δ 27.83, 29.72, 31.00, 33.14, 107.86, 122.00, 124.23 (q), 125.08 (q), 125.61, 129.45, 131.37 (q), 131.62, 136.09, 147.90, 151.00, 151.60, 155.31; EIMS *m/z* 352 (*M*⁺); HRMS calcd 352.11471; found: 352.11570.

4.3.5. (*E,E*)-8-(4-Phenylbutadien-1-yl)caffeine (**6a**)

The title compound was prepared from 1,3-dimethyl-5,6-diaminouracil (**7a**), (*E,E*)-5-phenyl-2,4-pentadienoic acid (**10a**), and iodomethane in a yield of 27%; mp 253 °C; ¹H NMR (CDCl_3) δ 3.37 (s, 3H), 3.58 (s, 3H), 3.96 (s, 3H), 6.44 (d, 1H, *J* = 15.0 Hz), 6.84–6.95 (m, 2H), 7.24–7.36 (m, 3H), 7.42–7.46 (m, 2H), 7.56 (dd, 1H, *J* = 15.0, 10.0 Hz); ¹³C NMR (CDCl_3) δ 27.86, 29.66, 31.35, 107.82, 114.46, 126.90, 127.30, 128.65, 128.77, 136.40, 138.14, 138.50, 148.61, 149.98, 151.64, 155.13; EIMS *m/z* 322 (*M*⁺); HRMS calcd 322.14298; found: 322.14186.

4.3.6. (*E,E*)-8-[4-(3-Chlorophenyl)butadien-1-yl]caffeine (**6b**)

The title compound was prepared from 1,3-dimethyl-5,6-diaminouracil (**7a**), (*E,E*)-5-(3-chlorophenyl)-2,4-pentadienoic acid (**10b**), and iodomethane in a yield of 10%; mp 249 °C; ¹H NMR (CDCl_3) δ 3.39 (s, 3H), 3.59 (s, 3H), 3.99 (s, 3H), 6.49 (d, 1H, *J* = 15.0 Hz), 6.80 (d, 1H, *J* = 15.5 Hz), 6.92–7.01 (m, 1H), 7.24–7.31 (m, 3H), 7.44 (d, 1H, *J* = 0.41 Hz), 7.55 (dd, 1H, *J* = 14.7, 10.9 Hz); ¹³C NMR (CDCl_3) δ 27.92, 29.71, 31.42, 108.01, 115.47, 125.15, 126.61, 128.48, 128.67, 130.01, 134.85, 136.34, 137.87, 138.32, 148.65, 149.72, 151.68, 155.21; EIMS *m/z* 357 (*M*⁺); HRMS calcd 356.10400; found: 356.10571.

4.3.7. (*E,E*)-8-[4-(3-Bromophenyl)butadien-1-yl]caffeine (**6c**)

The title compound was prepared from 1,3-dimethyl-5,6-diaminouracil (**7a**), (*E,E*)-5-(3-bromophenyl)-2,4-pentadienoic acid (**10c**), and iodomethane in a yield of 40%; mp 246 °C; ¹H NMR (CDCl_3) δ 3.38 (s, 3H), 3.58 (s, 3H), 3.98 (s, 3H), 6.49 (d, 1H, *J* = 15.0 Hz), 6.78 (d, 1H, *J* = 15.5 Hz), 6.95 (dd, 1H, *J* = 15.5, 10.9 Hz), 7.17–7.22 (m, 1H), 7.33–7.40 (m, 2H), 7.55 (dd, 1H, *J* = 14.6, 10.9 Hz), 7.59 (d, 1H, *J* = 1.8 Hz); ¹³C NMR (CDCl_3) δ 27.91, 29.70, 31.40, 108.00, 115.50, 123.01, 125.58, 128.70, 129.53, 130.27, 131.38, 136.20, 137.82, 138.60, 148.63, 149.70, 151.67, 155.20; EIMS *m/z* 400, 402 (*M*⁺); HRMS calcd 400.05349; found: 400.05193.

4.3.8. (*E,E*)-8-[4-(3-Fluorophenyl)butadien-1-yl]caffeine (**6d**)

The title compound was prepared from 1,3-dimethyl-5,6-diaminouracil (**7a**), (*E,E*)-5-(3-fluorophenyl)-2,4-pentadienoic acid

(**10d**), and iodomethane in a yield of 22.1%: mp 223 °C; $^1\text{H NMR}$ (CDCl_3) δ 3.22 (s, 3H), 3.44 (s, 3H), 3.95 (s, 3H), 6.87 (d, 1H, $J = 15.0$ Hz), 7.01 (d, 1H, $J = 15.4$ Hz), 7.03–7.15 (m, 1H), 7.26 (dd, 1H, $J = 15.4$, 11.0 Hz), 7.35–7.44 (m, 3H), 7.47 (dd, 1H, $J = 14.6$, 11.0 Hz); EIMS m/z 340 (M^+); HRMS calcd 340.13355; found: 340.13367.

4.3.9. (*E,E*)-1,3-Dimethyl-8-(4-phenylbutadien-1-yl)-7-ethylxanthine (**6e**)

The title compound was prepared from 1,3-dimethyl-5,6-diaminouracil (**7a**), (*E,E*)-5-phenyl-2,4-pentadienoic acid (**10a**), and iodoethane in a yield of 6.9%: mp 227 °C; $^1\text{H NMR}$ (CDCl_3) δ 1.46 (t, 3H, $J = 7.2$ Hz), 3.43 (s, 3H), 3.63 (s, 3H), 4.45 (q, 1H, $J = 7.2$ Hz), 6.50 (d, 1H, $J = 14.9$ Hz), 6.92 (d, 1H, $J = 15.5$ Hz), 7.01 (dd, 1H, $J = 15.5$, 11.0 Hz), 7.31 (t, 1H, $J = 7.3$ Hz), 7.38 (t, 2H, $J = 7.4$ Hz), 7.49 (d, 2H, $J = 7.4$ Hz), 7.63 (dd, 1H, $J = 14.9$, 10.9 Hz); $^{13}\text{C NMR}$ (CDCl_3) δ 16.65, 28.12, 29.93, 40.18, 107.76, 115.16, 127.73, 128.16, 129.48, 129.63, 137.30, 139.00, 139.40, 149.78, 150.10, 152.69, 155.77; EIMS m/z 336 (M^+); HRMS calcd 336.15863; found: 336.15872.

4.3.10. (*E,E*)-1,3-Diethyl-8-(4-phenylbutadien-1-yl)-7-methylxanthine (**6f**)

The title compound was prepared from 1,3-diethyl-5,6-diaminouracil (**7b**), (*E,E*)-5-phenyl-2,4-pentadienoic acid (**10a**), and iodomethane in a yield of 24%: mp 156–157 °C; $^1\text{H NMR}$ (CDCl_3) δ 1.19 (t, 3H, $J = 7.1$ Hz), 1.30 (t, 3H, $J = 7.0$ Hz), 3.93 (s, 3H), 4.01 (q, 2H, $J = 6.9$ Hz), 4.13 (q, 2H, $J = 7.0$ Hz), 6.41 (d, 1H, $J = 15.0$ Hz), 6.84 (d, 1H, $J = 15.5$ Hz), 6.92 (dd, 1H, $J = 15.5$, 11.2 Hz), 7.23 (m, 1H), 7.30 (t, 2H, $J = 7.4$ Hz), 7.40 (d, 2H, $J = 7.8$ Hz), 7.53 (dd, 1H, $J = 14.9$, 10.9 Hz); $^{13}\text{C NMR}$ (CDCl_3) δ 13.49, 29.90, 31.57, 36.60, 38.68, 108.76, 115.30, 127.73, 128.20, 129.48, 129.64, 137.33, 138.93, 139.38, 149.10, 150.90, 151.70, 156.00; EIMS m/z 350 (M^+); HRMS calcd 350.17428; found: 350.17277.

4.3.11. (*E,E*)-1,3-Diethyl-8-(4-phenylbutadien-1-yl)-7-ethylxanthine (**6g**)

The title compound was prepared from 1,3-diethyl-5,6-diaminouracil (**7b**), (*E,E*)-5-phenyl-2,4-pentadienoic acid (**10a**), and iodoethane in a yield of 21%: mp 177–178 °C; $^1\text{H NMR}$ (CDCl_3) δ 1.19 (t, 3H, $J = 7.1$ Hz), 1.31 (t, 3H, $J = 7.0$ Hz), 1.38 (t, 3H, $J = 7.2$ Hz), 4.01 (q, 2H, $J = 7.0$ Hz), 4.13 (q, 2H, $J = 7.0$ Hz), 4.36 (q, 2H, $J = 7.2$ Hz), 6.41 (d, 1H, $J = 14.9$ Hz), 6.84 (d, 1H, $J = 15.5$ Hz), 6.93 (dd, 1H, $J = 15.5$, 11.0 Hz), 7.22 (m, 1H), 7.29 (t, 2H, $J = 7.6$ Hz), 7.41 (d, 2H, $J = 8.0$ Hz), 7.55 (dd, 1H, $J = 14.9$, 11.0 Hz); $^{13}\text{C NMR}$ (CDCl_3) δ 13.47, 16.68, 29.89, 36.62, 38.64, 40.10, 108.00, 115.38, 127.70, 128.26, 129.43, 129.63, 137.37, 138.73, 139.23, 149.33, 149.98, 151.74, 155.57; EIMS m/z 364 (M^+); HRMS calcd 364.18993; found: 364.18904.

4.4. MAO-B inhibition studies

The mitochondrial fraction of baboon liver tissue was isolated as described previously⁴³ and stored at -70 °C. Following addition of an equal volume of sodium phosphate buffer (100 mM, pH 7.4) containing glycerol (50%, w/v) to the mitochondrial isolate, the protein concentration was determined by the method of Bradford using bovine serum albumin as reference standard.⁴⁴ MMTP ($K_m = 68.3 \pm 1.60$ μM for baboon liver MAO-B),³⁵ served as substrate for the inhibition studies. The enzymatic reactions were prepared in sodium phosphate buffer (100 mM, pH 7.4) and contained MMTP (30–120 μM), the mitochondrial isolate (0.15 mg protein/mL) and various concentrations of the test inhibitors. The final volume of the incubations was 500 μL . For the IC_{50} determinations, a fixed substrate concentration of 50 μM was used and the inhibitor concentrations spanned at least three

orders of a magnitude (3–1000 μM). The stock solutions of the inhibitors were prepared in DMSO and were added to the incubation mixtures to yield a final DMSO concentration of 4% (v/v). DMSO concentrations higher than 4% are reported to inhibit MAO-B.⁴⁵ The reactions were incubated at 37 °C for 10 min and then terminated by the addition of 10 μL perchloric acid (70%). The MAO-B catalyzed production of MMDP⁺ was found to be linear for the first 10 min of incubation under these conditions. The samples were centrifuged at 16,000g for 10 min, and the concentrations of the MAO-B generated product, MMDP⁺, were measured spectrophotometrically at 420 nm ($\epsilon = 25,000$ M^{-1}) in the supernatant fractions.³⁵ For the K_i determinations, the initial rates of oxidation at four different substrate concentrations (30–120 μM) in the absence and presence of three different concentrations of the inhibitors were used to construct Lineweaver–Burke plots. The slopes of the Lineweaver–Burke plots were plotted versus the inhibitor concentration and the K_i value were determined from the abscissa intercept (intercept = $-K_i$). Linear regression analysis was performed using the SigmaPlot software package (Systat Software Inc.). Each K_i value reported here is representative of a single determination where the correlation coefficient (R^2 value) of the replot of the slopes versus the inhibitor concentrations was at least 0.98. The IC_{50} values were determined by plotting the initial rates of oxidation versus the logarithm of the inhibitor concentrations to obtain a sigmoidal dose–response curve. This kinetic data were fitted to the one site competition model incorporated into the Prism 4 software package (GraphPad Software Inc.). The IC_{50} values were determined in duplicate and are expressed as mean \pm standard error of the mean (SEM).

4.5. Adenosine A_{2A} receptor antagonism studies

The adenosine A_{2A} receptor binding studies were carried out according to the procedure described in lit.³⁷ The striata of male Sprague–Dawley rats ($n = 40$) were dissected, immediately frozen in liquid nitrogen and stored at -70 °C. The striata were thawed on ice, weighed and disrupted for 30 s with the aid of a Polytron homogenizer in 10 volumes of ice-cold 50 mM Tris-HCl (pH 7.7 at 25 °C). The resulting homogenate was centrifuged at 50,000g for 10 min and the pellet was resuspended in 10 volumes of ice-cold Tris-HCl, again with the aid of a Polytron homogenizer as above. The resulting suspension was recentrifuged and the pellet obtained was suspended in Tris-HCl to a volume of 5 mL/g original striatal weight. The striatal membranes were aliquoted into microcentrifuge tubes and stored at -70 °C. The incubations were carried out in 4 mL polypropylene tubes, previously coated with Sigmacote (Sigma–Aldrich) and were prepared in 1 mL Tris-HCl containing 5 mg of the original tissue weight striatal membranes, 4 nM [^3H]NECA, 50 nM CPA, 10 mM MgCl_2 , 0.1 U/mL adenosine deaminase, and various concentrations of the test compounds. The stock solutions of the compounds to be tested as well as that of CPA were prepared in DMSO. On the day of the study, CPA and [^3H]NECA were diluted to concentrations of 500 nM and 40 nM, respectively. A membrane suspension was prepared that contained 5 mg/0.79 mL striatal membranes and sufficient amounts of MgCl_2 and adenosine deaminase to produce concentrations of 10 mM and 0.1 U/mL, respectively, in the final 1 mL incubation mixtures. The order of additions was as follows: test compound (10 μL), CPA (100 μL), [^3H]NECA (100 μL), and the membrane suspension (0.79 mL). The incubations were vortexed and incubated for 60 min at 25 °C in a shaking water bath. Halfway through the experiment, the incubations were vortexed again. The incubations were filtered through a prewetted 2.4 cm Whatman glass microfiber filter (grade GF/B) under reduced pressure. The tubes were washed with 4 mL ice-cold Tris-HCl and the filters were washed twice more with 4 mL ice-cold Tris-HCl. The damp filters were placed in scintillation vials, 4 mL of

Filter-Count (Perkin-Elmer) was added and the vials were incubated overnight before being counted. The IC_{50} values were determined by plotting the count values versus the logarithm of the inhibitor concentrations to obtain a sigmoidal dose–response curve. This kinetic data were fitted to the one site competition model incorporated into the Prism 4 software package (GraphPad Software Inc.). The K_i values for the competitive inhibition of [3H]NECA ($K_d = 15.3$ nM) binding by the test compounds were calculated according to the Cheng and Prusoff equation.²⁷ All incubations were carried out in duplicate and the K_i values are expressed as mean \pm SEM. An estimate of the nonspecific binding was obtained from binding studies in the presence of 100 μ M CPA.

Acknowledgments

We are grateful to Cor Bester and Antoinette Fick of the Animal Research Centre as well as the staff of the Laboratory for Applied Molecular Biology, North-West University for their support. The NMR and MS spectra were recorded by André Joubert, Johan Jordaan, and Louis Fourie of the SASOL Centre for Chemistry, North-West University. This work was supported by grants from the National Research Foundation and the Medical Research Council, South Africa.

References and notes

- Allain, H.; Bentué-Ferrer, D.; Akwa, Y. *Prog. Neurobiol.* **2008**, *84*, 25.
- Schwarzschild, M. A.; Agnati, L.; Fuxe, K.; Chen, J. F.; Morelli, M. *Trends Neurosci.* **2006**, *29*, 647.
- Dauer, W.; Przedborski, S. *Neuron* **2003**, *39*, 889.
- Xu, K.; Bastia, E.; Schwarzschild, M. *Pharmacol. Ther.* **2005**, *105*, 267.
- Chen, J. F.; Xu, K.; Petzer, J. P.; Staal, R.; Xu, Y. H.; Beilstein, M.; Sonsalla, P. K.; Castagnoli, K.; Castagnoli, N., Jr.; Schwarzschild, M. A. *J. Neurosci.* **2001**, *21*, RC143.
- Ikeda, K.; Kurokawa, M.; Aoyama, S.; Kuwana, Y. *J. Neurochem.* **2002**, *80*, 262.
- Bibbiani, F.; Oh, J. D.; Petzer, J. P.; Castagnoli, N., Jr.; Chen, J. F.; Schwarzschild, M. A.; Chase, T. N. *Exp. Neurol.* **2003**, *184*, 285.
- Bara-Jimenez, W.; Sherzai, A.; Dimitrova, T.; Favit, A.; Bibbiani, F.; Gillespie, M.; Morris, M. J.; Mouradian, M. M.; Chase, T. N. *Neurology* **2003**, *61*, 293.
- Kase, H.; Mori, A.; Jenner, P. *Drug Discov. Today Ther. Strat.* **2004**, *1*, 51.
- Shimada, J.; Koike, N.; Nonaka, H.; Shiozaki, S.; Yanagawa, K.; Kanda, T.; Kobayashi, H.; Ichimura, M.; Nakamura, J.; Kase, H.; Suzuki, F. *Bioorg. Med. Chem. Lett.* **1997**, *7*, 2349.
- Jacobson, K. A.; Gallo-Rodriguez, C.; Melman, N.; Fischer, B.; Maillard, M.; Van Bergen, A.; Van Galen, P. J. M.; Karton, Y. *J. Med. Chem.* **1993**, *36*, 1333.
- Müller, C. E.; Geis, U.; Hipp, J.; Schobert, U.; Frobenius, W.; Pawlowski, M.; Suzuki, F.; Sandoval-Ramirez, J. *J. Med. Chem.* **1997**, *40*, 4396.
- Petzer, J. P.; Steyn, S.; Castagnoli, K. P.; Chen, J. F.; Schwarzschild, M. A.; Van der Schyf, C. J.; Castagnoli, N., Jr. *Bioorg. Med. Chem.* **2003**, *11*, 1299.
- Vlok, N.; Malan, S. F.; Castagnoli, N., Jr.; Bergh, J. J.; Petzer, J. P. *Bioorg. Med. Chem.* **2006**, *14*, 3512.
- Youdim, M. B. H.; Edmondson, D.; Tipton, K. F. *Nat. Rev. Neurosci.* **2006**, *7*, 295.
- Riederer, P.; Lachenmayer, L.; Laux, R. *Curr. Med. Chem.* **2004**, *11*, 2033.
- Collins, G. G. S.; Sandler, M.; Williams, E. D.; Youdim, M. B. H. *Nature* **1970**, *225*, 817.
- Youdim, M. B. H.; Collins, G. G. S.; Sandler, M.; Bevan-Jones, A. B.; Pare, C. M.; Nicholson, W. J. *Nature* **1972**, *236*, 225.
- Birkmayer, W.; Riederer, P.; Youdim, M. B. H.; Linauer, W. J. *Neural Transm.* **1975**, *36*, 303.
- Finberg, J. P.; Wang, J.; Bankiewicz, K.; Harvey-White, J.; Kopin, I. J.; Goldstein, D. S. *J. Neural Transm. Suppl.* **1998**, *52*, 279.
- Barnham, K. J.; Masters, C. L.; Bush, A. I. *Nat. Rev.* **2004**, *3*, 205.
- Youdim, M. B. H.; Bakhle, Y. S. *Br. J. Pharmacol.* **2006**, *147*, S287.
- Nicotra, A.; Pierucci, F.; Parvez, H.; Senatori, O. *Neurotoxicology* **2004**, *25*, 155.
- Fowler, J. S.; Volkow, N. D.; Wang, G. J.; Logan, J.; Pappas, N.; Shea, C.; MacGregor, R. *Neurobiol. Aging* **1997**, *18*, 431.
- Levitt, P.; Pintar, J. E.; Breakefield, X. O. *Proc. Natl. Acad. Sci. U.S.A.* **1982**, *79*, 6385.
- Nagatsu, T.; Sawada, M. *J. Neural Transm. Suppl.* **2006**, *71*, 53.
- Cheng, Y. C.; Prusoff, W. H. *Biochem. Pharmacol.* **1973**, *22*, 3099.
- Morón, J. A.; Campillo, M.; Perez, V.; Unzeta, M.; Pardo, L. J. *Med. Chem.* **2000**, *43*, 1684.
- Suzuki, F.; Shimada, J.; Shiozaki, S.; Ichikawa, S.; Ishii, A.; Nakamura, J.; Nonaka, H.; Kobayashi, H.; Fuse, E. *J. Med. Chem.* **1993**, *36*, 2508.
- Blicke, F. F.; Godt, H. C., Jr. *J. Am. Chem. Soc.* **1954**, *76*, 2798.
- Gerber, N. N. *J. Am. Chem. Soc.* **1960**, *82*, 5216.
- Kurien, P. N.; Pandya, K. C.; Surange, V. R. *J. Indian Chem. Soc.* **1934**, *11*, 823.
- Baker, B. R.; Doll, M. H. *J. Med. Chem.* **1971**, *14*, 793.
- Baker, B. R.; Janson, E. E.; Vermeulen, N. M. J. *J. Med. Chem.* **1969**, *12*, 898.
- Inoue, H.; Castagnoli, K.; Van der Schyf, C. J.; Mabic, S.; Igarashi, K.; Castagnoli, N., Jr. *J. Pharmacol. Exp. Ther.* **1999**, *291*, 856.
- Van den Berg, D.; Zoellner, K. R.; Ogunrombi, M. O.; Malan, S. F.; Terre'Blanche, G.; Castagnoli, N., Jr.; Bergh, J. J.; Petzer, J. P. *Bioorg. Med. Chem.* **2007**, *15*, 3692.
- Bruns, R. F.; Lu, G. H.; Pugsley, T. A. *Mol. Pharmacol.* **1986**, *29*, 331.
- Pitts, S. M.; Markey, S. P.; Murphy, D. L.; Weisz, A. In *MPTP: A Neurotoxin Producing a Parkinsonian Syndrome*; Markey, S. P., Castagnoli, N., Jr., Trevor, A. J., Kopin, I. J., Eds.; Academic Press: New York, 1986; pp 703–716.
- Bissel, P.; Bigley, M. C.; Castagnoli, K.; Castagnoli, N., Jr. *Bioorg. Med. Chem.* **2002**, *10*, 3031.
- Werbel, L. M.; Headen, M.; Elslager, E. F. *J. Med. Chem.* **1967**, *10*, 366.
- Crombie, L.; Crombie, W. M. L. *J. Chem. Soc. Perkin Trans. 1* **1994**, *10*, 1267.
- Cook, A. H.; Thomas, G. H. *J. Chem. Soc.* **1950**, 1884.
- Salach, J. I.; Weyler, W. *Methods Enzymol.* **1987**, *142*, 627.
- Bradford, M. M. *Anal. Biochem.* **1976**, *72*, 248.
- Gnerre, C.; Catto, M.; Leonetti, F.; Weber, P.; Carrupt, P.-A.; Altomare, C.; Carotti, A.; Testa, B. *J. Med. Chem.* **2000**, *43*, 4747.